

Highway Concrete Pavement Technology Development and Testing: Volume I— Field Evaluation of Strategic Highway Research Program (SHRP) C-202 Test Sites (Alkali-Silica Reaction (ASR))

PUBLICATION NO. FHWA-RD-02-082

AUGUST 2006



U.S. Department of Transportation
Federal Highway Administration

Research, Development, and Technology
Turner-Fairbank Highway Research Center
6300 Georgetown Pike
McLean, VA 22101-2296



Foreword

Distress in portland cement concrete (PCC) pavements can be caused by aggregate that is reactive to alkalis in the environment. The Federal Highway Administration (FHWA) monitored test sections of various treatments designed to mitigate this type of distress in PCC pavements that contained aggregates known to be reactive with alkalis. The pavement treatments were part of the Strategic Highway Research Program (SHRP). The test sections were located in California, Nevada, New Mexico, and Delaware. Three pavement sites had suffered some degree of distress due to alkali-silica reaction (ASR) prior to treatment, and one pavement was newly constructed with known reactive aggregates.

The test sections in all four States were monitored annually for 5 years, from 1994 through 1998. The monitoring was done by Long-Term Pavement Performance (LTPP) visual surveys, faulting measurements, relative humidity testing, petrographic examination, and compressive strength and elastic modulus testing. Falling Weight Deflectometer (FWD) testing was also performed at all four test sites. This report describes and quantifies the differences between test sections and the results of the various treatments used.

Gary L. Henderson
Director
Office of Infrastructure
Research and Development

Notice

This document is disseminated under the sponsorship of the U.S. Department of Transportation in the interest of information exchange. The U.S. Government assumes no liability for its contents or use thereof. This report does not constitute a standard, specification, or regulation.

The U.S. Government does not endorse products or manufacturers. Trade and manufacturers' names appear in this report only because they are considered essential to the object of the document.

Technical Report Documentation Page

1. Report No. FHWA-RD-02-082	2. Government Accession No.	3. Recipient's Catalog No.	
4. Title and Subtitle Strategic Highway Research Program Highway Concrete Pavement Technology Development and Testing: Volume I—Field Evaluation of Strategic Highway Research Program (SHRP) C-202 Test Sites (Alkali-Silica Reaction (ASR))		5. Report Date August 2006	
7. Author(s) Paul Krauss—Wiss, Janney, Elstner Associates, Inc. Jagannath Mallela, Brian Aho—ERES Division of ARA, Inc.		6. Performing Organization Code	
9. Performing Organization Name and Address Wiss, Janney, Elstner Associates, Inc. ERES Division of Applied 330 Pfingsten Road Research Associates, Inc. Northbrook, IL 60062-2095 505 W. University Avenue Champaign, IL 61820-3915		8. Performing Organization Report No.	
12. Sponsoring Agency Name and Address Office of Engineering and Highway Operations R&D Federal Highway Administration 6300 Georgetown Pike McLean, VA 22101-2296		10. Work Unit No. (TRAIS)	
15. Supplementary Notes FHWA Contracting Officer's Technical Representative: Monte Symons, P.E. This work was conducted under subcontract by Wiss, Janney, Elstner Associates, Inc. The authors are thankful for the generous help from the participating transportation departments of Nevada, California, New Mexico, and Delaware. The authors also wish to thank Mathew Sherman (formerly with WJE) for his assistance in collecting field data for this project and Mr. Leslie Titus-Glover (ERES) for his help during statistical analysis of nondestructive evaluation data.		11. Contract or Grant No. DTFH61-94-C-00009	
16. Abstract This study consists of continued field evaluations of treatments to four pavements suffering from distress due to alkali-silica reaction (ASR). One set of treatments was evaluated on existing pavements in Delaware, California, and Nevada that already showed ASR-related distress. Two of the existing pavements were located in relatively dry environments, while the third (in Delaware) was located in a moderately wet environment. The fourth site, in New Mexico, consisted of treatments on newly constructed pavements built with known reactive aggregates. At the Nevada site, the pavement was treated with methacrylate (HMM), silane, linseed oil, or lithium hydroxide. The Delaware site used only lithium hydroxide, while the California site used only methacrylate. The test sections in New Mexico consisted of pavement that contained admixtures as ASR inhibitors. There were two rates of addition of lithium hydroxide, a 25 percent replacement of cement with combinations of Class C and F fly ashes, and a high-range water reducer (HRWR). This evaluation showed that, unfortunately, none of the treatments were significantly beneficial to pavements with moderate to advanced ASR damage. The methacrylate sealer was effective when applied to a bridge deck and extended the pavement service life 3 to 5 years or more when applied in two to three coats. The results indicate that, regardless of the treatment, upward moisture migration from the subgrade to the bottom of the pavement is sufficient to support continued ASR even in dry desert climates. Preliminary results from the New Mexico test sites show that Class F ash, LOMAR (HRWA), or blended Class C and Class F ash may improve resistance to ASR distress. However, Class C ash can make deterioration much worse. Careful selection of the fly ash is necessary when attempting to mitigate known reactive aggregate. Continued monitoring of this test site is recommended.		13. Type of Report and Period Covered Final Report	
17. Key Words Concrete pavement, durability, compressive strength, rapid chloride permeability test, AC impedance test, life cycle cost		14. Sponsoring Agency Code	
18. Distribution Statement No restrictions. This document is available to the public through the National Technical Information Service, Springfield, VA 22161.		15. Supplementary Notes	
19. Security Classif. (of this report) Unclassified	20. Security Classif. (of this page) Unclassified	21. No of Pages 185	22. Price

SI* (MODERN METRIC) CONVERSION FACTORS

APPROXIMATE CONVERSIONS TO SI UNITS

Symbol	When You Know	Multiply By	To Find	Symbol
LENGTH				
in	inches	25.4	millimeters	mm
ft	feet	0.305	meters	m
yd	yards	0.914	meters	m
mi	miles	1.61	kilometers	km
AREA				
in ²	square inches	645.2	square millimeters	mm ²
ft ²	square feet	0.093	square meters	m ²
yd ²	square yard	0.836	square meters	m ²
ac	acres	0.405	hectares	ha
mi ²	square miles	2.59	square kilometers	km ²
VOLUME				
fl oz	fluid ounces	29.57	milliliters	mL
gal	gallons	3.785	liters	L
ft ³	cubic feet	0.028	cubic meters	m ³
yd ³	cubic yards	0.765	cubic meters	m ³
NOTE: volumes greater than 1000 L shall be shown in m ³				
MASS				
oz	ounces	28.35	grams	g
lb	pounds	0.454	kilograms	kg
T	short tons (2000 lb)	0.907	megagrams (or "metric ton")	Mg (or "t")
TEMPERATURE (exact degrees)				
°F	Fahrenheit	5 (F-32)/9 or (F-32)/1.8	Celsius	°C
ILLUMINATION				
fc	foot-candles	10.76	lux	lx
fl	foot-Lamberts	3.426	candela/m ²	cd/m ²
FORCE and PRESSURE or STRESS				
lbf	poundforce	4.45	newtons	N
lbf/in ²	poundforce per square inch	6.89	kilopascals	kPa

APPROXIMATE CONVERSIONS FROM SI UNITS

Symbol	When You Know	Multiply By	To Find	Symbol
LENGTH				
mm	millimeters	0.039	inches	in
m	meters	3.28	feet	ft
m	meters	1.09	yards	yd
km	kilometers	0.621	miles	mi
AREA				
mm ²	square millimeters	0.0016	square inches	in ²
m ²	square meters	10.764	square feet	ft ²
m ²	square meters	1.195	square yards	yd ²
ha	hectares	2.47	acres	ac
km ²	square kilometers	0.386	square miles	mi ²
VOLUME				
mL	milliliters	0.034	fluid ounces	fl oz
L	liters	0.264	gallons	gal
m ³	cubic meters	35.314	cubic feet	ft ³
m ³	cubic meters	1.307	cubic yards	yd ³
MASS				
g	grams	0.035	ounces	oz
kg	kilograms	2.202	pounds	lb
Mg (or "t")	megagrams (or "metric ton")	1.103	short tons (2000 lb)	T
TEMPERATURE (exact degrees)				
°C	Celsius	1.8C+32	Fahrenheit	°F
ILLUMINATION				
lx	lux	0.0929	foot-candles	fc
cd/m ²	candela/m ²	0.2919	foot-Lamberts	fl
FORCE and PRESSURE or STRESS				
N	newtons	0.225	poundforce	lbf
kPa	kilopascals	0.145	poundforce per square inch	lbf/in ²

*SI is the symbol for the International System of Units. Appropriate rounding should be made to comply with Section 4 of ASTM E380.
(Revised March 2003)

TABLE OF CONTENTS

Chapter 1. Introduction.....	1
Chapter 2. Summary of Results from Winnemucca, NV	3
Summary of Pavement Condition by Section.....	5
Joint Distress.....	7
Severe Map Cracking at Joints	11
Wheelpath and Centerline Rating.....	14
Transverse Cracking	15
Modulus and Strength Testing.....	19
Relative Humidity Measurements.....	22
Petrographic Studies	23
Summary for Winnemucca, NV Test Site	25
Chapter 3. Summary of Results from Newark, DE	27
Summary of Pavement Section Condition.....	28
Joint Distress and Travel Lane Observations.....	32
Transverse Cracking	36
Modulus and Strength Testing.....	37
Relative Humidity Measurements.....	39
Petrographic Examination.....	40
Summary of Newark, DE Test Site.....	41
Chapter 4. Summary of Test Results From Boron, CA	43
Introduction.....	43
Boron Overhead.....	43
Pavement Sections	43
Observations	44
Status of Test Sections	44
Map Cracking.....	46
Joint Distress.....	49
Wheelpath Distress	55
Centerline Distress.....	56
Elastic Modulus and Compressive Strength	56
Relative Humidity Measurements.....	57
Petrographic Examination.....	59
Summary of Boron, CA Test Site.....	61
Chapter 5. Summary of Test Results From Albuquerque, NM	63
Condition of Pavement Sections.....	66
Transverse Joint Spalling.....	69
Map Cracking.....	71
Modulus Testing of Cores.....	72
Relative Humidity.....	74
Petrographic Examination.....	77
Summary of Lomas Boulevard, Albuquerque, NM, Test Site.....	77

Chapter 6. Falling Weight Deflectometer Results	81
Introduction.....	81
Methodology.....	81
Data Collection	81
Data Assembly.....	83
Performance Indicators and Their Significance.....	83
FWD Data Analysis for the Nevada Site	84
Subgrade k-value	85
D _o (Center Slab).....	86
E _{PCC} (Center Slab).....	86
D _o (Joint—Leave Side).....	87
FWD Data Analysis for the Delaware Site	89
Subgrade k-value	90
D _o (Center Slab).....	90
Backcalculated Concrete Modulus, E _{PCC}	91
D _o (Joint—Leave Side).....	92
LTE (Joint).....	93
FWD Data Analysis for the California Site	95
Subgrade k-value	95
D _o (Center Slab).....	95
Backcalculated Concrete Modulus, E _{PCC}	97
D _o (Joint—Leave Side).....	97
LTE (Joint).....	98
FWD Data Analysis for the New Mexico Site.....	100
Subgrade k-value	100
D _o (Center Slab).....	100
Backcalculated E _{PCC} (Center Slab).....	102
D _o (Joint—Leave Side).....	102
LTE (Joint).....	103
Summary of FWD Testing.....	105
Appendix A	107
Appendix B	127
Appendix C	145
Appendix D	159
References.....	173

LIST OF FIGURES

Figure 1. Overall view of Winnemucca, NV test site.	4
Figure 2. Winnemucca, NV test section layout.	4
Figure 3. Joint distress of high severity (Winnemucca, NV).....	7
Figure 4. Joint distress of medium severity (Winnemucca, NV).....	8
Figure 5. Joint distress for all sections of Winnemucca test site (1994).....	9
Figure 6. Joint distress for all sections of Winnemucca test site (1995).....	9
Figure 7. Joint distress for all sections of Winnemucca test site (1996).....	10
Figure 8. Joint distress for all sections of Winnemucca test site (1997).....	10
Figure 9. Joint distress for all sections of Winnemucca test site (1998).....	11
Figure 10. Actual joint length of each severity level for each section (Winnemucca, NV, 1998).	11
Figure 11. Photograph showing widespread map cracking in shoulder area of Winnemucca test site.	12
Figure 12. Close-up of map cracking with efflorescence (Winnemucca, NV).....	12
Figure 13. Number of areas of severe map cracking in each section from 1995 through 1998 (Winnemucca, NV).....	13
Figure 14. Total area of severe map cracking for each section for 1995 through 1998 (Winnemucca, NV).	14
Figure 15. Full-width transverse cracking in test section (Winnemucca, NV).....	16
Figure 16. Transverse cracking with intersecting longitudinal crack (Winnemucca, NV).	16
Figure 17. Amount and severity of transverse cracking for all sections (Winnemucca, NV, 1994).	17
Figure 18. Amount and severity of transverse cracking for all sections (Winnemucca, NV, 1995).	17
Figure 19. Amount and severity of transverse cracking for all sections (Winnemucca, NV, 1996).	18
Figure 20. Amount and severity of transverse cracking for all sections (Winnemucca, NV, 1997).	18
Figure 21. Amount and severity of transverse cracking for all sections (Winnemucca, NV, 1998).	19
Figure 22. North and south views of the Newark, DE site.	27
Figure 23. Typical longitudinal cracking (Newark, DE).	29
Figure 24. Typical longitudinal cracking and example of asphalt patching along joint between shoulder and travel lane (Newark, DE).	29

Figure 25. Area of each slab affected by map cracking over the 5 years of the study (Newark, DE).....	31
Figure 26. Area of each slab affected by map cracking expressed as a percentage of the total section area (Newark, DE).....	32
Figure 27. Asphalt concrete patching along transverse joint in travel lane (Newark, DE).	33
Figure 28. Asphalt patch in center of section in travel lane (Newark, DE).....	33
Figure 29. Length and severity of joint distress for all test sections (Newark, DE, 1994).....	34
Figure 30. Length and severity of joint distress for all test sections (Newark, DE, 1995).....	34
Figure 31. Length and severity of joint distress for all test sections (Newark, DE, 1996).....	35
Figure 32. Length and severity of joint distress for all test sections (Newark, DE, 1997).....	35
Figure 33. Length and severity of joint distress for all test sections (Newark, DE, 1998).....	36
Figure 34. Summary of transverse cracking in each section for the five inspections (Newark, DE).....	37
Figure 35. Treated section on Boron overhead structure over State Route 58 looking east (Boron, CA).....	43
Figure 36. Photograph showing part of Boron, CA, test site, M2, Station 250.....	45
Figure 37. Photograph showing part of Boron, CA, test site, M3, Station 160.....	45
Figure 38. Plan view of Boron, CA, test site.	46
Figure 39. Example of high-severity map cracking (Boron, CA).....	47
Figure 40. Close-up photograph showing typical map cracking (Boron, CA).....	47
Figure 41. Map cracking as a percentage for each level of severity (Boron, CA, 1995).....	48
Figure 42. Map cracking as a percentage for each level of severity (Boron, CA, 1996).....	48
Figure 43. Map cracking as a percentage for each level of severity (Boron, CA, 1997).....	49
Figure 44. Map cracking as a percentage for each level of severity (Boron, CA, 1998).....	49
Figure 45. Photograph showing medium-severity joint distress (Boron, CA).	50
Figure 46. Photograph showing an example of high-severity joint distress (Boron, CA).....	50
Figure 47. Amount and severity of joint distress (Boron, CA, 1995).....	51
Figure 48. Amount and severity of joint distress (Boron, CA, 1996).....	52
Figure 49. Amount and severity of joint distress (Boron, CA, 1997).....	52
Figure 50. Amount and severity of joint distress (Boron, CA, 1998).....	53
Figure 51. True length of joint spalls at each level of severity (Boron, CA, 1995).....	53
Figure 52. True length of joint spalls at each level of severity (Boron, CA, 1996).....	54
Figure 53. True length of joint spalls at each level of severity (Boron, CA, 1997).....	54
Figure 54. True length of joint spalls at each level of severity (Boron, CA, 1998).....	55

Figure 55. New Mexico ASR test section layout—westbound approach slabs to Lomas Boulevard (State Route 352) bridge over I-25.....	64
Figure 56. Lomas Boulevard westbound structure over I-40 (Albuquerque, NM).	65
Figure 57. Photographs of all sections in Albuquerque, NM.	68
Figure 58. Area of map cracking as a percentage of the total area (all sections, Albuquerque, NM).....	71
Figure 59. Modulus of elasticity test results for cores in the dry condition (all sections, Albuquerque, NM).....	73
Figure 60. Modulus of elasticity test results for cores in the saturated condition (all sections, Albuquerque, NM).....	74
Figure 61. Falling Weight Deflectometer.	81
Figure 62. Illustration of testing locations.	83
Figure 63. Static k-values for Nevada test section.....	85
Figure 64. Nevada test site— D_o from center slab.....	86
Figure 65. Nevada test site— E_{PCC} from center slab.	87
Figure 66. Nevada test site— D_o from leave side; deflection LTE (wheelpath).	88
Figure 67. Average LTE values for the various treatment sections for the Nevada site.	89
Figure 68. Average temperatures at time of joint testing for the Nevada site.	89
Figure 69. Static k-values for the Delaware site.	90
Figure 70. Delaware test site— D_o from center slab test.	91
Figure 71. Delaware test site— E_{PCC} from center slab.....	92
Figure 72. Delaware test site— D_o from leave side.	93
Figure 73. Delaware test site—LTE.	94
Figure 74. Average temperatures at time of joint testing for the Delaware site.	94
Figure 75. Static k-value for California test section.	96
Figure 76. California test site— D_o from center slab.....	96
Figure 77. California test site— E_{PCC} from center slab.....	97
Figure 78. California test site— D_o from leave side.	98
Figure 79. California test site—LTE.	99
Figure 80. Static k-value for New Mexico test.	101
Figure 81. New Mexico test site— D_o from center slab.	101
Figure 82. New Mexico test site— E_{PCC} from center slab.	102
Figure 83. New Mexico test site— D_o from leave side.....	103
Figure 84. Temperature variation during FWD testing for the New Mexico site.....	104

Figure 85. New Mexico test site—LTE.....	104
Figure A1. Photographs of typical joint sections for each test section (Winnemucca, NV).	107
Figure B1. Photographs of typical area of each section (Newark, DE).....	128
Figure C1. Photographs showing typical areas of each section (Boron, CA).....	145

LIST OF TABLES

Table 1. Inspection dates and conditions (Winnemucca, NV).....	5
Table 2. Wheelpath and centerline ratings for 1995 and 1998; number of slabs with each rating (Winnemucca, NV).	15
Table 3. Number of transverse cracks per section.	19
Table 4. Modulus of elasticity testing results for Winnemucca, NV (dry tested, x 10 ⁶ psi).....	20
Table 5. Modulus of elasticity testing results for Winnemucca, NV (wet tested, x 10 ⁶ psi).....	21
Table 6. Summary of average modulus data for Winnemucca, NV.	21
Table 7. Compressive strength testing results for Winnemucca, NV.	22
Table 8. Relative humidity measurements for Winnemucca, NV (December 1995).	22
Table 9. Relative humidity measurements for Winnemucca, NV (October 1997).....	23
Table 10. Relative humidity measurements for Winnemucca, NV (October 1998).....	23
Table 11. Summary of petrographic examinations for cores from Winnemucca, NV.	24
Table 12. Summary of petrographic results (average 1997-1998) for cores from Winnemucca, NV.....	25
Table 13. Summary of Winnemucca, NV test sections.	26
Table 14. Inspection dates and conditions.	28
Table 15. Condition of Delaware test pavement sections in 1998.....	30
Table 16. Newark, DE, core modulus testing results (psi x 10 ⁶ , dry tested).	38
Table 17. Newark, DE, core modulus testing results (psi x 10 ⁶ , wet tested).....	38
Table 18. Newark, DE, compressive strength results (psi).....	38
Table 19. Relative humidity testing at Newark, DE (1994).	39
Table 20. Relative humidity testing at Newark, DE (1995).	39
Table 21. Relative humidity testing at Newark, DE (1996).	40
Table 22. Relative humidity testing at Newark, DE (1997).	40
Table 23. Summary of petrographic findings for 1997 and 1998.....	41
Table 24. Wheelpath ratings for all sections, Boron, CA.	56
Table 25. Centerline ratings for all sections, Boron, CA.....	56
Table 26. Modulus dry tested elastic modulus (psi x 10 ⁶), Boron, CA.	57
Table 27. Modulus wet tested elastic modulus (psi x 10 ⁶), Boron, CA.....	57
Table 28. Compressive strength test results (Boron, CA).	57
Table 29. Relative humidity testing (1994).	58
Table 30. Relative humidity testing (1995).	58

Table 31. Relative humidity testing (1996).....	58
Table 32. Relative humidity testing (1997).....	59
Table 33. Relative humidity testing (1998).....	59
Table 34. Summary of petrographic findings for 1997 and 1998, Boron, CA.	60
Table 35. Test variables Lomas Boulevard, Albuquerque, NM.	63
Table 36. Visual inspection notes for October 1, 1998 (Albuquerque, NM).....	67
Table 37. Summary of transverse joint spalling (1998).....	70
Table 38. Elastic modulus test results dry condition (psi x 10 ⁶ , average of 2 cores) Albuquerque, NM.	72
Table 39. Elastic modulus test results wet condition (psi x 10 ⁶ , average of 2 cores), Albuquerque, NM.	73
Table 40. Relative humidity testing, Albuquerque, NM (1994).	75
Table 41. Relative humidity testing, Albuquerque, NM (1995).	75
Table 42. Relative humidity testing, Albuquerque, NM (1996).	76
Table 43. Relative humidity testing, Albuquerque, NM (1997).	76
Table 44. Relative humidity testing, Albuquerque, NM (1998).	77
Table 45. Summary of petrographic examination of cores for 1998 (S = Shakespeare, G = Grevey).....	79
Table 46. Summary of petrographic examination.....	80
Table 47. General cross section information.	82
Table 48. Results of Delaware Duncan grouping.	93
Table 49. Statistical analysis of California LTE.	99
Table A1. Summary of LTPP survey sheets for ASR investigation—control section.	116
Table A2. Summary of LTPP survey sheets for ASR investigation—section L2.	117
Table A3. Summary of LTPP survey sheets for ASR investigation—section S2.	118
Table A4. Summary of LTPP survey sheets for ASR investigation—section M2.	119
Table A5. Summary of LTPP survey sheets for ASR investigation—section SA1.	120
Table A6. Summary of LTPP survey sheets for ASR investigation—section LO1.	121
Table A7. Summary of LTPP survey sheets for ASR investigation—control 2.	122
Table A8. Summary of LTPP survey sheets for ASR investigation—section S1.	123
Table A9. Summary of LTPP survey sheets for ASR investigation—section L1.	124
Table A10. Summary of LTPP survey sheets for ASR investigation—control section 1.	125
Table A11. Summary of LTPP survey sheets for ASR investigation—section M1.	126

Table B1. Transverse joint observations of Route 72, Newark, DE (1998)	127
Table B2. Summary of LTPP survey sheets for ASR investigation—control section 1.	135
Table B3. Summary of LTPP survey sheets for ASR investigation—test section 1.....	136
Table B4. Summary of LTPP survey sheets for ASR investigation—test section 2.....	137
Table B5. Summary of LTPP survey sheets for ASR investigation—control section 2.	138
Table B6. Summary of LTPP survey sheets for ASR investigation—control section 3.	139
Table B7. Summary of LTPP survey sheets for ASR investigation—control section 4.	140
Table B8. Summary of LTPP survey sheets for ASR investigation—test section 3.....	141
Table B9. Summary of LTPP survey sheets for ASR investigation—test section 4.....	142
Table B10. Summary of LTPP survey sheets for ASR investigation—control section 5.	143
Table C1. Summary of LTPP survey sheets for ASR investigation—C1-boron.....	153
Table C2. Summary of LTPP survey sheets for ASR investigation—C2-boron.....	154
Table C3. Summary of LTPP survey sheets for ASR investigation—C3-boron.....	155
Table C4. Summary of LTPP survey sheets for ASR investigation—M1-boron.....	156
Table C5. Summary of LTPP survey sheets for ASR investigation—M2-boron.....	157
Table C6. Summary of LTPP survey sheets for ASR investigation—M3-boron.....	158
Table D1. Summary of LTPP survey sheets for ASR investigation—1-1% LiOH.	162
Table D2. Summary of LTPP survey sheets for ASR investigation—2-0.5% LiOH.	163
Table D3. Summary of LTPP survey sheets for ASR investigation—3-Lomar.....	164
Table D4. Summary of LTPP survey sheets for ASR investigation—4-class F fly ash.....	165
Table D5. Summary of LTPP survey sheets for ASR investigation—5-class F fly ash.....	166
Table D6. Summary of LTPP survey sheets for ASR investigation—6-control.	167
Table D7. Summary of LTPP survey sheets for ASR investigation—7-blended C&F.....	168
Table D8. Summary of LTPP survey sheets for ASR investigation—8-class F.	169
Table D9. Summary of LTPP survey sheets for ASR investigation—9-control.	170
Table D10. Summary of LTPP survey sheets for ASR investigation—10-1% LiOH.	171
Table D11. Summary of LTPP survey sheets for ASR investigation—11-class C ash.....	172

CHAPTER 1. INTRODUCTION

In 1994, the Federal Highway Administration (FHWA) began monitoring test sections of various treatments designed to mitigate distress in portland cement concrete (PCC) pavements that contained aggregates known to be reactive with alkalis. The pavement treatments were part of the Strategic Highway Research Program (SHRP). The test sections were located in California, Nevada, New Mexico, and Delaware. Three pavement sites had suffered some degree of distress due to alkali-silica reaction (ASR) prior to treatment, and one pavement was newly constructed with known reactive aggregates.

The test sections of existing distressed pavement in California were treated with high molecular weight methacrylate (HMWM); the existing pavement sections in Nevada were also treated with HMWM, plus linseed oil, lithium hydroxide, and silane; and the existing pavement sections in Delaware were treated with lithium hydroxide. Various application rates were used at each test section.

The test sections in New Mexico consisted of a newly constructed pavement that contained mineral and chemical admixtures as ASR inhibitors. These were: two rates of addition of lithium hydroxide, a 25 percent replacement of cement with combinations of Class C and Class F fly ashes, and a high-range, water-reducing (HRWR) admixture.

The test sections in all four States were monitored annually for 5 years, from 1994 through 1998. The monitoring was done by Long-Term Pavement Performance (LTPP) visual surveys, faulting measurements, relative humidity testing, petrographic examination, and compressive strength and elastic modulus testing. Falling Weight Deflectometer (FWD) testing also was performed. The FWD results for all four test sites are included in a section near the end of the report.

The standard LTPP visual rating system sometimes had to be modified to accurately describe the differences between test sections. The LTPP criteria only rate the area of map cracking, not its severity. All of the older pavements (Nevada, California, and Delaware) already exhibited nearly 100 percent map cracking at the time of the first survey. Each pavement was in moderate to advanced stages of ASR deterioration before surface treatment. Therefore, additional gradings to rate the severity of map cracking had to be developed for each site. This allowed differences between test sections to be described and quantified.

CHAPTER 2. SUMMARY OF RESULTS FROM WINNEMUCCA, NV

This test site is the pavement described in the SHRP C-343 report, "Eliminating or Minimizing Alkali-Silica Reactivity." The test section consists of eleven 24.4-meter (m) groups of five-slab panels on the travel (number 2) lane of U.S. Interstate 80 (I-80) just east of Winnemucca, NV. The pavement was built in 1981. It consists of a plain, jointed, 20.3-centimeter (cm)-thick concrete slab over a 15.2-cm portland cement-treated base and a 7.6-cm gravel subbase. An asphalt concrete bondbreaker was used between the base and subbase. Non-doweled, skewed transverse joints are spaced at a repeating pattern of 3.66, 3.97, 5.49, and 5.80 m. Coarse aggregate was reportedly obtained from a commercial source in Winnemucca, and an American Society of Testing Materials (ASTM) Type II low-alkali cement was used. An overall view of the section is shown in figure 1. A key to the sections is given in figure 2.

Different surface treatment materials were applied to each five-slab-long test section. The materials tested were a high-molecular weight methacrylate resin (Sika Pronto 19TF), a polysiloxane resin sealer (Sikagard 70), a lithium hydroxide solution, a silane sealer (SilAct), and a linseed oil. There are also three five-slab-long untreated control sections. The treatments were applied in 1991 and 1992. Two different sets of test slabs were treated. One section, on the east end of the test site, includes the sections methacrylate 1 (M1), control 1 (C1), lithium 1 (L1), siloxane 1 (S1), and control 2 (C2). A second group of the same materials was applied on slabs on the west end of the test site; methacrylate (M2), siloxane (S2), lithium (L2), and control 3 (C3). The pavement in the west end of the test area was less severely distressed than the sections in the east end. Within 1 year, two additional treatments were applied to the sections. One section used SilAct silane and was designated silane number 2 section 1 (SA1). The other material was a linseed oil and was designated linseed oil section 1 (LO1). Two additional applications of 10 percent LiOH solution were applied to the existing LiOH test areas. The following excerpt describes the application of the test materials (letter, Stark to Surdahl, October 8, 1987):

During the SHRP program in 1991, a search was made for an existing pavement where several candidate techniques for mitigating ASR might be investigated. Mr. Richard Moore, Materials and Testing Engineer of the State of Nevada, Department of Transportation (DOT), and the writer concluded that the above-mentioned I-80 pavement exhibited the intended severity of cracking due to ASR to be the test pavement. It was preferred that ASR be only moderate so that traffic loading would not render such severe distress that remediation efforts would have no potential to arrest ASR-related distress. Based on SHRP laboratory work, LiOH was considered a satisfactory candidate. The intent was to spray the solution on the top of the wearing surface several times to allow penetration into the concrete, thereby arresting ASR. The second surface-applied treatment was a high-molecular weight methacrylate known as Sika Pronto 19 TF. It was a two-component, rapid curing, solvent-free product intended to penetrate and bond near-surface ASR and other cracks, thereby strengthening the pavement concrete against further distress.



Figure 1. Overall view of Winnemucca, NV test site.

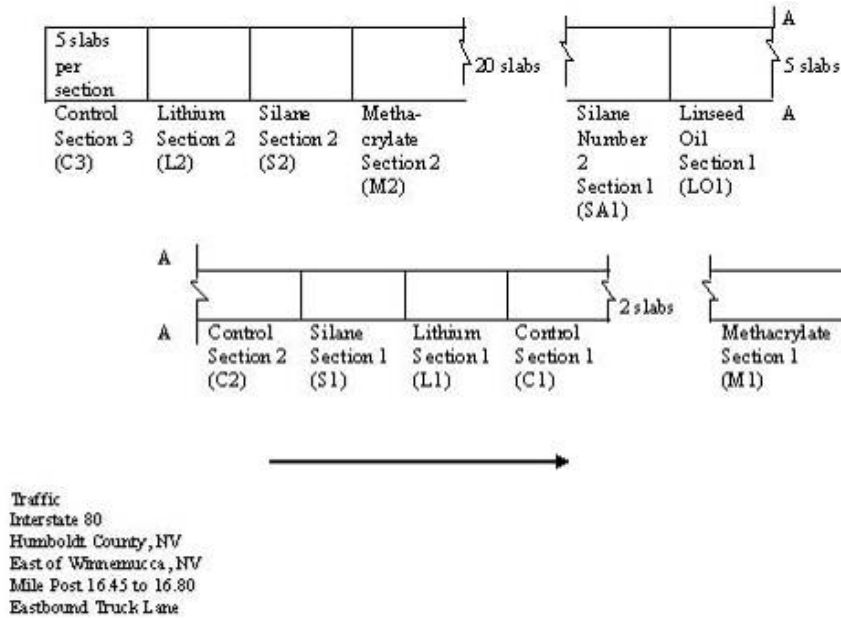


Figure 2. Winnemucca, NV test section layout.

A third surface treatment was Sikagard 70. It was a blend of polysiloxane resins that was a colorless, nonfilm-forming, nonvapor barrier formulation to seal absorbent cementitious surfaces. The intent was to minimize penetration of atmospheric moisture into the concrete pavement, thereby reducing additional cracking from swelling of ASR gel reaction products. Figure 2 shows the location of the individual test sections.

The first three surface treatments were applied on October 2, 1991. Prior to the initial application, all surfaces, including the nontreated control sections were sand- and air-blasted to remove adhered surface debris to facilitate penetration of the treatment. The Sikagard 70 polysiloxane sealant was sprayed on at the recommended rate of (9.3 m²/3.8 liter (L)) (100 square

feet per gallon (ft²/gal)) in a single application. Sika Pronto 19 Tack Free was squeegeed and broomed on the surface at a rate of 6.5 to 7.4 m²/3.8 L (70 to 80 ft²/gal), then treated with fine (sandblasting) sand to minimize stickiness during setting that day.

A 283.88 L quantity of a 10 percent LiOH solution was used for the two treatment areas. The LiOH was dissolved in a wheeled spray tank on October 1, 1991, and stored at the maintenance garage in Winnemucca. The following day, after surface cleaning, four individual applications of LiOH solution were sprayed on immediately following atmospheric surface drying during the late morning and middle afternoon. The rate of application was calculated at 5.6 m²/3.8 L (60 ft²/gal) for the 10 percent LiOH solution.

On October 7, 1992, one year after the initial testing, three additional surface treatments were applied on the same region of Eastbound I-80 near Winnemucca. One application of linseed oil and one of SilAct silane each were applied to test sections as shown in figure 2. Also, two applications of the 10 percent LiOH solution were applied to the same test sections, at the same locations as before. These were applied at the rate of 1.7 m²/3.8 L (18 ft²/gal).

The Winnemucca pavement test section was inspected each fall for the 5 years of the study. Table 1 shows the inspection dates for this site. Annual tests included visual inspection and crack mapping, faulting measurements, relative humidity measurements, FWD readings (performed by the Nevada DOT), and core removal for wet and dry modulus testing and petrographic studies. The cores were taken by Nevada DOT personnel.

Table 1. Inspection dates and conditions (Winnemucca, NV).

Year	Inspection Dates	Weather Conditions
1994	October 18, 1994	Warm, 65–90 °F
1995	December 12, 1995	Rainy, breezy, 50 °F
1996	December 5, 1996	Rain, snow, 40 °F
1997	October 9, 1997	Cold, became clear, 50–60 °F
1998	October 28, 1998	Cold, showers, 40 °F

$$^{\circ}\text{C} = (^{\circ}\text{F}-32)/1.8$$

SUMMARY OF PAVEMENT CONDITION BY SECTION

The condition of the pavement test section was determined by visual inspection. Notes were made as to the extent of map cracking, transverse cracking, etc. Generally, all sections had extensive map cracking, but some sections were worse than others. The condition of one section was compared to others. The results of the final visual inspection (1998) are given below. Photographs of typical sections are shown in appendix A.

- Control 3 (C3)—This section is in slightly better condition than the other two control sections except that it has more transverse cracking. A considerable amount of high-severity spalling exists at the joints; however, a few areas within the transverse joints have not yet spalled.
- Lithium 2 (L2)—This section is performing better than the lithium 1 section, but it was initially in better condition. Some areas along the transverse joints are not spalled, and the

amount of high-severity spalling is less. The map cracking in the wheelpath is mostly medium severity with some low severity, and the cracking in the centerline area is roughly half low and half medium severity.

- Siloxane 2 (S2)—The transverse joint condition of this section is much better than that of S1, but it was initially in better condition. Some joints have no areas of high-severity spalling, and where joints have some high-severity spalling it is only for a short length. The map cracking in the wheelpath is mostly medium with some high and some low severity. The cracking in the centerline area is of medium severity.
- Methacrylate (M2)—This section is performing better than most with respect to joint spalling. Transverse joints are rated as medium or high severity, but the actual length of high-severity spalling is small for each joint. The majority of the total joint length has a rating of low severity, but it is tabulated higher because of the rating criteria defined in the LTPP rating system. There are several large longitudinal cracks and a few transverse cracks. The amount of severe map cracking at the joints for this section is average compared to the other sections. The cracking in the wheelpath areas between joints is predominantly medium severity, and the centerline area is rated low severity.
- Silane Number 2-1 (SA1)—The total length of joint spalling for this section is less than some sections but is still considerable. The severity of the spalling is less, with most being medium severity. There are some areas of severe map cracking in the wheelpaths at the joints, as well as several areas associated with large transverse cracks. The map cracking associated with the wheelpaths and centerline areas between joints is rated as medium severity.
- Linseed Oil 1 (LO1)—This section has the same level of severity of joint spalling as control 1. Almost all the joint length has some spalling, and most joints have some areas of high-severity spalling. The heavy map cracking in the wheelpath areas at the joints in this section is among the most severe of all sections, but not as bad as section S1. The map cracking in the wheelpaths between joints is of medium severity, and the cracking in the centerline areas is of low to medium severity.
- Control 2 (C2)—This section is worse than control 1. Map cracking is well advanced, although discrete longitudinal cracking has become less pronounced. Almost all of the transverse joint length has spalling, and most has some high-severity spalling. The wheelpath map cracking is of high to medium severity, and the centerline cracking is of medium severity.
- Siloxane 1 (S1)—This section has the most severe joint spalling of any section. High-severity spalling had occurred along 45 percent of the total transverse joint length. The map cracking in the wheelpath area is of medium to high severity, and in the centerline area it is of medium severity. The areas of heavy map cracking, where the wheelpaths cross the joints, are more severe for this section than the other sections.
- Lithium 1 (L1)—This section is in the same condition as control 2. The entire transverse joint length has spalling, and all joints have some areas of high-severity spalling. The map cracking in the wheelpath area is of medium severity, while that in the centerline area is of low to medium severity.

- Control 1 (C1)—Some major longitudinal cracks exist, but they are becoming less noticeable due to an increase in the amount and severity of the map cracking. Almost all of the transverse joint length has spalling, and most joints have at least one area of high-severity spalling. Most of the wheelpath and centerline map cracking is of medium severity.
- Methacrylate 1 (M1)—Joint spalling in this section is comparable to that in sections C1 and LO1. The entire length of transverse joints has some spalling. The spalling ranges from mostly medium and low severity for some joints, to other joints with half their length rated as high severity. The area associated with the severe map cracking in the wheelpaths at the joints is the second highest after section S1. The map cracking in the wheelpath between joints is rated from medium to high severity, and in the centerline area it is rated from low to medium severity.

JOINT DISTRESS

The joint ratings categorized the length of crack or joint at each severity level. This provided more information than the overall rating, based on the 10 percent rule defined in the LTPP rating system. Using the 10 percent rule rating method it is sometimes difficult to describe the actual visual difference between two sections. In the LTPP rating system, as long as a joint has at least 10 percent high-severity spalling, it is labeled high. The joint distress ratings for this project and test site were further defined using the following rating scale.

- Low—cracks are 3.175 millimeters (mm) wide or less, no adjacent parallel cracks, and no interconnection of parallel and perpendicular cracks.
- Medium—cracks are >3.175 mm and <6.35 mm wide, or adjacent parallel cracks with interconnection of parallel and perpendicular cracks, with no loss of material.
- High—cracks are >6.35 mm wide, or adjacent parallel cracks with interconnection of parallel and perpendicular cracks, with loss of material.

Figure 3 shows an example of joint distress of high severity, and figure 4 shows an example of joint distress of medium severity.



Figure 3. Joint distress of high severity (Winnemucca, NV).



Figure 4. Joint distress of medium severity (Winnemucca, NV).

Figures 5 through 9 show the amount and severity of joint distress for each section over the 4 years of the study. The figures are based on the 10 percent rule defined in the LTPP rating system. The amount and severity of joint distress has increased considerably during the study period. In 1994, all the joint distress was rated low except for small areas in sections SA1, C3, LO1, and M2 where the rating was medium. At that time, there were a large number of joints that had lengths without cracking or spalling. The deterioration increased to a point in 1998 where almost the entire length of all transverse joints in each test section is distressed. The only section with any joint length rated low was section S2 (figure 9). The joints in several sections (C2, L1, C3, and S1) are rated high using the 10 percent rule.

Figure 10 shows the actual measured joint length at each level of severity for all the sections in 1998. If the true joint length at each severity is considered, all sections have some areas of low-severity spalling. The length of high-severity joint spalling per section is less than the length of low- and medium-severity spalling. The section with the most high-severity joint distress is S1. The sections with the least amount of high joint distress are SA1 and S2, but these slabs were in better condition at the start of the study. Of the sections in the same group or beginning condition as S1, the section with least amount of high-severity spalling is section C1 (control). The next best is section L1. In the second group of sections, which were initially in better shape, the one with the most high-severity spalling is C3, followed by section LO1.

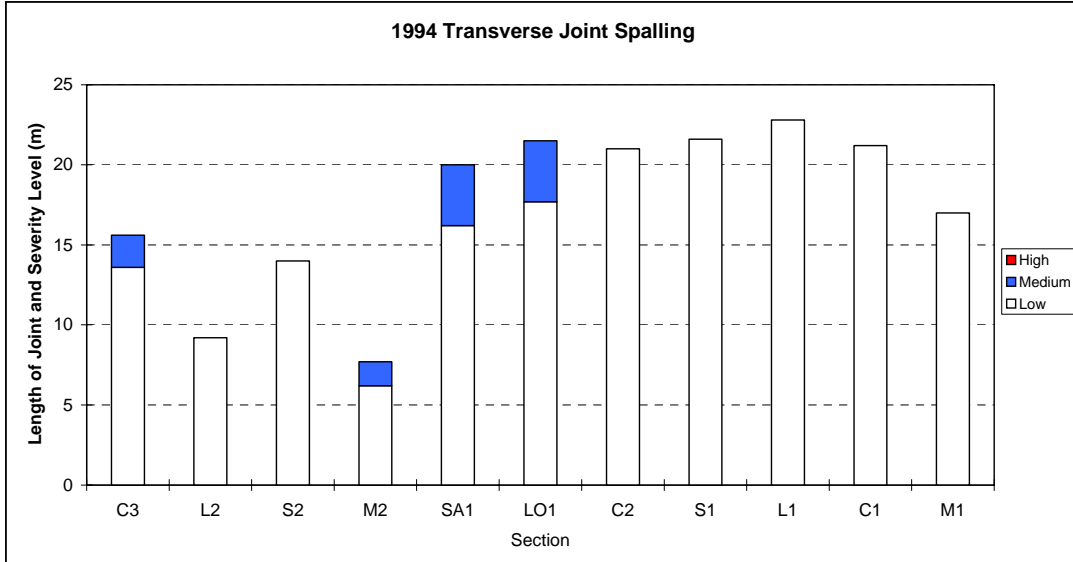


Figure 5. Joint distress for all sections of Winnemucca test site (1994).

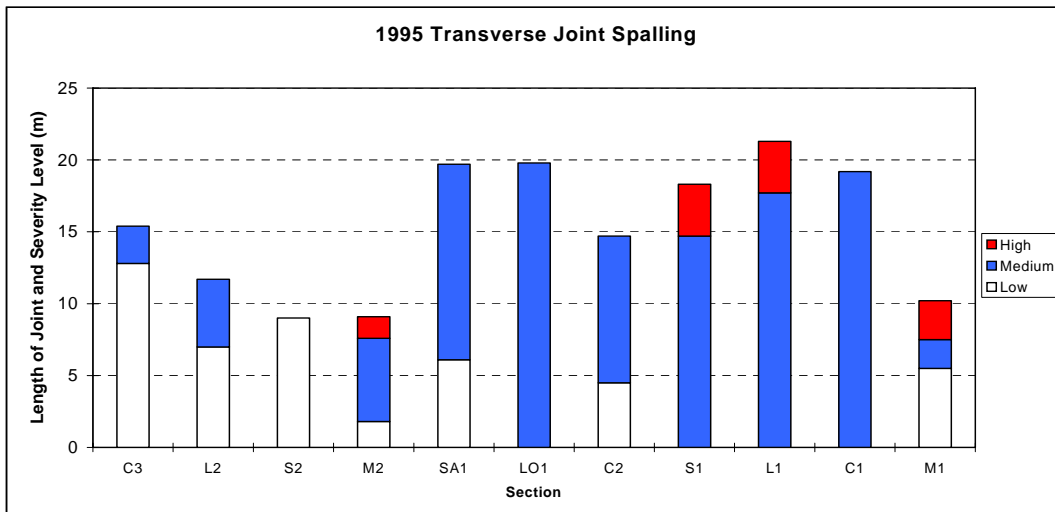


Figure 6. Joint distress for all sections of Winnemucca test site (1995).

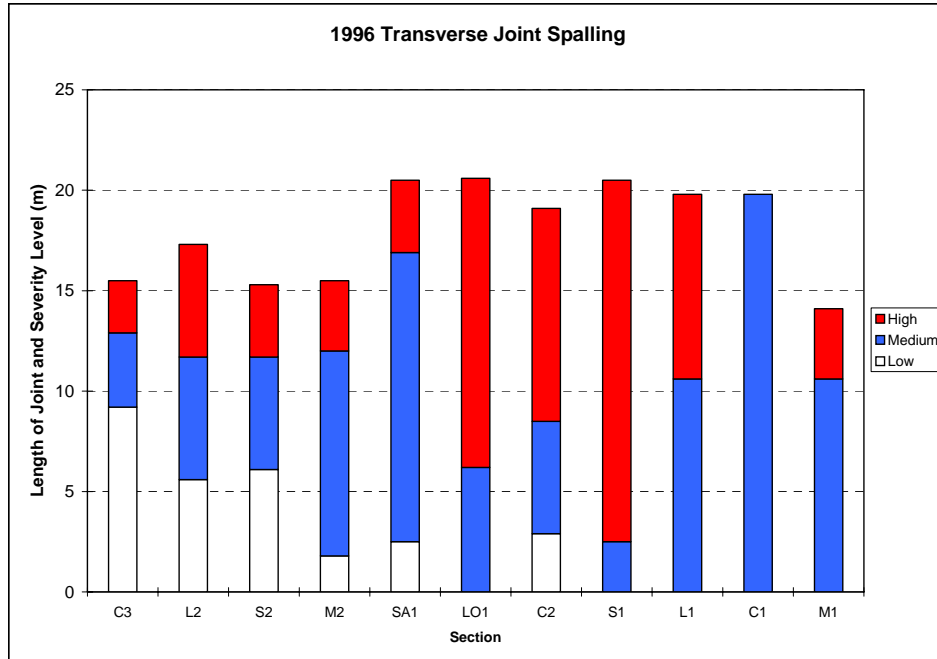


Figure 7. Joint distress for all sections of Winnemucca test site (1996).

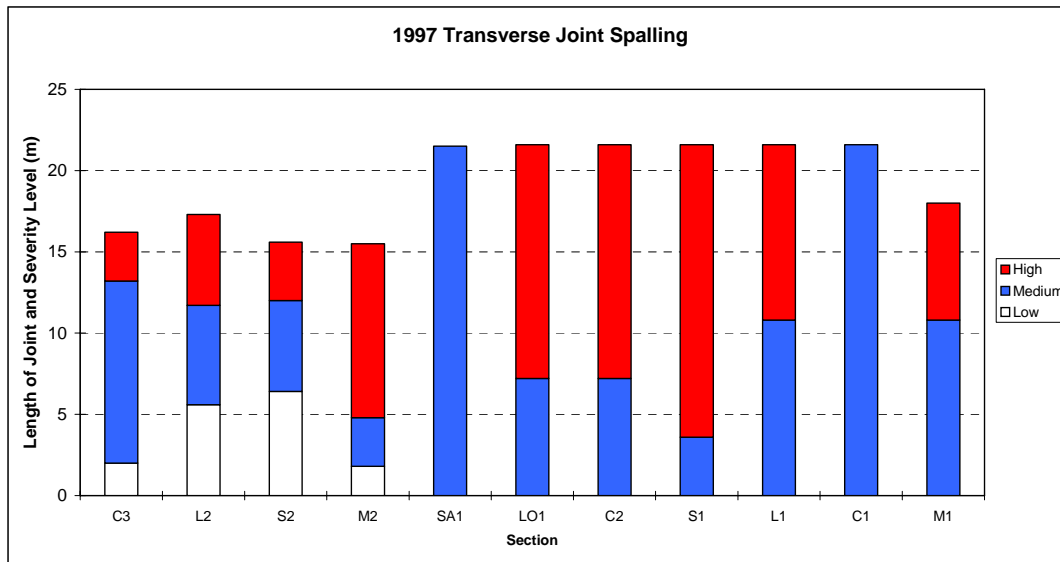


Figure 8. Joint distress for all sections of Winnemucca test site (1997).

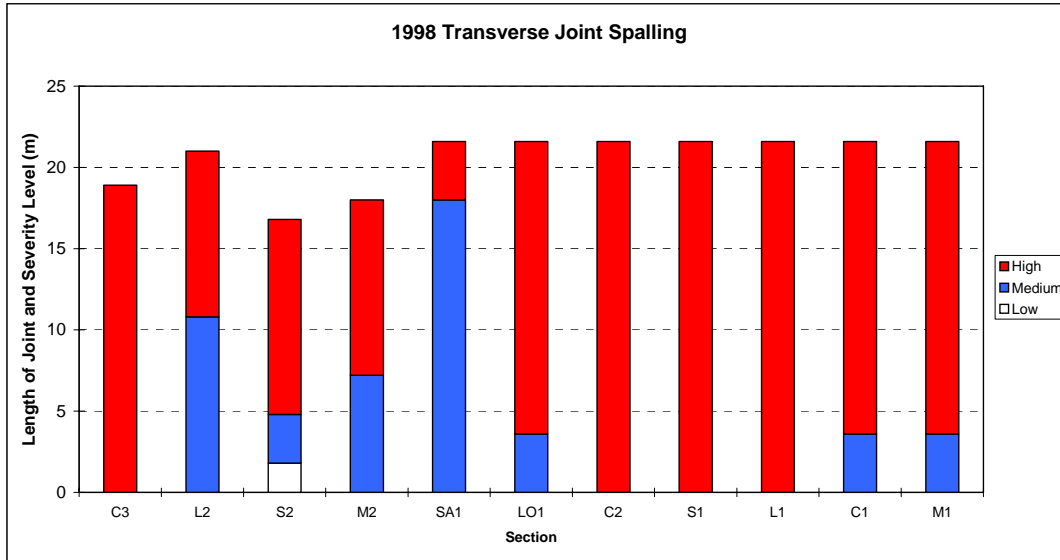


Figure 9. Joint distress for all sections of Winnemucca test site (1998).

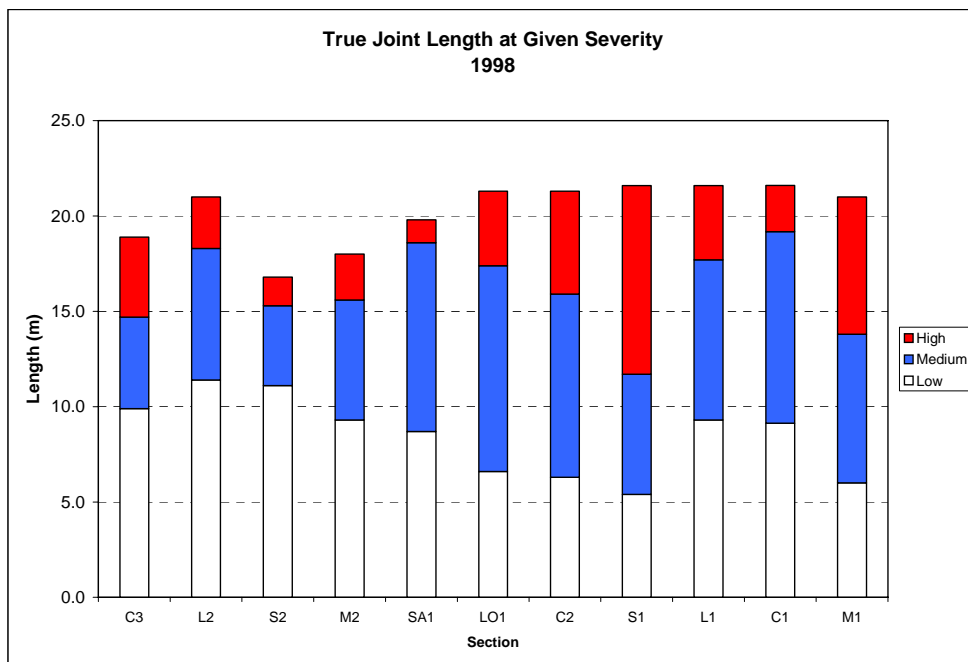


Figure 10. Actual joint length of each severity level for each section (Winnemucca, NV, 1998).

SEVERE MAP CRACKING AT JOINTS

Almost the entire test site was covered with map cracking when the study began in 1994. The cracking is more visible in the wheelpaths and shoulder areas (figure 11), but it does cover the entire pavement surface. Many of the cracks have efflorescence, as shown in figure 12. Because the entire test site is covered with fine map cracking, it is meaningless to compare sections on the basis of map cracking according to LTPP criteria. Therefore, only areas of severe map cracking

will be discussed and used to compare the sections. The severely map cracked areas typically appeared in the wheelpaths, especially at the joints. These areas represent locations where spalling or loss of concrete pieces has occurred or is likely to occur in the near future. Sometimes loss of base support and depressions occur. The number and area of interconnected “pockets” of severe cracking were noted during the visual survey and were recorded in category 8a in the SHRP LTPP recording sheets.

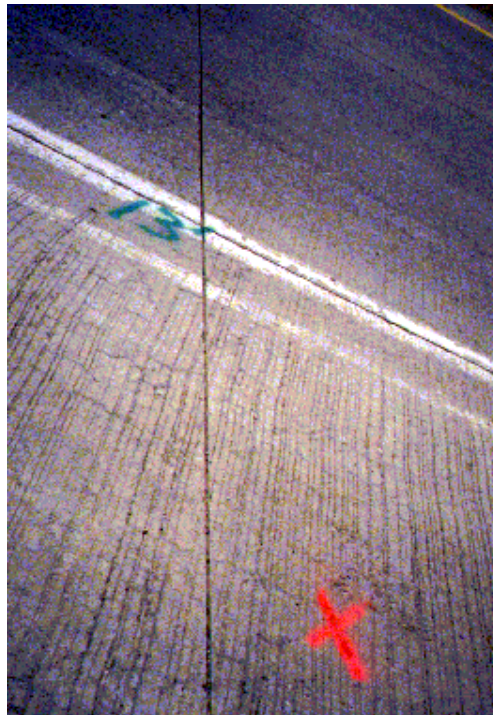


Figure 11. Photograph showing widespread map cracking in shoulder area of Winnemucca test site.

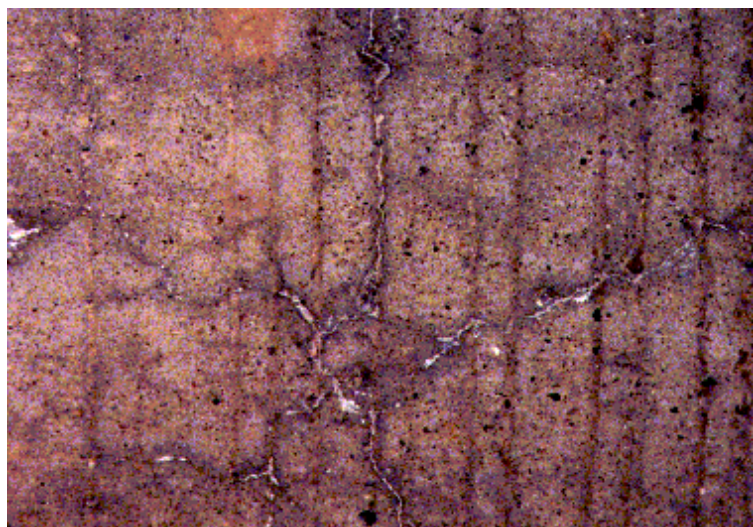


Figure 12. Close-up of map cracking with efflorescence (Winnemucca, NV).

The number of areas of severe map cracking in each section has increased each year over the 4 years. However, sections C2, LO1, and M2 have remained nearly constant for the last 2 years. Figure 13 shows the number of areas of severe map cracking in each section for the years 1995 through 1998. The sections with the most severe map cracking in 1998 are sections M1 and S1 with 16 and 18 areas, respectively. The sections with the least number of areas are sections L2 with eight areas and M2 and S2 with nine areas.

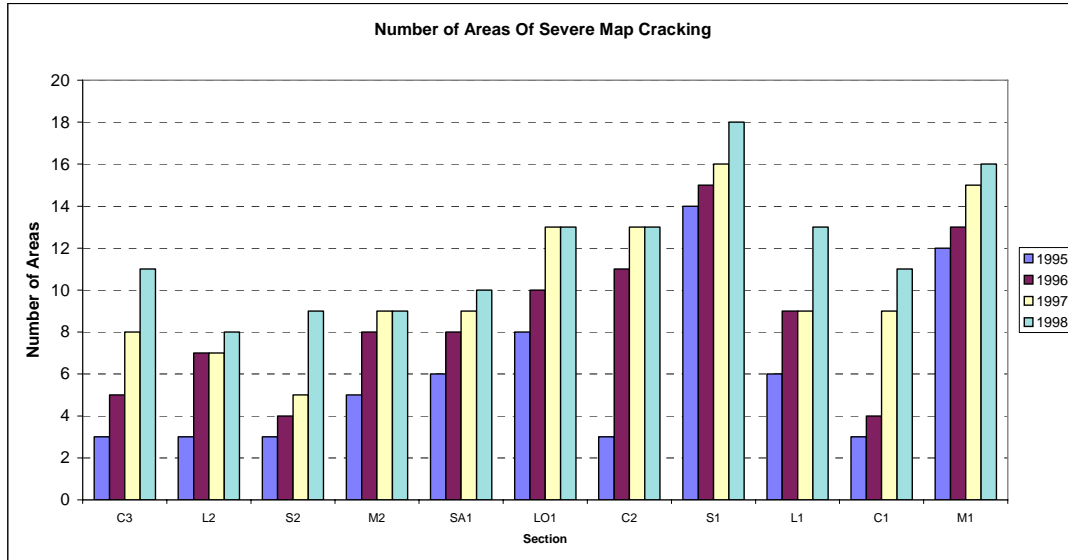


Figure 13. Number of areas of severe map cracking in each section from 1995 through 1998 (Winnemucca, NV).

Figure 14 shows the total area of severe map cracking for each section for the years 1995 and 1998. The most distressed sections are the S1 and M1 sections, which have approximately 16 and 15 square meters (m²) of severe cracking, respectively. These sections also had the most distress at the start of the study. They are followed by section LO1 with approximately 11 m² and section C2 with about 9 m². These sections are all at the eastern end of the test site, which had the more severe cracking at the start of the test. sections L1 and C1 have the least area affected of the sections in the eastern end. Of the sections in the western end of the site, section M2, with over 7 m² of severe map cracked area, is the worst. The best performing section in this group is section L2, with 4 m².

Overall, the only treatment that shows minor improvement in severe map cracking over the control sections is the LiOH (sections L1 and L2). In 1998, section L2 had less area affected than control 3 in the western end of the site. Section L1 in the eastern end had less area affected than control 2 and about the same amount as control 1. In general, all the test sections are performing similar to or worse than the control sections.

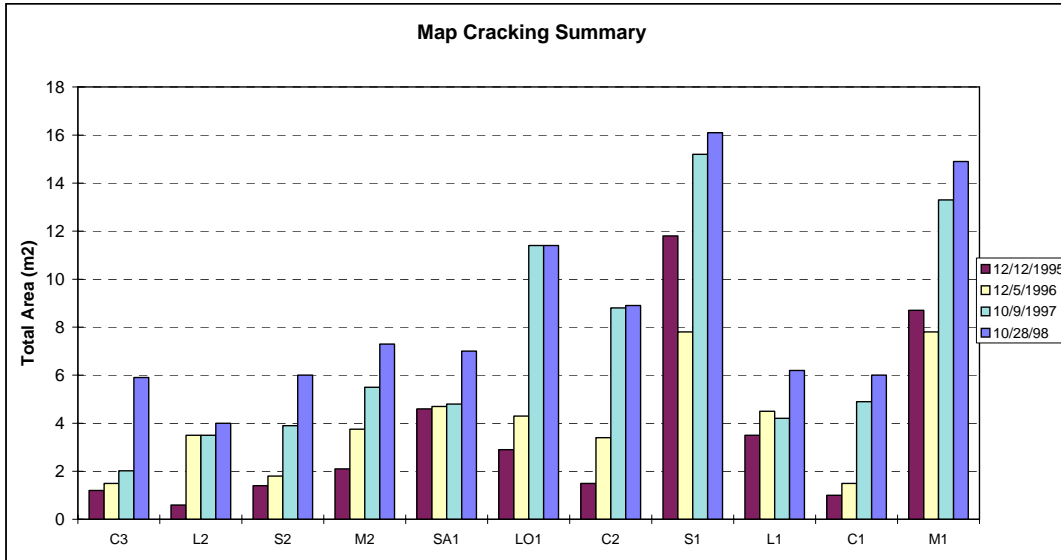


Figure 14. Total area of severe map cracking for each section for 1995 through 1998 (Winnemucca, NV).

WHEELPATH AND CENTERLINE RATING

The severity of the wheelpath and centerline map cracking at the center of the slabs, away from the transverse joints, was rated as low, medium, or high, as follows:

- Low—cracking is primarily longitudinal with little or no interconnection of longitudinal cracks and very few transverse interconnected cracks.
- Medium—cracking is both longitudinal and transverse with interconnection of cracks, easily defined longitudinal cracks exist and are included in the category “3” damage ratings of the SHRP LTPP ratings.
- High—heavy transverse and longitudinal cracking occurs with interconnections, pockets of heavy damage exist with small pieces, and some pieces may be spalled.

The wheelpath and centerline ratings for all sections for 1995 and 1998 are given in table 2. In general, the map cracking areas have increased in severity from 1995 to 1998. In 1995, no sections of wheelpath or centerline areas were rated high severity. The wheelpath areas were approximately 50 percent low and 50 percent medium severity in 1995, but in 1998 they were mostly of medium severity with some low- and occasional high-severity ratings.

**Table 2. Wheelpath and centerline ratings for 1995 and 1998;
number of slabs with each rating (Winnemucca, NV).**

Section		C3	L2	S2	M2	SA1	LO1	C2	S1	L1	C1	M1
1995	WP L	2	3	3	4	3	1	2	0	0	0	5
	M	3	2	2	1	2	4	3	5	5	5	0
	H	0	0	0	0	0	0	0	0	0	0	0
1998	WP L	0	1	1	1	0	0	0	0	0	0	0
	M	4	4	2	4	5	5	3	3	5	4	3
	H	1	0	2	0	0	0	2	2	0	1	2
1995	CL L	4	5	5	5	3	3	5	3	4	4	5
	M	1	0	0	0	2	2	0	2	1	1	0
	H	0	0	0	0	0	0	0	0	0	0	0
1998	CL L	1	3	0	5	0	1	0	0	2	1	4
	M	4	2	5	0	5	4	5	5	3	4	1
	H	0	0	0	0	0	0	0	0	0	0	0

In 1995, the centerline areas were mostly of low severity with some medium-severity areas, but in 1998, the centerlines are mostly of medium severity with some low-severity areas. In 1998, there were no areas of high-severity cracking in the centerline areas.

In 1998, sections M1, C2, and S1 had the highest levels of distress in the wheelpaths with three panels rated medium severity and two panels rated high severity. Section M2 and L2 had the lowest wheelpath distress in 1998 with one panel rated low severity and four panels rated medium severity. Sections L2, LO1, and L1 had moderately low relative distress. Sections S2, SA1, C2, and S1 all had the highest level of centerline distress in 1998 with all five panels rated medium severity. Section M2 had the lowest distress in the centerline area with all five panels rated low severity.

TRANSVERSE CRACKING

All of the test sections have several transverse cracks, such as that shown in figure 15. Some extend full width while others only reach partway across the lane. Some other transverse cracks, such as the one in figure 16, intersect with longitudinal cracks. A comparison of the transverse cracking for each year is shown in figures 17 through 21. Table 3 indicates the number of transverse cracks in each section for all years of the study. A transverse crack consists of a single distinct crack or a single crack with only a few branches. The number of transverse cracks in a section can decrease if the crack becomes part of an area of severe map cracking.

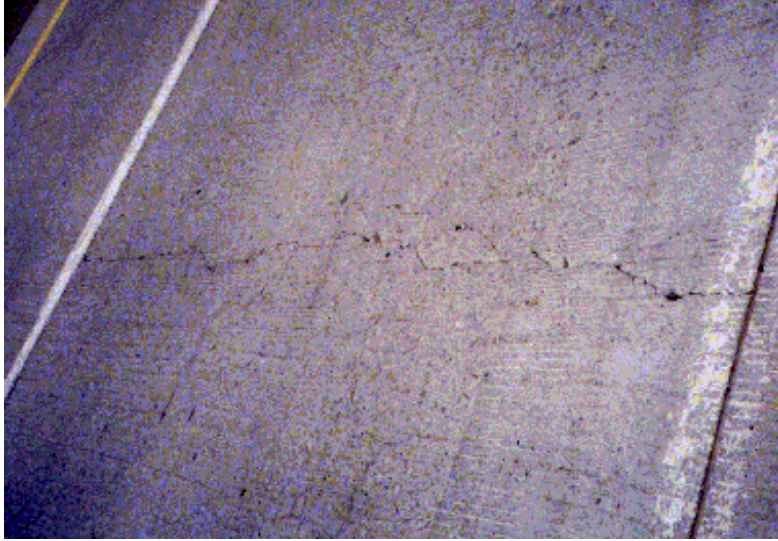


Figure 15. Full-width transverse cracking in test section (Winnemucca, NV).

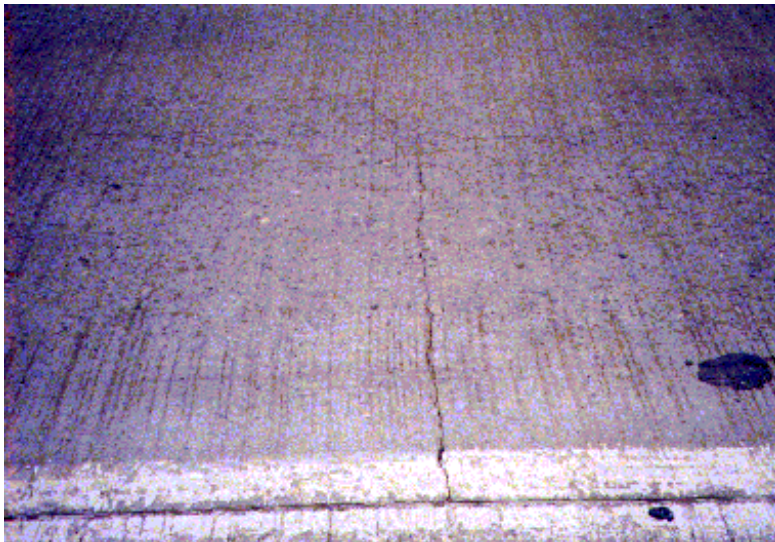


Figure 16. Transverse cracking with intersecting longitudinal crack (Winnemucca, NV).

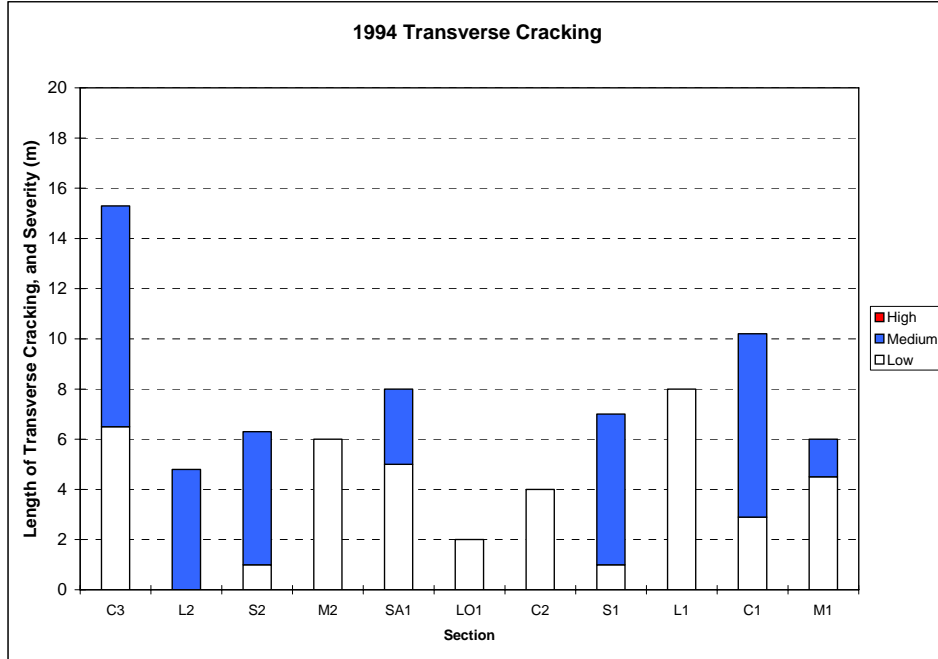


Figure 17. Amount and severity of transverse cracking for all sections (Winnemucca, NV, 1994).

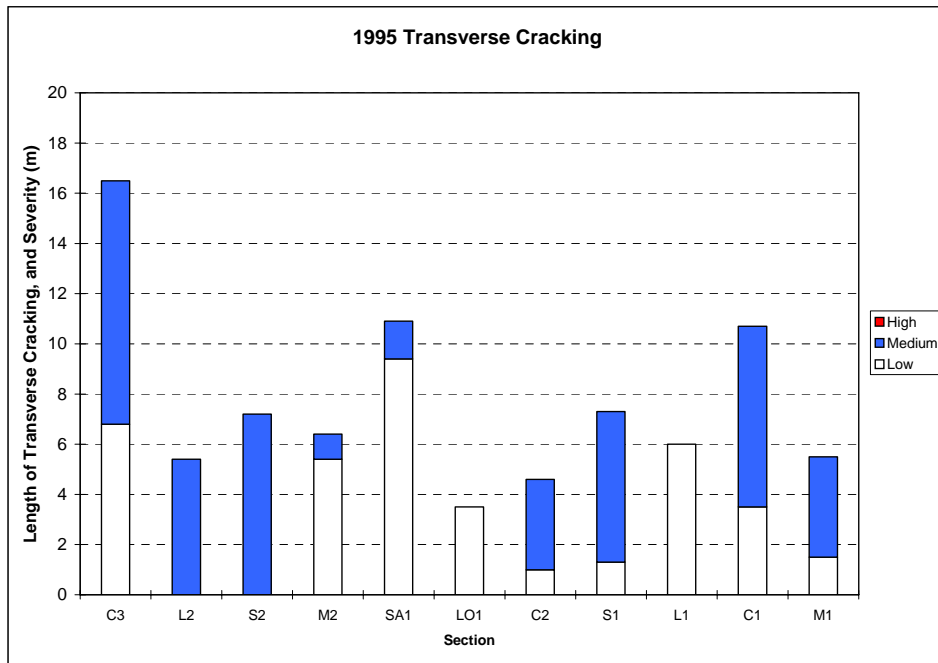


Figure 18. Amount and severity of transverse cracking for all sections (Winnemucca, NV, 1995).

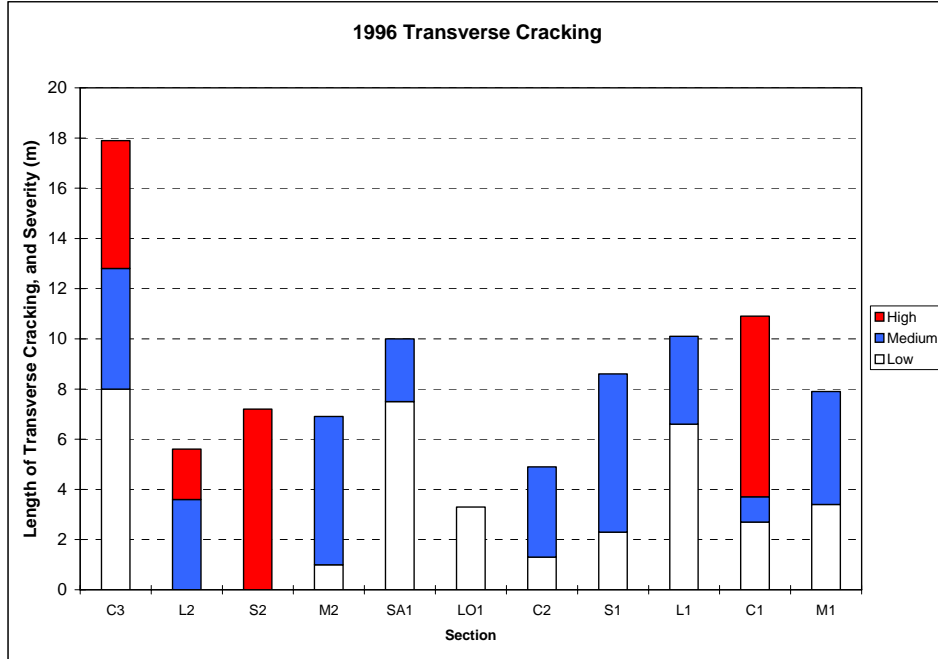


Figure 19. Amount and severity of transverse cracking for all sections (Winnemucca, NV, 1996).

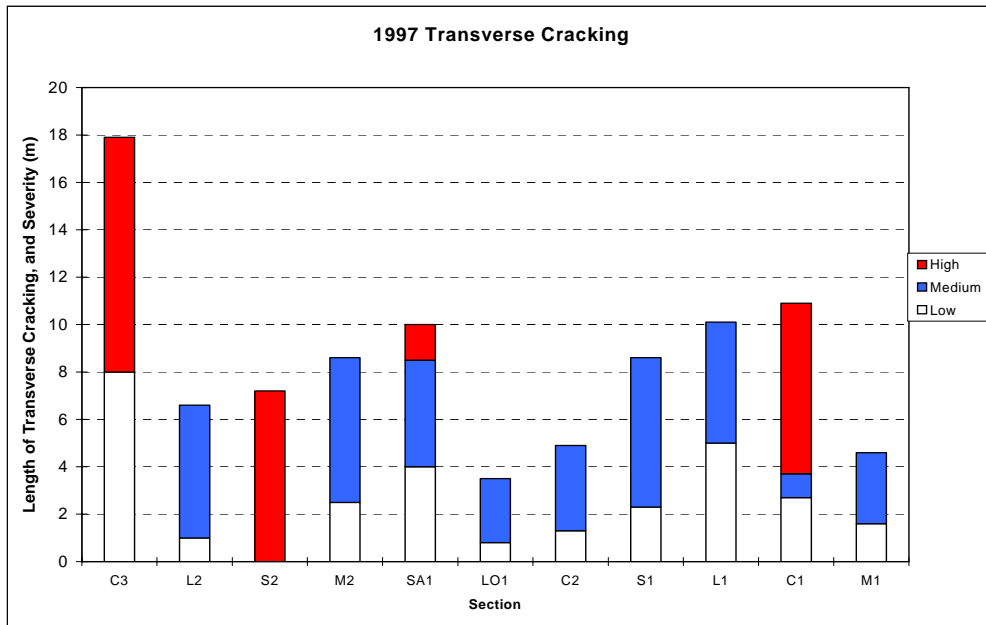


Figure 20. Amount and severity of transverse cracking for all sections (Winnemucca, NV, 1997).

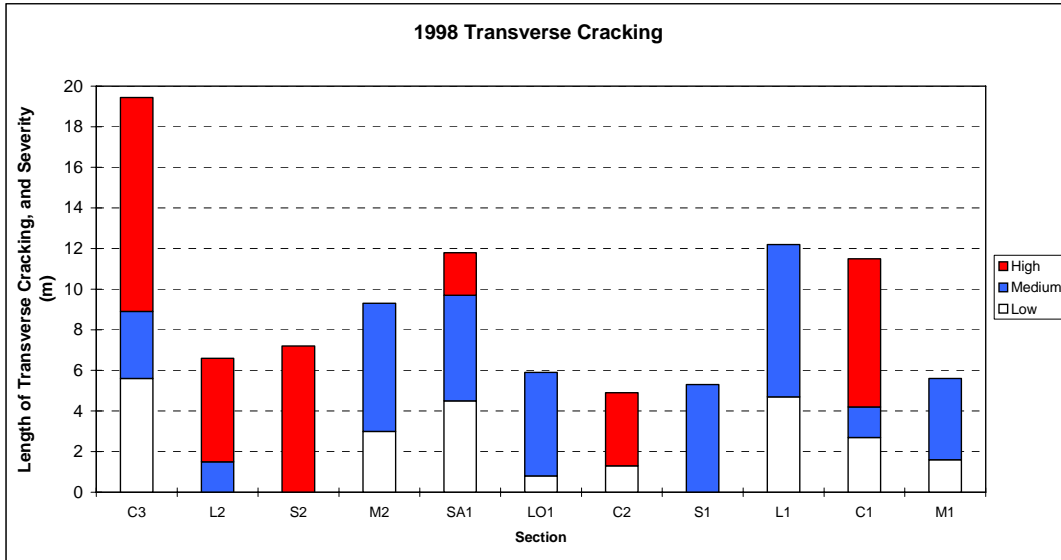


Figure 21. Amount and severity of transverse cracking for all sections (Winnemucca, NV, 1998).

Table 3. Number of transverse cracks per section.

Section ID	Year				
	1994	1995	1996	1997	1998
C3	11	10	11	11	11
L2	3	2	2	3	3
S2	3	2	2	2	2
M2	5	4	4	5	5
SA1	8	8	8	8	8
LO-1	2	3	3	3	3
C2	3	2	2	2	2
S1	7	7	8	8	4
L1	7	7	7	7	8
C1	7	6	6	6	6
M1	4	4	4	4	5

Section C3 (control) has the most cracks at 11, and the greatest length of high-severity cracking. However, the section with the lowest total number and length of transverse cracking is section C2 (control). Section S2 also has the fewest number of cracks, but all cracks are high severity. The section with the lowest overall severity of transverse cracking is section M1. Transverse cracking does not appear to be a good indicator of relative performance of these ASR test sections.

MODULUS AND STRENGTH TESTING

Core samples were removed from each test section and tested for modulus of elasticity in both dry and wet conditions. In the field, after some cores came out in several pieces, an additional core had to be taken. The dry-tested and wet-tested moduli of elasticity for the test sections over

the 4-year test duration are shown in tables 4 and 5. The cores taken in 1994 were only tested in the dry condition. A summary of the average data is shown in table 6.

There is no obvious trend from 1994 to 1998. The measured modulus fluctuated up and down over the test period. There is, however, a trend when the test sections from different groups are studied. For all sections in 1998, the average dry modulus of elasticity is 13.92×10^6 kilopascals (kPa) (2.02×10^6 pounds per square inch (psi)).

The average for the group of test sections at the eastern end that were originally in worse condition (C1, C2, L1, M1, and S1) is 11.78×10^6 kPa (1.71×10^6 psi) while the sections on the western end (C3, L2, M2, and S2) have an average modulus of 15.71×10^6 kPa (2.28×10^6 psi). For the wet-tested modulus, shown in tables 5 and 6, the trend is the same. The east group of sections has an average modulus of elasticity of 10.82×10^6 kPa (1.57×10^6 psi) compared to 14.33×10^6 kPa (2.08×10^6 psi) for the west group.

The same trend is also found in the compressive strength results listed in table 7. All compressive strength tests were conducted on dry cores. No compressive strength tests were conducted on cores from 1994 or 1995 since compressive strength was not in the original scope of work. In 1998, the average strength of the sections in the east group is 32,564 kPa (4,723 psi) compared to 37,101 kPa (5,381 psi) for the sections in the west group. In general, it appears the concrete in the western end of the site was in better condition at the beginning of the study and suffered a lesser amount of distress during the study. There is no trend to indicate which surface treatment is performing better than the others.

**Table 4. Modulus of elasticity testing results for Winnemucca, NV
(dry tested, $\times 10^6$ psi).**

Section ID	Year				
	1994	1995	1996	1997	1998
C3	2.28	2.77	2.73	2.60	1.97
L2	3.41	2.31	3.49	4.06	2.74
S2	1.74	1.84	3.25	2.34	1.88
M2	2.04	1.59	1.96	2.02	2.35
SA1	1.67	2.69	1.75	2.34	2.28
LO1	2.31	1.46	1.19	2.49	2.47
C2	–	1.46	1.99	2.83	1.20
S1	1.67	1.11	1.93	1.49	1.97
L1	2.17	1.62	–	1.72	1.53
C1	2.71	2.06	–	1.72	2.45
M1	0.97	1.71	–	1.19	1.40
Average	2.10	1.87	2.29	2.25	2.02

1 psi = 6.89 kPa

**Table 5. Modulus of elasticity testing results for Winnemucca, NV
(wet tested, x 10⁶ psi).**

Section ID	Year				
	1994	1995	1996	1997	1998
C3	–	3.08	2.23	2.39	2.20
L2	–	2.59	3.51	3.90	2.51
S2	–	1.96	3.00	2.72	1.84
M2	–	1.70	1.72	1.64	2.08
SA1	–	2.86	1.84	2.22	2.12
LO1		1.52	1.28	2.37	1.70
C2	–	1.56	1.82	3.60	1.64
S1	–	1.04	1.93	1.23	1.03
L1	–	1.62	–	1.80	1.04
C1	–	2.12	–	1.25	2.46
M1	–	1.81	–	1.24	1.66
Average	–	1.99	2.17	2.21	1.84

1 psi = 6.89 kPa

Table 6. Summary of average modulus data for Winnemucca, NV.

Average	Year				
	1994	1995	1996	1997	1998
E-dry	2.09	1.87	2.29	2.25	2.02
E-dry east	1.88	1.59	1.96	1.79	1.71
E-dry west	2.24	2.11	2.40	2.64	2.28
E-wet	–	1.99	2.17	2.21	1.84
E-wet east	–	1.63	1.88	1.82	1.57
E-wet west	–	2.29	2.26	2.54	2.08

1 psi = 6.89 kPa

**Table 7. Compressive strength testing results
for Winnemucca, NV.**

Section	Year		
	1996	1997	1998
C3	6951	4968	4831
L2	6230	5028	5811
S2	6210	5511	4837
M2	5968	5132	5875
SA1	6785	5244	5633
LO1	5444	5573	5297
C2	5395	5141	4305
S1	6401	4250	4279
L1	–	4494	4749
C1	–	5113	5107
M1	4510	4920	5175
Average	6173	5034	5082

1 psi = 6.89 kPa

RELATIVE HUMIDITY MEASUREMENTS

Powdered samples of the concrete pavement were taken from various locations in 1995, 1997, and 1998. The samples were taken at four different depths, as shown in tables 8, 9, and 10. A rotary hammer drill with a 2.858-cm (1.125-inch) diameter drill bit was used to drill the concrete. The powder samples were sealed in glass containers. The humidity within the containers was measured using a resistance humidity probe.

**Table 8. Relative humidity measurements for
Winnemucca, NV (December 1995).**

Section	Depth (inches)			
	0.5–1	2–2.5	4–4.5	6–6.5
C3	47	76	86	91
L2	38	60	83	89
S2	52	86	89	98
M2	40	68	89	91
SA1	44	73	92	86
LO1	38	61	85	81
C2	96	98	90	100
S1	44	96	99	97
L1	56	74	88	95
C1	40	58	86	91
M1	59	80	69	93

1 inch = 2.54 cm

Table 9. Relative humidity measurements for Winnemucca, NV (October 1997).

Section	Depth (inches)			
	0.5–1	2–2.5	4–4.5	6–6.5
C3	78	95	96	97
L2	87	94	99	99
S2	39	62	96	97
M2	88	97	92	99
SA1	71	88	96	93
LO1	100	100	100	100

1 inch = 2.54 cm

Table 10. Relative humidity measurements for Winnemucca, NV (October 1998).

Section	Depth (inches)			
	0.5–1	2–2.5	4–4.5	6–6.5
C3	100	100	100	100
L2	100	100	100	100
S2	100	100	100	100
M2	100	100	100	100
SA1	100	100	100	100
LO1	100	100	100	100

1 inch = 2.54 cm

Intermittent heavy rain occurred during the 1998 inspection. Light rain occurred after sampling in 1995. For all samples taken deeper than 10.2 cm (4.016 inch) below the surface, the relative humidity is typically more than 80 percent. This would indicate that even though the test site is in a dry climate, there is enough moisture migrating up from the soil underneath the pavement to sustain the ASR.

PETROGRAPHIC STUDIES

Petrographic examinations were made of at least one core from each test section at selected years. The core was cut into the largest possible rectangular prism, and two faces of the prism were lapped. Parallel sections were marked on each lapped face to delineate each traverse and ensure that the entire lapped surface was examined. Evidence of an ASR in the form of gel, cracks characteristic of ASR, and reacted particles were then counted. Cracks were counted more than once if they were encountered in more than one traverse.

The relative number of reacted coarse and fine aggregate particles should be regarded as approximate, since alkali-silica gel is highly mobile and may have migrated away from the originating particle. For example, gel may be present on the surface of a potentially reactive coarse aggregate particle that shows no other signs of distress. This particle would be counted as a reacted coarse aggregate particle although it is entirely possible the gel originated from an adjacent fine aggregate particle.

The petrographic reports are in appendix A. Table 11 gives a summary of the findings for the years 1996, 1997, and 1998. Generally, there is a significant increase in the number of cracks, particles that have reacted, and gel locations for all treatment sections in 1997 and 1998. Table 12 shows a summary and ranking of each section relative to the average number of cracks, reacted particles, and gel spots for 1997 and 1998.

Table 11. Summary of petrographic examinations for cores from Winnemucca, NV.

Core ID	Year	Cracks		Reacted particles		Gel
		Micro	Large	Fine	Coarse	Locations
C1	1996	–	–	–	0	–
	1997	61	0	22	8	54
	1998	40	0	115	17	129
C2	1996	54	0	11	0	10
	1997	34	0	42	9	58
	1998	139	3	129	35	104
C3	1996	38	0	20	0	23
	1997	11	0	27	3	50
	1998	72	1	134	16	84
M1	1996	–	–	–	–	–
	1997	185	0	42	13	81
	1998	196	7	102	47	105
M2	1996	22	0	8	0	22
	1997	48	0	27	5	75
	1998	75	0	65	35	73
SA1	1996	7	0	1	0	10
	1997	77	0	64	10	41
	1998	114	1	156	43	78
S1	1996	70	0	12	0	31
	1997	97	0	23	13	85
	1998	113	2	173	58	90
S2	1996	15	0	7	0	8
	1997	29	0	53	14	40
	1998	153	3	102	45	116
L1	1996	45	0	4	0	11
	1997	65	0	21	1	39
	1998	121	1	81	31	69
L2	1996	1	0	4	0	20
	1997	20	0	22	0	32
	1998	23	0	126	16	88
LO-1	1996	19	0	7	0	40
	1997	73	0	32	5	62
	1998	46	0	69	27	84

**Table 12. Summary of petrographic results (average 1997-1998)
for cores from Winnemucca, NV.**

Section	Cracks	Reacted Particles	Gel	Total
C3	84	180	134	398
L2	43	164	120	327
S2	185	214	156	555
M2	123	132	148	403
SA1	192	273	119	584
LO-1	119	133	146	398
C2	176	215	162	553
S1	212	267	175	654
L1	187	134	108	429
C1	101	162	183	446
M1	388	204	186	778

SUMMARY FOR WINNEMUCCA, NV TEST SITE

Table 13 summarizes selected data for the Winnemucca, NV test site. Overall, little difference was seen in the performance of the test sections. None of the treatments stopped the progression of ASR distress. The humidity in the pavement was sufficient to allow continued ASR in each section. Review of all data indicates that sections L2 and M2 may have improved the durability slightly over the controls. None of treatments (LO1, S1, L1, M1) applied to the eastern pavement section, which started in the worst condition, improved performance. This indicates that the timing of the treatment may be important and treatment should be performed before the pavement is seriously distressed.

Table 13. Summary of Winnemucca, NV test sections.

Section ID	Percent Joint Distress 1998		Severe Map Cracking (m ²) 1998	Wheelpath Ratings 1998-High	Centerline Ratings 1998-Med.	Average Modulus (10 ⁻⁶ psi) 1997-1998		Average Compressive Strength (psi) 1997-1998	Average Relative Humidity (%) 1995-1997		Total Petrographic Defects 1997-1998
	Medium	High				Dry	Wet		Dry	0.75 in.	
C3	24	23	6	1	4	2.29	2.30	4900	75	90	398
L2	32	13	4	0	2	3.40	3.21	5420	75	85	327
S2	24	10	6	2	5	2.11	2.28	5174	64	83	555
M2	34	14	7	0	0	2.19	1.86	5504	76	88	403
SA1	49	7	7	0	5	2.31	2.17	5439	72	87	584
LO1	49	19	11	0	4	2.48	2.04	5435	79	87	398
C2	44	26	9	2	5	2.02	2.62	4723	96	98	553
S1	28	46	16	2	5	1.73	1.13	4265	44	96	654
L1	37	18	6	0	3	1.63	1.42	4622	56	74	429
C1	46	11	6	1	4	2.09	1.86	5110	40	58	446
M1	36	35	15	2	1	1.30	1.45	5048	59	80	778

1 psi = 6.89 kPa

1 m = 3.281 ft

CHAPTER 3. SUMMARY OF RESULTS FROM NEWARK, DE

The test section consists of nine 12.2-m-long slabs on the northbound shoulder of Route 72 in Newark, DE. There are five control sections with no treatment and four test sections that had lithium hydroxide applied as a surface treatment to mitigate ASR damage. The test site starts with the second full slab past the entrance to the University of Delaware Agricultural Experimentation Station. The sections are ordered as follows: control 1, test 1, test 2, control 2, control 3, control 4, test 3, test 4, control 5. The test location includes a gradual right-hand turn and sag vertical curve, with section control 3 containing drains at the low point. Sections control 1, test 1, test 2, control 2, and control 3 are sloped more steeply downward toward the drains than the other sections. Because of the grade changes and the location of the test area, sections control 1, 2, and 3 and test sections 1 and 2 could be expected to carry significantly more water during storms than test sections 3 and 4 and control sections 4 and 5. An overall view of the section is shown in figure 22.



(a) (site looking north)



(b) (site looking south)

Figure 22. North and south views of the Newark, DE site.

For the Newark test site, visual surveys for map cracking and joint spalling, relative humidity sampling, and drilling of cores for modulus and strength were performed for each of the 5 years of study. FWD tests were performed, and the results are presented in a section near the end of this report. Table 14 lists when the site inspections were performed and the weather conditions.

Table 14. Inspection dates and conditions.

Inspection Date	Weather
November 29, 1994	Cool, sunny
November 28, 1995	Cloudy, 50–60 °F
November 21, 1996	Cold, overcast, 35–45 °F
December 9, 1997	Cold, Sunny
October 22, 1998	Cool, breezy, sunny, 40–45 °F, pavement wet

$$^{\circ}\text{C} = (^{\circ}\text{F}-32)/1.8$$

Since the FHWA LTPP structurally oriented rating system did not adequately describe the pavement condition, the LTPP sheets were filled out using the following conventions:

1. The longitudinal cracking was recorded as a map-cracked area. This was necessary because no length could be assigned to the extensive cracking. Only one area exhibited some minor interconnection with transverse cracks, so all areas were considered to be affected at equal severity.
2. Transverse joints separating test sections were graded as part of the next section, that is, the northernmost section.
3. The transverse joint damage was listed as the length of joint intersected by the longitudinal cracking. Ratings were as given in the LTPP handbook.

The cracking was principally longitudinal with only minor transverse cracks that sometimes interconnected the longitudinal cracks. The cracking appears to be related to ASR damage, but it has not manifested itself in the typical pattern or map cracking. The longitudinal cracking pattern may be related to the restraint conditions of the shoulder. Expansion of the shoulder concrete may be easier toward the soil side of the pavement than against more rigid pavement. Lower restraint allows cracking to occur easier in the longitudinal direction. This type of cracking is commonly seen in prestressed beams with ASR, where cracking is seen only parallel to the prestressing strand.

SUMMARY OF PAVEMENT SECTION CONDITION

Extensive longitudinal cracking, with cracks more closely spaced near the longitudinal joint with the adjacent travel lane, was noted in all sections. The longitudinal cracks were usually short with no inter-connecting transverse cracks. Figures 23 and 24 show photographs of typical longitudinal cracking. Figure 24 also shows some of the typical asphalt patching along the longitudinal joint between the shoulder and travel lanes. The only areas within the sections not covered with longitudinal cracking are along the curb side. Table 15 gives a brief description of the condition of each section in 1998. The table follows the position of the test sections from the south to the north.



Figure 23. Typical longitudinal cracking (Newark, DE).

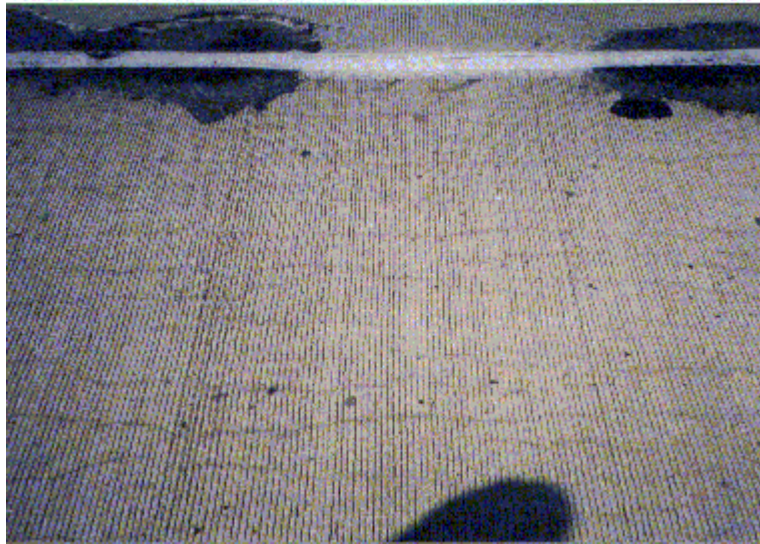


Figure 24. Typical longitudinal cracking and example of asphalt patching along joint between shoulder and travel lane (Newark, DE).

Table 15. Condition of Delaware test pavement sections in 1998.

Section	Description
Control 1	Longitudinal cracking (map cracking) covers the area from 1.22 to 3.36 m from the edge of pavement (EP). Cracks are typically spaced 10.2 cm apart. Cracking extends full width at ends of section. Most of cracks are stained. One full width transverse crack and one spall were observed on the south end of the section. This section has almost as severe cracking as TS2.
Test section 1	Longitudinal cracking (map cracking) covers the area from 1.07 to 3.36 m from EP, with a typical 10.2-cm spacing. Cracking extends the full width of the slabs at the ends of section. More severe map cracking exists at the south end of the section. Cracking is obvious (medium) due to the staining. One 1.22-m-long transverse crack exists at the 3.97-m mark of section. Slightly less severe cracking than TS2.
Test section 2	Longitudinal cracking (map cracking) covers area from 1.22 to 3.36 m from the EP, with 10.2- to 12.7-cm spacing in center area of section and 7.6- to 10.2-cm spacing at the south end. Cracking extends full width at ends of section especially at south end. All cracking is medium with heavy stains. This section has the most severe cracking and staining.
Control 2	Longitudinal cracking (map cracking) covers the area from 1.22 to 3.36 m from the EP, with 10.2-cm spacing at the south end and 15.2- to 25.4-cm spacing in the center area of slab. Staining of cracks is noticeable, especially near the joints. Fine cracking exists over the area 0.92 to 1.83 m from the EP. Cracking and staining are not as severe as TS2, TS1, or C1.
Control 3	Fine longitudinal cracking (map cracking) covers the area from 1.22 to 3.36 m from the EP, with staining along lane edge and ends of the section. Some larger longitudinal cracks are present in center area of the section. One transverse crack is present from the corner of drain to the edge of the lane. Cracking is less frequent than on C4.
Control 4	Short fine cracks are present from 0.61 to 3.36 m from EP, spaced about 8 to 11 inches apart. No cracks were noted within 0.61 m of the curb. Some larger longitudinal cracks (medium) are present. Cracking is slightly less severe than first three control sections.
Test section 3	Fine short cracks are present over the entire area 0.61 to 3.36 m from EP. No cracks are present within 0.61 m of the curb. Cracks extend farther into the section near the south end. This section has the least severe cracking of the test sections.
Test section 4	Very fine cracks (2-inch spacing) cover an area from 0.61 to 3.36 m from the EP. From 2.75 to 3.36 m, cracks are more obvious and have staining but are spaced farther apart. Several larger new cracks are present at approximately 0.92 m from the EP. This section has somewhat more severe cracking than section TS3.
Control 5	Very fine cracks (finer than TS4) extend from 0.61 to 3.36 m from EP, and are typically spaced 7.6 cm apart. Cracks from 0.61 to 0.92 m have staining. Cracking is slightly more severe than section TS4.

It appears the nine sections can be divided into two groups of almost equal severity of cracking. The group with the most severe cracking and staining include control sections 1, 2, and 3 and test sections 1 and 2. These are also the first five sections of the site and carry the most runoff water. The other group includes control section 4 and 5, and test sections 3 and 4.

The area of each slab affected by map cracking has increased over the 4 years of the study. Figure 25 shows a graph of the area affected in each section over the 4 years of the study. Two levels of distress are apparent. One group, which consists of control 1, test section 1, test section 2, and control 3, has approximately the same area affected by map cracking. The area has gradually been increasing over the 5 years. The other group consists of control 2, test section 3, test section 4, control 4, and control 5. The area of these sections affected increased gradually over the first 4 years but at a lower level than the other group. However, the area affected increased sharply in the last year of the study and was at the same level as the other group. This can also be seen in figure 26, which shows the area affected by map cracking as a percentage of the total section area. All sections had more than 60 percent of their area affected by map cracking in 1998. There is no value for control 4 in 1998. Test section 3, test section 4, and control 5 have the most area affected, at over 80 percent, but these areas had the smallest affected areas the year before. All the map cracking was of low severity.

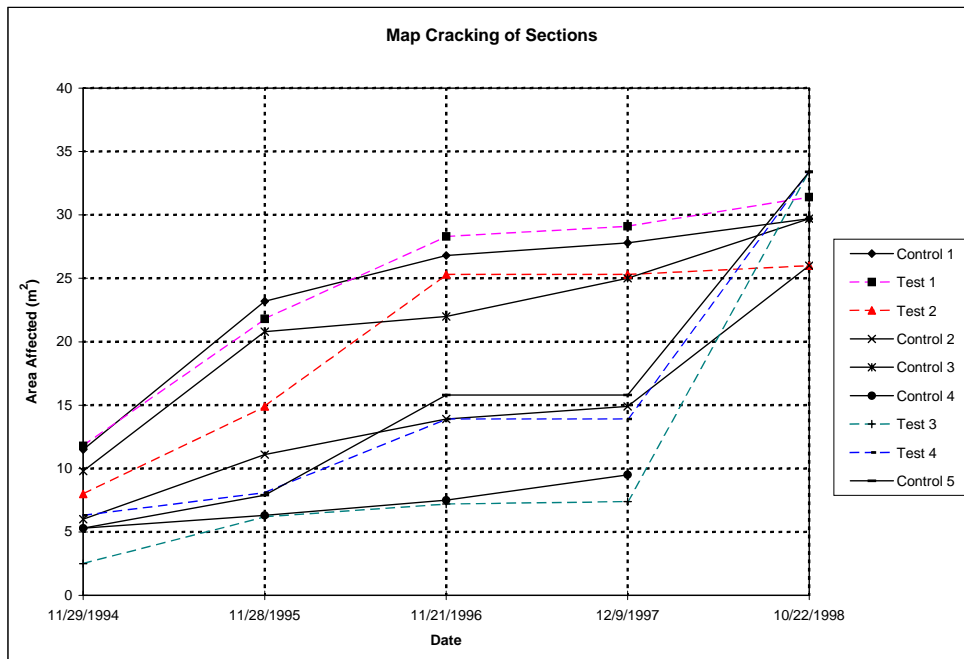


Figure 25. Area of each slab affected by map cracking over the 5 years of the study (Newark, DE).

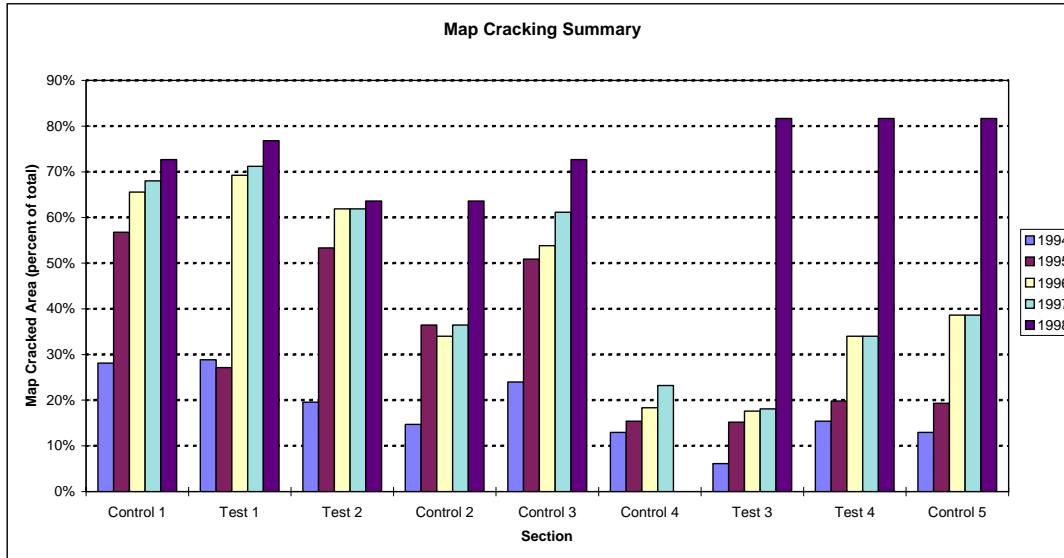


Figure 26. Area of each slab affected by map cracking expressed as a percentage of the total section area (Newark, DE).

JOINT DISTRESS AND TRAVEL LANE OBSERVATIONS

Spalling of transverse joints has increased over the 4 years of the study. A description of the joint observations in the shoulder lane and the travel lane from 1998 is given in appendix B (table B-1). The joints were rated both by SHRP guidelines and by noting how many longitudinal cracks intersected the joint. The travel lane was observed from the shoulder lane because of the difficulty in setting up a lane closure. A marked increase in damage in the travel lane was noted.

Many of the joints had been patched in the wheelpath areas with large asphaltic concrete patches. Figure 27 shows a typical asphalt concrete patch along a transverse joint in the travel lane. Also, extensive patching was noted on the traffic side of the longitudinal joint along test section 2. Figure 28 shows a patch in the center of the travel lane. Visual observations of the joints along the pavement were made of both the travel and passing lanes.



Figure 27. Asphalt concrete patching along transverse joint in travel lane (Newark, DE).



Figure 28. Asphalt patch in center of section in travel lane (Newark, DE).

Figures 29 through 33 show the amount and severity of joint spalling over the 5 years of the study. In 1994, the control 3, control 4, control 5, and test section 2 had joint spalling. At this time the spalling was all low severity. In 1998, all sections except test section 4 have transverse joint spalling. All sections have low-severity spalling except control 4 and control 5, which have spalling of medium severity. Test sections 3 and 4 are performing much better than test sections 1 and 2 with respect to transverse joint spalling. This likely is due to the different exposure conditions previously discussed.

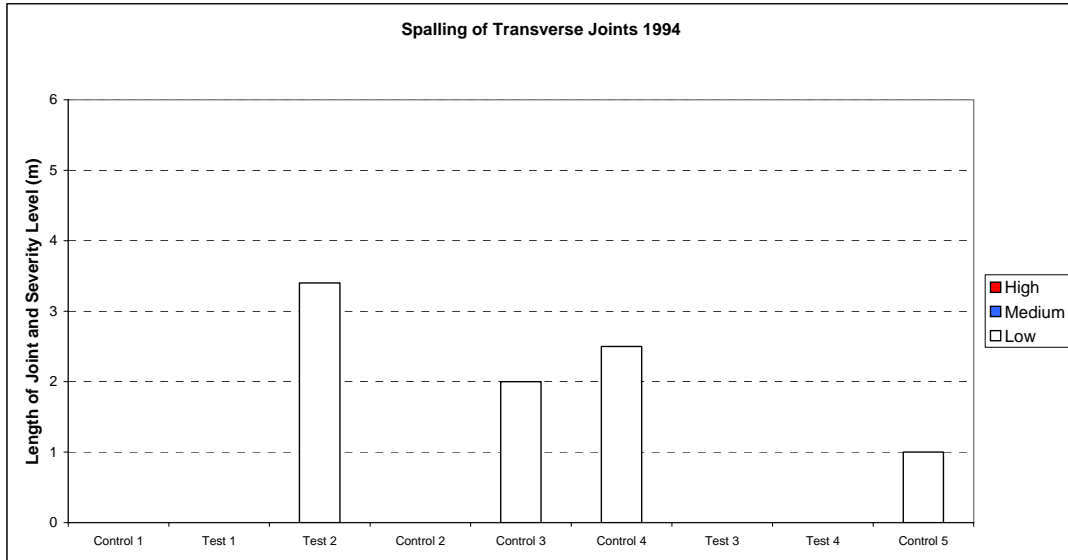


Figure 29. Length and severity of joint distress for all test sections (Newark, DE, 1994).

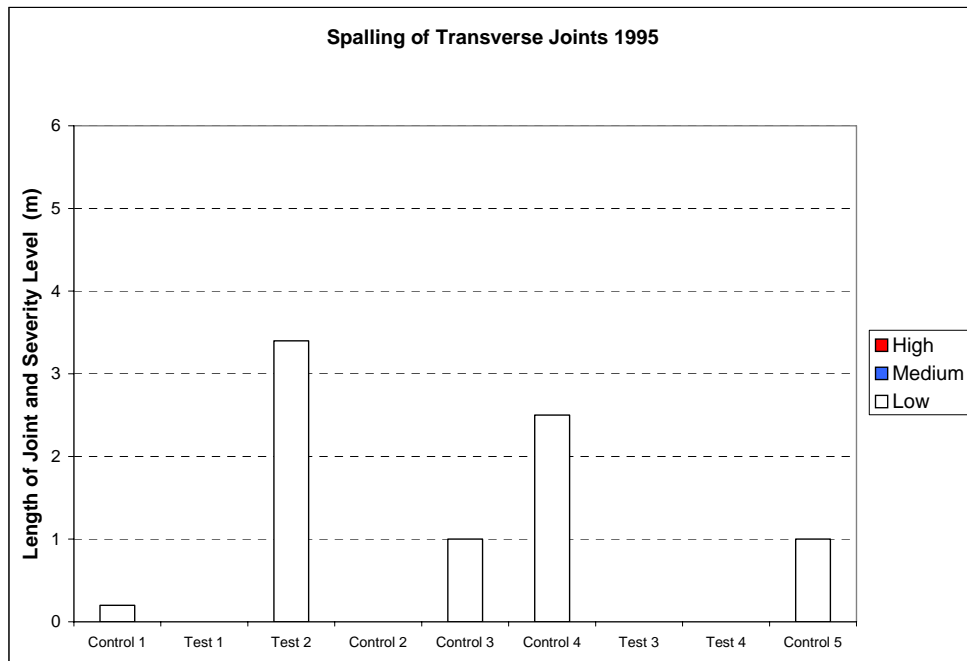


Figure 30. Length and severity of joint distress for all test sections (Newark, DE, 1995).

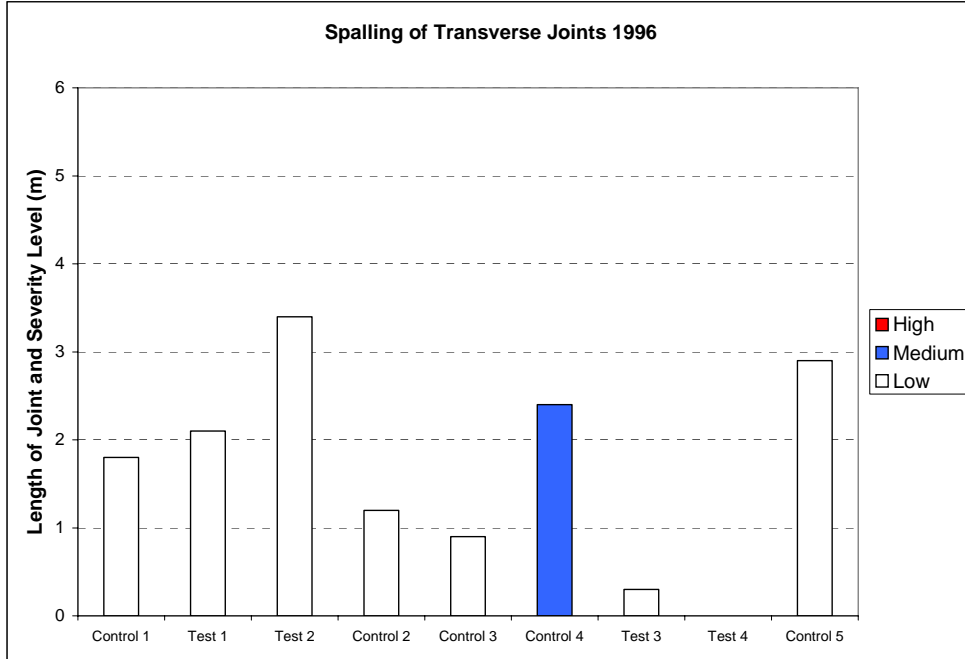


Figure 31. Length and severity of joint distress for all test sections (Newark, DE, 1996).

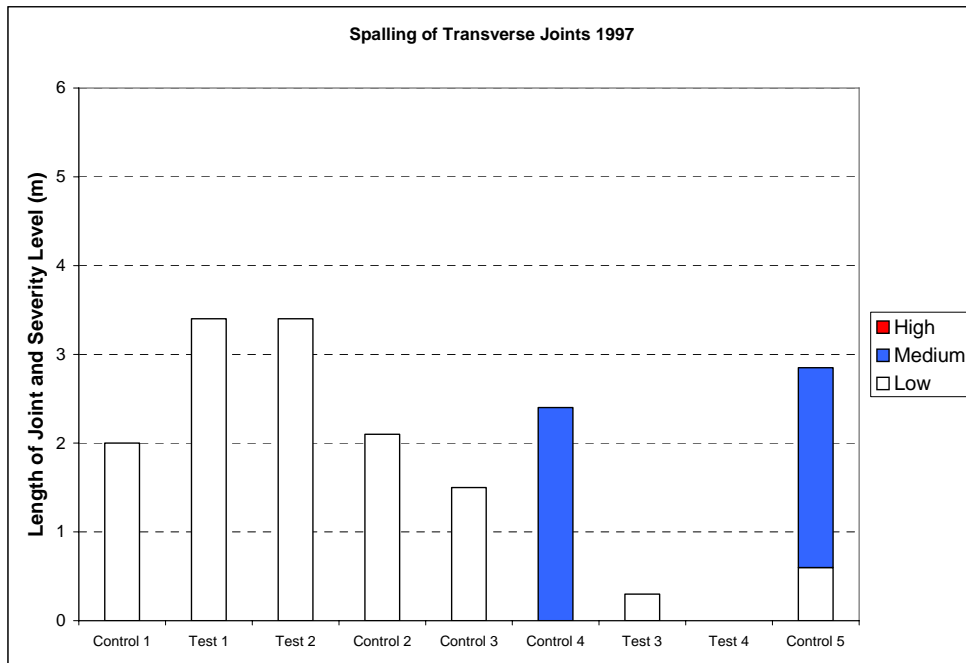


Figure 32. Length and severity of joint distress for all test sections (Newark, DE, 1997).

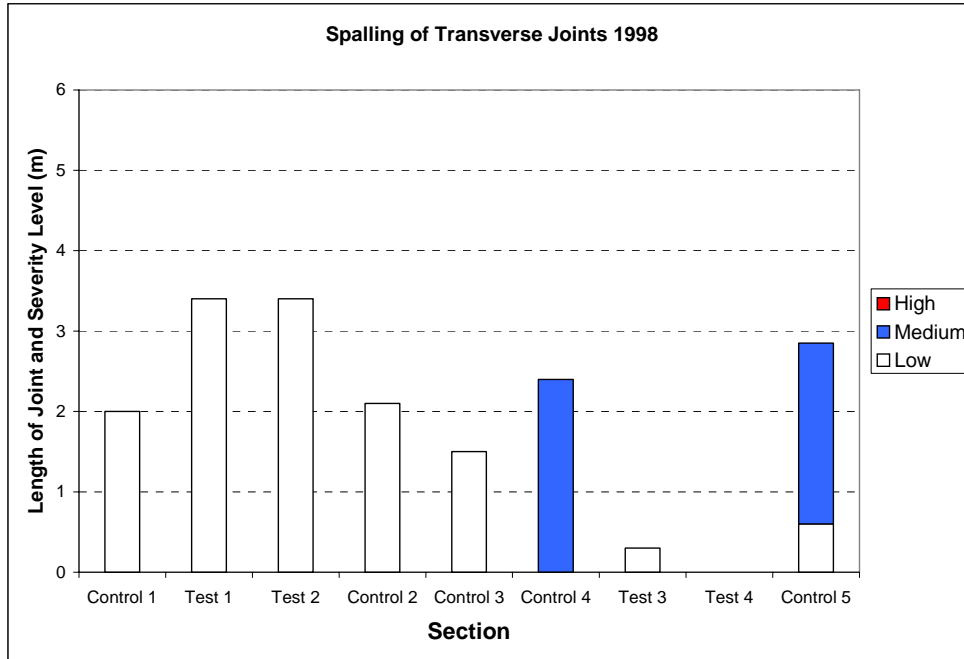
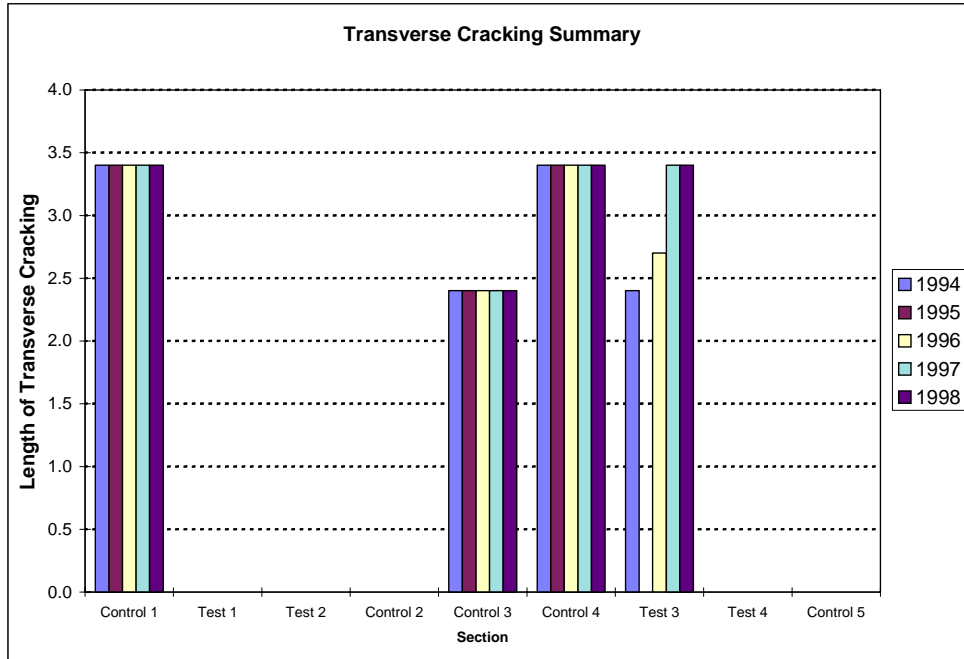


Figure 33. Length and severity of joint distress for all test sections (Newark, DE, 1998).

TRANSVERSE CRACKING

A summary of the transverse cracking in each section over the 5 years is shown in figure 34. The only sections with transverse cracking are control 1, control 3, control 4, and test section 3. The cracking in the three control sections had occurred before the first year of the study and did not increase in length or severity during the next 4 years of the study. The cracking in test section 3 had also occurred before the first year of the study but increased in length over the 4 years. There was no increase in severity, and all severity ratings are low. Generally, the transverse cracking of the Delaware test sections were there before the study began and do not appear to be getting more severe.



(Note: Length of Transverse Cracking (y-axis) is in meters.)

Figure 34. Summary of transverse cracking in each section for the five inspections (Newark, DE).

MODULUS AND STRENGTH TESTING

Each year cores were taken for modulus and strength testing. Subsequent cores were taken 0.61 m and 0.92 m from the previous year's cores along the same travel line on the downstream or "leave" side of the panel. The cores were labeled with the test panel designation and the letters "A" and "B," with A being the upstream (approach) core. The state crew removed the cores using a trailer-mounted coring machine. Selected cores were tested to determine the compressive strength and elastic modulus of the concrete in both wet and dry conditions.

A single core from each section was tested for wet and dry modulus and compressive strength testing. The cores were tested in a dry as-received condition, then soaked in lime saturated water for 2 weeks and retested. After the wet modulus tests were performed, the cores were allowed to dry for approximately 1 week, then tested to determine their compressive strength. The results of the dry modulus testing are shown in table 16, and results of the wet modulus testing are shown in table 17. In 1994 the cores were only tested for modulus in the dry condition. Wet modulus testing and compressive strength testing was not performed. In 1995, wet and dry modulus testing was performed but compressive strength testing was not since strength testing was not part of the original work plan.

Table 16. Newark, DE, core modulus testing results (psi x 10⁶, dry tested).

Section	Year				
	1994	1995	1996	1997	1998
Control 1	2.05	2.04	1.62	2.12	1.50
Test 1	1.77	1.76	0.96	2.34	Failed
Test 2	1.50	1.71	1.00	1.36	1.20
Test 3	1.87	2.08	1.79	2.33	1.66
Test 4	1.95	2.46	2.17	2.43	1.98
Control 5	2.04	2.09	1.87	2.19	1.71

1 psi = 6.89 kPa

Table 17. Newark, DE, core modulus testing results (psi x 10⁶, wet tested).

Section	1994	1995	1996	1997	1998
Control 1	–	1.80	1.69	1.70	1.40
Test 1	–	1.77	1.31	1.88	–
Test 2	–	1.67	1.00	1.19	1.38
Test 3	–	2.01	1.68	1.97	1.86
Test 4	–	2.27	1.96	2.17	2.20
Control 5	–	1.81	1.76	1.77	2.10

1 kPa = 6.89 psi

The measured modulus values for the cores were generally lower for 1998 than those in previous years, especially for the dry-tested moduli. The core from test section 1 failed during the pre-load, so there is no value for 1998. The results from 1997 show an increase in modulus over the previous years. The results from 1998 decreased, with a few exceptions, to less than the 1996 values. This follows the increase in distress noted in the sections.

The compressive strength results shown in table 18 do not indicate any trend except that test section 4 and control 5 have considerably higher compressive strengths than the other sections. These sections are at the far north end of the test area. The strength results are generally lower in 1998 than in 1996 but the concrete still has considerable compressive strength.

Table 18. Newark, DE, compressive strength results (psi).

Section	1994	1995	1996	1997	1998
Control 1	–	–	5320	5171	4325
Test 1	–	–	5837	4947	–
Test 2	–	–	4799	4014	4520
Test 3	–	–	4947	3989	4107
Test 4	–	–	6058	5849	5720
Control 5	–	–	5891	5565	5533

1 psi = 6.89 kPa

RELATIVE HUMIDITY MEASUREMENTS

After the visual surveys were completed and as the cores were being taken, six relative humidity locations were sampled, one each in sections control 1, test 1, test 2, test 3, test 4, and control 5. Section control 2, control 3, and control 4 were not sampled. The relative humidity samples were taken at various depths. The sample depths and results of the relative humidity testing are shown in tables 19 through 22. The relative humidity measurements were not made in 1998 due to very wet pavement conditions.

Table 19. Relative humidity testing at Newark, DE (1994).

Section	Relative Humidity, Percent (at given depth interval) (inches)			
	0.5–1	2–2.5	4–4.5	5.5–6
Control 1	70	81	90	95
Test section 1	72	95	97	98
Test section 2	85	93	97	101
Test section 3	84	97	100	100
Test section 4	–	–	–	–
Control 5	71	93	92	94

1 inch = 2.54 cm

Table 20. Relative humidity testing at Newark, DE (1995).

Section	Relative Humidity, Percent (at given depth interval) (inches)			
	0.5–1	2–2.5	4–4.5	5.5–6
Control 1	67	84	93	95
Test section 1	75	87	96	99
Test section 2	87	92	97	100
Test section 3	83	92	96	94
Test section 4	77	90	92	98
Control 5	69	85	94	96

1 inch = 2.54 cm

Table 21. Relative humidity testing at Newark, DE (1996).

Section	Relative Humidity, Percent (at given depth interval) (inches)			
	0.5–1	2–2.5	4–4.5	5.5–6
Control 1	69	95	96	87
Test section 1	71	82	94	93
Test section 2	52	84	48	83
Test section 3	54	83	91	80
Test section 4	57	85	94	83
Control 5	80	87	74	83

1 inch = 2.54 cm

Table 22. Relative humidity testing at Newark, DE (1997).

Section	Relative Humidity, Percent (at given depth interval) (inches)			
	0.5–1	2–2.5	4–4.5	5.5–6
Control 1	45	54	61	54
Test section 1	36	46	51	54
Test section 2	58	53	38	–
Test section 3	–	–	–	–
Test section 4	43	–	–	–
Control 5	42	50	53	70

1 inch = 2.54 cm

Generally, below 5.1 cm in depth, the relative humidity of samples is more than 80 percent. This is enough moisture for ASR to proceed.

PETROGRAPHIC EXAMINATION

Each year, one core from each test section was examined using methods of ASTM C 856, *Petrographic Examination of Hardened Concrete*. Sections from each of the cores were cut and lapped. These sections were then soaked overnight and dried, and the entire lapped surface was traversed under a stereo microscope. Each lapped surface was divided into five or more traverse areas and examined at magnifications of 10 to 30 times. All instances of cracks, alkali-silica gel, and deteriorated or reacted aggregate particles were counted. The petrographic observations are presented in appendix B. Table 23 gives a summary of the petrographic findings for the years 1997 and 1998. In the previous year's petrographic studies, the reactive particles and gel locations were not counted. From the petrographer's notes in appendix B, signs of ASR became widespread in the 1996 cores and continued to spread in the cores from 1997 and 1998. Notes from the 1996 core study indicate there was no significant difference between the cores from the control sections and those from the treated sections. All examined surfaces had abundant distressed fine aggregate and most potentially reactive particles had reacted to some extent. Microcracks and incipient microcracks were widespread. Gel was widely

distributed throughout the cores. There also appeared to be a tendency for the cores to fracture parallel to the wearing surface.

Table 23 indicates there is little difference in the amount of reacting particles and gel locations in cores from all the sections for 1997 and 1998. The test areas had, on average, slightly less cracking, reacted particles, and visible gel locations than the control areas. Generally in these 2 years, all cores were moderately to severely distressed from the effects of ASR. Reactive particles and gel locations were widespread.

Table 23. Summary of petrographic findings for 1997 and 1998.

Core ID	Year	Cracks		Reactive Particles		Gel Locations
		Micro	Large	Fine	Coarse	
C1	1997	40	1	24	3	27
	1998	77	1	39	0	49
C5	1997	34	1	27	3	31
	1998	57	0	42	0	79
TS1	1997	87	0	31	0	42
	1998	50	2	38	0	61
TS2	1997	43	0	29	0	33
	1998	64	1	23	0	58
TS3	1997	17	0	23	0	25
	1998	25	0	15	0	43
TS4	1997	8	0	31	0	13
	1998	14	0	15	0	44
Average for control sections (97 and 98)		52.0	0.8	33.0	1.5	46.5
Average for treated sections (97 and 98)		38.5	0.4	25.6	0.0	39.9

SUMMARY OF NEWARK, DE TEST SITE

Five control sections and four test sections treated with lithium hydroxide were evaluated. All sections increased in distress over the 4-year evaluation. Significant differences between all sections were seen between the north and south ends of the test area due to differences in exposure to moisture. The lithium hydroxide did not appear to be effective in stopping or significantly slowing the ASR deterioration at this test site.

CHAPTER 4. SUMMARY OF TEST RESULTS FROM BORON, CA

INTRODUCTION

This site consists of two eastbound lanes of State Route 58 eastbound in Boron, CA, as well as an overhead structure carrying State Route 58 over a rail spur immediately before the test section. The individual test sites and test results are described in the following sections.

BORON OVERHEAD

The Boron overhead, Bridge No. 50-353R 9-KER-58-R141.5, consists of two parallel structures carrying State Route 58 over the rail spur leading to the U.S. Borax mine in Boron, CA. Each structure consists of a three-span continuous bridge with no expansion joints. Each bridge has two traffic lanes and a shoulder. The bridge beams were cast integrally with the deck slab. The entire deck appears to be undergoing significant ASR, as manifested by widespread visible map cracking. The deck surface was treated with a methacrylate (HMWM) in 1995, into which a coarse, rounded sand was broadcast. Figure 35 shows a photograph of the deck surface.



Figure 35. Treated section on Boron overhead structure over State Route 58 looking east (Boron, CA).

Pavement Sections

The following information was excerpted from the CTL report (Stark to Surdahl letter, dated October 8, 1997):

This pavement section is located on State Route 58 between Barstow and Mojave near Boron on the Kern-San Bernardino county line in California. The pavement of interest was built between 1971 and 1974 as part of a four-lane divided section with 20.32-cm (8-inch) portland cement concrete slip-formed onto 10.16 to 15.24 cm (4 to 6 inches) of cement-treated base. The concrete was made using low-alkali cement (less than 0.60 percent equivalent to Na_2O) and natural sand and

gravel from a source in Barstow. In the early to middle 1980s, observations of this and several other concrete structures containing aggregate from the same source revealed deleterious ASR. In 1991, SHRP discussion with CALTRANS [California Department of Transportation] personnel revealed major surface cracking had been observed in the State Route 58 pavement. In 1988, a high molecular weight methacrylate (HMWM) had been applied to the pavement wearing surface in selected westbound sections near Boron to minimize cracking development and improve and prolong traffic service life, particularly with truck loading. A side effect would be to minimize any effects of deleterious ASR. In 1991, cores were taken as part of the SHRP program to confirm the occurrence of ASR and estimate the depth of penetration of the HMWM into the pavement concrete.

Observations

As noted in SHRP-C-343, six full-depth 10.16-cm (4-inch) diameter cores were taken from the experimental pavement section of Route 58, and sawed and finely lapped in the longitudinal direction for microscopic examination. The examinations confirmed that deleterious ASR had developed in the pavement concrete, and that the reactive aggregate constituents were cryptocrystalline volcanics of rhyolite to andesite composition. These were evidenced by reaction rims on aggregate particles, microcracks in the concrete, and ASR gel in cracks and voids. The examinations revealed that the applied HMWM penetrated and filled surface cracks to maximum depths of 51 to 62 mm (2 to 2.25 inch). Also, HMWM was found to have penetrated and filled cracks as little as 0.05 m (0.002 in) wide.

Status of Test Sections

For a period of years since 1988 when HMWM was applied, improved performance was noted, compared with sections with no treatment. For more than 5 years, only minor additional surface cracking appeared, while more severe surface cracks continued to develop along transverse joints, and adjacent to other random cracks in untreated sections. Also, numerous small surface spalls continued to develop in the untreated sections but not in the treated sections.

By 1995, 7 years after application of HMWM on State Route 58, it became apparent to CALTRANS that pavement performance both with and without the treatment reached a state of deterioration that required full-surface overlay. In 1996, this asphalt overlay was completed. However, CALTRANS agreed to retain a short section of exposed pavement with HMWM. This is presently the only section still available for visual inspection.

The test section described herein consists of two lanes of U.S. Route 52. Figures 36 and 37 show different views of the test pavement site, and figure 38 shows a plan of the test sections. The original test sections consisted of control 1, methacrylate 1, and methacrylate 2, all of which are located in the travel lane (number 2). Sections methacrylate 1 and methacrylate 2 were treated

with a single coat of methacrylate into which a sand was broadcast. In 1995, three test sections in the passing lane (number 1); control 2, control 3, and methacrylate 3 were added alongside the existing test areas in the travel lane (number 2) by CALTRANS to evaluate the effect of traffic loading on the ASR damage. The Boron Overhead section was also added at this time. Lane 1 does not have the extreme damage present at the joints that lane 2 had. A coat of methacrylate was applied to the methacrylate 3 section in 1995, at the same time the bridge deck was treated. At that time, a second coat of methacrylate was added to section methacrylate 2 in the travel lane. Also, in 1995, the pavement on either side of the test section was overlaid with asphaltic concrete. The asphalt overlays were placed to reduce the maintenance liability of the large length of exposed ASR pavement adjacent to the test sections.



Figure 36. Photograph showing part of Boron, CA, test site, M2, Station 250.



Figure 37. Photograph showing part of Boron, CA, test site, M3, Station 160.

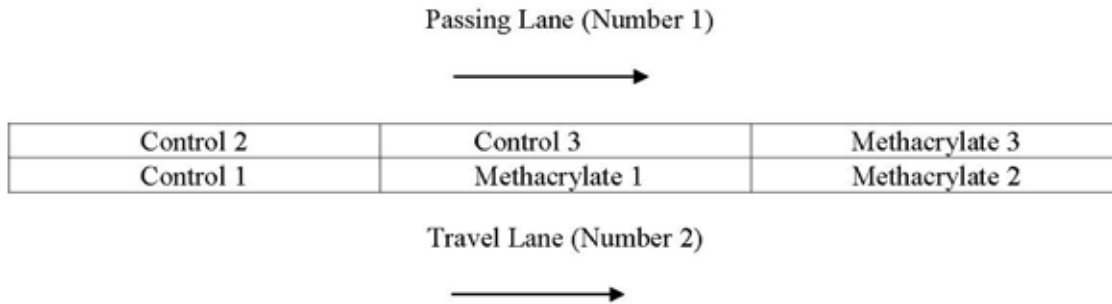


Figure 38. Plan view of Boron, CA, test site.

MAP CRACKING

All the sections making up the Boron, CA, test site had map cracking over 100 percent of their area in 1998. Most of the map cracking was of low severity, but there was some medium and high severity also. Figure 39 shows an example of high-severity map cracking. Figure 40 shows a close-up view of typical map cracking at the Boron site. Figures 41 through 44 show the amount of each level of severity as a percentage of the total area for each section for all 5 years of the study. In the travel lane, control section 1 (C1) had more severe map cracking than the methacrylate sections (M1 and M2). The cracking was less severe in M2 than in M1. It appears that the second application of methacrylate to section M2 in 1995 has helped reduce cracking. In the passing lane, methacrylate section 3 (M3) is performing better than control section 3 (C3). Overall, the passing lane sections are performing better than the travel lane sections. A description of the map cracking in each section is as follows:

- Control 1—the map cracking in this section progressed from more than 90 percent low severity and the remainder medium in 1994, to about 70 percent low severity and 15 percent each for medium and high severity in 1998.
- Methacrylate 1—the map cracking in 1998 in this section was less severe than C1, with just over 80 percent low severity and 20 percent medium severity.
- Methacrylate 2—the map cracking in 1998 was less than in section M1. There was also some redirection in the severity levels after the second application of methacrylate in 1995. The level in 1998 was 90 percent low severity and 10 percent medium severity. The deterioration increased only slightly during the four years of study.
- Control 3—the map cracking of 1998 in this section is at about the same level of severity as M2 in 1998, but the rate of increase in deterioration appears to be greater in C3 than in M2.
- Methacrylate 3—this section has the least severe map cracking of all the sections. Approximately 95 percent of the section is low severity and 5 percent is medium severity. The amount of medium-severity distress has increased only slightly during the 4 years of study.



Figure 39. Example of high-severity map cracking (Boron, CA).



Figure 40. Close-up photograph showing typical map cracking (Boron, CA).

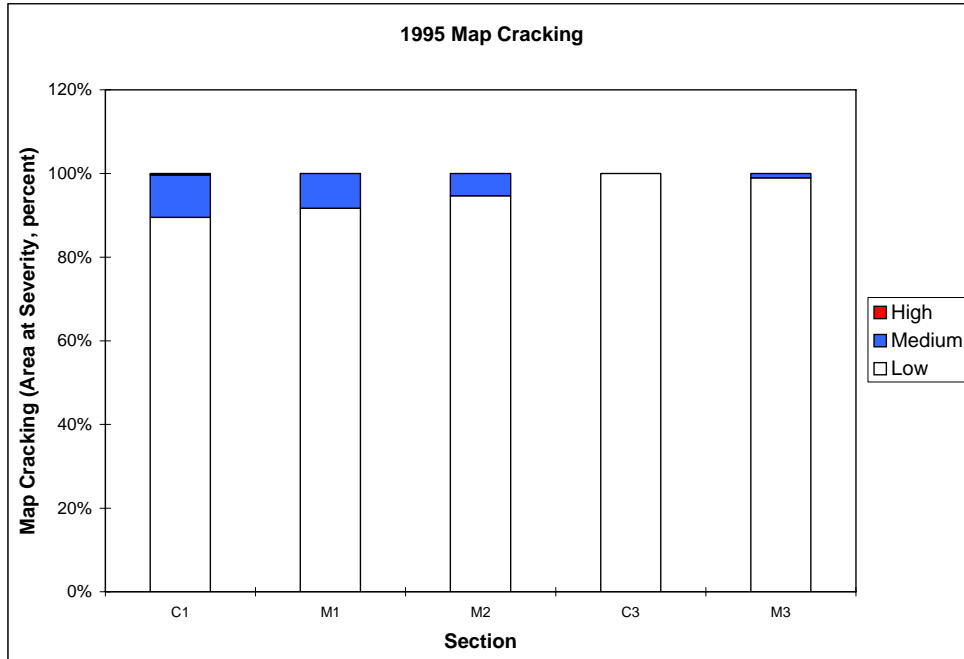


Figure 41. Map cracking as a percentage for each level of severity (Boron, CA, 1995).

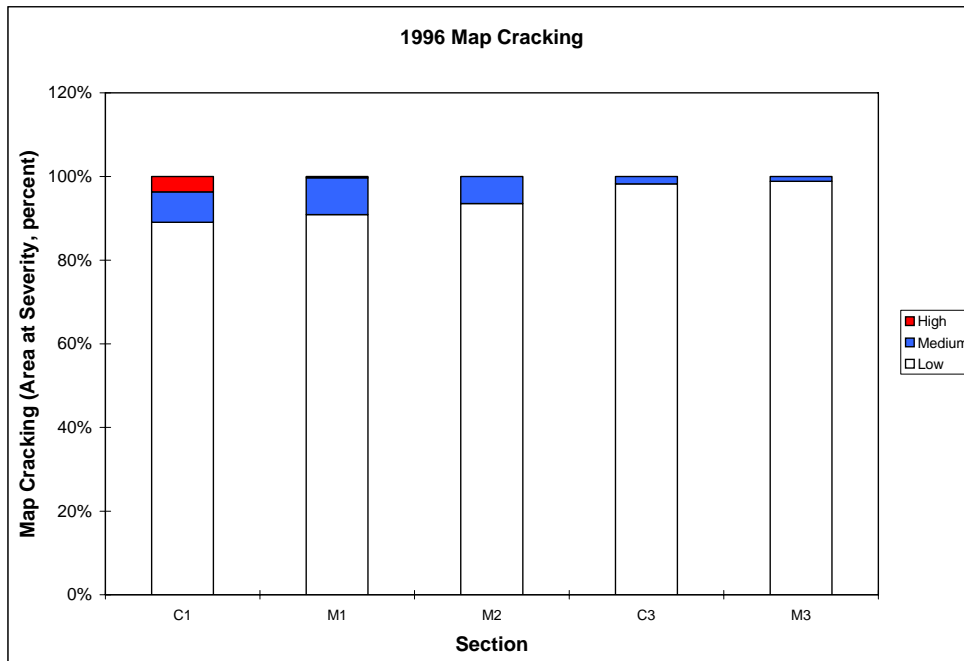


Figure 42. Map cracking as a percentage for each level of severity (Boron, CA, 1996).

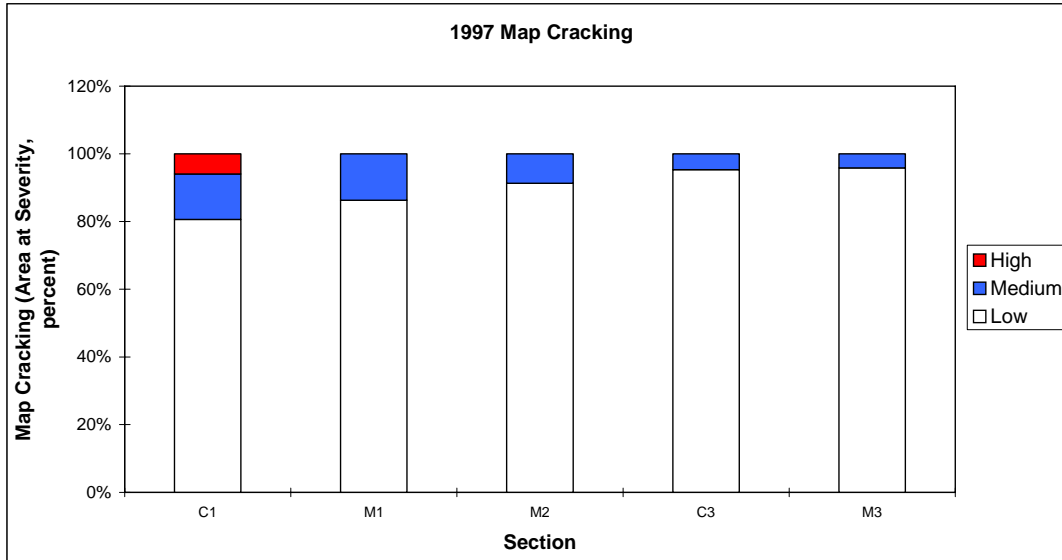


Figure 43. Map cracking as a percentage for each level of severity (Boron, CA, 1997).

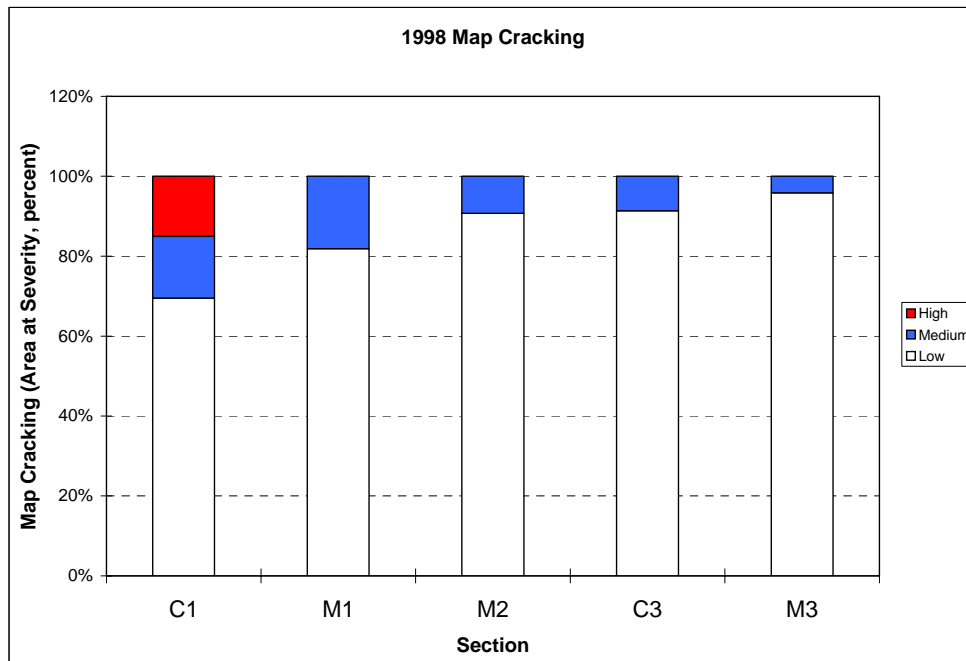


Figure 44. Map cracking as a percentage for each level of severity (Boron, CA, 1998).

JOINT DISTRESS

The widespread map cracking in the test sections made exact crack recording impossible. Therefore, only the large, clearly visible cracks were noted. The transverse joints were all completely distressed, with cracks and spalled areas occurring over the entire length of the joints. Figure 45 shows a photograph with an example of medium-severity joint distress. Figure 46

shows an example of high-severity joint distress. According to the LTPP criteria for rating joint distress, the entire length of each joint was rated at the highest severity level if at least 10 percent of the joint length had the higher severity distress.



Figure 45. Photograph showing medium-severity joint distress (Boron, CA).



Figure 46. Photograph showing an example of high-severity joint distress (Boron, CA).

Figures 47 through 50 are a series of graphs illustrating the amount and severity of joint distress for each section. There is also a series of graphs showing the actual lengths of distress at each level in figures 51 through 54. Both series compare all sections for each year. The 1998 observations of the joint distress for individual sections are as follows:

- Control 1—the severity of joint distress in section C1 had increased from almost entirely low severity in 1994 to mostly high severity in 1998. This was the worst section of the five. At least 10 percent of the length of almost all joints in this section had at least some high-severity joint distress. The graph of actual length of each distress condition (figure 54) indicates that for 1998 most of the length was of medium severity.
- Methacrylate 1—the methacrylate-1 section was the second worst section after C1. It had deteriorated from almost all low-severity distress in 1994 to 75 percent medium and 25 percent high in 1998. The rating system used showed no joints of low severity, while the graph of actual lengths of distressed joint indicates there were some areas of low-severity distress.
- Methacrylate 2—the methacrylate-2, with the second application of methacrylate, appeared to be performing better than the M1 section, which only had one application. This section was the best in the travel lane and second overall to the M3 section. The rating scheme rules imply that almost all the joint length was of medium-severity distress with a small amount of high-severity distress. The actual joint lengths show about one-third low severity, two-thirds medium, and a very small amount of high severity.
- Control 3—section control 3 has a rating of medium severity over the full joint length using the 10 percent rating scheme, but the true lengths show a small amount of low severity. Section C3 in the passing lane is much better than the control C1 in the travel lane.
- Methacrylate 3—the joint distress in section M3 appears to be more severe than that of C3 when using the 10 percent rule. Using this rule, C3 is performing better than M3 with C3 having all medium severity and M3 having mostly medium-, some high-, and a very small amount of low-severity distress. The actual length of each severity shows M3 has about two-thirds of its joint length rated as low severity, one-third medium severity, and a very small amount of high severity. If the actual length of each severity is used for comparison, M3 is performing much better than C3.

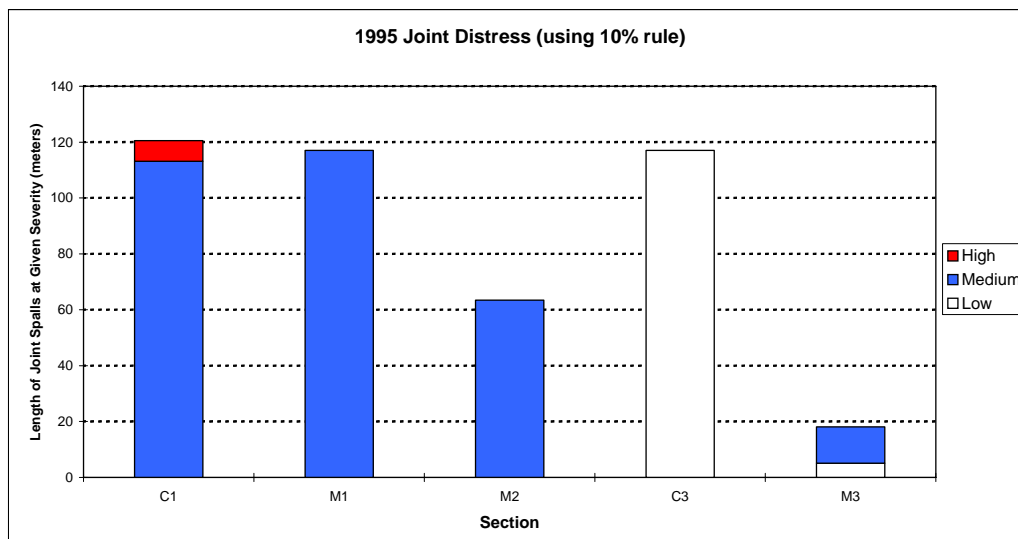


Figure 47. Amount and severity of joint distress (Boron, CA, 1995).

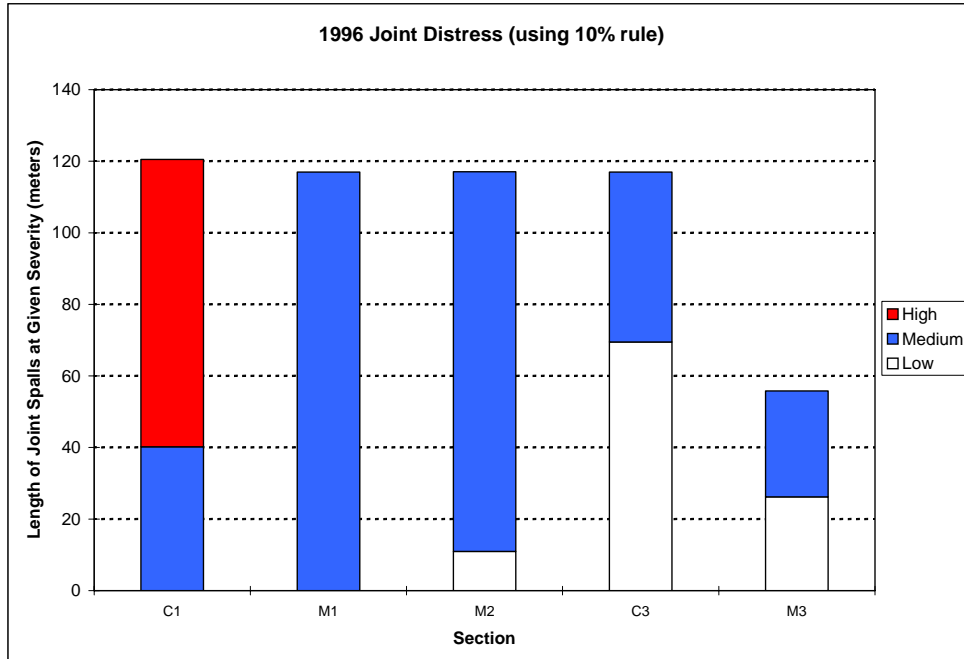


Figure 48. Amount and severity of joint distress (Boron, CA, 1996).

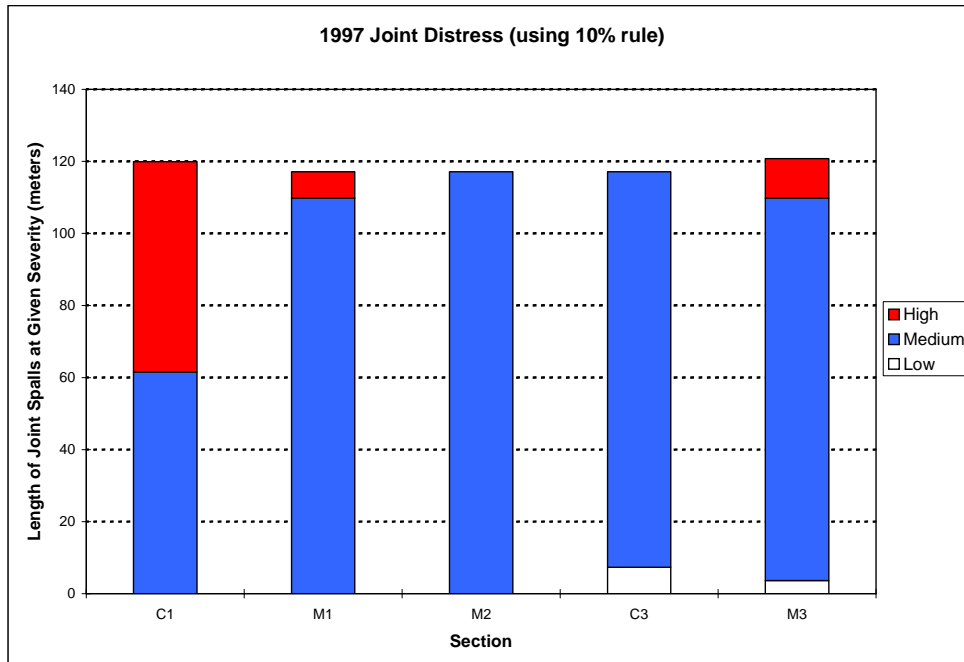


Figure 49. Amount and severity of joint distress (Boron, CA, 1997).

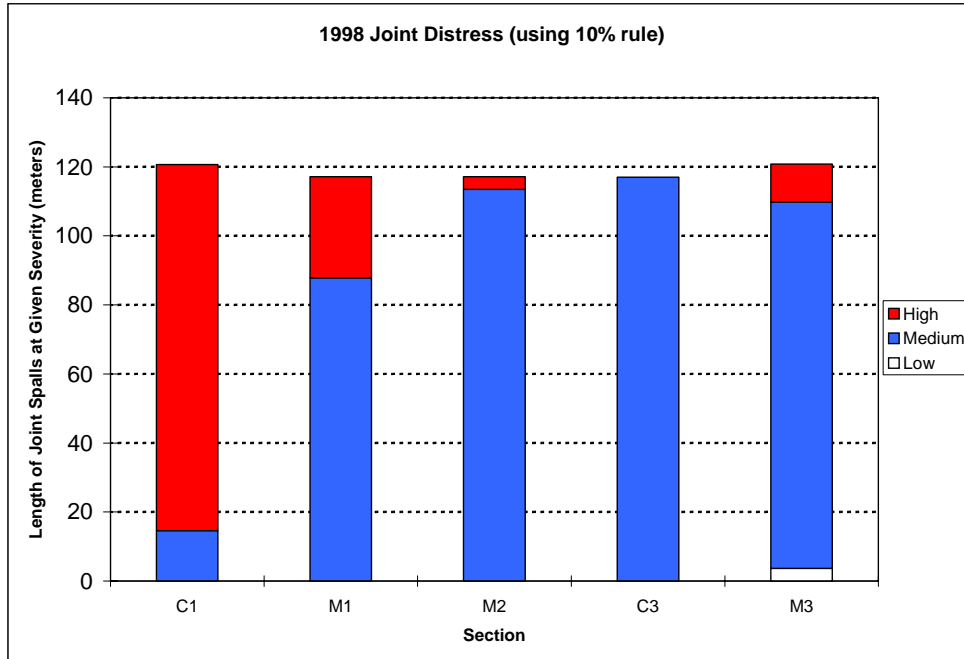


Figure 50. Amount and severity of joint distress (Boron, CA, 1998).

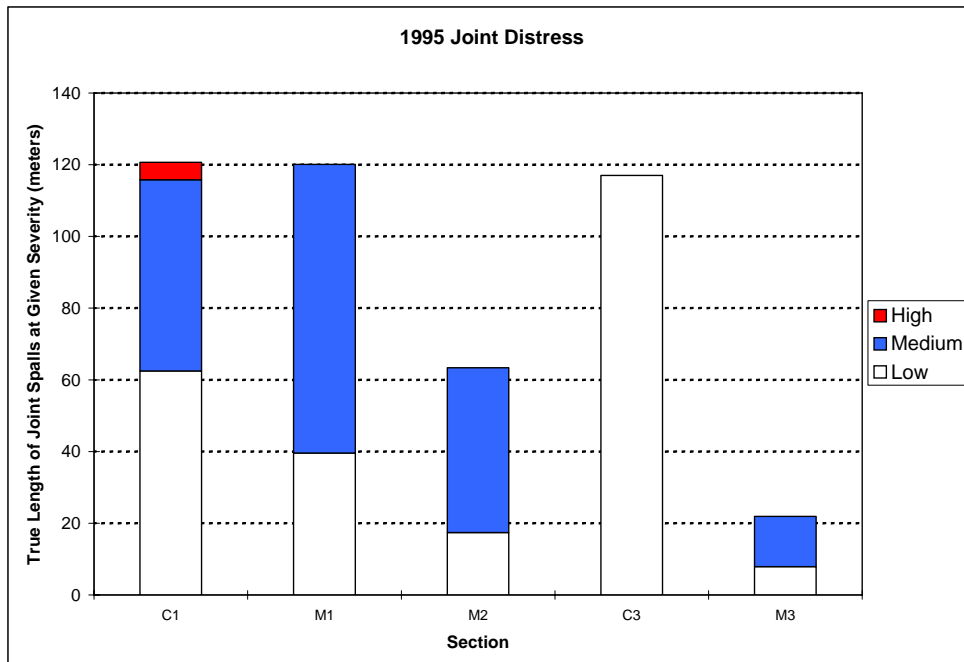


Figure 51. True length of joint spalls at each level of severity (Boron, CA, 1995).

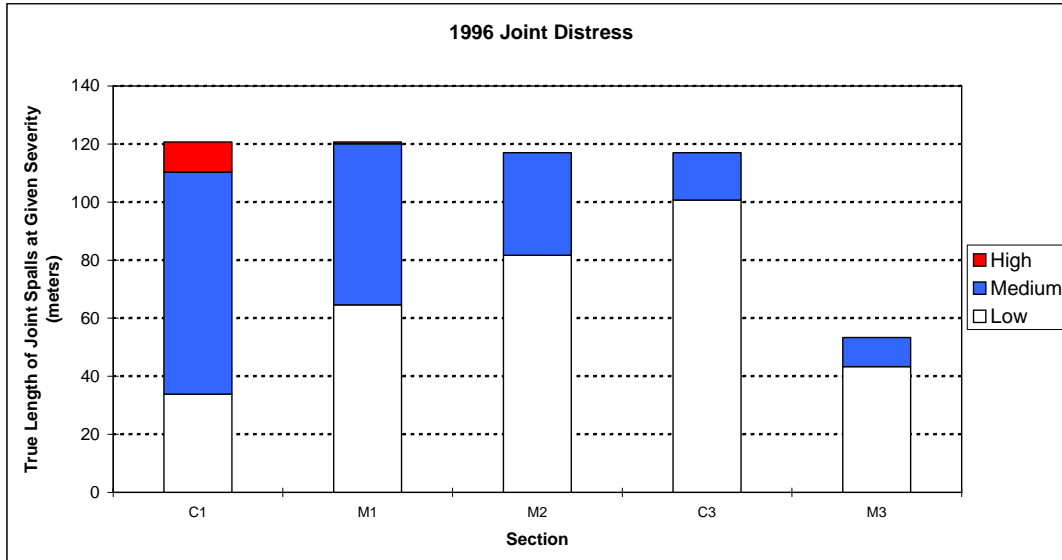


Figure 52. True length of joint spalls at each level of severity (Boron, CA, 1996).

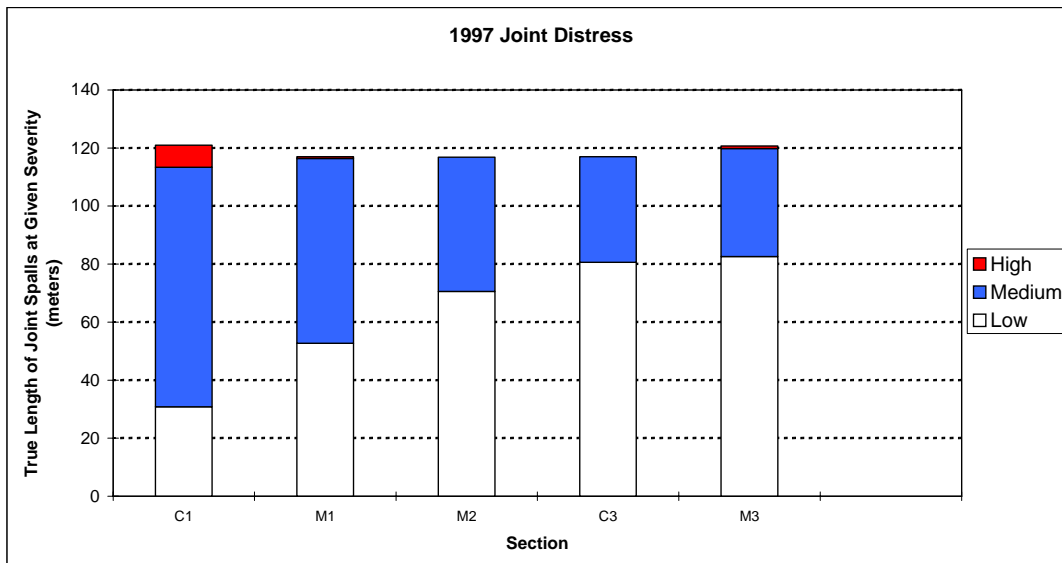


Figure 53. True length of joint spalls at each level of severity (Boron, CA, 1997).

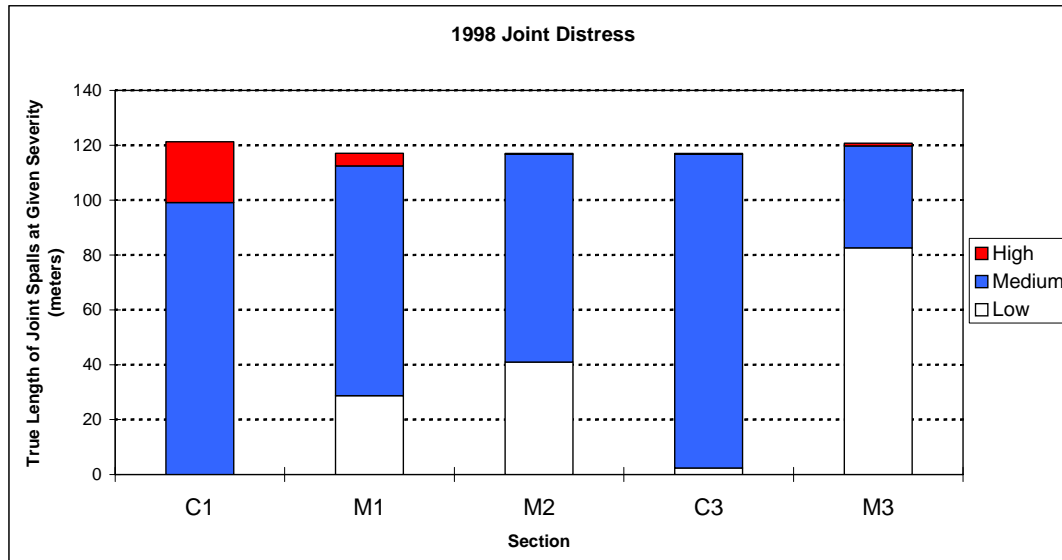


Figure 54. True length of joint spalls at each level of severity (Boron, CA, 1998).

In general, the sections in the travel lane had more severe joint distress than those sections in the passing lane. The control sections had the most severe joint distress in each lane relative to the treated areas. The second application of methacrylate to section M2 appeared to have helped, the severity of distress in M2 being less than that in section M1.

WHEELPATH DISTRESS

Visual surveys of the pavement sections were performed as previously done, with the wheelpath and centerline grading system changed to include sections with small, loose pieces in the high-severity (H) category. The wheelpaths and centerline were rated as follows:

- Low—no clear longitudinal cracking pattern developed.
- Medium—clear longitudinal cracking pattern developed with no spalls greater than 7.6 cm.
- High—clear longitudinal cracking pattern developed with spalls greater than 7.6 cm, or small, loose pieces.

Table 24 shows the number of slabs in each section at each level of severity for all years of the study. Some variability in the ratings occurred due to site lighting conditions and other inspection variations. In 1997, all the methacrylate-treated systems had a combination of low- and medium-severity cracking. There was little difference between section M2, which had the second application of methacrylate, and section M1, which only had one application. Both control sections had the most severe cracking with control section C1, which is in the No. 2 travel (truck) lane, having the most severe cracking. Section C1 had medium- and high-severity cracking while C3 had mostly medium severity with a small amount of low-severity cracking. In 1998, C1 still had the most severe cracking. The severity of cracking in all the other sections but M3 had increased. Sections M1 and M2 had medium-severity cracking over the wheelpaths of all slabs in 1998.

Table 24. Wheelpath ratings for all sections, Boron, CA.

Year	C1			M1			M2			C3			M3		
	L	M	H	L	M	H	L	M	H	L	M	H	L	M	H
1994	0	27	5	1	32	0	0	32	1	–	–	–	–	–	–
1995	0	0	32	0	33	0	0	33	0	2	31	0	–	–	–
1996	0	6	26	3	30	0	17	15	1	5	28	0	32	2	0
1997	0	10	22	22	11	0	19	14	0	1	32	0	17	17	0
1998	0	10	22	0	33	0	0	33	0	0	29	4	17	17	0

CENTERLINE DISTRESS

Table 25 shows the number of slabs in each section at each level of severity for all 5 years of the study for the centerline area of the sections. The same trend is evident here as in the wheelpath ratings. The ratings for all sections except M3 were more severe in 1998. Sections M1 and M2 were actually rated less severe than M3 in 1997, but in 1998 they were rated more severe than in previous years. The two control sections were rated the most severely distressed with C1 rated more severe than C3. Overall, the ratings in the centerline areas were much less severe than for the wheelpath areas.

Table 25. Centerline ratings for all sections, Boron, CA.

Year	C1			M1			M2			C3			M3		
	L	M	H	L	M	H	L	M	H	L	M	H	L	M	H
1994	26	6	0	31	2	0	33	0	0	–	–	–	–	–	–
1995	0	32	0	13	20	0	33	0	0	32	1	0	–	–	–
1996	3	22	7	33	0	0	30	3	0	30	3	0	33	0	0
1997	1	26	5	33	0	0	33	0	0	30	3	0	30	3	0
1998	7	25	0	8	25	0	27	6	0	4	29	0	30	3	0

ELASTIC MODULUS AND COMPRESSIVE STRENGTH

At least four cores were removed from each section, with many of the removed cores extracted in small, already fractured pieces. The cores were 1.22 and 1.83 m from the shoulder stripe to reflect wheelpath and centerline areas, respectively. The specific locations were chosen to avoid interfering with previous cores. If a core was retrieved in a broken or damaged condition, another core was taken approximately 0.61 m east of the original core at the same distance from the shoulder stripe.

The cores were tested to determine the compressive strength and elastic modulus of the concrete in both wet and dry conditions. The cores were tested in a dry as-received condition, then soaked in lime-saturated water for 2 weeks and retested. After the wet modulus tests were performed, the cores were tested to determine their compressive strength. The results of the dry modulus testing are shown in table 26. The results of the wet modulus testing are shown in table 27.

Table 26. Modulus dry tested elastic modulus (psi x 10⁶), Boron, CA.

Section	1995	1996	1997	1998
Control 1 (C1)	1.60	0.98	1.15	1.25
Methacrylate 1 (M1)	1.28	1.13	1.14	1.47
Methacrylate 2 (M2)	1.42	1.34	1.16	1.18
Control 3 (C3)	–	0.92	1.26	1.28
Methacrylate 3 (M3)	–	0.69	1.09	1.18

1 psi = 6.89 kPa

Table 27. Modulus wet tested elastic modulus (psi x 10⁶), Boron, CA.

Section	1995	1996	1997	1998
Control 1 (C1)	1.28	1.10	1.08	1.47
Methacrylate 1 (M1)	1.00	0.99	1.12	1.82
Methacrylate 2 (M2)	1.19	1.30	1.09	1.49
Control 3 (C3)	–	0.90	1.05	1.50
Methacrylate 3 (M3)	–	0.72	0.99	1.12

1 psi = 6.89 kPa

The results of the modulus testing show there is not much difference in modulus from one section to another. The wet and dry modulus values were generally similar. The one consistent trend is that the modulus for section M3 was the lowest in every year.

The wet lime-saturated compressive strength results are given in table 28. The compressive strength results show no significant difference between the sections. Generally, there has been a decrease in strength of each section over the test years.

Table 28. Compressive strength test results (Boron, CA).

Section	1995	1996	1997	1998
Control 1 (C1)	4788	4270	3605	3731
Methacrylate 1 (M1)	4052	4510	4041	4371
Methacrylate 2 (M2)	4302	5137	3803	3609
Control 3 (C3)	–	3985	3495	3684
Methacrylate 3 (M3)	–	4280	3688	3744

The cores tested may represent a minimum strength or modulus for intact cores. If a core was taken and it fell apart as it was being removed, another core was drilled. This biases the results because only solid cores can be tested.

RELATIVE HUMIDITY MEASUREMENTS

Relative humidity samples were removed from one or two locations in each section at various depth intervals, using a 38.1-mm-diameter bit and rotary hammer. The depth intervals and results of the relative humidity testing are shown in tables 29 through 33. Most of the relative humidity measurements were above 80 percent, especially below a depth of 10.2 cm. These results

indicate that even though the pavement is located in a very dry climate, sufficient moisture is still present to sustain the ASR. The humidity results for the bridge were much lower than the pavement. This is encouraging and indicates that methacrylate treatment of bridge decks may be much more effective at slowing ASR than when treating pavements.

Table 29. Relative humidity testing (1994).

Test Area and Section Number		Relative Humidity, Percent (at given depth interval) (inches)			
		0.5–1	2–2.5	4–4.5	6–6.5
Number 1 (Passing) Lane	C3	88	89	93	92
	M3	69	81	87	87
Number 2 (Travel) Lane	C1	93	87	93	90
	M1	78	91	97	92
	M2	59	97	96	90

1 inch = 2.54 cm

Table 30. Relative humidity testing (1995).

Test Area and Section Number		Relative Humidity, Percent (at given depth interval) (inches)			
		0.5–1	2–2.5	4–4.5	6–6.5
Number 1 (Passing) Lane	C3	36	63	62	86
	M3	46	72	86	90
Number 2 (Travel) Lane	M1	45	70	62	89
	M2	72	84	86	89
	C1	68	64	90	89
	Bridge	37	55	66	65

1 inch = 2.54 cm

Table 31. Relative humidity testing (1996).

Test Area and Section Number		Relative Humidity, Percent (at given depth interval) (inches)			
		0.5–1	2–2.5	4–4.5	6–6.5
Number 1 (Passing) Lane	C3	65	90	92	87
	M3	69	79	87	83
Number 2 (Travel) Lane	C1	56	89	84	80
	M1	81	90	86	72
	M2	44	74	70	78

1 inch = 2.54 cm

Table 32. Relative humidity testing (1997).

Test Area and Section Number		Relative Humidity, Percent (at given depth interval) (inches)			
		0.5–1	2–2.5	4–4.5	6–6.5
Number 1 (Passing) Lane	C3	–	–	–	–
	M3	40	62	86	96
Number 2 (Travel) Lane	M1	46	93	81	98
	M2	43	48	79	87
	C1	50	76	92	90
	Bridge	32	46	44	56

1 inch = 2.54 cm

Table 33. Relative humidity testing (1998).

Test Area and Section Number		Relative Humidity, Percent (at given depth interval) (inches)			
		0.5–1	2–2.5	4–4.5	6–6.5
Number 1 (Passing) Lane	C3	48	75	100	100
	M3	58	76	97	96
Number 2 (Travel) Lane	M1	100	100	100	100
	M2	100	54	100	93
	C1	100	100	100	100
	Bridge	32	39	52	62

1 inch = 2.54 cm

PETROGRAPHIC EXAMINATION

Two cores from each section were examined petrographically to document the condition of the concrete. The cores were cut length-wise and polished. These sections were then soaked overnight and dried, and the entire lapped surface was traversed under a stereo microscope. Each lapped surface was divided into five or more traverse areas and examined at magnifications of 10 to 30 times. Because of their smaller diameters (6.99 cm (2.75 inches)), the Boron overhead bridge cores were divided into four traverses. All instances of cracks, alkali-silica gel, and deteriorated or reacted aggregate particles were counted. The petrographer’s notes for each year are included in appendix C. Table 34 gives a numerical summary of the findings for 1997 and 1998.

Table 34. Summary of petrographic findings for 1997 and 1998, Boron, CA.

Core ID	Year	Cracks		Reactive Particles		Gel Locations
		Micro	Large	Fine	Coarse	
C1-1	1997	190	0	20	8	67
	1998	86	5	21	22	49
C1-2	1997	–	–	–	–	–
	1998	60	0	21	23	41
C3-1	1997	174	0	23	11	24
	1998	50	3	8	11	28
C3-2	1997	190	0	30	26	44
	1998	63	23	10	12	14
M1-1	1997	191	0	33	23	65
	1998	51	1	9	9	20
M1-2	1997	–	–	–	–	–
	1998	84	6	15	17	32
M2-1	1997	135	0	24	29	59
	1998	72	3	7	12	12
M2-2	1997	–	–	–	–	–
	1998	89	3	16	8	23
M3-1	1997	134	0	32	31	46
	1998	66	0	7	14	29
M3-2	1997	–	–	–	–	–
	1998	67	0	13	10	24
OH-1 Bridge	1997	22	0	0	0	0
	1998	29	2	8	7	29
OH-2 Bridge	1997	–	–	–	–	–
	1998	29	1	7	11	36

A summary description of the cores from each section follows:

- Boron overhead (bridges)—cores from 1997 and 1998 have shown moderately severe distress. This concrete is also poorly air-entrained. The top surface appeared moderately worn and partially coated with methacrylate.
- Control 1—the wearing surface of the cores for the past 3 years (1996, 1997, 1998) was moderately to severely worn with frequently exposed fine aggregate particles. All of these cores appeared to be air-entrained with approximately 5 percent entrained air. The condition of the cores was classified as moderately distressed in 1996 and severely distressed in 1997 and 1998. Observations indicated moderately frequent popouts over fine and coarse aggregates in the past 2 years. Microcracks, reacted particles, and gel locations are abundant and widespread within the concrete for all 3 years. Most, if not all, potentially reactive particles have reacted to some extent.
- Control 3—the cores from 1996, 1997, and 1998 were classified as severely distressed with extensive microcracking throughout the cores. Multiple generations of alkali-silica gel are abundant and ubiquitous. The top surface of the cores, from 1997 and 1998, was severely

worn and had frequent exposed aggregate particles and worn popouts. The cores seemed to be well air-entrained with approximately 5 to 6 percent air content.

- Methacrylate 1—the surface of the cores taken in 1997 and 1998 were severely worn with frequently exposed fine aggregate particles. The cores were classified as moderately severely to severely distressed. There was an abundance of reacted particles, microcracks, and gel locations within the concrete matrix. All potentially reactive aggregate particles appeared to have reacted and some were deteriorated. The core from 1996 showed microcracks perpendicular to the wearing surface filled with resin. The cores appeared to be marginally air-entrained, with an estimated air content of 4 to 5 percent.
- Methacrylate 2—the wearing surface was severely worn. Aggregate particles were frequently exposed and polished. The cores were classified as moderately severe to severely distressed. The core from 1996 had a darkened area of the paste in the top 5 millimeters from the surface treatment. Distress was not prevalent in that area. The rest of that core and the cores from 1997 and 1998 had microcracks widespread throughout the core. Multiple generations of gel were generally ubiquitous and moderately abundant to abundant. The cores were marginally air-entrained, with an estimated air content of 4 percent.
- Methacrylate 3—the surface of the 1997 core was worn and partially coated. Occasional popouts over aggregates were evident. The core from 1998 had a severely worn surface with frequently exposed and polished aggregate particles. The cores were classified as moderately severely distressed. All potentially reactive particles appeared to have reacted to varying degrees. Multiple generations of gel were abundant.

SUMMARY OF BORON, CA TEST SITE

HMWM resin was topically applied to desert pavement sections with moderate to severe ASR distress. The methacrylate has extended the pavement life by filling cracks bonding the pieces of concrete and reducing spalling, especially near joints. The service life extension of one coat of HMWM appears to be about 3 to 5 years. Two coats of resin improved performance further. It is envisioned that periodic reapplication of HMWM would reduce future concrete spalling and continue to extend the pavement life.

HMWM resin was also applied to a bridge deck having low to moderate ASR distress. The resin had been effective in bonding and sealing almost all of the cracks. No new visible cracking was noted over the study period. The relative humidity in the deck concrete is moderately low and to a level that should slow ASR deterioration. Preliminary results are promising and continued monitoring of this structure is recommended.

CHAPTER 5. SUMMARY OF TEST RESULTS FROM ALBUQUERQUE, NM

The New Mexico State Highway and Transportation Department constructed test sections in June 1992 of a new highway to evaluate the capability of concrete admixtures to prevent expansion due to ASR. The pavement is a three-lane, uphill, left-turning approach to a bridge carrying Lomas Boulevard westbound over Interstate 40 (I-40) in eastern Albuquerque. The surface was smooth-finished, with no tining or grooving. An overall view of the test site and variables are shown in figures 55 and 56. Eleven test sections described in tables 35, each 12.2 to 18.3 m in length, were constructed.

Table 35. Test variables Lomas Boulevard, Albuquerque, NM.

Test Section	Aggregate Source	Treatment
1	Shakespeare	1 percent LiOH
2	Shakespeare	0.5 percent LiOH
3	Shakespeare	Lomar—HRWR at 0.59 L/45.6 kg (20 oz/hundredweight (cwt))
4	Shakespeare	Class F fly ash, 25 percent replacement of cement
5	Shakespeare	Class C fly ash, 25 percent replacement of cement
6	Shakespeare	Control
7	Shakespeare	Blend of Class C and F fly ash (1:1), 25 percent replacement of cement
8	Grevey	Class F fly ash, 25 percent replacement of cement
9	Grevey	Control
10	Grevey	1 percent LiOH
11	Grevey	Class C fly ash, 25 percent replacement of cement

A single source of portland cement with 0.55 percent total alkalies [as Na₂O] was used throughout the project. The complete concrete mix characteristics are given in appendix D.

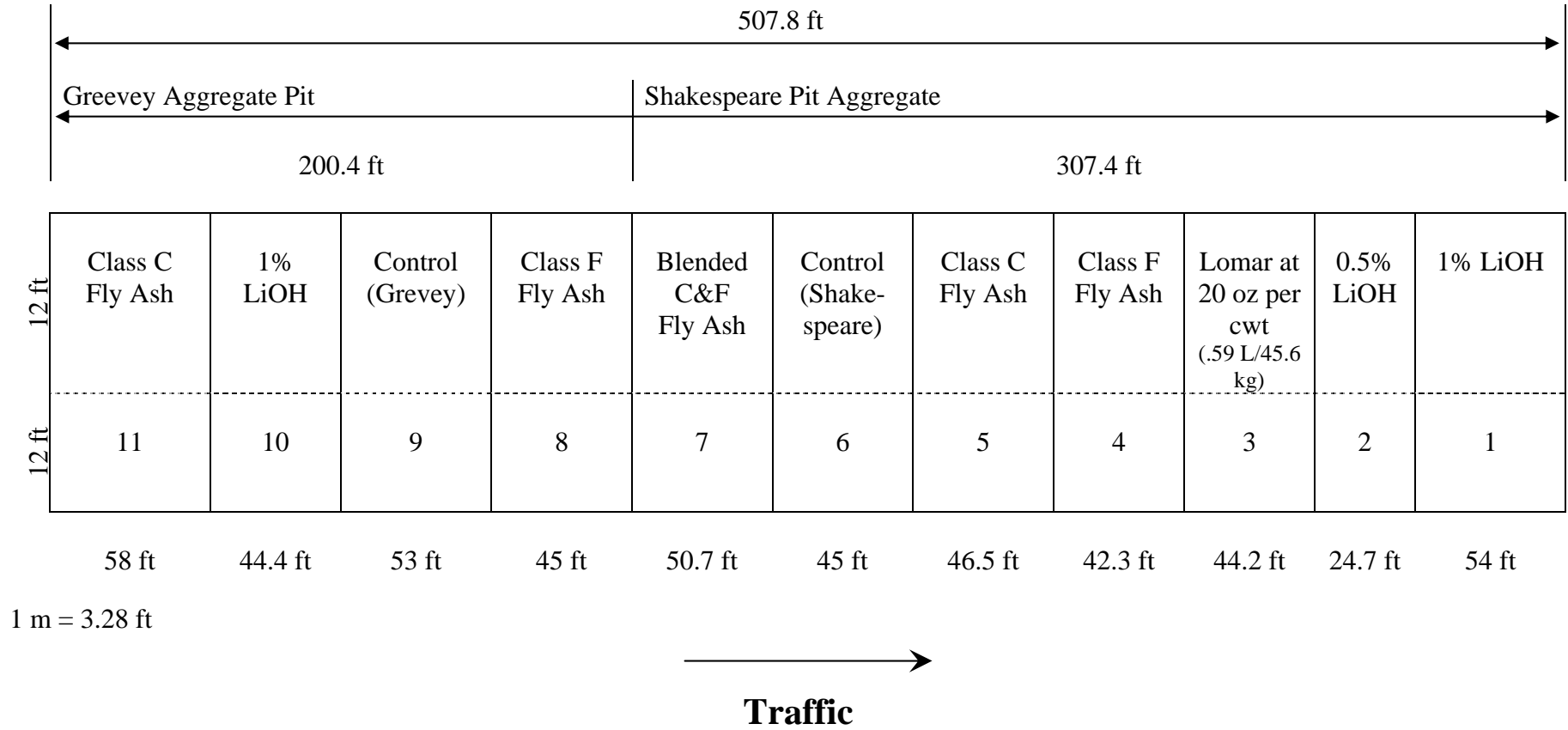


Figure 55. New Mexico ASR test section layout—westbound approach slabs to Lomas Boulevard (State Route 352) bridge over I-25.



Figure 56. Lomas Boulevard westbound structure over I-40 (Albuquerque, NM).

The following information was reported:

- This project was designed under the SHRP program to evaluate the relative effectiveness of certain mineral and chemical admixtures in preventing deleterious ASR in new pavement construction. For this purpose, two similar, well-documented, highly reactive coarse and fine aggregates from Albuquerque, and a low-alkali cement, were used as the major components of the test pavement. ASTM Class F and Class C fly ash, and lithium hydroxide monohydrate ($\text{LiOH}\cdot\text{H}_2\text{O}$), were included as admixtures.
- The concrete test section is a 9.15-m (30.02-ft) wide, three-lane pavement, 20.3 cm (8 inches) thick, and is placed on a 15.2-cm (6-inch) thick cement-treated base. This base layer is underlain full-width by a filter fabric layer.
- In view of favorable laboratory test results demonstrating its capability to prevent expansion due to ASR, the New Mexico State Highway and Transportation Department agreed to use LiOH in new highway construction in Albuquerque. Location of the experimental pavement was the approach lanes to a bridge on Lomas Boulevard (State Route 352) over I-40.
- Ten test sections, each 12.2 to 18.3 m (40.03 to 60.04 ft) long, were included in the experimental pavement. Two local sources of sand and gravel, including AL, were used separately in various test sections. In addition to LiOH, a Class F and a Class C fly ash were used separately with each aggregate at approximately 25 percent mass replacement of cement. A single section made with aggregate AL contained 25 percent mass replacement fly ash consisting of 50 percent Class F (the same source) and 50 percent Class C (different source) ash. $\text{LiOH}\cdot\text{H}_2\text{O}$ was added at the rate of 0.5 percent and 1 percent by mass of cement with aggregate AL, but only 1 percent by mass of cement with aggregate from the other, nearby source. Control sections also were built in which neither fly ash or LiOH was

included. A single source of portland cement with approximately 0.55 percent equivalent Na_2O was used through the project. Installation was carried out in June 1992.

- One concern with using LiOH was its uniform dispersion in the concrete batches in the ready-mix trucks. To maximize uniformity, mixing water was introduced into the trucks the night before placement and the appropriate amount of powdered LiOH·H₂O added to the water. The trucks were batched the next day, driven to the job site and the concrete discharged in the forms 20 to 30 minutes after the beginning of mixing. It was found that the presence of LiOH in the concrete had no discernible effect on slump or air content compared with the control concrete. Also, joint-sawing could be carried out on the schedule for the control concrete. Overall, no schedule allowances were required in the mixing and placing sequences for the LiOH additions.
- Subsequent to placement, unused materials were evaluated in the rapid immersion test method to evaluate the ability of the fly ashes to suppress expansive ASR with aggregates from the two sources used in the experiment pavement. Mortar bars also were made to evaluate the effect of LiOH on ASR, using C 227 storage conditions. The proportions of fly ash and LiOH to cement were the same as those used in the pavement. Cement B, with 0.18 percent equivalent Na_2O , was used for rapid immersion tests in 1N NaOH solution. Data indicate that both coarse and fine aggregate from both sources are potentially deleteriously reactive since they all greatly exceed the 0.08 percent test criterion. This confirms previous field performance observations. These results also indicate the use of the Class C fly ash had little beneficial effect on suppressing ASR, whereas the Class F ash reduced expansions below the test criterion. Specimens containing the Class C + Class F mixture produced expansion somewhat greater than the test criterion. Continued monitoring of this experimental pavement over a period of years should validate these test results. Test mixtures containing LiOH admixtures and stored under C 227 conditions are too young to provide meaningful results. Thus, they are not reported here.

The Albuquerque pavement test section was inspected in the fall in each of the 5 years following construction. The most recent inspection was performed on October 1, 1998. Annual tests performed included visual inspection and crack mapping, faulting measurements, relative humidity measurements, FWD readings, and core removal for wet and dry modulus testing and petrographic studies. The cores were taken by New Mexico DOT personnel.

CONDITION OF PAVEMENT SECTIONS

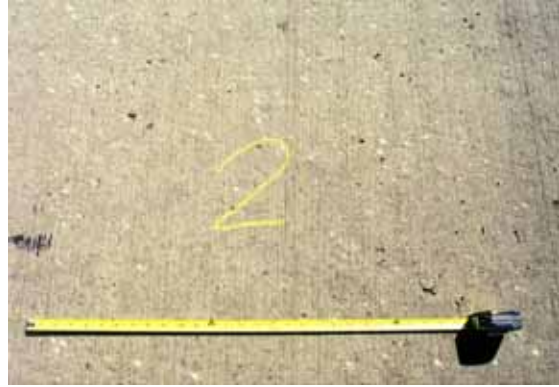
The condition of the pavement test section was determined by visual inspection. Notes were made as to extent of map cracking, transverse cracking, joint spalling, joint seal condition, patching, popouts, and other LTPP criteria. The condition of each section relative to the others in the test area was also noted. The results of the 1998 visual inspection are given in table 36. Photographs of the various test sections are shown in figure 57.

Table 36. Visual inspection notes for October 1, 1998 (Albuquerque, NM).

Test Section	Treatment –Aggregate Source	Observations
1	1 percent LiOH—Shakespeare	Fine map cracking developing in areas of the right wheelpath. In the left wheelpath, there is slightly visible map cracking. The centerline has light, barely visible map cracking. In general, the entire section except along the curb has faint to light map cracking.
2	0.5 percent LiOH—Shakespeare	The entire section has light map cracking that is slightly more visible than in section 1. The left wheelpath has slightly more visible cracking than the right wheelpath.
3	Lomar—Shakespeare	Occasional cracking was noted but no map cracking except for one faint area in the right wheelpath. Very rough original surface texture in approximately 80 percent of the test area due to rain damage while plastic.
4	Class F Fly Ash—Shakespeare	Areas of occasional very light surface cracking exist in first slab in left wheelpath. A few cracks exist near the lane centerline.
5	Class C Fly Ash—Shakespeare	Two full-width transverse cracks, well-defined transverse and longitudinal cracks, well-defined map cracking over entire surface with some raveling of the cracks were observed. Cracking is worse in wheelpaths. The average size of the pieces between cracks is 7.6 cm (3 inches).
6	Control—Shakespeare	Entire section, except along curb, has faint map cracking. Fine cracks have developed at a transverse joint.
7	Blended C & F Fly Ash—Shakespeare	Some areas of faint map cracking were found.
8	Class F Fly Ash—Grevey	The entire area has faint to light map cracking. Concentrated in the left wheelpath. Some joint spalling is present.
9	Control—Grevey	Very faint map cracking was observed over the entire section.
10	1 percent LiOH—Grevey	Very faint map cracking was found but less visible than in section 9. Areas of rough and irregular finish exist.
11	Class C Fly Ash—Grevey	Longitudinal cracks were found in left wheelpath and along centerline, fine wheelpath map cracking and transverse cracks were also developing, and areas of rough and irregular finish exist. Severity of map cracking is between that of sections 9 and 10.



(a) 1% LiOH—Shakespeare aggregate



(b) 0.5% LiOH—Shakespeare aggregate



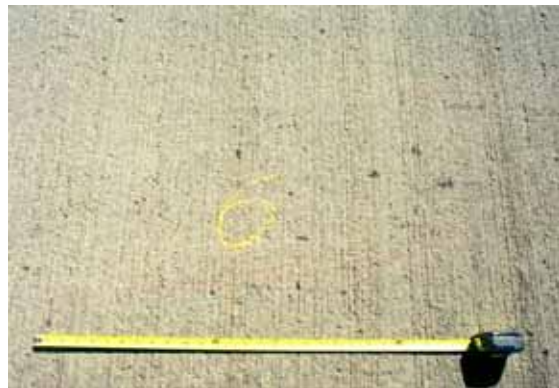
(c) Lomar—Shakespeare aggregate



(d) Class F Ash—Shakespeare



(e) Class C Ash—Shakespeare



(f) Control—Shakespeare

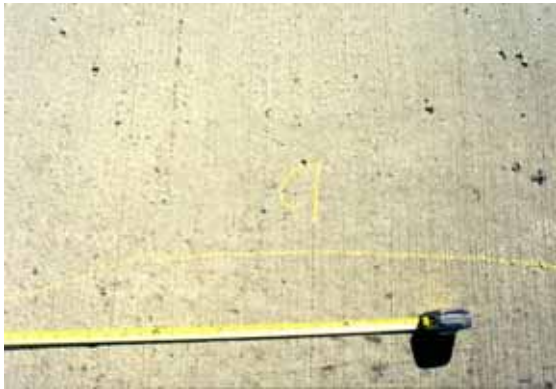
Figure 57. Photographs of all sections in Albuquerque, NM.



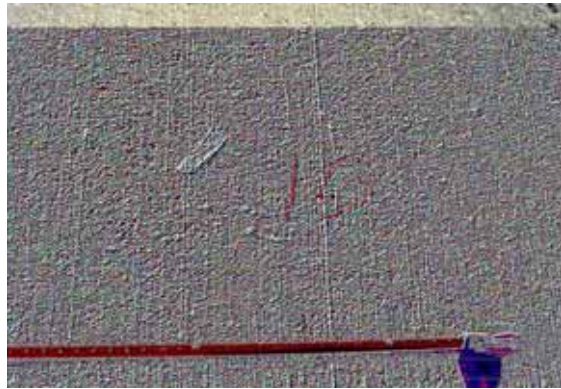
(g) Blended C & F Ash—Shakespeare



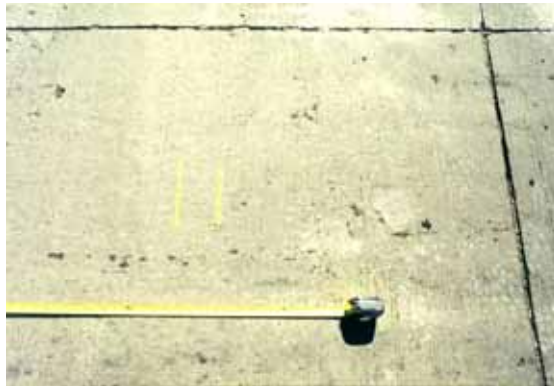
(h) Class F Ash—Grevey Aggregate



(i) Control—Grevey



(j) 1% LiOH—Grevey



(k) Class C Ash—Grevey

Figure 57. Photographs of all sections in Albuquerque, NM (continued).

TRANSVERSE JOINT SPALLING

The amount and severity of transverse joint spalling was used as an indicator of the section condition. The amount of transverse joint spalling in the years 1994 to 1998 is shown in the series of figures in appendix D. The amount of joint spalling for all sections increased over the 4 years of the study. The largest increase in this deterioration occurred between 1997 and 1998. The severity of the joint spalling was rated high, medium, or low. LTPP criteria define spalling of transverse joints as follows:

- Low—7.6-cm (3-inch) wide pieces with or without loss of concrete (just cracking).
- Medium—7.6- to 15.2-cm (3- to 6-inch) pieces with loss of concrete.
- High—greater than 15.2-cm (6-inch) pieces with loss of concrete.

The highest level of severity that occurred along the joint was then used to designate the entire length of the joint. There are significant differences between the performances of the sections. However, joint distress is not as good an indicator of ASR damage as map cracking. Each section has only 2 or 3 interior joints, while the remaining joints are at transition areas between test sections. Table 37 summarizes the percent transverse joint spalling and notes the highest level of severity.

Table 37. Summary of transverse joint spalling (1998).

Test Section	Treatment	Length of Transverse Spalling (meters)	Total Length (meters)	Percent of Total	Highest Severity
1	1 percent LiOH (S)	5.8	10.6	55	H
2	0.5 percent LiOH (S)	5.5	7.1	77	M
3	Lomar (S)	4.3	7.1	60	H
4	Class F Ash (S)	5.2	10.6	49	L
5	Class C Ash (S)	7.1	7.1	100	M
6	Control (S)	7.0	10.6	66	L
7	Blended C & F (S)	7.0	10.6	66	L
8	Class F Ash (G)	5.5	7.1	77	H
9	Control (G)	8.1	10.6	76	L
10	1 percent LiOH (G)	5.5	7.1	77	L
11	Class C Ash (G)	11.0	10.6	100	L

For the sections made with Shakespeare aggregate, the section with the best performance was the section that contains Class F fly ash, with just over 49 percent of the joint affected with low-severity joint spalling (cracking). The next best sections were the control section and the section containing blended Class F and Class C fly ashes. Both had about 66 percent of low-severity joint spalling. The worst performances were in the sections that contain Lomar, which had approximately 60 percent of high-severity spalling, and the 1 percent LiOH section, which had 55 percent of low- and high-severity spalling. The sections with 0.5 percent LiOH or Class C fly ash were between the others with about 77 percent and 100 percent of moderate-severity joint spalling, respectively.

For the sections made with the Grevey aggregate, the best performing sections were the control and the 1 percent LiOH. Each had about 76 percent of low severity spalling. The Class C fly ash section was performing better than the Class F fly ash section. The Class C had only low severity spalling over 100 percent of the joints while the Class F section had high severity spalling over 77 percent of the entire joint length.

There are some contradictory results when comparing the sections with the two aggregates. With the Shakespeare aggregate, the Class F fly ash outperformed the Class C fly ash, while with the Grevey aggregate, the Class C fly ash performed better than the Class F fly ash. With the Shakespeare aggregate, the section with the 1 percent LiOH had higher severity spalling than the 0.5 percent LiOH section. The section with Grevey aggregate and 1 percent LiOH performed better than either LiOH test section made with Shakespeare aggregate. The control sections with both aggregates had the same, low amount and severity of joint spalling.

MAP CRACKING

The amount and severity of map cracking is a good early indicator of the extent of ASR occurring in each section. The area of map cracking as a percent of the total area is shown in figure 58. This figure shows that, for most sections, the area of map cracking had increased substantially between 1996 and 1998. The section with Class C fly ash and Shakespeare aggregate had extensive map cracking over the entire test area in 1995, except for a small area along the curb. The section with Class F fly ash and Shakespeare aggregate was performing the best of all the sections, with less than 10 percent of its area covered by map cracking. The Lomar section was the next best with about 15 percent map cracking. Several sections, especially those with Grevey aggregate, had extensive map cracking appear only within the last 2 years of the study.

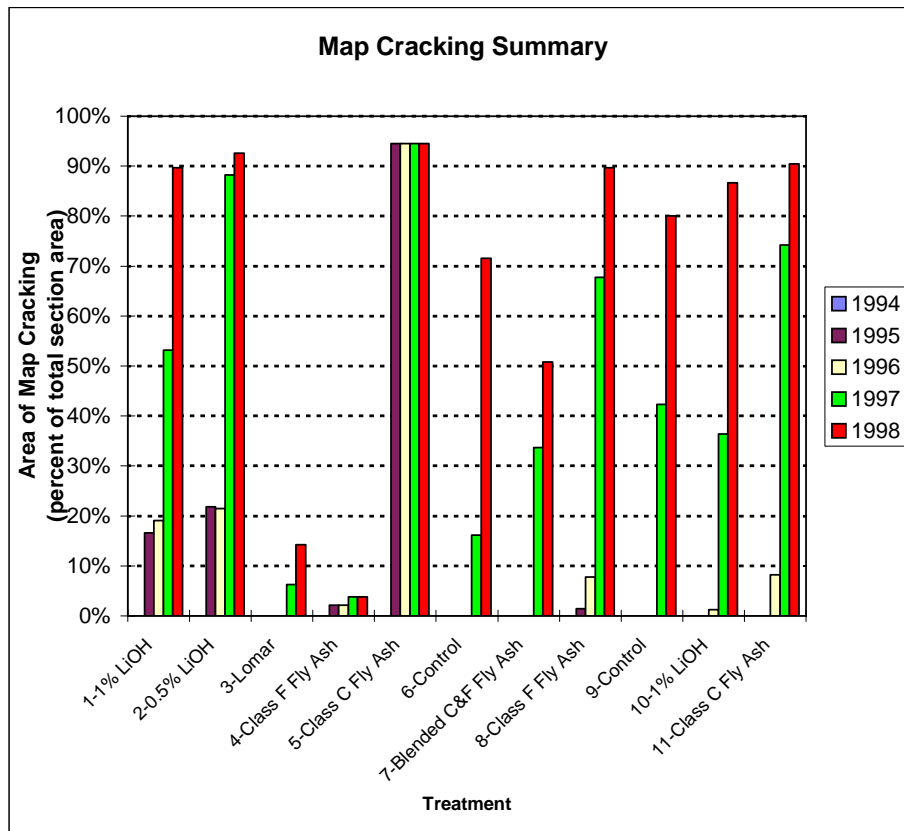


Figure 58. Area of map cracking as a percentage of the total area (all sections, Albuquerque, NM).

MODULUS TESTING OF CORES

Cores taken by New Mexico DOT personnel were shipped to laboratories for testing. Some of the cores were prepared by cutting them to length and squaring the ends. These cores were first tested for elastic modulus in the as-received, dry condition, then soaked for 2 weeks in lime-saturated water and retested. The elastic modulus tests were performed using an external compressometer.

The results of the modulus of elasticity tests cores in the dry condition for all 5 years are given in table 38. The test results for the cores in the wet or saturated condition are shown in table 39. The cores were not tested in the wet condition in 1994. Except from 1994 to 1995, the overall annual average moduli, both wet and dry, declined. The overall standard deviation generally increased over this same time. The moduli of all the sections did not decrease the same amount. Figure 59 shows the modulus of elasticity tested in the as-received state for all the sections over the four years. There are no obvious trends in most sections. The Class C fly ash section with the Shakespeare aggregate (S) is the only section that showed a uniform decrease in the modulus over the past four years. The modulus results from testing in the wet state are shown in figure 60. Here, the trend of decreasing modulus over the four years is more distinct. Most sections show a decrease in elastic modulus from 1995 to 1998. Again the Class C fly ash with Shakespeare aggregate section has the largest and most consistent decrease in modulus. The other sections maintained moderately high modulus properties.

**Table 38. Elastic modulus test results dry condition
(psi x 10⁶, average of 2 cores) Albuquerque, NM.**

Section No.	Description*	Dry					Percent Loss From 1994–1998
		1994	1995	1996	1997	1998	
1	1 percent LiOH (S)	4.10	4.68	5.11	4.09	3.89	4
2	0.5 percent LiOH (S)	4.06	4.43	4.71	3.61	3.69	8
3	Lomar (S)	4.15	4.91	4.75	3.83	4.18	-1
4	Class F Ash (S)	3.80	3.95	3.89	4.14	4.02	-6
5	Class C Ash (S)	2.16	2.90	2.39	1.72	1.24	32
6	Control (S)	3.52	4.08	3.29	3.59	3.47	1
7	Class C & F Ash (S)	3.30	3.67	3.66	3.60	3.28	1
8	Class F Ash (G)	3.53	4.24	3.77	4.04	3.31	5
9	Control (G)	3.33	4.02	3.50	3.31	3.57	-6
10	1 percent LiOH (G)	3.20	3.28	3.15	3.74	3.70	-1
11	Class C Ash (G)	3.71	4.34	3.85	4.26	3.62	2
Average		3.53	4.05	3.82	3.63	3.45	2
Standard Deviation		0.56	0.59	0.79	0.70	0.78	

*(S) = Shakespeare aggregate; (G) = Grevey aggregate

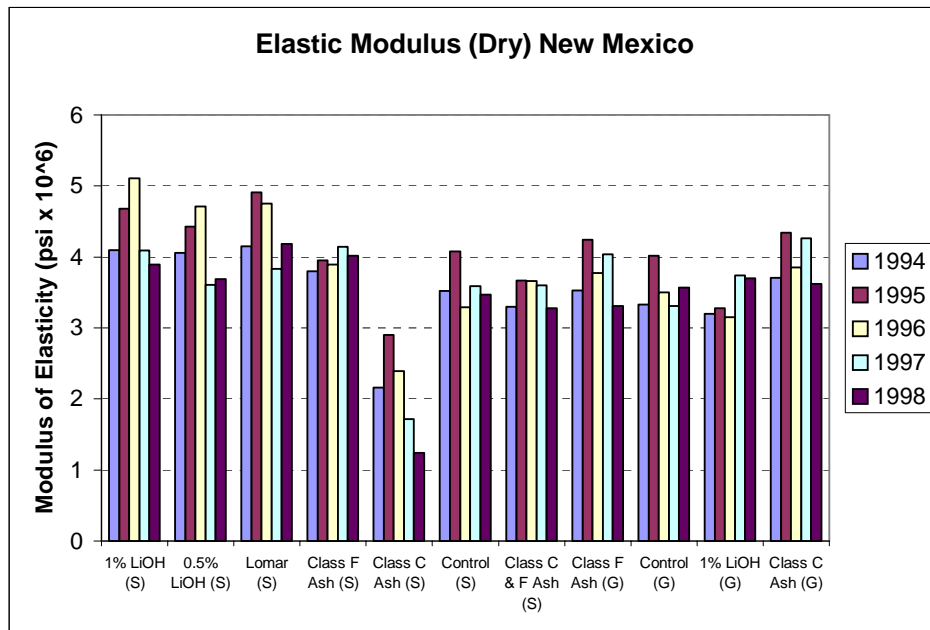
1 psi = 6.89 kPa

**Table 39. Elastic modulus test results wet condition
(psi x 10⁶, average of 2 cores), Albuquerque, NM.**

Section No	Description*	Wet					Percent Loss From 1995–1998
		1994	1995	1996	1997	1998	
1	1 percent LiOH (S)	–	5.06	4.47	4.08	4.02	21
2	0.5 percent LiOH (S)	–	4.05	4.09	3.46	3.46	15
3	Lomar (S)	–	5.07	4.54	3.96	3.87	24
4	Class F Ash (S)	–	4.08	4.03	4.05	3.43	16
5	Class C Ash (S)	–	3.22	2.57	1.79	1.39	57
6	Control (S)	–	3.89	3.20	3.40	3.30	15
7	Class C & F Ash (S)	–	3.82	3.66	3.69	3.36	12
8	Class F Ash (G)	–	4.57	3.54	3.82	3.54	23
9	Control (G)	–	4.02	3.82	3.56	3.50	13
10	1 percent LiOH (G)	–	3.29	3.09	3.58	3.65	-11
11	Class C Ash (G)	–	4.44	3.96	3.46	3.58	19
Average		–	4.14	3.72	3.53	3.37	18
Standard Deviation		–	0.61	0.60	0.63	0.69	–

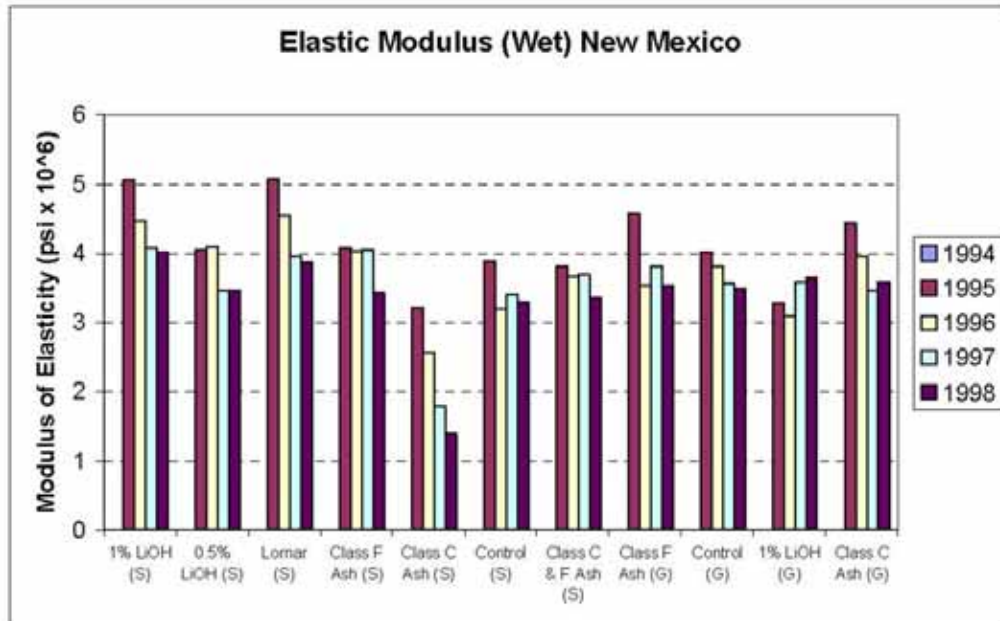
*(S) = Shakespeare aggregate; (G) = Grevey aggregate

1 psi = 6.89 kPa



1 psi = 6.89 kPa

Figure 59. Modulus of elasticity test results for cores in the dry condition (all sections, Albuquerque, NM).



1 psi = 6.89 kPa

Figure 60. Modulus of elasticity test results for cores in the saturated condition (all sections, Albuquerque, NM).

The increased scatter in the dry-tested results may be due to the cores being tested in the as-shipped condition. Depending on the storage conditions and time elapsed from coring to testing, the moisture content of the cores from one year's testing to another could change considerably. When tested in the saturated state, the condition of the cores from one year to the next are similar. This results in more consistent results and less scatter. If the concrete has internal cracking and gel due to ASR, the concrete modulus is expected to decrease. Wetting causes the gel to imbibe water and swell. This swelling should reduce the modulus further than if the concrete is tested dry.

RELATIVE HUMIDITY

The relative humidity values of the concrete pavement sections as they vary with depth are given in tables 40 through 44. The relative humidity values are similar from year to year, with levels increasing with depth. Generally, all of the samples had relative humidities of approximately 70 percent or higher at the deepest level measured, from 15.2- to 16.5-cm (6- to 6.5-inch) depths. The 100 percent humidity values for the top portions in 1998 were caused by rain showers that occurred during the site inspection. None of the test variables are expected to alter the humidity within the concrete. The data shows the wide variability of concrete humidity in pavements and confirms that sufficient moisture is normally available to promote ASR within the concrete.

Table 40. Relative humidity testing, Albuquerque, NM (1994).

Section No.	Description*	Relative Humidity, Percent (at given depth interval) (inches)			
		0.5–1	2–2.5	4–4.5	6–6.5
1	1 percent LiOH (S)	76	78	95	95
2	0.5 percent LiOH (S)	56	64	75	82
3	Lomar (S)	42	68	78	80
4	Class F Ash (S)	63	74	85	90
5	Class C Ash (S)	90	87	86	87
6	Control (S)	44	78	82	85
7	Class C & F Blend (S)	58	60	80	83
8	Class F (G)	59	82	87	91
9	Control (G)	54	73	84	88
10	1 percent LiOH (G)	62	77	87	88
11	Class C (G)	65	70	80	84

*(S) = Shakespeare aggregate; (G) = Grevey aggregate

1 inch = 2.54 cm

Table 41. Relative humidity testing, Albuquerque, NM (1995).

Section No.	Description*	Relative Humidity, Percent (at given depth interval) (inches)			
		0.5–1	2–2.5	4–4.5	6–6.5
1	1 percent LiOH (S)	–	59	–	90
2	0.5 percent LiOH (S)	38	–	–	76
3	Lomar (S)	41	53	–	63
4	Class F Ash (S)	51	50	80	81
5	Class C Ash (S)	60	73	74	80
6	Control (S)	42	56	73	70
7	Class C & F Blend (S)	39	59	73	74
8	Class F (G)	41	61	77	72
9	Control (G)	43	60	76	71
10	1 percent LiOH (G)	44	55	74	76
11	Class C (G)	41	61	72	70

*(S) = Shakespeare aggregate; (G) = Grevey aggregate

1 inch = 2.54 cm

Table 42. Relative humidity testing, Albuquerque, NM (1996).

Section No.	Description*	Relative Humidity, Percent (at given depth interval) (inches)			
		0.5-1	2-2.5	4-4.5	6-6.5
1	1 percent LiOH (S)	63	79	78	87
2	0.5 percent LiOH (S)	42	68	81	90
3	Lomar (S)	48	66	77	85
4	Class F Ash (S)	82	68	62	81
5	Class C Ash (S)	82	67	60	69
6	Control (S)	58	66	59	75
7	Class C & F Blend (S)	59	61	66	82
8	Class F (G)	31	72	79	82
9	Control (G)	64	62	74	81
10	1 percent LiOH (G)	55	63	75	82
11	Class C (G)	47	59	73	79

*(S) = Shakespeare aggregate; (G) = Grevey aggregate

1 inch = 2.54 cm

Table 43. Relative humidity testing, Albuquerque, NM (1997).

Section No.	Description*	Relative Humidity, Percent (at given depth interval) (inches)			
		0.5-1	2-2.5	4-4.5	6-6.5
1	1 percent LiOH (S)	63	67	72	81
2	0.5 percent LiOH (S)	93	66	74	83
3	Lomar (S)	35	47	58	80
4	Class F Ash (S)	65	73	83	88
5	Class C Ash (S)	52	93	96	90
6	Control (S)	38	55	77	73
7	Class C & F Blend (S)	41	65	80	77
8	Class F (G)	83	63	100	88
9	Control (G)	37	55	90	99
10	1 percent LiOH (G)	38	63	92	100
11	Class C (G)	36	37	95	100

*(S) = Shakespeare aggregate; (G) = Grevey aggregate

1 inch = 2.54 cm

Table 44. Relative humidity testing, Albuquerque, NM (1998).

Section No.	Description*	Relative Humidity, Percent (at given depth interval) (inches)			
		0.5–1	2–2.5	4–4.5	6–6.5
1	1 percent LiOH (S)	33	42	88	69
2	0.5 percent LiOH (S)	100	100	71	89
3	Lomar (S)	100	100	49	51
4	Class F Ash (S)	100	100	53	79
5	Class C Ash (S)	100	100	100	100
6	Control (S)	100	100	100	100
7	Class C & F Blend (S)	100	100	100	100
8	Class F (G)	100	100	100	100
9	Control (G)	100	100	100	100
10	1 percent LiOH (G)	100	100	100	100
11	Class C (G)	100	100	100	100

*(S) = Shakespeare aggregate; (G) = Grevey aggregate

1 inch = 2.54 cm

PETROGRAPHIC EXAMINATION

A petrographic examination was done on one core from each test section each year. The core was cut into the largest possible square prism, and two faces of the prism were lapped. Parallel sections were marked on each lapped face to delineate each traverse and ensure that the entire lapped surface was examined. Evidence of reaction, in the form of gel and cracks characteristic of ASR and associated with aggregate particles and reactive particles, were then counted on both lapped faces.

As discussed previously, the relative numbers of reactive coarse and fine aggregate particles should be regarded as approximate, since alkali-silica gel is highly mobile and may have migrated away from the originating particle. The petrographer's observations are in appendix D. A summary of the observations from the cores for 1998 is given in tables 45 and 46.

SUMMARY OF LOMAS BOULEVARD, ALBUQUERQUE, NM, TEST SITE

Some test sections show visual indications of distress after 6 years of service. Based on the visual inspection, area of map cracking, and transverse joint spalling, only three sections appear to be performing better than the controls:

Section

- 4 Class F Fly Ash—Shakespeare
- 3 Lomar (HRWA)—Shakespeare
- 7 Blend Class C and F Ash—Shakespeare

Section 5 (Class C fly ash—Shakespeare) and section 11 (Class C fly ash—Grevey) are clearly performing the worst and considerable worse than the control concretes. Sections 2 (0.5 percent LiOH) and section 8 (Class F fly ash—Grevey) may be slightly worse than the controls. Section 10 (1 percent LiOH—Grevey) and section 1 (1 percent LiOH—Shakespeare) appear similar to the controls.

Section 5 (Class C fly ash—Shakespeare) was the only section to exhibit a large decrease in the wet concrete modulus of elasticity. 1998 modulus values for section 5 were half the value of the other test sections. Section 5 cores also had the most microcracking, gel, and reacted aggregate particles, identified by petrographic examination.

From petrographic studies of one core in 1998, sections 1 (1 percent LiOH (S)) and 2 (0.5 percent LiOH (S)) had fewer microcracks, gel, and reacted particles than the control. However, section 10 (1 percent LiOH (G)) with Grevey aggregate had similar distress as the control.

Sections 3 (Lomar (S)) and 4 (Class F (S)) had less microcracking than the control but similar numbers of reacted particles. All cores exhibit some internal microcracking, gel, and reacted particles.

ASR has not reduced serviceability of any of the test sections after 6 years. However, Class C fly ash addition with Shakespeare aggregate has accelerated deterioration. The addition of Class F fly ash, combined Class F and Class C fly ash, and Lomar (HRWA) may have improved the ASR resistance of concrete made with Shakespeare aggregate. However, none of the test materials has eliminated ASR only affected its rate. No clear or significant differences have been seen when using Class F fly ash, Class C fly ash, or 1 percent LiOH with Grevey aggregate. Continued monitoring of this test pavement is recommended.

**Table 45. Summary of petrographic examination of cores for 1998
(S = Shakespeare, G = Grevey).**

Section	Description
1 1% LiOH (S)	Few instances of deterioration. The wearing surface has a slightly to moderately worn surface with occasional popouts over aggregate particles. Three microcracks were counted, and 24 occurrences of alkali-silica gel. Three coarse and 36 fine aggregate particles show slight evidence of reaction.
2 0.5% LiOH (S)	The wearing surface has a moderately worn surface on which aggregate particles are occasionally exposed. The core is very slightly distressed. Seven cracks and 24 instances of alkali-silica gel were counted. Two coarse and 27 fine aggregate particles show evidence of reaction. One fine aggregate particle was severely distressed.
3 Lomar (S)	The wearing surface is moderately severely worn with frequent exposed aggregate particles, some apparently in old, worn popouts. The core shows abundant evidence of reaction but little distress. Two microcracks and 68 occurrences of gel were detected. Two coarse and 35 fine aggregate particles show evidence of reaction or distress.
4 Class F Fly Ash (S)	The wearing surface is severely worn with frequent exposed coarse and fine aggregate particles. Surface wear is too great to determine whether it included any popouts. The core shows evidence of reaction but little distress. Five microcracks were detected, and 51 instances of alkali-silica gel. Ten coarse and 51 fine aggregate particles showed evidence of distress or reaction.
5 Class C Fly Ash (S)	The wearing surface is severely worn, with numerous exposed coarse and fine aggregate particles, one empty coarse aggregate particle socket, and five visible cracks, three of which intersect near the center of the core. The core is severely distressed. In addition to the features noted above, Two hundred fifty-four microcracks and 135 instances of alkali-silica gel were counted. Fifty-two coarse and 75 fine aggregate particles show evidence of reaction or distress.
6 Control (S)	The wearing surface is moderately worn with occasional exposed coarse and fine aggregate particles. The core shows slight evidence of distress or deterioration. Twenty-six microcracks and 25 instances of alkali-silica gel were counted. Fourteen coarse and 32 fine aggregate particles show evidence of reaction or distress.
7 Blended C & F Fly Ash (S)	The wearing surface is moderately worn with frequently exposed aggregate particles. The core shows considerable evidence of reaction but little evidence of distress. Ten microcracks and 92 occurrences of alkali-silica gel were counted. Twenty-four coarse and 54 fine aggregate particles showed evidence of distress or reaction.
8 Class F Fly Ash (G)	The wearing surface is severely worn with frequent exposed aggregate particles. There is considerable evidence of reaction but little evidence of distress. Twenty-one microcracks, chiefly contained within reacted aggregate particles, and 45 occurrences of alkali-silica gel were counted. Sixteen coarse and 36 fine aggregate particles showed evidence of reaction or distress.
9 Control (G)	The wearing surface is moderately severely worn with frequent exposed aggregate particles. Although the core contains substantial evidence of ASR, apparent distress is slight. Twenty-one microcracks—chiefly limited to aggregate particles—and 58 instances of alkali-silica gel were counted. Sixteen coarse and 45 fine aggregate particles show evidence of distress or reaction.
10 1% LiOH (G)	The wearing surface is moderately worn with moderately frequent exposed aggregate particles. The core contains abundant evidence of reaction, but little evidence of distress. Eighteen microcracks—all contained in aggregate particles—and 77 instances of alkali-silica gel were counted. Twenty-one coarse and 51 fine aggregate particles showed evidence of reaction or distress.
11 Class C Fly Ash (G)	The wearing surface is severely worn with frequent exposed aggregate particles. The core contains frequent evidence of reaction, but little evidence of distress. Eleven microcracks were counted, and 55 instances of alkali-silica gel. Sixteen coarse and 60 fine aggregate particles show evidence of distress or reaction.

Table 46. Summary of petrographic examination.

Section No.	Microcracks	Gel	Reacted Coarse Particles	Reacted Fine Particles	Total Events
1	3	24	3	36	66
2	7	24	2	27	60
3	2	68	2	35	107
4	5	51	10	51	117
5	254	135	52	75	516
6	26	25	14	32	97
7	10	93	24	54	181
8	21	45	16	36	118
9	21	58	16	45	140
10	18	77	21	51	167
11	11	55	16	60	142

CHAPTER 6. FALLING WEIGHT DEFLECTOMETER RESULTS

INTRODUCTION

The FWD is an impulse loading device used to simulate moving wheel loads and measure the corresponding pavement response. The FWD applies a dynamic load by dropping a mass from a predetermined height, as illustrated in figure 61. The mass drops onto a foot plate connected to a rigid 30-cm diameter base plate by means of thick rubber buffers, which act as springs. The falling weight subassembly is furnished so that different load magnitudes can be applied by varying the mass and drop height. The FWD load signal is a transient pulse with a duration of 25 to 35 milliseconds. Seismic transducers, known as geophones, measure the resulting pavement deflection.

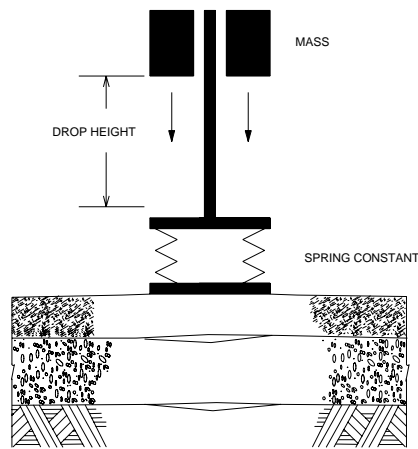


Figure 61. Falling Weight Deflectometer.

METHODOLOGY

Data Collection

The FWD was specified in the contract to test the experimental pavement sections in Nevada, Delaware, California, and New Mexico in an effort to detect ASR. The treatment types, number of slabs per section, and section lengths were variable between the four test sites. Detailed information regarding treatments and test site layout is contained in the previous sections of this report. A brief summary of general cross section information for each site is shown in table 47.

Table 47. General cross section information.

Site	Joint Spacing, ft	Mean Slab Thickness ¹ , inches	Base Type	Base Thickness, inches	Shoulder Type
Nevada	12-13-19-18	8.0	CTB	6.0	PCC
Delaware	40	8.0	CTB	6.0	Curb and Gutter
California	12-13-19-18	8.25	CTB	4.0	AC
New Mexico	18	8.8	CTB	6.0	Curb and Gutter

1 The actual slab thicknesses varied from section to section within each site.

1 m = 3.28 ft

1 inch = 2.54 cm

For each of the concrete slabs located at each test site, FWD testing was conducted at the center of slab, edge of slab, and in the right wheelpath at the joint. At each test point, at least one drop at each of three load levels—40.03, 53.38, and 71.17 kilonewtons (kN) (9, 12, and 16 kips)—was made. Figure 62 provides an illustration of the testing locations within each slab. Except where otherwise stated, the data was collected with the following sensor and load configuration for the slab center and joint tests:

- *Mid-Slab or Basin Test*—sensors were placed at (0, 0), (0, 8), (0, 12), (0, 24), (0, 36), (0, 48), and (0, 60) for the center of slab test (or basin test). In this scheme, the coordinates (0, 0) represent sensor placement at center of the FWD load plate, (0, 8) represent sensor placement 20.32 cm (8 inches) from the center of the load plate, and so on. The load itself is placed at the geometric center of the slab for this test.
- *Joint Test*—deflection data was collected with the FWD load placed both on the approach (position 2 in figure 62) and the leave side (position 3 in figure 62). In both cases, data was collected with sensors placed at the locations identical to those noted above for the mid-slab test along with two additional sensors placed at (0, -12) and (12, 0) positions.

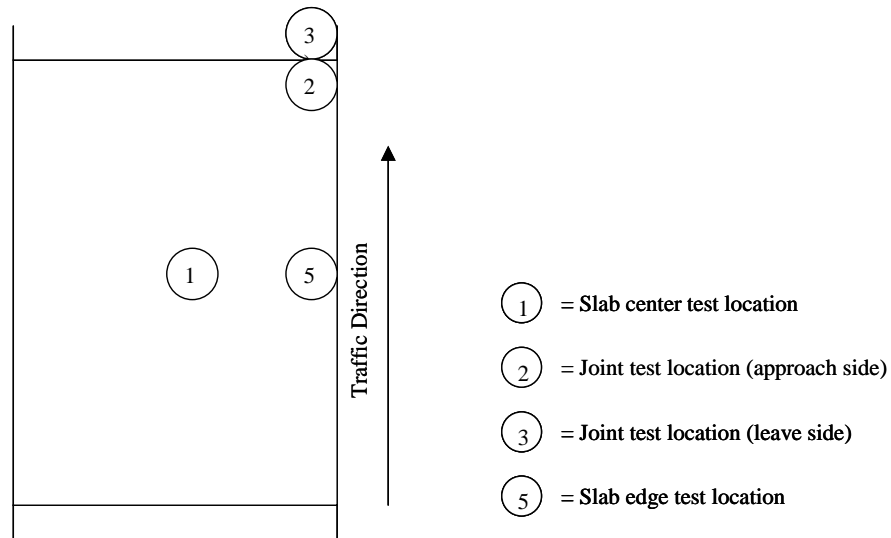


Figure 62. Illustration of testing locations.

FWD testing was conducted on all sites in all 5 years of the performance monitoring period—1994 through 1998. The testing was generally conducted between the months of October and December of each year. Weather-related problems (rain and snow) prevented the collection of FWD data other than the center slab deflections in the year 1996 for the California and Nevada sites.

Data Assembly

Before analyzing any of the deflection data collected, the data were normalized to a 4,086-kg load to account for slight variations in the actual load applied by the FWD. This normalization process was done using standard linear extrapolation techniques and is a routine operation. Further, to make valid performance comparisons on a year-to-year basis, it was necessary to ensure that the testing was done at approximately the same locations within each site. This was an important step in establishing the analysis database. Comparisons of the raw FWD data from each year and each site were made to ensure that test points were indeed collected in the same location. In a few cases, additional test points were discovered in a given year that did not have corresponding test points in the other years. Such data was not considered in further analysis; however, the data was retained in the final deflection database.

PERFORMANCE INDICATORS AND THEIR SIGNIFICANCE

The elastic modulus of the concrete, E_{PCC} , and the joint deflection load transfer efficiency were selected as the primary indicators of the performance of the pavement sections considered in this study. The E_{PCC} values were obtained from the FWD data collected at the center slab location through a process known as backcalculation, whereas the joint load transfer efficiencies (LTE) were obtained from the data collected at the joint by taking a ratio (expressed as a percentage) of the deflections on the unloaded and loaded slabs. Data obtained by placing the load in position 3 in figure 62 was used to estimate the LTE. Other parameters that were also studied include the maximum deflection, D_o , obtained from the basin test and the joint test locations. The deflection response was analyzed since it is a direct indicator of performance and is not subjected to process

errors unlike the backcalculated E_{PCC} values. Further, the modulus of subgrade reaction, k , determined from the backcalculation process was also analyzed because this has a big impact on the backcalculated pavement layer modulus values and the deflection responses.

The backcalculation routine employed in this study is outlined in the American Association of State Highway and Transportation Officials (AASHTO) *Design Supplement* (AASHTO, 1998) as well as in the research report *LTPP Data Analysis*.⁽¹⁾ Another backcalculation routine known as the “best fit” method was also considered initially. This method has been developed recently and is based on minimization of error between the predicted and measured deflections. One advantage of this method over the AASHTO method is that it is far less sensitive to irregularities in the deflection profile. However, preliminary comparisons of these two methods did not reveal any significant differences. Therefore, the AASHTO method was retained for further analysis. Unlike many iterative methods, the AASHTO method is based on closed-form solutions. The method models the pavement system as a rigid plate resting on a dense-liquid foundation. Based on the deflection data from the seven FWD sensors, the routine backcalculates the composite elastic modulus for combinations of all bound layers above the subgrade and the subgrade modulus of reaction (k -value). Once the composite modulus is known, it can be separated into component layer moduli based on the pavement layer types and thicknesses. The backcalculated k -value, unlike the moduli of the overlying pavement layers, is independent of the overlying pavement structure and is not susceptible to process errors arising from assuming uniform layer thicknesses along a given section.

As stated above, the primary parameter of interest derived from the FWD basin test data was the PCC elastic modulus, E_{PCC} . Monitoring E_{PCC} over time gives an indication of the structural integrity of the concrete within a given section. If a slab shows extensive map cracking due to ASR, as was the case with most of the sections considered in this study, it is hoped that it will be reflected in its backcalculated E_{PCC} . Further, as the ASR progresses with time, the E_{PCC} is expected to drop due to increased map cracking. The existence of these correlations between E_{PCC} and the total area affected by map cracking (determined from distress surveys) were investigated in this study. A correlation between maximum deflection, D_o , at the slab center and the area affected by map cracking was also investigated to evaluate the FWD’s ability to pick up on ASR-related distress. Another parameter that was carefully analyzed was the joint load transfer. Most materials-durability problems such as ASR manifest themselves in their most severe forms around the transverse joints and cracks of the pavement. This, in turn, proportionately reduces the LTE of the joint. Therefore, by observing the changes in the joint LTE values over time, an indirect measure of the structural integrity of the pavement can be obtained. It was hoped that a correlation could be developed between LTE and joint distress data. Further, the joint spalling can be expected to be more severe on the leave side of the slab. Therefore, the maximum leave slab deflection, D_o , from the joint test was also evaluated.

FWD DATA ANALYSIS FOR THE NEVADA SITE

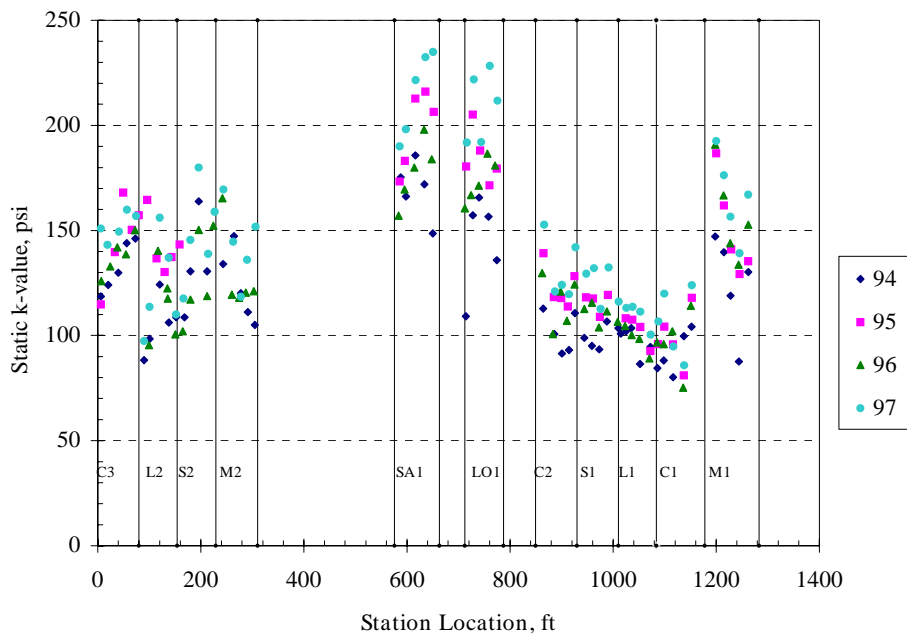
The Nevada test site had a 20.3-cm PCC pavement resting on a 15.2-cm cement-treated base, and 7.6-cm granular subbase. The joints were undoweled and skewed, and the joint spacing had a repeating pattern (see table 47). The site was treated with four different types of materials and had three control sections with no treatment. Some of the treatments were repeated along the site

to yield a total of 11 test sections. Figure 2 presents the layout of the site with the different sections and their respective acronyms identified.

The FWD testing within this site contained a minimum of four test points per treatment with some treatment sections containing as many as six test points. An exception to this is the 1998 data, which contained only one test point for the SA1 section, two test points for the C2 section, and three test points for the S1 section. The wheelpath joint data was collected with the following sensor configuration: (0, -12) (0, 0) (0, 12) (0, 18) (0, 24) (0, 36) (0, 60). The center slab data and the wheelpath data were analyzed, and their results are discussed below.

Subgrade k-value

A plot of the static k-value determined for the Nevada site for years 1994 through 1997 from the basin test data is shown in figure 63. Note that the k-value reported is the composite value, which takes into account both the existing subgrade and the 7.6-cm granular subbase layer. Further, the values reported in the plot are static k-values obtained by multiplying the backcalculated value by 0.5.



1 psi = 6.89 kPa
 1 m = 3.28 ft

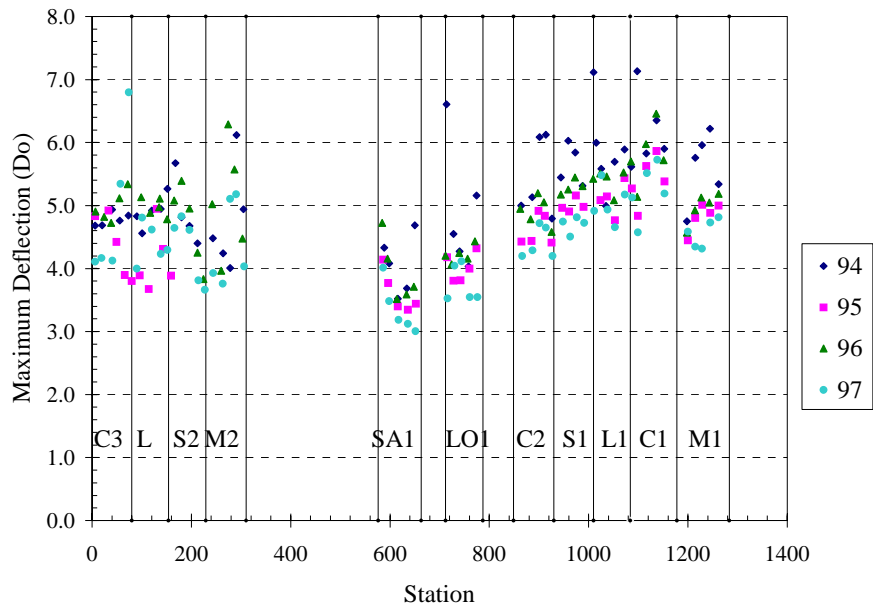
Figure 63. Static k-values for Nevada test section.

It can be noted from figure 63 that the subgrade k-value continually changes from one end of the site to the other. For example, the mean k-values of the C2, L2, S2, and M2 sections are approximately at the same level and are lower than the mean k-values for the SA1 and LO1 sections. Further, there does not seem to be a clear time-series trend to the subgrade values between the various years of testing. The k-value ranges from 517 kPa to about 1,724 kPa (75 psi

to about 250 psi) if the entire site is taken into consideration. This could potentially cause significant differences in the pavement responses along the test section.

D_o (Center Slab)

In figure 64, the variation of the maximum pavement deflection, D_o , measured from the basin test, was plotted for the various treatment sections. Each year in which the data was collected was plotted as a separate series. It can be seen from the figure that D_o varies greatly from section to section and from year to year. Comparing figures 63 and 64, the main cause of variation between the sections appears to be due to differences in subgrade support. For example, it can be noted from figure 63 the static k-value for the SA1 and LO1 treatment sections have the highest value for subgrade support. Thus, it is not surprising that these sections have the lowest deflection. However, what is unexpected is that the average deflection for each section appears to be decreasing slightly from year to year. Thus, the D_o parameter does not appear to have any correlation with the observed map cracking, which was noted to be increasing with time.



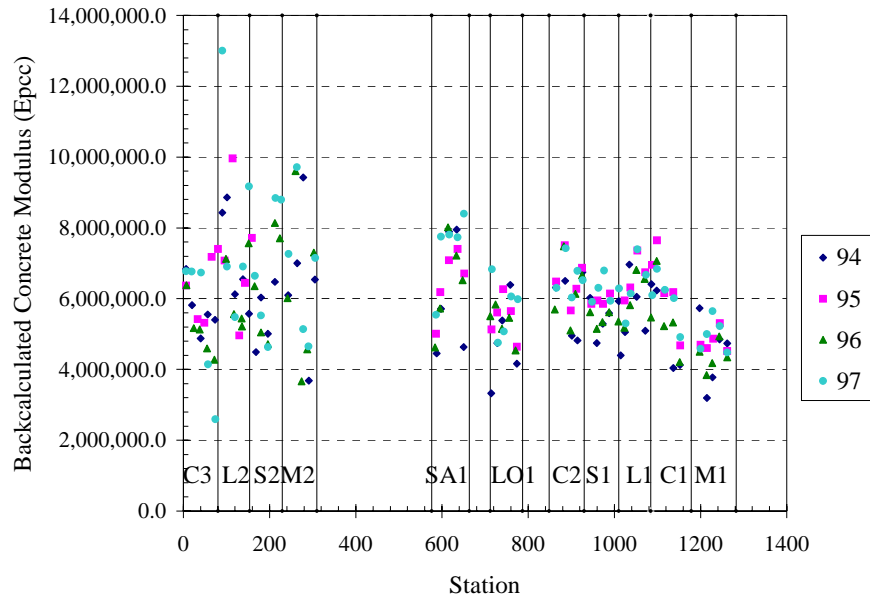
(Station location is in feet; 1 m = 3.28 ft)

Figure 64. Nevada test site— D_o from center slab.

E_{PCC} (Center Slab)

Figure 65 presents the section-to-section and year-to-year variation of backcalculated E_{PCC} for the Nevada site. Unlike the center slab D_o data, the backcalculated E_{PCC} data shown in the figure is relatively consistent between the sections throughout the site. Because the k-value is accounted for in the backcalculation process, the difference in subgrade support conditions does not cause the large section-to-section variability seen with the D_o parameter. Further, unlike what was found from laboratory modulus testing, no significant difference was noted in the modulus values between sections located on the east end (C1, C2, L1, M1, and S1) and west end (C3, L2, M2, S2) of the test site. However, the times series trends show that the average E_{PCC} for each

section increases slightly with time. This trend is contrary to what was expected, since the increase in map cracking over time should result in a lower E_{PCC} .



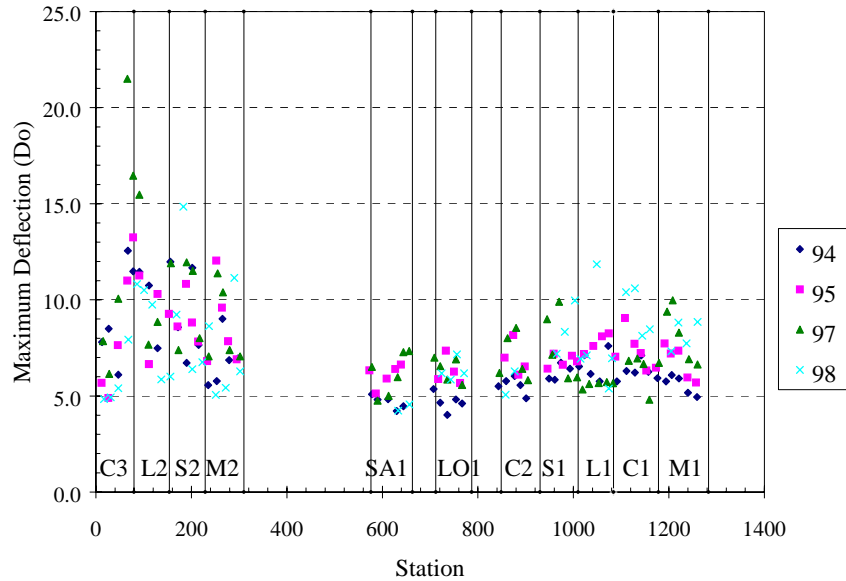
(Station location is in feet; 1 m = 3.28 ft)

Figure 65. Nevada test site— E_{PCC} from center slab.

Note that in figure 65, the values of E_{PCC} range from 27,579 to 55,158 megapascals (mPa) (4 to 8 million psi). These numbers are higher than the previously reported laboratory values and also are relatively high for a pavement showing medium-to-high severity map cracking. However, it should be kept in mind that the backcalculated moduli do not necessarily agree with laboratory values since the loading rates and test conditions are quite different. Further, in backcalculating the pavement layer moduli, constant pavement and base layer thicknesses were assumed for the pavement layer—an assumption seldom realized in the field due to construction variability. However, despite these discrepancies, the higher E_{PCC} values should not be of concern since only the relative change of modulus along the project and between the various testing instances is being evaluated.

D_o (Joint—Leave Side)

The D_o data collected on the leave side of the joint, shown in figure 66, remained relatively consistent throughout the 5-year period. Some variation was identified between the years, but D_o was increasing in some years and decreasing in others. The variation in D_o appears to be temperature-related rather than ASR-related. No trend of increasing D_o with time was observed, belying expectations. Thus, this parameter did not correlate with the observed joint distress data, which was increasing with time. However, as expected, the mean D_o values for each treatment section were relatively greater than those at the mid-slab location.



(Station location is in feet; 1 m = 3.28 ft)

Figure 66. Nevada test site— D_o from leave side; deflection LTE (wheelpath).

The average joint load transfer data for each treatment section is plotted in figure 67 for each year in which testing was conducted. The LTE values do not show a downward trend corresponding to the increased joint distress, as was noted in figure 10. LTE values range from approximately 30 to 88 percent with a significant amount of the data above 50 percent. The higher LTE values are inconsistent with a deteriorated, undoweled joint. A careful examination of the data revealed that the temperature at the time of testing was major confounding factor affecting the LTE values computed and can be used to explain some of the inconsistent and highly variable results. The average temperatures at the time of FWD testing for each treatment section are presented in figure 68. Ideally, the pavement temperature should be relatively constant for the entire data collection effort to make valid comparisons.

However, this condition seldom is realized in the field. It can be noted from figure 68 that the temperature varied from section-to-section during each visit (with some years, such as 1994, having a higher fluctuation than the others) as well as between visits. Comparing the temperature at the time of testing with the deflection LTE along the project length, it can be observed that the higher LTE values correspond to the higher test temperatures and vice versa. This is expected since the joints lock up at the higher test temperatures and produce higher load transfer values. Further, the fluctuation of the LTE values for each section seem to correlate more with the temperature at testing than any change in the real condition of the pavement.

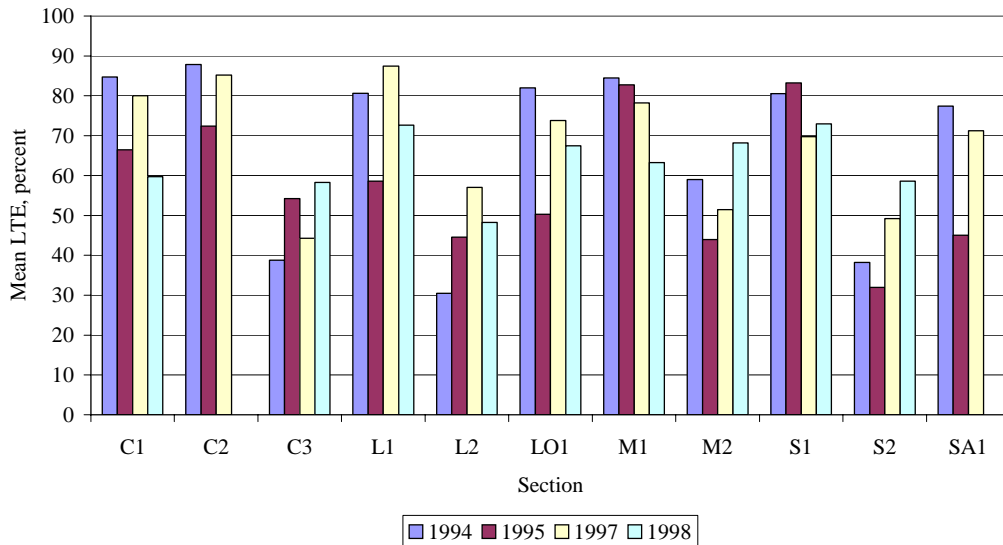
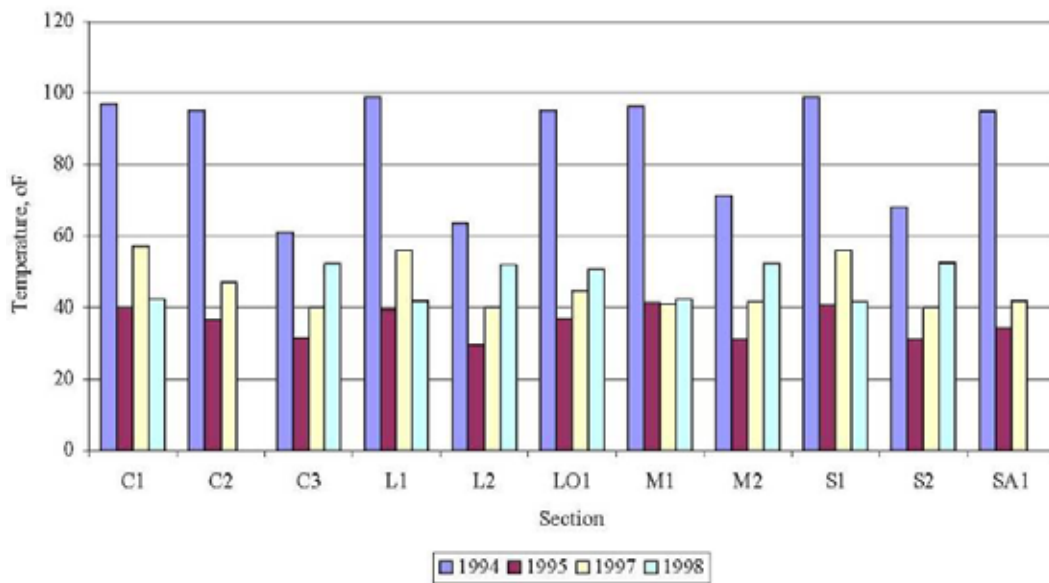


Figure 67. Average LTE values for the various treatment sections for the Nevada site.



$$^{\circ}\text{C} = (^{\circ}\text{F} - 32) / 1.8$$

Figure 68. Average temperatures at time of joint testing for the Nevada site.

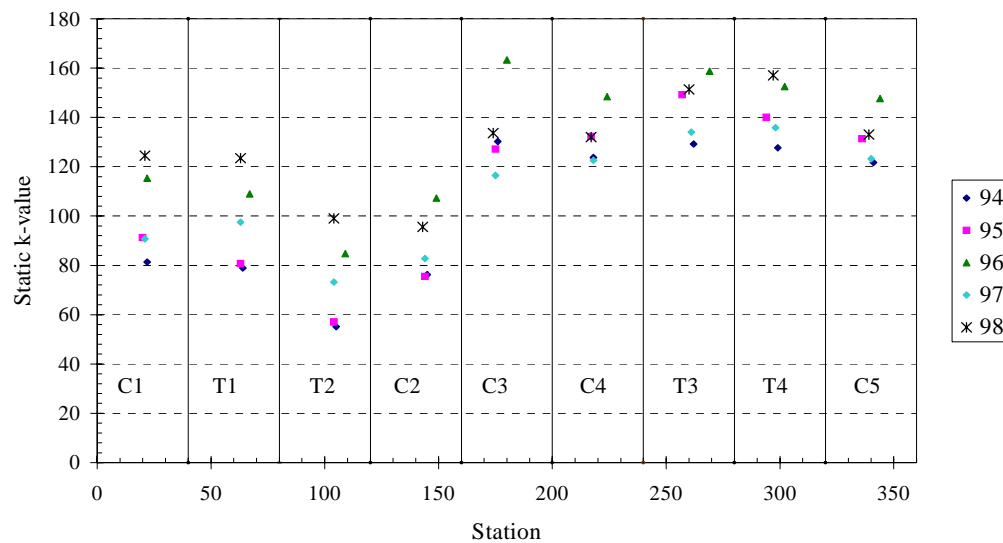
FWD DATA ANALYSIS FOR THE DELAWARE SITE

The test section in Newark, DE, was a relatively short section with a total project length of approximately 109.8 m. Only one type of treatment (lithium hydroxide—LIOH) was applied to this site to mitigate the ASR, and its performance was compared with side-by-side control sections. In all, there were four treatment sections (T1 through T4) and five control sections (C1 through C5). A description of the test section layout and the differential drainage conditions was presented in earlier sections of this report.

All of the Delaware data, with the exception of data from 1995, was collected using the standard sensor spacing described in the introduction. The 1995 data was also collected with the standard sensor spacing with the exception that the (12, 0) side sensor was not used. The Delaware testing locations consisted of one center slab and one leave side LTE test point per treatment in each year. An exception to this was that the C2 and C3 sections for LTE locations were not tested in 1995. Also, the LTE test points for the C5 section could not be collected in 1998. The various conclusions drawn from analyzing this data are presented below.

Subgrade k-value

The variation of the subgrade support along the project was analyzed as a first step. Figure 69 presents a plot of the static subgrade k-value for the various sections.



(Station location is in feet; 1 m = 3.28 ft)

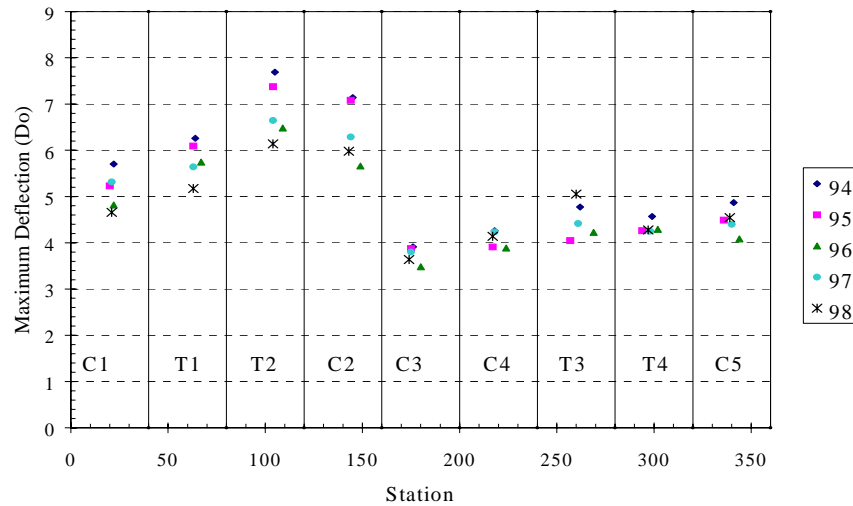
Figure 69. Static k-values for the Delaware site.

The static k-values were derived from the dynamic values obtained from backcalculation by multiplying the latter by a factor of 0.5. Note that the layout of the sections in the figure is the exact sequential order in which they are arranged in the field. It can be observed from the figure that the site can be divided into two groups based on the spatial variability of the k-values. The group with sections C1, T1, T2, and C2 has a lower mean k-value than the group with sections C3, C4, T3, T4, and C5. Also, there is some variability in the data on a year-to-year basis within each section. Overall, the k-values ranged from 414 to 1,103 kPa/2.54 cm (60 to 160 psi/inch).

D_o (Center Slab)

The variation of the maximum pavement deflection, D_o, measured from the center slab test is plotted in figure 70 for the various treatment sections. Section-by-section analysis of the data revealed that the C2, T1, T2, and C2 sections have a substantially higher D_o than the other test sections. This result does correspond to the observed distress data, which also showed higher level of map cracking in these areas. This can be explained by the drainage and subgrade

conditions. As described in the visual distress portion of this report, the first few sections of the Delaware test site were located in the low portion of a sag vertical curve and thus were exposed to more water during the wet months. This higher exposure could have weakened the pavement layers and increased the potential for materials-related distresses, including ASR. Further, as noted in figure 69, static mean k-value for this group of sections is lower than that for the remaining sections. This could be due to poor drainage or soil conditions. Regardless of the cause, the lower k-values could also have led to poorer structural performance.



(Station location is in feet; 1 m = 3.28 ft)

Figure 70. Delaware test site—Do from center slab test.

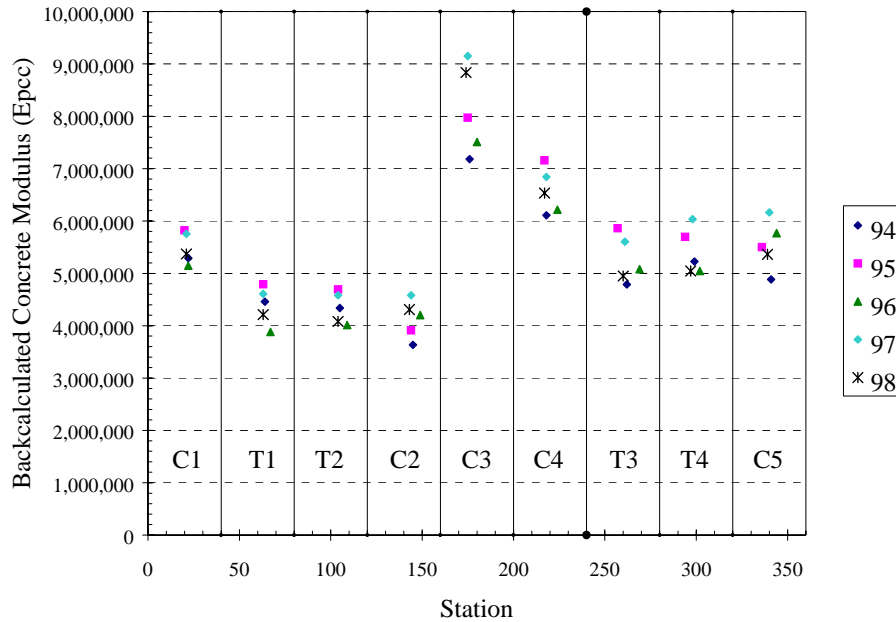
It can be noted from figure 70 that D_o varies slightly from year to year. When each section was analyzed individually on a year-to-year basis, D_o remained relatively constant for most sections, with some sections showing a slight downward trend. This result is contrary to the observed distress data, which shows map cracking is increasing with time. Variations in layer thicknesses, which were assumed to be constant in the backcalculation procedure, and variations in subgrade support conditions are likely responsible for this apparent discrepancy.

Backcalculated Concrete Modulus, E_{PCC}

Figure 71 shows the variation of the E_{PCC} along the section. Once again, there is a clear distinction in the modulus values of sections C1, T1, T2, and C2 compared to the remaining sections. The modulus values for these sections are lower and, as explained before for the D_o data, are perhaps influenced by the map cracking prevalent in these sections. A similar trend was observed from the laboratory tested modulus values. However, the absolute magnitudes of the backcalculated moduli are far greater than their laboratory counterparts.

An examination of the time series data reveals that, similar to the D_o pavement response, the backcalculated E_{PCC} remained relatively constant with time. A few sections showed a slight upward trend with time. Based on these results, the E_{PCC} parameter is not able to pick up on the observed data, which shows map cracking to be increasing with time. Thus, map cracking is not affecting the apparent structural capacity of the pavement, or more likely, the effects of slight

variations in layer thickness and subgrade support conditions are interfering with the FWD's ability to distinguish between the different levels of map cracking observed in this section.



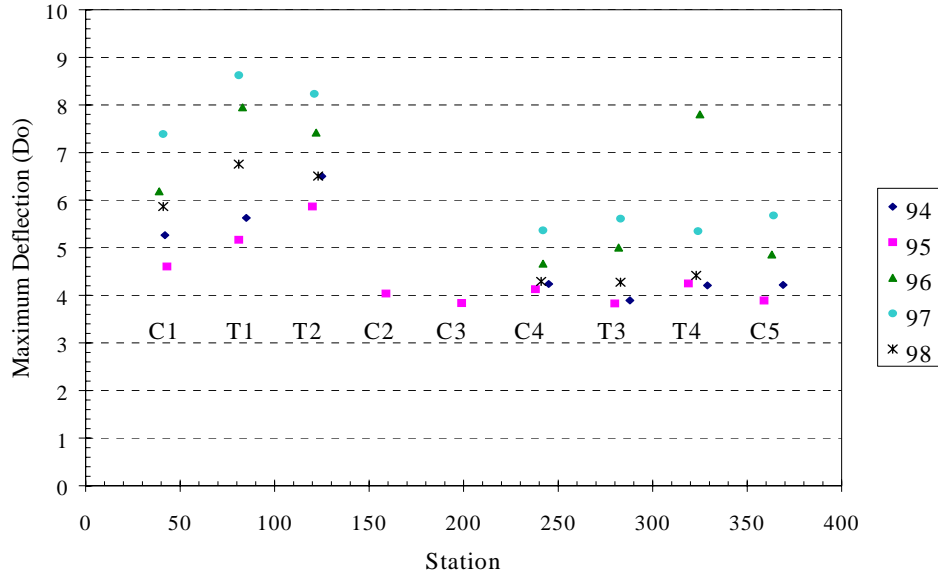
(Station location is in feet; 1 m = 3.28 ft)

Figure 71. Delaware test site—EPCC from center slab.

D_o (Joint—Leave Side)

Figure 72 presents the variation of the maximum deflection data collected at the joints along the Delaware site. The data in the figure suggests that D_o did show a slight increasing trend with time from 1994 through 1997. However, the measured D_o dropped sharply in 1998, and overall the leave side D_o response did not reveal a difference between the treated and the non-treated sections. For the Delaware test site, both the FWD data and the observed distress data indicated that the drainage differences between the sections has a far greater influence on pavement performance than the treatment type.

Of the four pavement response parameters analyzed, D_o on the leave side of the joint showed the best correlation with the observed joint distress data. A statistical analysis consisting of a Duncan grouping was performed on this data. Because the Delaware site contained only one test point per section, the data from all years was grouped together. The Duncan grouping confirmed that the D_o parameter mirrored the observed joint distress data. The observed data showed that sections in the poor drainage areas of the site exhibited the highest levels of joint distress. Likewise, the Duncan grouping showed that maximum mean deflection for treatment sections C1, T1, and T2 were higher than and statistically different from the maximum mean deflections in sections C4, C5, T3, and T4. The results of the Duncan grouping are shown in table 48.



(Station location is in feet; 1 m = 3.28 ft)

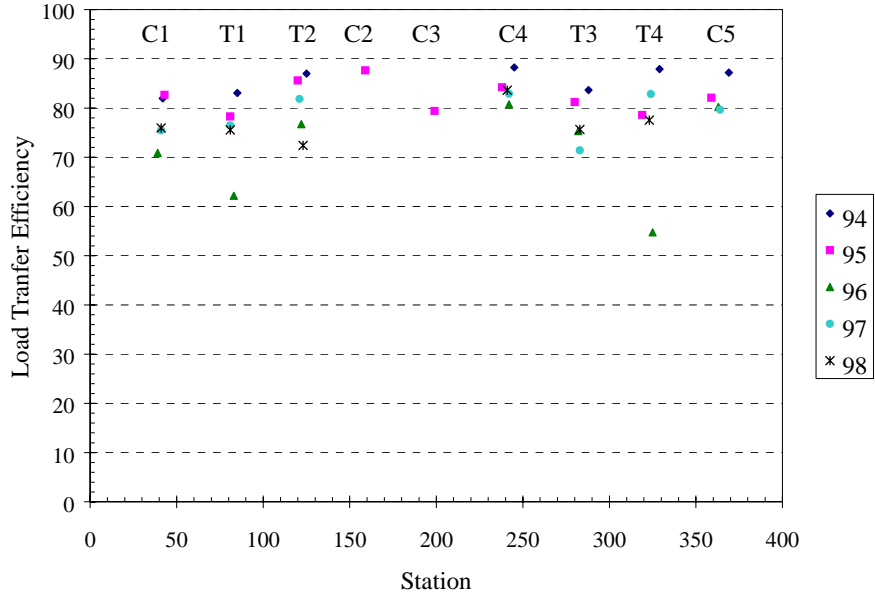
Figure 72. Delaware test site—Do from leave side.

Table 48. Results of Delaware Duncan grouping.

Treatment	Mean Leave Side D_o	Duncan Grouping
T1	7.24	A
T2	7.16	A
C1	6.18	A, B
T4	5.44	C, B
C5	4.92	C, B
T3	4.70	C
C4	4.64	C

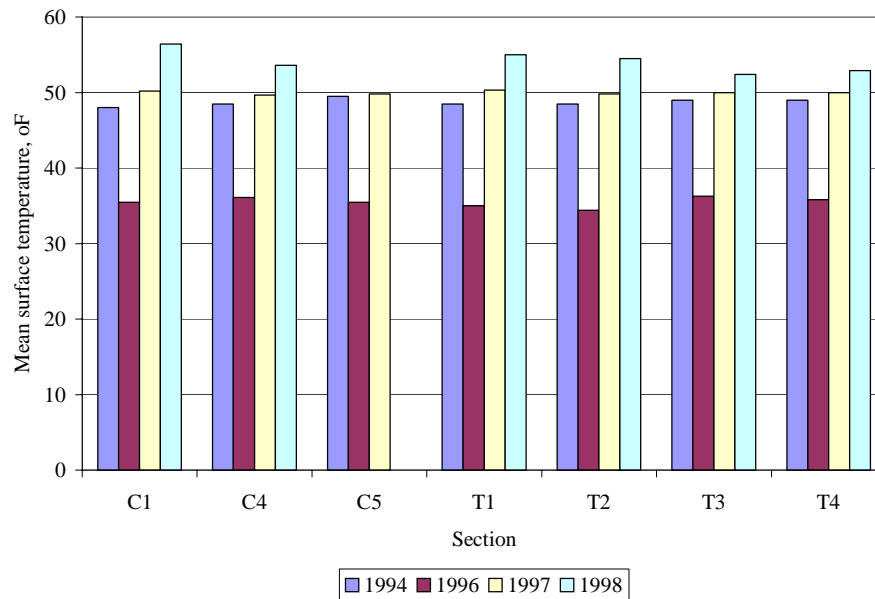
LTE (Joint)

The variation of the LTE values along the project is presented in figure 73. The LTE data is presented both on a yearly and treatment section basis. In both cases, the calculated LTE values remained relatively constant. The magnitudes of the LTE values were also in the high range (between 70 and 90). This is not a totally unexpected finding since most of the joint deterioration (spalling) observed was of low severity. It is possible that the low severity spalling did not cause deterioration to an extent that would destroy the LTE at the joints. Further, unlike the Nevada section, temperature was not a confounding variable. Figure 74 presents the average testing temperature for each year in which the survey was performed. It can be observed from the figure that the temperature was fairly consistent between visits, as well as from the first to the last section during each visit.



(Station location is in feet; 1 m = 3.28 ft)

Figure 73. Delaware test site—LTE.



$$^{\circ}\text{C} = (^{\circ}\text{F} - 32) / 1.8$$

Figure 74. Average temperatures at time of joint testing for the Delaware site.

The test temperatures in all the years were below 15.56 °C, reducing the possibility of the joint lockup.

FWD DATA ANALYSIS FOR THE CALIFORNIA SITE

As noted earlier in the report, the California site had two experimental sites. One of the sites was an overhead structure, and the other was a conventional highway pavement. The pavement test sections were constructed in the early 1970s and had undergone an ASR mitigating treatment in the form of a methacrylate coating. The site consists of three sections coated with methacrylate (M1, M2, and M3) and three control sections (C1, C2, and C3). Figure 38 presented details of the section layout. FWD testing was performed on sections C1, M1, and M2, which are located in the passing lane. The treatment section M2 received an additional coating of the methacrylate in 1995. As noted in table 47, the sections consist of a 21.0-cm PCC layer resting on a 10.2-cm cement-treated base.

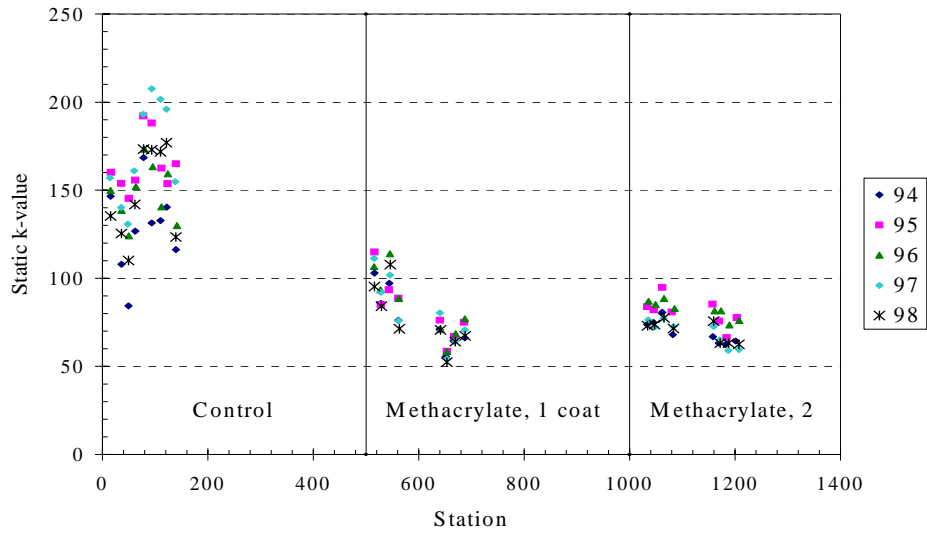
The testing locations contained a minimum of nine test points in the control section and at least eight test points in each of the methacrylate treated sections. Some years contained additional test points in various locations. For data analysis purposes, the data collected on 2/28/95 was designated as 1994 data. Center slab data was analyzed for each of the years 1994 through 1998. Joint test data was analyzed for 1994, 1997, and 1998. The 1995 joint data was not included in the analysis because only the approach side of the joint was tested in 1995. However, this omission is not expected to pose any significant problems in evaluating the performance of the test sections. The 1996 joint data could not be collected due to weather-related problems, as noted earlier.

Subgrade k-value

The variation of the subgrade support along the project was analyzed as a first step. Figure 75 presents a plot of the static subgrade k-value for the various sections. It can be observed from the figure that the control section C1 has a higher k-values on an average compared to the methacrylate sections M1 and M2. The mean k-value of section C1 is approximately 1034 kPa/2.54 cm (150 psi/inch) with a range of 689 to 1,379 kPa (100 to 200 psi), whereas the mean k-value for treatment sections M1 and M2 is approximately 517 kPa (75 psi) with a range of 345 to 689 kPa/25.4 cm (50 to 100 psi/inch). Further, the variability in the k-value on a year-to-year basis is higher for the treatment section C1 than for M1 and M2. These observations will likely assume significance in evaluating the FWD data.

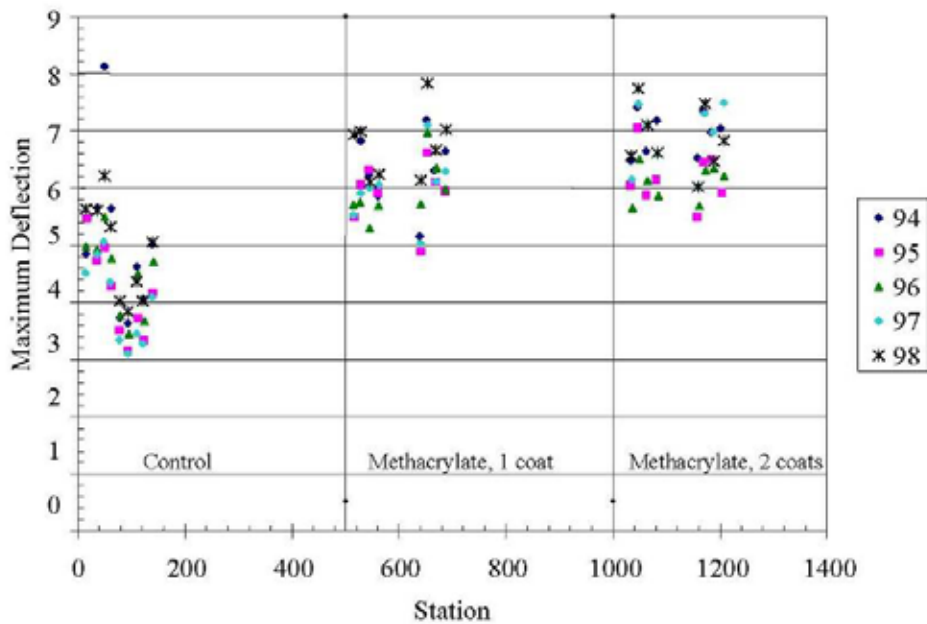
D_o (Center Slab)

Figure 76 shows a plot of the variation of the maximum mid-slab deflection, D_o , along the project length. As expected, the control section, which had a lower subgrade support value, also had higher average deflections than treatment sections M1 and M2. Also, the D_o varies greatly from year to year. Because of this variation, no clear trend of increasing or decreasing deflection in relation to time could be identified.



(Station location is in feet; 1 m = 3.28 ft)

Figure 75. Static k-value for California test section.



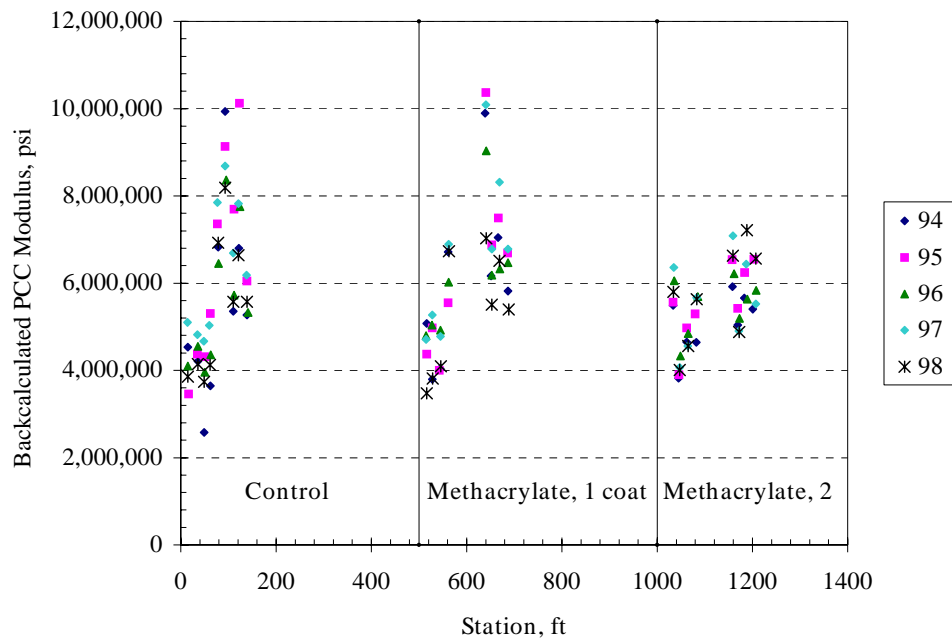
(Station location is in feet; 1 m = 3.28 ft)

Figure 76. California test site— D_o from center slab.

Rather, D_o remains relatively constant over the 5-year testing period, and because of this, no correlation between center slab deflection and map cracking could be developed.

Backcalculated Concrete Modulus, E_{PCC}

The backcalculated concrete modulus is plotted against station location in figure 77. Similar conclusions can be drawn from this figure as from the D_o data. The mean E_{PCC} values are relatively consistent between the treatment sections and over time. There appear to be some spurious deflections in the dataset that result in unrealistic numbers for the E_{PCC} . But if these points are discounted, the E_{PCC} for all the sections range from 27,579 to 55,158 mPa (4 to 8 million psi), which is still relatively high for an old pavement section showing signs of ASR. It was noted from coring data that the thickness of the pavement sections varied along the project length, with some sections substantially thicker than the 21 cm adopted in backcalculation. This could be a plausible explanation for the higher E_{PCC} values.



1 psi = 6.89 kPa

1 m = 3.28 ft

Figure 77. California test site—EPCC from center slab.

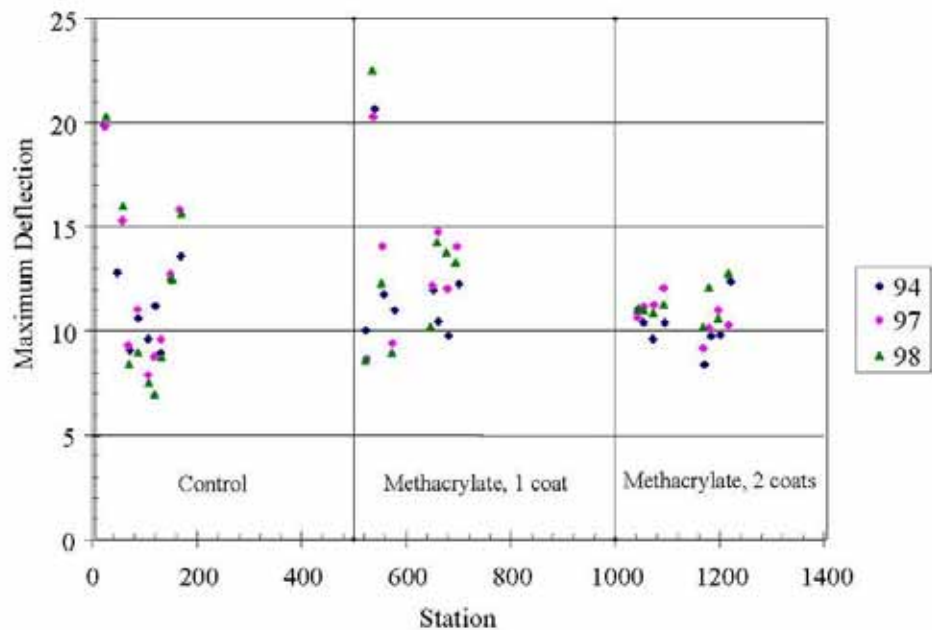
This discrepancy in the magnitudes of modulus values, nevertheless, does not diminish the value of the data presented since only relative trends were being examined here in an effort to correlate E_{PCC} with the amount of map cracking. Based on the data presented there does not appear to be a consistent time-series trend to the modulus values. It was expected that the modulus values will drop with time corresponding to the proportional increase in map cracking. It may be that, just as with D_o at the mid-slab location, the backcalculated moduli are not sensitive to the map cracking since most of the distress at mid-slab was at low severity.

D_o (Joint—Leave Side)

An analysis of the maximum joint deflection data shown in figure 78 showed that the D_o values have a slight increasing trend over time. However, the differences were relatively slight and are

not proportional to the increase in the amount of observed joint distress data. Overall, the levels of maximum joint deflection were about double the maximum interior deflection (mid-slab values), which is as expected. An examination of the average values for each section revealed that the methacrylate 1 section had the highest deflection, followed by the control and the methacrylate 2 sections. It is difficult to postulate what the expected joint deflection over time is expected on jointed pavement having ASR distress. In jointed pavements, without dowels, joint deflection and curling can be large. As ASR develops, the concrete expands reducing joint openings and increasing aggregate interlock across the joint. Joint curling is essentially eliminated and the ride (smoothness) is improved.

As ASR deterioration continues, spalling and loss of integrity at the joints occurs. However, even though the concrete is disintegrating, the joints remain very tight.



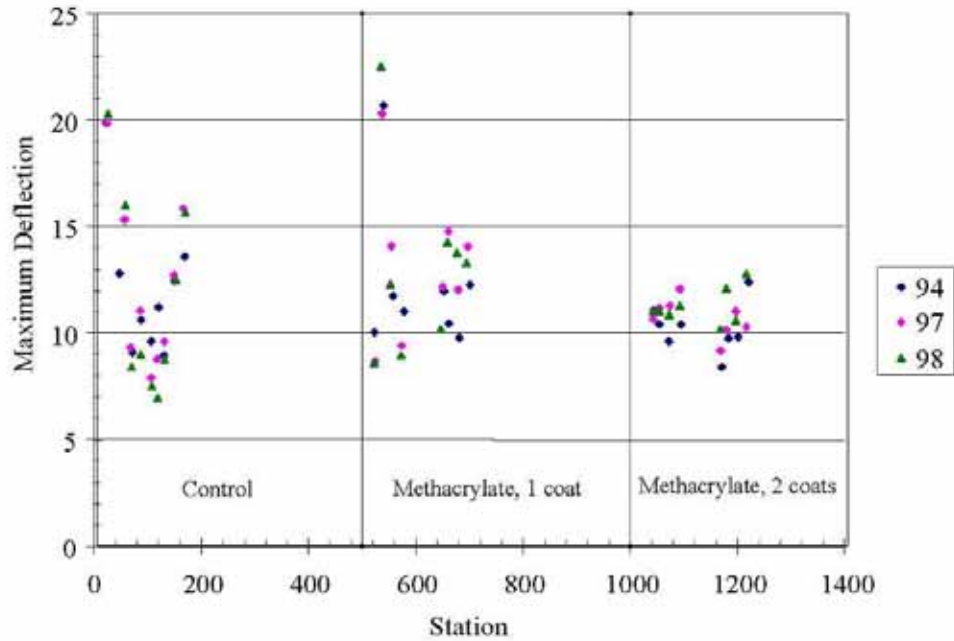
(Station location is in feet; 1 m = 3.28 ft)

Figure 78. California test site—D_o from leave side.

LTE (Joint)

The variation of the LTE along the project is shown in figure 79. Although the load transfer efficiencies are relatively high, the LTE has the best correlation with the observed joint distress data. The average values for each section decrease substantially from 1994 through 1997. There is a slight increase in the LTE from 1997 to 1998 in the methacrylate 1 and control sections, but this is expected given the temperature at the time of testing. For these sections, the test temperature in 1998 was approximately 10 degrees higher than in 1997. For the methacrylate 2 section, the 1997 and 1998 test temperatures were approximately equal, and the LTE continued to decrease. Ranking the average LTE for each section shows the expected correlation with the joint distress data. The methacrylate 2 section has the highest average LTE, followed by the methacrylate 1 section, followed by the control section. A statistical analysis was performed to

determine if the difference in LTE between the treatment types was significantly different. This analysis consisted of a Duncan grouping at an alpha level of 0.05. This analysis confirmed that the LTE for the methacrylate-treated sections was significantly higher than the LTE for the control section. The results of the Duncan grouping are shown in table 49.



(Station location is in feet; 1 m = 3.28 ft)

Figure 79. California test site—LTE.

Table 49. Statistical analysis of California LTE.

1994		
Treatment	Mean LTE	Duncan Grouping
Methacrylate, 2	84.3	A
Methacrylate, 1	80.0	A
Control	63.9	B
1997		
Treatment	Mean LTE	Duncan Grouping
Methacrylate, 2	73.0	A
Methacrylate, 1	69.5	A
Control	52.0	B
1998		
Treatment	Mean LTE	Duncan Grouping
Methacrylate, 1	73.3	A
Methacrylate, 2	71.3	A
Control	61.5	B

FWD DATA ANALYSIS FOR THE NEW MEXICO SITE

The New Mexico test pavement was built specifically to support SHRP ASR research. Details regarding the section layout and treatment types were explained in earlier sections. The pavement is 20.3 cm thick with a 15.2-cm cement-treated base layer. Two different aggregate sources were used in the construction of the various test sections. Class C and F fly ash and lithium hydroxide were the main ASR mitigating treatments. Side-by-side control sections were also provided for comparison. In all, 11 treatment sections were available for comparison. The sections are numbered from 1 through 11 as shown in figure 55.

The New Mexico test locations for the center slab testing consisted of two test points per treatment, except for section 10, which contained only one test point. The test locations for the LTE testing consisted of two test points per treatment with the exception of sections 8, 9, and 10. Sections 8 and 10 contained one test point in each year, and section 9 contained three test points in each year. All data was collected using the standard sensor spacing described earlier.

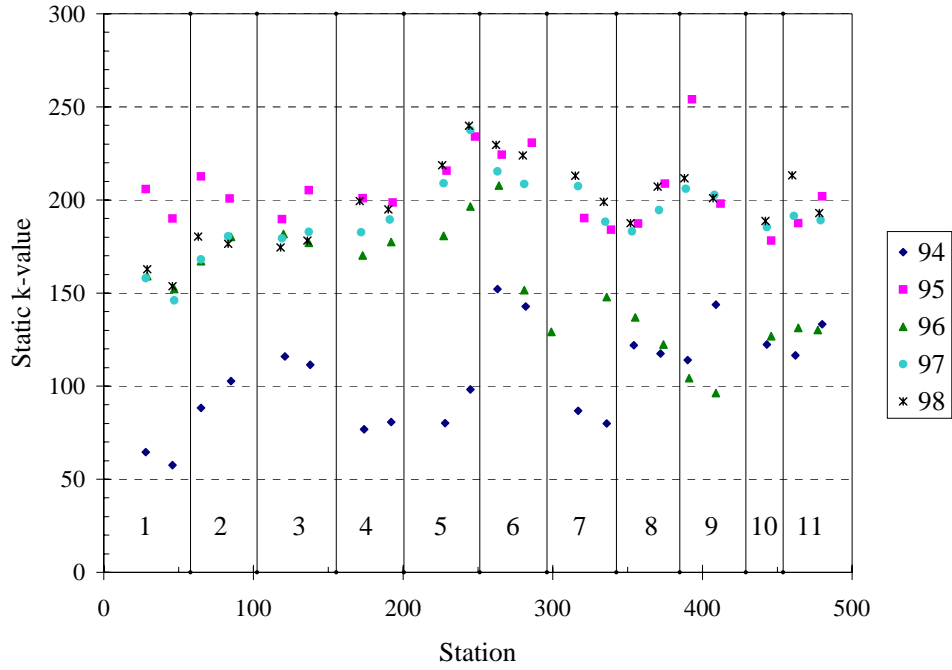
Subgrade k-value

A plot of the variation of the backcalculated subgrade support value along the project is presented in figure 80 for each year the data was collected. The subgrade support value is relatively constant within each visit and between visits for the years 1995, 1997, and 1998. The mean k-value for the various sections based on this data is 1,379 kPa/2.54 cm (200 psi/inch). The k-value is quite variable in 1994 and 1996, with the lowest k-values being recorded in the former year. The type of subgrade soils present at the site location and the saturation state of the soils during the time at which the FWD testing was conducted could likely explain these findings. For example, an intense rainfall event a few days prior to the testing in combination with a moisture-sensitive subgrade soil and poor drainage conditions could lead to a weak subgrade support condition. However, actual occurrence of this event could not be ascertained from the data collected.

D_o (Center Slab)

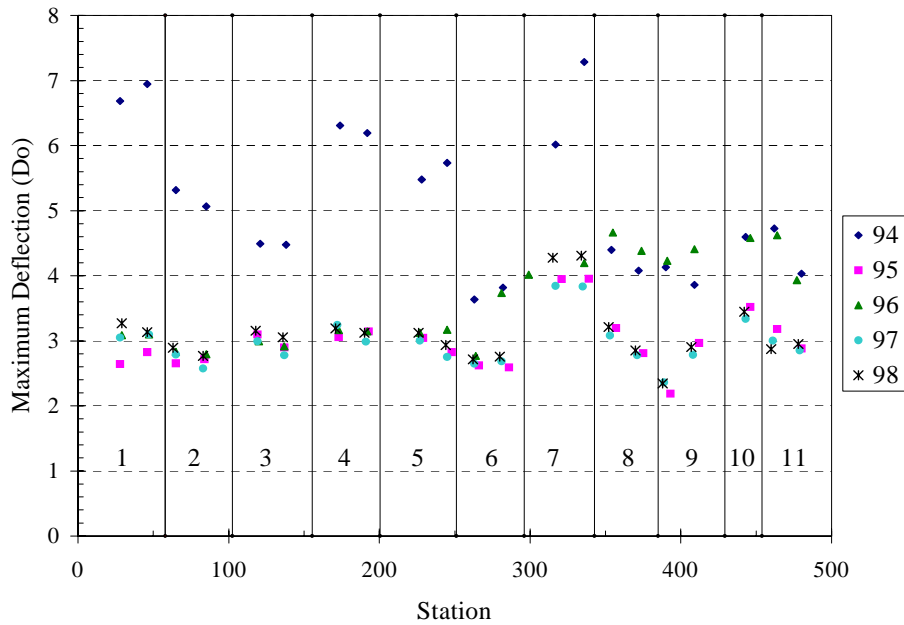
In figure 81, the project variation of D_o is presented for the multiple years in which data was collected. From this figure it can be seen that D_o varies greatly, especially for the 1994 data. The D_o values follow the expected trends based on the subgrade support conditions shown in figure 80. It seems likely that saturated subgrade conditions were present during the 1994 data collection. This would explain the substantially higher D_o values obtained for that year.

An examination of the data on a section-by-section basis and on a year-to-year basis did not indicate any clear trend regarding D_o . There does not appear to be any apparent correlation between D_o and map cracking for this section. Recall that map cracking has been reported to increase in all sections between 1994 and 1998, with the exception of sections 3 and 4; with the last 2 years registering a dramatic increase. However, most of the map cracking reported was of low severity, and it is assumed that the FWD test was not sensitive enough to register this distress.



(Station location is in feet; 1 m = 3.28 ft)

Figure 80. Static k-value for New Mexico test.

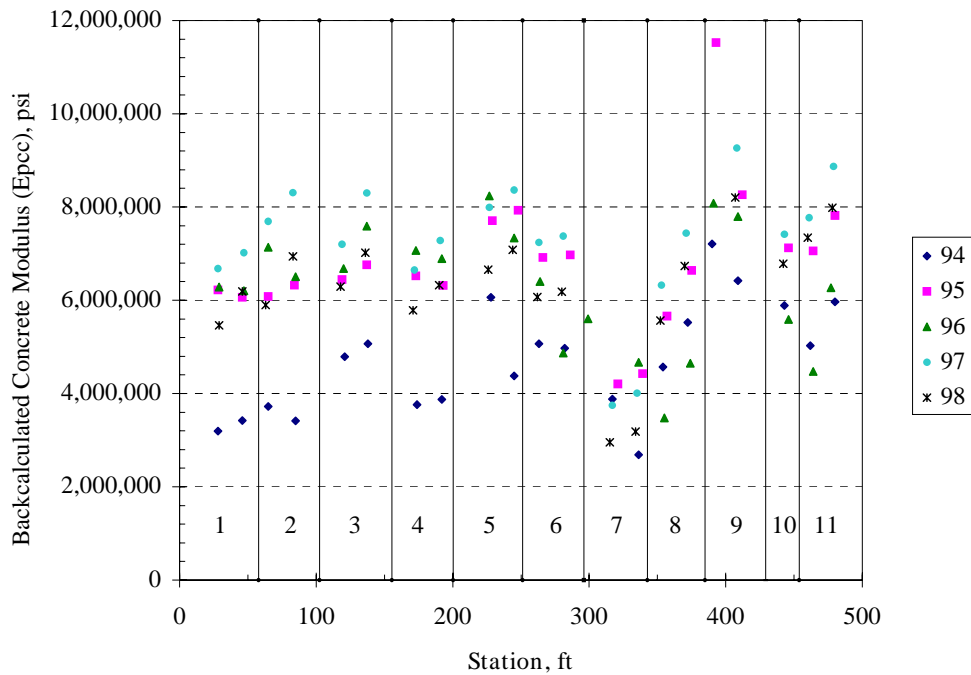


(Station location is in feet; 1 m = 3.28 ft)

Figure 81. New Mexico test site—Do from center slab.

Backcalculated E_{PCC} (Center Slab)

In figure 82, the backcalculated E_{PCC} is plotted for all the treatment sections. Similar to the D_0 pavement response, the backcalculated E_{PCC} remained relatively constant over time. Based on these results, the E_{PCC} parameter is not able to corroborate the observed distress data, which shows map cracking to be increasing over time. Thus, the map cracking is not affecting the apparent structural capacity of the pavement, or more likely, the effects of slight variations in layer thickness and subgrade support conditions are interfering with the FWD's ability to distinguish between the different levels of map cracking observed in this section.



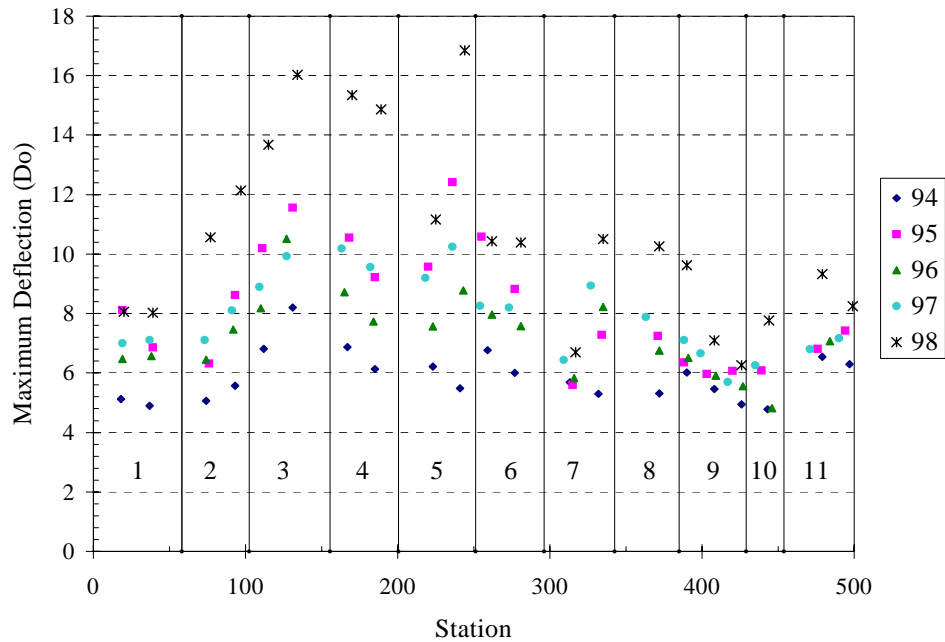
1 psi = 6.89 kPa

1 m = 3.28 ft

Figure 82. New Mexico test site—EPCC from center slab.

D_0 (Joint– Leave Side)

Figure 83 presents the maximum pavement deflection collected from joint testing. As with the D_0 center slab data, the D_0 data taken from the leave side of the joint showed rather large variability. Overall, the data did show a slight upward trend over time corresponding to increased joint distress. However, this trend was not consistent, as the data was confounded by differences in temperatures at testing between sections during each visit. A pictorial representation of the average temperature at the time of FWD testing for each section is presented in figure 84. Other confounding factors include variations in slab thickness due to construction variability and changing subgrade support conditions.



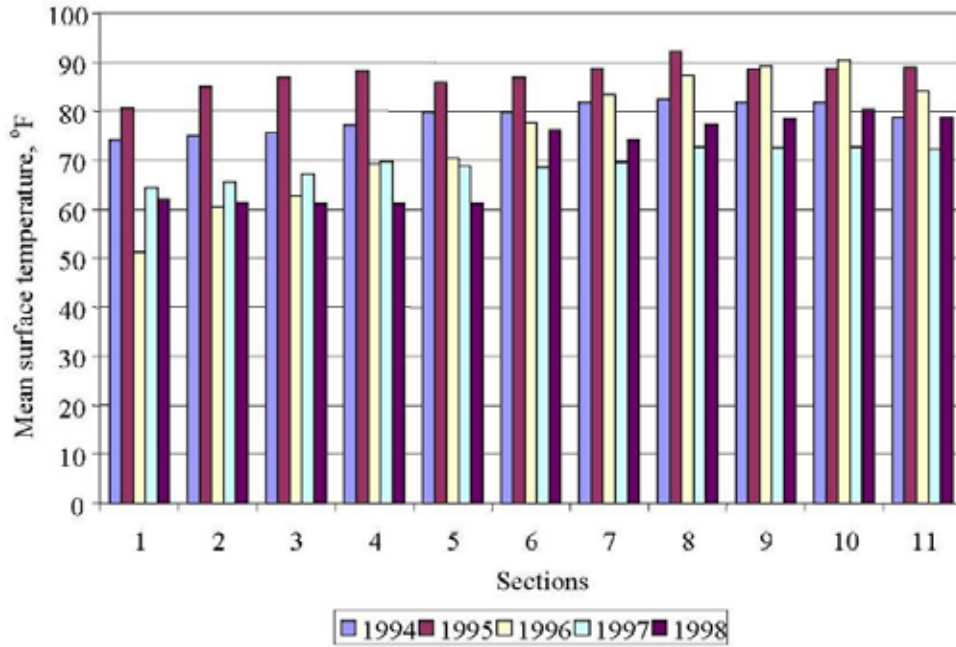
(Station location is in feet; 1 m = 3.28 ft)

Figure 83. New Mexico test site— D_0 from leave side.

Because the D_0 data did at least show the expected trend of increasing with time, a statistical analysis was performed. This analysis revealed some differences between the treatment types; however, these differences appear to be more closely related to temperature and subgrade support conditions than to ASR-related deterioration.

LTE (Joint)

The variation of the LTE along the project is plotted in figure 85. An examination of the LTE data on both a yearly and section-by-section basis revealed that LTE remained relatively constant. The LTE data did not have a significant correlation with the observed joint distress data, and it could not be used to corroborate the benefit of the Class F fly ash treatment. A statistical analysis revealed that the average LTE values for each section belonged to the same group. Thus, no significant differences in LTE values existed between any of the treatment types.



$^{\circ}\text{C} = (^{\circ}\text{F} - 32) / 1.8$

Figure 84. Temperature variation during FWD testing for the New Mexico site.

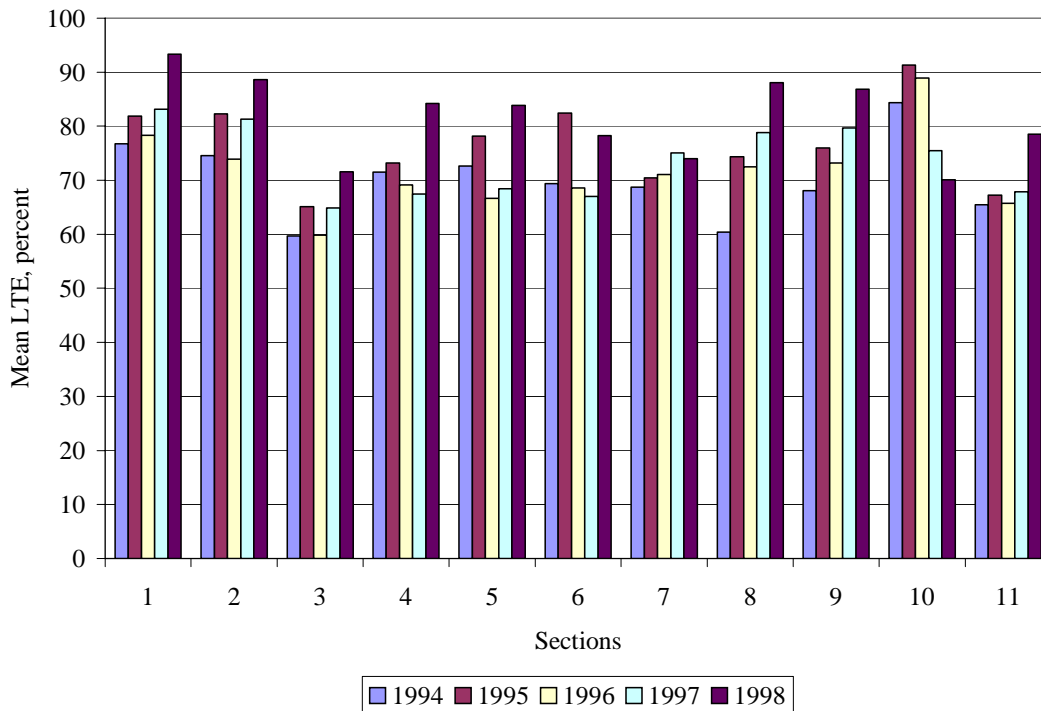


Figure 85. New Mexico test site—LTE.

SUMMARY OF FWD TESTING

Visual surveys confirmed that each of the four experiment sites were accumulating increased amounts of ASR-related distress over the 5-year experiment time frame. It was hoped that correlations could be developed which would relate pavement responses collected by the FWD to the observed ASR-related distresses. To assess the FWD's ability to identify ASR related distress, four pavement response parameters were examined in detail: maximum deflection and backcalculated modulus collected from center slab tests, and D_o and LTE collected from joint tests. It was believed that these four parameters offered the best chance to develop a meaningful correlation to the observed distress data. Attempts were made to correlate center slab D_o and E_{PCC} to the map cracking data. It was expected that D_o would increase and that E_{PCC} would decrease as the observed map cracking increased.

Attempts were also made to correlate D_o and LTE measured at the joints to the observed joint distress data. It was expected that D_o would increase and that LTE would decrease in relation to observed increase joint distress severity.

Based on the analysis results, no significant correlations could be developed linking the FWD data to the observed distresses, particularly when the distresses were of low severity. For all four sites, center slab D_o and E_{PCC} proved to be very poor indicators of ASR-related map cracking. In each of the four sites, D_o and E_{PCC} remained relatively constant over time, and differences between treatment sections at any given site were found to correlate with variations in subgrade support conditions, rather than to the observed differences in map cracking. Further complicating the E_{PCC} analysis is the issue of slight variations in layer thickness. It seems apparent that the effects of subgrade support, temperature, and possible variation from assumed layer thickness far outweigh the FWD's ability to distinguish between varying levels of map cracking.

FWD data collected from joint tests was slightly more promising. The LTE data from the California site correlated well with the observed joint distress data, as did the D_o data from the Delaware site. However, these results are far from conclusive, and overall, the majority of the joint data did not correlate well with the observed distress.

APPENDIX A



(a) Control section 3 (C3)



(b) Lithium Hydroxide section 2 (L2)

Figure A1. Photographs of typical joint sections for each test section (Winnemucca, NV).



(c) Silane section 2 (S2)



(d) Methacrylate section 2 (M2)

**Figure A1. Photographs of typical joint sections for each test section(Winnemucca, NV).
(continued)**



(e) Silane #2 section 1 (SA1)



(f) Linseed oil section 1 (LO1)

**Figure A1. Photographs of typical joint sections for each test section (Winnemucca, NV).
(continued)**



(g) Control section 2 (C2)



(h) Silane section 1 (S1)

**Figure A1. Photographs of typical joint sections for each test section (Winnemucca, NV).
(continued)**



(i) Lithium hydroxide section 1 (L1)



(j) Control section 1 (C1)

**Figure A1. Photographs of typical joint sections for each test section (Winnemucca, NV).
(continued)**



(k) Methacrylate section 1 (M1)

Figure A1. Photographs of typical joint sections for each test section (Winnemucca, NV).
(continued)

Petrographic Report for Winnemucca, NV, 1997

Two sections from each of the cores were cut and lapped. These sections were then soaked overnight and dried, and the entire lapped surface was traversed under a stereo microscope. The lapped surface was divided into five or more traverses and examined at magnifications of 10 to 30 times. All instances of cracks, alkali-silica gel, and deteriorated or reacted aggregate particles were counted.

Core 97-C1-B: The core is classed as slightly to moderately distressed. The wearing surface is severely worn, exposing coarse and fine aggregate particles. Popouts are occasionally identifiable. Sixty-one cracks (chiefly microscopic) and 54 instances of alkali-silica gel were counted. Eight coarse and 22 fine aggregate particles were distressed or had reacted. The core is marginally air-entrained with an estimated air content of 5 percent.

Core 97-C2-A: The core is classed as slightly distressed. The wearing surface is severely worn, exposing coarse and fine aggregate particles. Popouts are occasionally identifiable. Thirty-four cracks and 58 instances of alkali-silica gel were counted. Nine coarse and 42 fine aggregate particles were distressed or had reacted. The core is well air-entrained with an estimated air content of 6.5 percent.

Core 97-C3-A: The core is classified as slightly distressed. The wearing surface is severely worn, exposing coarse and fine aggregate particles. Popouts are occasionally identifiable. Eleven cracks and 50 instances of alkali-silica gel were counted. Three coarse and 27 aggregate particles show evidence of distress or reaction. The core is air-entrained with an estimated air content of 5.5 percent.

Core 97-L1-C: The core is classified as moderately distressed. The wearing surface is severely worn, exposing coarse and fine aggregate particles. Popouts are frequently identifiable. Sixty-five cracks and 39 instances of alkali-silica gel were counted. One coarse and 21 fine aggregate particles show evidence of distress or reaction. The core is air-entrained with an estimated air content of 6 percent.

Core 97-L2-B: The core is classified as slightly distressed. The wearing surface is worn, exposing aggregate particles. Twenty cracks and 32 instances of alkali-silica gel were counted. Twenty-two fine aggregate particles showed evidence of distress or reaction. The core is air-entrained with an estimated air content of 6 percent.

Core 97-LO1-B: The core is classified as moderately severely distressed. The wearing surface is worn, exposing numerous fine and coarse aggregate particles. Popouts are occasionally evident. Seventy-three cracks and 62 instances of alkali-silica gel were counted. Five coarse and 32 fine aggregate particles showed evidence of distress or reaction. The core is marginally to poorly air-entrained with an estimated air content that varies between 4 and 5 percent.

Core 97-M1-C: The core is classed as severely distressed. The wearing surface is worn, exposing coarse and fine aggregate particles. Popouts are occasionally evident. One hundred eighty-five cracks and 81 instances of alkali-silica gel were counted. Several of the cracks are macroscopic. Thirteen coarse and 42 fine aggregate particles showed evidence of distress or reaction. The core is poorly air-entrained with an estimated air content of 4 percent.

Core 97-M2-B: The core is classified as slightly to moderately distressed. The wearing surface is worn, revealing fine and occasionally coarse aggregate particles; 48 cracks and 75 instances of alkali-silica gel were counted. Five coarse and 27 fine aggregate particles showed evidence of distress or reaction. The core is poorly air-entrained with an estimated air content of 4 percent.

Core 97-S1-C: The core is classified as moderately severely distressed. The wearing surface is moderately worn, exposing fine and occasionally coarse aggregate particles. Ninety-seven cracks and 85 instances of alkali-silica gel were counted. Thirteen coarse and 23 fine aggregate particles showed evidence of distress or reaction. The core is air-entrained with an estimated air content of 5.5 percent.

Core 97-SA1-C: The core is classified as moderately distressed. The wearing surface is worn, and popouts over aggregate particles are present. Seventy-seven cracks and 41 instances of alkali-silica gel were counted. Ten coarse and 64 fine aggregate particles showed evidence of reaction or distress. The core is air-entrained with an estimated air content of 6 percent.

Core 97-S2-A: The core is classified as slightly distressed. The wearing surface is worn; shallow popouts over coarse and fine aggregate particles are frequent; 29 cracks and 40 instances of alkali-silica gel were counted. Fourteen coarse and 53 fine aggregate particles show evidence of reaction or distress. The core is air-entrained with an estimated air content of 6 percent.

Petrographic report for Winnemucca, NV, 1998

Sections from each of the cores were cut and lapped. These sections were then soaked overnight and dried, and the entire lapped surface was traversed under a stereo microscope. Each lapped surface was divided into five or more traverse areas and examined at magnifications of 10 to 30 times. All instances of cracks, alkali-silica gel, and deteriorated or reacted aggregate particles were counted.

98-C1-2: The wearing surface appears to be a worn, mechanically ground surface. The core contains abundant evidence of reaction but little distress. Forty microcracks and 129 instances of alkali-silica gel were counted. Seventeen coarse and 115 fine aggregate particles show evidence of reaction or distress. The core is air-entrained with an estimated air content of 7 percent.

98-C2-1: The wearing surface is severely worn with very frequently exposed and polished aggregate particles. The core is severely distressed. Three large cracks, 139 microcracks, and 104 instances of alkali-silica gel were counted; 35 coarse and 129 fine aggregate particles show evidence of reaction or distress. The core is air-entrained with an estimated air content of 6.5 percent.

98-C3-2: The wearing surface is very severely worn with frequently exposed and polished aggregate particles. The core is severely distressed. One large crack, 72 microcracks, and 84 instances of alkali-silica gel were counted. Sixteen coarse and 134 fine aggregate particles show evidence of reaction or distress. The core is air-entrained with an estimated air content of 7.5 percent.

98-LI-1: The wearing surface is severely worn with frequently exposed and polished aggregate particles, and three prominent but tightly closed cracks. The core is moderately to severely

distressed. One large crack, 121 microcracks, and 69 instances of alkali-silica gel were counted. Thirty-one coarse and 81 fine aggregate particles show evidence of distress or reaction. The core is air-entrained with an estimated air content of 5 percent.

98-L2-1: The wearing surface is moderately severely worn with frequent exposed and polished aggregate particles. The core is slightly distressed. Twenty-three microcracks and 88 instances of alkali-silica gel were counted. Sixteen coarse and 126 fine aggregate particles show evidence of reaction or distress. The core is air-entrained with an estimated air content of 5 percent.

98-LOI-2: The wearing surface is moderately to severely worn with frequently exposed and polished aggregate particles. The core is slightly to moderately distressed. Forty-six microcracks and 84 instances of alkali-silica gel were counted. Twenty-seven coarse and 69 fine aggregate particles show evidence of reaction or distress. The core is air-entrained with an estimated air content of 4.5 percent.

98-M1-1: The wearing surface is severely worn or possibly worn and mechanically ground, with frequently exposed and polished aggregate particles. The core is very severely distressed. Seven major cracks, 196 microcracks, and 105 occurrences of alkali-silica gel were counted. Forty-seven coarse and 102 fine aggregate particles show evidence of reaction or distress. The core is air-entrained with an estimated air content of 5.5 percent.

98-M2-2: The wearing surface is severely worn with frequent exposed and polished aggregate particles. The core is moderately distressed. Seventy-five microcracks and 73 instances of alkali-silica gel were counted. Thirty-five coarse and 65 fine aggregate particles show evidence of distress or reaction. The core is air-entrained with an estimated air content of 5.5 percent.

98-S1-2: The wearing surface is severely worn with frequent exposed aggregate particles and occasional popouts. The core is very severely distressed. Two major cracks, 113 microcracks, and 90 occurrences of alkali-silica gel were counted. Fifty-eight coarse and 173 fine aggregate particles show evidence of reaction or distress. The core is air-entrained with an estimated air content of 5.5 percent.

98-S2-2: The wearing surface is worn with frequent exposed and polished aggregate particles. The surface appears to have been machine grooved at one time. One crack and a popout are apparent on the wearing surface. The core is very severely distressed. Three major and 153 microcracks, and 116 occurrences of alkali-silica gel were counted. Forty-five coarse and 102 fine aggregate particles showed evidence of reaction or distress. The core is poorly to marginally air-entrained with an estimated air content of 5 percent.

98-SA1-2: The wearing surface is severely worn with frequent exposed aggregate particles and occasional popouts. The core is severely distressed. One major crack, 114 microcracks, and 78 occurrences of alkali-silica gel were counted; 43 coarse and 156 fine aggregate particles showed evidence of reaction or distress. The core is air-entrained with an estimated air content of 6 percent.

**Table A1. Summary of LTPP survey sheets
for ASR investigation—control section.**

Type	Identification code	Unit	10/18/94	12/12/95	12/5/96	10/9/97	10/28/98
Corner breaks	1L	no.	0	0	0	0	0
	1M	no.	0	0	0	0	0
	1H	no.	0	0	0	0	0
Durability cracking	2L	no.	0	0	0	0	0
	2L	m2	0	0	0	0	0
	2M	no.	0	0	0	0	0
	2M	m2	0	0	0	0	0
	2H	no.	0	0	0	0	0
	2H	m2	0	0	0	0	0
Longitudinal cracking	3L	m	-	6.5	8	9	5.5
	3L (sealed)	m	-	0	0	0	0
	3M	m	16	8.5	12.5	12.5	18.1
	3M (sealed)	m	0	0	0	0	0
	3H	m	0	0	0	0	0
Transverse cracking	3H (sealed)	m	0	0	0	0	0
	4L	no.	6	6	7	7	5
	4L	m	6.5	6.8	8	8	5.6
	4L (sealed)	m	0	0	0	0	0
	4M	no.	5	4	2	0	2
	4M	m	8.8	9.7	4.8	0	3.3
	4M (sealed)	m	0	0	0	0	0
	4H	no.	0	0	2	4	4
4H	m	0	0	5.1	9.9	10.54	
Transverse joint seal damage	4H (sealed)	m	0	0	0	0	0
	Sealed	y/n	Y	Y	Y	Y	Y
	5A1	no.	0	0	0	0	0
	5aM	no.	0	0	0	0	0
Longitudinal joint seal damage	5aH	no.	0	0	0	0	0
	No. sealed	no.	2	2	2	2	2
Spalling of longitudinal joints	5b	m	0	0	0	0	0
	6L	m	0	0	0	0	0
	6M	m	0	0	0	0	0
Spalling of transverse joints	6H	m	0	0	0	0	0
	7L	no.	5	4	3	1	0
	7L (length)	m	13.6	12.8	9.2	2	0
	7M	no.	1	2	2	4	0
	7M (length)	m	2	2.6	3.7	11.2	0
Map cracking	7H	no.	0	0	1	1	6
	7H (length)	m	0	0	2.6	3	18.9
Scaling	8a	no.	-	3	5	8	11
	8a	m2	-	1.2	1.5	2.02	5.9
Polished aggregate	8b	no.	0	0	0	0	0
	8b	m2	0	0	0	0	0
Popouts	9	m2	0	0	0	0	0
Blowups	10	no./m2	1.2	0	0	0	0
Faulting	11	no.	0	0	0	0	0
Lane-shoulder dropoff	12	-	-	-	-	-	-
Lane-shoulder separation	13	-	-	-	-	-	-
Other	14	-	-	-	-	-	-
	WP-L	no.	-	2	-	-	0
	WP-M	no.	-	3	-	-	4
	WP-H	no.	-	0	-	-	1
	CL-L	no.	-	4	-	-	1
	CL-M	no.	-	1	-	-	4
Longitudinal cracking	CL-H	no.	-	0	-	-	0
	Total	m	16	15	20.5	21.5	23.6
	Percent L	-	0	43	39	42	23
	Percent M	-	100	57	61	58	77
	Percent H	-	0	0	0	0	0
Transverse cracking	Total	no	11	10	11	11	11
	Total	m	15.3	16.5	17.9	17.9	19.44
	Percent L	-	42	41	45	45	29
	Percent M	-	58	59	27	0	17
	Percent H	-	0	0	28	55	54
Spalling of transverse joints	Total	no.	6	6	6	6	6
	Total	m	15.6	15.4	15.5	16.2	18.9
	Percent L	-	87	83	59	12	0
	Percent M	-	13	17	24	69	0
	Percent H	-	0	0	17	19	100

**Table A2. Summary of LTPP survey sheets
for ASR investigation—section L2.**

Type	Identification code	Unit	10/18/94	12/12/95	12/5/96	10/9/97	10/28/98
Corner breaks	1L	no.	0	0	0	0	0
	1M	no.	0	0	0	0	0
	1H	no.	0	0	0	0	0
Durability cracking	2L	no.	0	0	0	0	0
	2L	m2	0	0	0	0	0
	2M	no.	0	0	0	0	0
	2M	m2	0	0	0	0	0
	2H	no.	0	0	0	0	0
	2H	m2	0	0	0	0	0
Longitudinal cracking	3L	m	6	5	5	11.5	1
	3L (sealed)	m	0	0	0	0	0
	3M	m	16	13	6.5	7	17
	3M (sealed)	m	0	0	0	0	0
	3H	m	0	0	9	3.5	3.5
	3H (sealed)	m	0	0	0	0	0
Transverse cracking	4L	no.	0	0	0	1	0
	4L	m	0	0	0	1	0
	4L (sealed)	m	0	0	0	0	0
	4M	no.	3	2	1	2	1
	4M	m	4.8	5.4	3.6	5.6	1.5
	4M (sealed)	m	0	0	0	0	0
	4H	no.	0	0	1	0	2
	4H	m	0	0	2	0	5.1
Transverse joint seal damage	4H (sealed)	m	0	0	0	0	0
	Sealed	y/n	Y	Y	Y	Y	Y
	5aL	no.	0	0	0	0	0
	5aM	no.	0	0	0	0	0
Longitudinal joint seal damage	5aH	no.	0	0	0	0	0
	No. sealed	no.	2	2	2	2	2
Spalling of longitudinal joints	5b	m	0	0	0	0	0
	6L	m	0	0	0	0	0
	6M	m	0	0	0	0	0
Spalling of transverse joints	6H	m	0	0	0	0	0
	7L	no.	6	4	2	2	0
	7L (length)	m	9.2	7	5.6	5.6	0
	7M	no.	0	2	2	2	3
	7M (length)	m	0	4.7	6.1	6.1	10.8
Map cracking	7H	no.	0	0	2	2	3
	7H (length)	m	0	0	5.6	5.6	10.2
Scaling	8a	no.	-	3	7	7	8
	8a	m2	85	0.6	3.5	3.5	4
Polished aggregate	8b	no.	0	0	0	0	0
	8b	m2	0	0	0	0	0
Popouts	9	m2	0	0	0	0	0
Blowups	10	no./m2	1.4	0.4	0	0	0
Faulting	11	no.	0	0	0	0	0
Lane-shoulder dropoff	12	-	-	-	-	-	-
Lane-shoulder separation	13	-	-	-	-	-	-
Other	14	-	-	-	-	-	-
	WP-L	no.	-	3	-	-	1
	WP-M	no.	-	2	-	-	4
	WP-H	no.	-	0	-	-	0
	CL-L	no.	-	5	-	-	3
	CL-M	no.	-	0	-	-	2
Longitudinal cracking	CL-H	no.	-	0	-	-	0
	Total	m	22	18	20.5	22	21.5
	Percent L	-	27	28	24	52	5
	Percent M	-	73	72	32	32	79
	Percent H	-	0	0	44	16	16
Transverse cracking	Total	no	3	2	2	3	3
	Total	m	4.8	5.4	5.6	6.6	6.6
	Percent L	-	0	0	0	15	0
	Percent M	-	100	100	64	85	23
	Percent H	-	0	0	36	0	77
Spalling of transverse joints	Total	no.	6	6	6	6	6
	Total	m	9.2	11.7	17.3	17.3	21
	Percent L	-	100	60	32	32	0
	Percent M	-	0	40	35	35	51
	Percent H	-	0	0	32	32	49

**Table A3. Summary of LTPP survey sheets
for ASR investigation—section S2.**

Type	Identification code	Unit	10/18/94	12/12/95	12/5/96	10/9/97	10/28/98
Corner breaks	1L	no.	0	0	0	0	0
	1M	no.	0	0	0	0	0
	1H	no.	0	0	0	0	0
Durability cracking	2L	no.	0	0	0	0	0
	2L	m2	0	0	0	0	0
	2M	no.	0	0	0	0	0
	2M	m2	0	0	0	0	0
	2H	no.	0	0	0	0	0
	2H	m2	0	0	0	0	0
Longitudinal cracking	3L	m	17	9.5	11	11.5	6.5
	3L (sealed)	m	0	0	0	0	0
	3M	m	17	12.5	12.5	8	17.5
	3M (sealed)	m	0	0	0	0	0
	3H	m	0	0	0	0	0
Transverse cracking	4L	no.	1	0	0	0	0
	4L	m	1	0	0	0	0
	4L (sealed)	m	0	0	0	0	0
	4M	no.	2	2	0	0	0
	4M	m	5.3	7.2	0	0	0
	4M (sealed)	m	0	0	0	0	0
	4H	no.	0	0	2	2	2
	4H (sealed)	m	0	0	7.2	7.2	7.2
Transverse joint seal damage	Sealed	y/n	Y	Y	Y	Y	Y
	5aL	no.	6	6	6	6	6
	5aM	no.	0	0	0	0	0
	5aH	no.	0	0	0	0	0
Longitudinal joint seal damage	No. sealed	no.	2	2	2	2	2
	5b	m	0	0	0	0	0
Spalling of longitudinal joints	6L	m	0	0	0	0	0
	6M	m	0	0	0	0	0
	6H	m	0	0	0	0	0
Spalling of transverse joints	7L	no.	6	6	3	3	1
	7L (length)	m	14	9	6.1	6.4	1.8
	7M	no.	0	0	2	2	1
	7M (length)	m	0	0	5.6	5.6	3
	7H	no.	0	0	1	1	4
Map cracking	8a	no.		3	4	5	9
	8a	m2	84.1	1.4	1.8	3.9	6
Scaling	8b	no.	0	0	0	0	0
	8b	m2	0	0	0	0	0
Polished aggregate	9	m2	0	0	0	0	0
Popouts	10	no./m2	0.9	0	0	0	0
Blowups	11	no.	0	0	0	0	0
Faulting	12	-	-	-	-	-	-
Lane-shoulder dropoff	13	-	-	-	-	-	-
Lane-shoulder separation	14	-	-	-	-	-	-
Other	WP-L	no.	-	3	-	-	1
	WP-M	no.	-	2	-	-	2
	WP-H	no.	-	0	-	-	2
	CL-L	no.	-	5	-	-	0
	CL-M	no.	-	0	-	-	5
	CL-H	no.	-	0	-	-	0
Longitudinal cracking	Total	m	34	22	23.5	19.5	24
	Percent L	-	50	43	47	59	27
	Percent M	-	50	57	53	41	73
	Percent H	-	0	0	0	0	0
Transverse cracking	Total	no	3	2	2	2	2
	Total	m	6.3	7.2	7.2	7.2	7.2
	Percent L	-	16	0	0	0	0
	Percent M	-	84	100	0	0	0
	Percent H	-	0	0	100	100	100
Spalling of transverse joints	Total	no.	6	6	6	6	6
	Total	m	14	9	15.3	15.6	16.8
	Percent L	-	100	100	40	41	11
	Percent M	-	0	0	37	36	18
Percent H	-	0	0	24	23	71	

**Table A4. Summary of LTPP survey sheets
for ASR investigation—section M2.**

Type	Identification code	Unit	10/18/94	12/12/95	12/5/96	10/9/97	10/28/98
Corner breaks	1L	no.	0	0	0	0	0
	1M	no.	0	0	0	0	0
	1H	no.	0	0	0	0	0
Durability cracking	2L	no.	0	0	0	0	0
	2L	m2	0	0	0	0	0
	2M	no.	0	0	0	0	0
	2M	m2	0	0	0	0	0
	2H	no.	0	0	0	0	0
	2H	m2	0	0	0	0	0
Longitudinal cracking	3L	m	11	11	11	15	5
	3L (sealed)	m	0	0	0	0	0
	3M	m	8	9	7	6	15.9
	3M (sealed)	m	0	0	0	0	0
	3H	m	0	0	4	6.5	8
Transverse cracking	3H (sealed)	m	0	0	0	0	0
	4L	no.	5	3	1	2	2
	4L	m	6	5.4	1	2.5	3
	4L (sealed)	m	0	0	0	0	0
	4M	no.	0	1	3	3	3
	4M	m	0	1	5.9	6.1	6.3
	4M (sealed)	m	0	0	0	0	0
	4H	no.	0	0	0	0	0
Transverse joint seal damage	4H	m	0	0	0	0	0
	4H (sealed)	m	0	0	0	0	0
	Sealed	y/n	Y	Y	Y	Y	Y
	5aL	no.	6	5	5	5	5
Longitudinal joint seal damage	5aM	no.	0	0	0	0	0
	5aH	no.	0	0	0	0	0
	No. sealed	no.	2	2	2	2	2
Spalling of longitudinal joints	5b	m	0	0	0	0	0
	6L	m	0	0	0	0	0
	6M	m	0	0	0	0	0
Spalling of transverse joints	6H	m	0	0	0	0	0
	7L	no.	4	1	1	1	0
	7L (length)	m	6.2	1.8	1.8	1.8	0
	7M	no.	1	3	3	1	2
	7M (length)	m	1.5	5.8	10.2	3	7.2
Map cracking	7H	no.	0	1	1	3	3
	7H (length)	m	0	1.5	3.5	10.7	10.8
Scaling	8a	no.		5	8	9	9
	8a	m2	93	2.1	3.75	5.5	7.3
Polished aggregate	8b	no.	0	0	0	0	0
	8b	m2	0	0	0	0	0
Popouts	9	m2	0	0	0	0	0
Blowups	10	no./m2	0.3	0	0	0	0
Faulting	11	no.	0	0	0	0	0
Lane-shoulder dropoff	12	-	-	-	-	-	-
Lane-shoulder separation	13	-	-	-	-	-	-
Other	14	-	-	-	-	-	-
	WP-L	no.	-	4	-	-	1
	WP-M	no.	-	1	-	-	4
	WP-H	no.	-	0	-	-	0
	CL-L	no.	-	5	-	-	5
	CL-M	no.	-	0	-	-	0
Longitudinal cracking	CL-H	no.	-	0	-	-	0
	Total	m	19	20	22	27.5	28.9
	Percent L	-	58	55	50	55	17
	Percent M	-	42	45	32	22	55
	Percent H	-	0	0	18	24	28
Transverse cracking	Total	no	5	4	4	5	5
	Total	m	6	6.4	6.9	8.6	9.3
	Percent L	-	100	84	14	29	32
	Percent M	-	0	16	86	71	68
	Percent H	-	0	0	0	0	0
Spalling of transverse joints	Total	no.	5	5	5	5	5
	Total	m	7.7	9.1	15.5	15.5	18
	Percent L	-	81	20	12	12	0
	Percent M	-	19	64	66	19	40
	Percent H	-	0	16	23	69	60

**Table A5. Summary of LTPP survey sheets
for ASR investigation—section SA1.**

Type	Identification code	Unit	10/18/94	12/12/95	12/5/96	10/9/97	10/28/98
Corner breaks	1L	no.	0	0	0	0	0
	1M	no.	0	0	0	0	0
	1H	no.	0	0	0	0	0
Durability cracking	2L	no.	0	0	0	0	0
	2L	m2	0	0	0	0	0
	2M	no.	0	0	0	0	0
	2M	m2	0	0	0	0	0
	2H	no.	0	0	0	0	0
	2H	m2	0	0	0	0	0
Longitudinal cracking	3L	m	4	5.5	8	7	7.4
	3L (sealed)	m	0	0	0	0	0
	3M	m	11	9.5	9.5	11	21.2
	3M (sealed)	m	0	0	0	0	0
	3H	m	0	0	0	0	0
Transverse cracking	4L	no.	6	7	6	4	4
	4L	m	5	9.4	7.5	4	4.5
	4L (sealed)	m	0	0	0	0	0
	4M	no.	2	1	2	4	3
	4M	m	3	1.5	2.5	4.5	5.2
	4M (sealed)	m	0	0	0	0	0
	4H	no.	0	0	0	1	1
	4H (sealed)	m	0	0	0	1.5	2.1
Transverse joint seal damage	Sealed	y/n	Y	Y	Y	Y	Y
	5aL	no.	6	6	6	6	6
	5aM	no.	0	2	0	0	0
	5aH	no.	0	0	0	0	0
Longitudinal joint seal damage	No. sealed	no.	2	2	2	2	2
	5b	m	0	0	0	0	0
Spalling of longitudinal joints	6L	m	0	0	0	0	0
	6M	m	0	0	0	0	0
	6H	m	0	0	0	0	0
Spalling of transverse joints	7L	no.	5	2	1	0	0
	7L (length)	m	16.2	6.1	2.5	0	0
	7M	no.	1	4	4	6	5
	7M (length)	m	3.8	13.6	14.4	21.6	18
	7H	no.	0	0	1	0	1
Map cracking	8a	no.		6	8	9	10
	8a	m2	87.8	4.6	4.7	4.8	7
Scaling	8b	no.	0	0	0	0	0
	8b	m2	0	0	0	0	0
Polished aggregate	9	m2	0	0	0	0	0
Popouts	10	no./m2	1	0.3	0	0	0
Blowups	11	no.	0	0	0	0	0
Faulting	12	-	-	-	-	-	-
Lane-shoulder dropoff	13	-	-	-	-	-	-
Lane-shoulder separation	14	-	-	-	-	-	-
Other	WP-L	no.	-	3	-	-	0
	WP-M	no.	-	2	-	-	5
	WP-H	no.	-	0	-	-	0
	CL-L	no.	-	3	-	-	0
	CL-M	no.	-	2	-	-	5
	CL-H	no.	-	0	-	-	0
Longitudinal cracking	Total	m	15	15	17.5	18	28.6
	Percent L	-	27	37	46	39	26
	Percent M	-	73	63	54	61	74
	Percent H	-	0	0	0	0	0
Transverse cracking	Total	no	8	8	8	9	8
	Total	m	8	10.9	10	10	11.8
	Percent L	-	63	86	75	40	38
	Percent M	-	38	14	25	45	44
	Percent H	-	0	0	0	15	18
Spalling of transverse joints	Total	no.	6	6	6	6	6
	Total	m	20	19.7	20.5	21.6	21.6
	Percent L	-	81	31	12	0	0
	Percent M	-	19	69	70	100	83
Percent H	-	0	0	18	0	17	

**Table A6. Summary of LTPP survey sheets
for ASR investigation—section LO1.**

Type	Identification code	Unit	10/18/94	12/12/95	12/5/96	10/9/97	10/28/98
Corner breaks	1L	no.	1	0	0	0	0
	1M	no.	0	0	0	0	0
	1H	no.	0	0	0	0	0
Durability cracking	2L	no.	0	0	0	0	0
	2L	m2	0	0	0	0	0
	2M	no.	0	0	0	0	0
	2M	m2	0	0	0	0	0
	2H	no.	0	0	0	0	0
	2H	m2	0	0	0	0	0
	3L	m	15	13	15.5	8	5.5
Longitudinal cracking	3L (sealed)	m	0	0	0	0	0
	3M	m	1.5	4.2	4.2	12	25.1
	3M (sealed)	m	0	0	0	0	0
	3H	m	0	0	0	0	0
	3H (sealed)	m	0	0	0	0	0
Transverse cracking	4L	no.	2	3	3	1	1
	4L	m	2	3.5	3.3	0.8	0.8
	4L (sealed)	m	0	0	0	0	0
	4M	no.	0	0	0	2	2
	4M	m	0	0	0	2.7	5.1
	4M (sealed)	m	0	0	0	0	0
	4H	no.	0	0	0	0	0
	4H (sealed)	m	0	0	0	0	0
Transverse joint seal damage	Sealed	y/n	Y	Y	Y	Y	Y
	5aL	no.	6	6	6	6	6
	5aM	no.	0	0	0	0	0
	5aH	no.	0	0	0	0	0
Longitudinal joint seal damage	No. sealed	no.	2	2	2	2	2
	5b	m	0	0	0	0	0
Spalling of longitudinal joints	6L	m	0	0	0	0	0
	6M	m	0	0	0	0	0
	6H	m	0	0	0	0	0
Spalling of transverse joints	7L	no.	5	0	0	0	0
	7L (length)	m	17.7	0	0	0	0
	7M	no.	1	6	2	2	1
	7M (length)	m	3.8	19.8	6.2	7.2	3.6
	7H (length)	m	0	0	14.4	14.4	18
Map cracking	8a	no.		8	10	13	13
	8a	m2	81	2.9	4.3	11.4	11.4
Scaling	8b	no.	0	0	0	0	0
	8b	m2	0	0	0	0	0
Polished aggregate	9	m2	0	0	0	0	0
Popouts	10	no./m2	0.4	0	0	0	0
Blowups	11	no.	0	0	0	0	0
Faulting	12	-	-	-	-	-	-
Lane-shoulder dropoff	13	-	-	-	-	-	-
Lane-shoulder separation	14	-	-	-	-	-	-
Other	WP-L	no.	-	1	-	-	0
	WP-M	no.	-	4	-	-	5
	WP-H	no.	-	0	-	-	0
	CL-L	no.	-	3	-	-	1
	CL-M	no.	-	2	-	-	4
	CL-H	no.	-	0	-	-	0
Longitudinal cracking	Total	m	16.5	17.2	19.7	20	30.6
	Percent L	-	91	76	79	40	18
	Percent M	-	9	24	21	60	82
	Percent H	-	0	0	0	0	0
Transverse cracking	Total	no	2	3	3	3	3
	Total	m	2	3.5	3.3	3.5	5.9
	Percent L	-	100	100	100	23	14
	Percent M	-	0	0	0	77	86
	Percent H	-	0	0	0	0	0
Spalling of transverse joints	Total	no.	6	6	6	6	6
	Total	m	21.5	19.8	20.6	21.6	21.6
	Percent L	-	82	0	0	0	0
	Percent M	-	18	100	30	33	17
Percent H	-	0	0	70	67	83	

**Table A7. Summary of LTPP survey sheets
for ASR investigation—control 2.**

Type	Identification code	Unit	10/18/94	12/12/95	12/5/96	10/9/97	10/28/98
Corner breaks	1L	no.	0	0	0	0	0
	1M	no.	0	0	0	0	0
	1H	no.	0	0	0	0	0
Durability cracking	2L	no.	0	0	0	0	0
	2L	m2	0	0	0	0	0
	2M	no.	0	0	0	0	0
	2M	m2	0	0	0	0	0
	2H	no.	0	0	0	0	0
	2H	m2	0	0	0	0	0
Longitudinal cracking	3L	m	4.5	8	10.5	8.5	12.4
	3L (sealed)	m	0	0	0	0	0
	3M	m	0	0	1.5	1.5	15.5
	3M (sealed)	m	0	0	0	0	0
	3H	m	0	0	0	0	0
	3H (sealed)	m	0	0	0	0	0
Transverse cracking	4L	no.	3	1	1	1	1
	4L	m	4	1	1.3	1.3	1.3
	4L (sealed)	m	0	0	0	0	0
	4M	no.	0	1	1	1	0
	4M	m	0	3.6	3.6	3.6	0
	4M (sealed)	m	0	0	0	0	0
	4H	no.	0	0	0	0	1
	4H	m	0	0	0	0	3.6
Transverse joint seal damage	4H (sealed)	m	0	0	0	0	0
	Sealed	y/n	Y	Y	Y	Y	Y
	5aL	no.	6	6	6	6	6
	5aM	no.	0	0	0	0	0
Longitudinal joint seal damage	5aH	no.	0	0	0	0	0
	No. sealed	no.	2	2	2	2	2
Spalling of longitudinal joints	5b	m	0	0	0	0	0
	6L	m	0	0	0	0	0
	6M	m	0	0	0	0	0
Spalling of transverse joints	6H	m	0	0	0	0	0
	7L	no.	6	2	1	0	0
	7L (length)	m	21	4.5	2.9	0	0
	7M	no.	0	4	2	2	0
	7M (length)	m	0	10.2	5.6	7.2	0
Map cracking	7H	no.	0	0	3	4	6
	7H (length)	m	0	0	10.6	14.4	21.6
Scaling	8a	no.	4	3	11	13	13
	8a	m2	3	1.5	3.4	8.8	8.9
Polished aggregate	8b	no.	0	0	0	0	0
	8b	m2	0	0	0	0	0
Popouts	9	m2	0	0	0	0	0
Blowups	10	no./m2	0.6	1	0	0	0
Faulting	11	no.	0	0	0	0	0
Lane-shoulder dropoff	12	-	-	-	-	-	-
Lane-shoulder separation	13	-	-	-	-	-	-
Other	14	-	-	-	-	-	-
	WP-L	no.	-	2	-	-	0
	WP-M	no.	-	3	-	-	3
	WP-H	no.	-	0	-	-	2
	CL-L	no.	-	5	-	-	0
	CL-M	no.	-	0	-	-	5
Longitudinal cracking	CL-H	no.	-	0	-	-	0
	Total	m	4.5	8	12	10	27.9
	Percent L	-	100	100	88	85	44
	Percent M	-	0	0	13	15	56
	Percent H	-	0	0	0	0	0
Transverse cracking	Total	no	3	2	2	2	2
	Total	m	4	4.6	4.9	4.9	4.9
	Percent L	-	100	22	27	27	27
	Percent M	-	0	78	73	73	0
	Percent H	-	0	0	0	0	73
Spalling of transverse joints	Total	no.	6	6	6	6	6
	Total	m	21	14.7	19.1	21.6	21.6
	Percent L	-	100	31	15	0	0
	Percent M	-	0	69	29	33	0
	Percent H	-	0	0	55	67	100

**Table A8. Summary of LTPP survey sheets
for ASR investigation—section S1.**

Type	Identification code	Unit	10/18/94	12/12/95	12/5/96	10/9/97	10/28/98
Corner breaks	1L	no.	0	0	0	0	0
	1M	no.	0	0	0	0	0
	1H	no.	0	0	0	0	0
Durability cracking	2L	no.	0	0	0	0	0
	2L	m2	0	0	0	0	0
	2M	no.	0	0	0	0	0
	2M	m2	0	0	0	0	0
	2H	no.	0	0	0	0	0
	2H	m2	0	0	0	0	0
Longitudinal cracking	3L	m	10	12.5	13	0	7.7
	3L (sealed)	m	0	0	0	0	0
	3M	m	0	0	0	13.5	21
	3M (sealed)	m	0	0	0	0	0
	3H	m	0	0	0	0	0
Transverse cracking	3H (sealed)	m	0	0	0	0	0
	4L	no.	1	2	2	2	0
	4L	m	1	1.3	2.3	2.3	0
	4L (sealed)	m	0	0	0	0	0
	4M	no.	6	5	6	6	4
	4M	m	6	6	6.3	6.3	5.3
	4M (sealed)	m	0	0	0	0	0
	4H	no.	0	0	0	0	0
Transverse joint seal damage	4H	m	0	0	0	0	0
	4H (sealed)	m	0	0	0	0	0
	Sealed	y/n	Y	Y	Y	Y	Y
	5aL	no.	6	6	6	6	6
Longitudinal joint seal damage	5aM	no.	0	0	0	0	0
	5aH	no.	0	0	0	0	0
	No. sealed	no.	2	2	2	2	2
Spalling of longitudinal joints	5b	m	0	0	0	0	0
	6L	m	0	0	0	0	0
	6M	m	0	0	0	0	0
Spalling of transverse joints	6H	m	0	0	0	0	0
	7L	no.	6	0	0	0	0
	7L (length)	m	21.6	0	0	0	0
	7M	no.	0	5	1	1	0
	7M (length)	m	0	14.7	2.5	3.6	0
Map cracking	7H	no.	0	1	5	5	6
	7H (length)	m	0	3.6	18	18	21.6
Scaling	8a	no.	7	14	15	16	18
	8a	m2	6	11.8	7.8	15.2	16.1
Polished aggregate	8b	no.	0	0	0	0	0
	8b	m2	0	0	0	0	0
Popouts	9	m2	0	0	0	0	0
Blowups	10	no./m2	0.8	0	0	0	0
Faulting	11	no.	0	0	0	0	0
Lane-shoulder dropoff	12	-	-	-	-	-	-
Lane-shoulder separation	13	-	-	-	-	-	-
Other	14	-	-	-	-	-	-
	WP-L	no.	-	0	-	-	0
	WP-M	no.	-	5	-	-	3
	WP-H	no.	-	0	-	-	2
	CL-L	no.	-	3	-	-	0
	CL-M	no.	-	2	-	-	5
Longitudinal cracking	CL-H	no.	-	0	-	-	0
	Total	m	10	12.5	13	13.5	28.7
	Percent L	-	100	100	100	0	27
	Percent M	-	0	0	0	100	73
	Percent H	-	0	0	0	0	0
Transverse cracking	Total	no	7	7	8	8	4
	Total	m	7	7.3	8.6	8.6	5.3
	Percent L	-	14	18	27	27	0
	Percent M	-	86	82	73	73	100
	Percent H	-	0	0	0	0	0
Spalling of transverse joints	Total	no.	6	6	6	6	6
	Total	m	21.6	18.3	20.5	21.6	21.6
	Percent L	-	100	0	0	0	0
	Percent M	-	0	80	12	17	0
	Percent H	-	0	20	88	83	100

**Table A9. Summary of LTPP survey sheets
for ASR investigation—section L1.**

Type	Identification code	Unit	10/18/94	12/12/95	12/5/96	10/9/97	10/28/98
Corner breaks	1L	no.	0	0	0	0	0
	1M	no.	0	0	0	0	0
	1H	no.	0	0	0	0	0
Durability cracking	2L	no.	0	0	0	0	0
	2L	m2	0	0	0	0	0
	2M	no.	0	0	0	0	0
	2M	m2	0	0	0	0	0
	2H	no.	0	0	0	0	0
	2H	m2	0	0	0	0	0
Longitudinal cracking	L	m	5.5	7.8	10	3.5	10.7
	3L (sealed)	m	0	0	0	0	0
	3M	m	0	1.5	1.5	7	20
	3M (sealed)	m	0	0	0	0	0
	3H	m	0	0	0	0	0
Transverse cracking	4L	no.	7	5	5	4	4
	4L	m	8	6	6.6	5	4.7
	4L (sealed)	m	0	2	0	0	0
	4M	no.	0	2.5	2	3	4
	4M	m	0	0	3.5	5.1	7.5
	4M (sealed)	m	0	0	0	0	0
	4H	no.	0	0	0	0	0
	4H	m	0	0	0	0	0
Transverse joint seal damage	Sealed	y/n	Y	Y	Y	Y	Y
	5aL	no.	6	6	6	6	6
	5aM	no.	0	0	0	0	0
	5aH	no.	0	0	0	0	0
Longitudinal joint seal damage	No. sealed	no.	2	2	2	2	2
	5b	m	0	0	0	0	0
Spalling of longitudinal joints	6L	m	0	0	0	0	0
	6M	m	0	0	0	0	0
	6H	m	0	0	0	0	0
Spalling of transverse joints	7L	no.	6	0	0	0	0
	7L (length)	m	21.6	0	0	0	0
	7M	no.	0	5	3	3	0
	7M (length)	m	0	17.7	10.6	10.8	0
	7H	no.	0	1	3	3	6
Map cracking	8a	no.	3	6	9	9	13
	8a	m2	2	3.5	4.5	4.2	6.2
Scaling	8b	no.	0	0	0	0	0
	8b	m2	0	0	0	0	0
Polished aggregate	9	m2	0	0	0	0	0
Popouts	10	no./m2	1	0	0	0	0
Blowups	11	no.	0	0	0	0	0
Faulting	12	-	-	-	-	-	-
Lane-shoulder dropoff	13	-	-	-	-	-	-
Lane-shoulder separation	14	-	-	-	-	-	-
Other	WP-L	no.	-	0	-	-	0
	WP-M	no.	-	5	-	-	5
	WP-H	no.	-	0	-	-	0
	CL-L	no.	-	4	-	-	2
	CL-M	no.	-	1	-	-	3
	CL-H	no.	-	0	-	-	0
Longitudinal cracking	Total	m	5.5	9.3	11.5	10.5	30.7
	Percent L	-	100	84	87	33	35
	Percent M	-	0	16	13	67	65
	Percent H	-	0	0	0	0	0
Transverse cracking	Total	no	7	7.5	7	7	8
	Total	m	8	6	10.1	10.1	12.2
	Percent L	-	100	100	65	50	39
	Percent M	-	0	0	35	50	61
	Percent H	-	0	0	0	0	0
Spalling of transverse joints	Total	no.	6	6	6	6	6
	Total	m	21.6	21.3	19.8	21.6	21.6
	Percent L	-	100	0	0	0	0
	Percent M	-	0	83	54	50	0
Percent H	-	0	17	46	50	100	

**Table A10. Summary of LTPP survey sheets
for ASR investigation—control section 1.**

Type	Identification code	Unit	10/18/94	12/12/95	12/5/96	10/9/97	10/28/98
Corner breaks	1L	no.	0	0	0	0	0
	1M	no.	0	0	0	0	0
	1H	no.	0	0	0	0	0
Durability cracking	2L	no.	0	0	0	0	0
	2L	m2	0	0	0	0	0
	2M	no.	0	0	0	0	0
	2M	m2	0	0	0	0	0
	2H	no.	0	0	0	0	0
	2H	m2	0	0	0	0	0
Longitudinal cracking	3L	m	14	19	11	4	13
	3L (sealed)	m	0	0	0	0	0
	3M	m	0	0	3	10	18.8
	3M (sealed)	m	0	0	0	0	0
	3H	m	0	0	0.8	0.8	0
Transverse cracking	3H (sealed)	m	0	0	0	0	0
	4L	no.	5	4	3	3	3
	4L	m	2.9	3.5	2.7	2.7	2.7
	4L (sealed)	m	0	0	0	0	0
	4M	no.	2	2	1	1	1
	4M	m	7.3	7.2	1	1	1.5
	4M (sealed)	m	0	0	0	0	0
	4H	no.	0	0	2	2	2
Transverse joint seal damage	4H	m	0	0	7.2	7.2	7.3
	4H (sealed)	m	0	0	0	0	0
	Sealed	y/n	Y	Y	Y	Y	Y
	5aL	no.	0	0	0	0	0
Longitudinal joint seal damage	5aM	no.	0	0	0	0	0
	5aH	no.	0	0	0	0	0
	No. sealed	no.	2	2	2	2	2
Spalling of longitudinal joints	5b	m	0	0	0	0	0
	6L	m	0	0	0	0	0
	6M	m	0	0	0	0	0
Spalling of transverse joints	6H	m	0	0	0	0	0
	7L	no.	6	0	0	0	0
	7L (length)	m	21.2	0	0	0	0
	7M	no.	0	6	6	6	1
	7M (length)	m	0	19.2	19.8	21.6	3.6
Map cracking	7H	no.	0	0	0	0	5
	7H (length)	m	0	0	0	0	18
Scaling	8a	no.	5	3	4	9	11
	8a	m2	4	1	1.5	4.9	6
Polished aggregate	8b	no.	0	0	0	0	0
	8b	m2	0	0	0	0	0
Popouts	9	m2	0	0	0	0	0
Blowups	10	no./m2	1	0.8	0	0	0
Faulting	11	no.	0	0	0	0	0
Lane-shoulder dropoff	12	-	-	-	-	-	-
Lane-shoulder separation	13	-	-	-	-	-	-
Other	14	-	-	-	-	-	-
	WP-L	no.	-	0	-	-	0
	WP-M	no.	-	5	-	-	4
	WP-H	no.	-	0	-	-	1
	CL-L	no.	-	4	-	-	1
	CL-M	no.	-	1	-	-	4
Longitudinal cracking	CL-H	no.	-	0	-	-	0
	Total	m	14	19	14.8	14.8	31.8
	Percent L	-	100	100	74	27	41
	Percent M	-	0	0	20	68	59
	Percent H	-	0	0	5	5	0
Transverse cracking	Total	no	7	6	6	6	6
	Total	m	10.2	10.7	10.9	10.9	11.5
	Percent L	-	28	33	25	25	23
	Percent M	-	72	67	9	9	13
	Percent H	-	0	0	66	66	63
Spalling of transverse joints	Total	no.	6	6	6	6	6
	Total	m	21.2	19.2	19.8	21.6	21.6
	Percent L	-	100	0	0	0	0
	Percent M	-	0	100	100	100	17
Percent H	-	0	0	0	0	83	

**Table A11. Summary of LTPP survey sheets
for ASR investigation—section M1.**

Type	Identification code	Unit	10/18/94	12/12/95	12/5/96	10/9/97	10/28/98
Corner breaks	1L	no.	0	0	0	0	0
	1M	no.	0	0	0	0	0
	1H	no.	0	0	0	0	0
Durability cracking	2L	no.	0	0	0	0	0
	2L	m2	0	0	0	0	0
	2M	no.	0	0	0	0	0
	2M	m2	0	0	0	0	0
	2H	no.	0	0	0	0	0
	2H	m2	0	0	0	0	0
	3L	m	6	13	13	4	11
Longitudinal cracking	3L (sealed)	m	0	0	0	0	0
	3M	m	0	0	0	14	24.7
	3M (sealed)	m	0	0	0	0	0
	3H	m	0	0	0	0	0
	3H (sealed)	m	0	0	0	0	0
Transverse cracking	4L	no.	3	1	4	2	2
	4L	m	4.5	1.5	3.4	1.6	1.6
	4L (sealed)	m	0	0	0	0	0
	4M	no.	1	3	3	2	3
	4M	m	1.5	4	4.5	3	4
	4M (sealed)	m	0	0	0	0	0
	4H	no.	0	0	0	0	0
	4H (sealed)	m	0	0	0	0	0
Transverse joint seal damage	Sealed	y/n	Y	Y	Y	Y	Y
	5aL	no.	5	5	5	5	5
	5aM	no.	0	0	0	0	0
	5aH	no.	0	0	0	0	0
Longitudinal joint seal damage	No. sealed	no.	2	2	2	2	2
	5b	m	0	0	0	0	0
Spalling of longitudinal joints	6L	m	0	0	0	0	0
	6M	m	0	0	0	0	0
	6H	m	0	0	0	0	0
Spalling of transverse joints	7L	no.	5	3	0	0	0
	7L (length)	m	17	5.5	0	0	0
	7M	no.	0	1	4	3	1
	7M (length)	m	0	2	10.6	10.8	3.6
	7H (length)	m	0	2.7	3.5	7.2	18
Map cracking	8a	no.	9	12	13	15	16
	8a	m2	7.5	8.7	7.8	13.3	14.9
Scaling	8b	no.	0	0	0	0	0
	8b	m2	0	0	0	0	0
Polished aggregate	9	m2	0	0	0	0	0
Popouts	10	no./m2	0.4	0.07	0	0	0
Blowups	11	no.	0	0	0	0	0
Faulting	12	-	-	-	-	-	-
Lane-shoulder dropoff	13	-	-	-	-	-	-
Lane-shoulder separation	14	-	-	-	-	-	-
Other	WP-L	no.	-	5	-	-	0
	WP-M	no.	-	0	-	-	3
	WP-H	no.	-	0	-	-	2
	CL-L	no.	-	5	-	-	4
	CL-M	no.	-	0	-	-	1
	CL-H	no.	-	0	-	-	0
Longitudinal cracking	Total	m	6	13	13	18	35.7
	Percent L	-	100	100	100	22	31
	Percent M	-	0	0	0	78	69
	Percent H	-	0	0	0	0	0
Transverse cracking	Total	no	4	4	7	4	5
	Total	m	6	5.5	7.9	4.6	5.6
	Percent L	-	75	27	43	35	29
	Percent M	-	25	73	57	65	71
	Percent H	-	0	0	0	0	0
Spalling of transverse joints	Total	no.	5	5	5	5	6
	Total	m	17	10.2	14.1	18	21.6
	Percent L	-	100	54	0	0	0
	Percent M	-	0	20	75	60	17
Percent H	-	0	26	25	40	83	

APPENDIX B

Table B1. Transverse joint observations of Route 72, Newark, DE (1998)

Joint	Shoulder Lane Observations	Travel Lane Observations
Start of C1	Joint is intact and well sealed. Cracking perpendicular to the joint along entire joint. No nearby transverse cracks. Twenty-one cracks along joint. Spalling at joint with shoulder.	Four spalls, 1 large in right wheelpath. All patched, but subsequent loss of material in center patch. More PCC spalling pieces.
C1-T1	Joint intact and well sealed. Perpendicular cracks intercepting full width of the joint. Transverse cracks in outer 3.05 m at 0.305 m from the joint.	Heavy spalls in 3.05 m of lane, all patched with asphalt. Concrete is lost in outer 0.61 m in two separate spalls. All joints spalled. AC patch 0.92 m by 3.05 m.
T1-T2	Joint intact and well sealed. Intersecting cracks perpendicular to the joint at 0.305 m on center along the whole joint. Twenty-four cracks along joint.	Heavy loss of material over 10 feet of joint, all patched with asphalt. Patch largest at joint with shoulder. AC patch 0.61 m x 3.05 m. Also patch at shoulder joint 0.305 m x 3.05 m.
T2-C2	Joint intact and well sealed. Cracks perpendicular to and intersecting the whole joint. No nearby transverse cracks. Twenty-one cracks along joint.	Unpatched small (less than .305 m from joint) spalls over 1.83 m of joint. Spalling also along longitudinal shoulder joint.
C2-C3	Joint intact and well sealed. Cracks perpendicular to and intersecting the joint along 0.92 m of joint. Light cracking over remainder of joint. Scattered nearby transverse cracks. Sixteen cracks along joint.	Spalls over 3.05 m of joint, all patched with asphalt. Patch widest at longitudinal joint.
C3-C4	Joint intact and well sealed. .305 m spall 50.8 mm wide near longitudinal joint. Cracks perpendicular to joint stop .305 m from joint, with cracks extending to joint all of joint. Light cracking, no staining. Seventeen cracks along joint.	Spall along 2.44 m of joint, all patched with asphalt. Patch approximately 0.305 m wide on either side of joint, with wider patch (0.92 m x 0.92 m) at longitudinal joint. Some new PCC spalling.
C4-T3	Joint intact and well sealed. Very light perpendicular cracking along joint. No nearby transverse cracking. Ten cracks along joint.	Right wheelpath patch over 0.92 m x 0.305 m area, 0.61 m x 0.61 m patch in center with some concrete loss around edge of patch. Transverse crack 0.92 m from joint with 0.305 m x 0.305 m spall.
T3-T4	Joint intact and well sealed. Cracking along joint. Eleven cracks along joint.	Small spall 20.3 cm x 20.3 cm at longitudinal joint.

Table B1. Transverse joint observations of Route 72, Newark, DE (1998). (continued)

Joint	Shoulder Lane Observations	Travel Lane Observations
T4-C5	Joint intact and well sealed. Very light perpendicular cracking at joint with 15.2 cm corner spall in C5. All cracks narrow with brown staining. Fourteen cracks along joint.	20.3 to 30.5-cm wide asphalt patch along 0.92 m of C5 section. New PCC spalling.
C5-end	Joint intact and well sealed. Light widely-spaced cracking perpendicular to joint and along entire joint. Thirteen cracks along joint.	Small .305 m x .305 m patch near longitudinal joint at transverse joint.



(a) Control section 1 (C1)

Figure B1. Photographs of typical area of each section (Newark, DE).



(b) Test section 1 (TS1)



(c) Test section 2 (TS2)

Figure B1. Photographs of typical area of each section (Newark, DE). (continued)

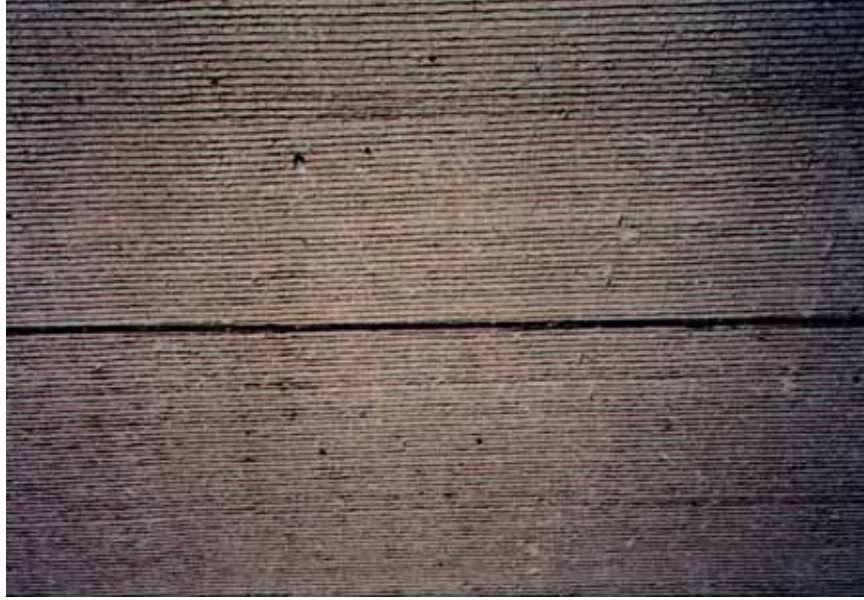


(d) Control section 2 (C2)



(e) Control section 3 (C3)

Figure B1. Photographs of typical area of each section (Newark, DE). (continued)



(f) Control section 4 (C4)



(g) Test section 3 (TS3)

Figure B1. Photographs of typical area of each section (Newark, DE). (continued)



(h) Test section 4 (TS4)



(i) Control section 5 (C5)

Figure B1. Photographs of typical area of each section (Newark, DE). (continued)

Petrographic Report for Newark, DE, 1997

Sections from each of the cores were cut and lapped. These sections were then soaked overnight, dried, and the entire lapped surface was traversed under a stereo microscope. The lapped surface was divided into five or more traverses and examined at magnifications of 10 to 30 times. All instances of cracks, alkali-silica gel, and deteriorated or reacted aggregate particles were counted.

Core 97C1A: the core is poorly and nonuniformly air-entrained, with an estimated air content of 4.5 percent. Distress to the wearing surface appears limited to small popouts over fine aggregate particles. The core is moderately severely distressed. One major crack bisects the core into top and bottom halves. Additionally, 40 microcracks and 27 instances of alkali-silica gel were

counted. Three coarse aggregate particles appear to have reacted slightly; 24 fine aggregate particles were distressed or had reacted.

Core 97C5A: the core is poorly and nonuniformly air-entrained with an estimated air content of 5 percent. Distress to the wearing surface appears limited to small popouts over fine aggregate particles. The core is moderately severely distressed. One major crack bisects the core into top and bottom halves. Thirty-four other microcracks were counted, and 31 occurrences of alkali-silica gel. Three coarse aggregate particles appear to have reacted slightly. Twenty-seven fine aggregate particles are distressed or have reacted.

Core 97T51A: the core is poorly and nonuniformly air-entrained with an estimated air content of 4 percent. Distress to the wearing surface appears limited to small popouts over fine aggregate particles. The core is severely distressed. Eighty-seven cracks were counted, along with 42 occurrences of alkali-silica gel. Thirty-one reacted or distressed fine aggregate particles were counted.

Core 97T52B: the core is marginally air-entrained with an estimated air content of 5 percent. Distress to the wearing surface appears limited to small popouts over fine aggregate particles. The core is moderately severely distressed. Forty-three cracks and 33 instances of alkali-silica gel were detected. Twenty-nine reacted or distressed fine aggregate particles were detected.

Core 97T53B: the core is well air-entrained with an estimated air content of 6.5 percent. Distress to the wearing surface appears limited to small popouts over fine aggregate particles. Distress is relatively minor. Seventeen cracks were counted, and 25 instances of alkali-silica gel. Twenty-three fine aggregate particles had reacted or were distressed.

Core 97T54B: the core is poorly air-entrained with an estimated air content of 3.5 percent. Distress to the wearing surface is apparently limited to small popouts over fine aggregate particles. Distress is minor. Eight cracks and 13 occurrences of alkali-silica gel were counted. Thirty-one fine aggregate particles had reacted or were distressed.

Distress is relatively severe in all but the last two cores. We do not have sufficient information to interpret the possible reason, since all were treated with lithium compounds, but we have not been told what differences there were.

Petrographic Report for Newark, DE, 1998

Sections from each of the cores were cut and lapped. These sections were then soaked overnight, dried, and the entire lapped surface was traversed under a stereo microscope. Each lapped surface was divided into five or more traverses areas and examined at magnifications of 10 to 30 times. All instances of cracks, alkali-silica gel, and deteriorated or reacted aggregate particles were counted.

Core 98-C1-A: the core is severely distressed. The wearing surface is grooved and worn. Fine aggregate particles on the wearing surface are frequently exposed, occasionally in popouts. Seventy-seven microcracks, one large crack, and 49 instances of alkali-silica gel were counted. Thirty-nine reacted or distressed fine aggregate particles were counted. The core is air-entrained with an estimated air content of 6.5 percent.

Core 98-C5-B: the core is severely distressed. The wearing surface is grooved and worn. Fine aggregate particles on the wearing surface are frequently exposed, occasionally in popouts. Fifty-seven microcracks and 79 instances of alkali-silica gel were counted. Forty-two fine aggregate particles showed evidence of distress or reaction. The core is air-entrained with an estimated air content of 6 percent.

Core 98-TS1-A: the core is severely distressed. The wearing surface is grooved and worn, with fine and coarse aggregate particles partially exposed. Fine aggregate particles are occasionally exposed in popouts. Two major cracks and fifty microcracks were counted. Sixty-one instances of alkali-silica gel and 38 reacted or distressed fine aggregate particles were counted. The core is air-entrained with an estimated air content of 5.5 percent.

Core 98-TS-2B: the core is severely distressed. The grooved wearing surface is severely worn, exposing fine and coarse aggregate particles. Fine aggregate particles are frequently exposed in popouts. One major and 64 microcracks were detected. Fifty-eight instances of alkali-silica gel and 23 reacted or distressed fine aggregate particles were counted. The core is air-entrained with an estimated air content of 7.5 percent.

Core 98-TS-3A: the core is slightly to moderately distressed. The grooved wearing surface is moderately worn with both fine and coarse aggregate particles exposed on it, but with few identifiable popouts. Twenty-five microcracks and 43 instances of alkali-silica gel were counted. Fifteen fine aggregate particles had reacted or showed distress. The core is highly air entrained with an estimated air content of 8.5 percent.

Core 98-TS-4B: the core is slightly distressed. The grooved wearing surface is severely worn with no other distinct evidence of distress. Fourteen microcracks and 44 instances of alkali-silica gel were detected. Fifteen fine aggregate particles showed evidence of distress or reaction. The core is air entrained with an estimated air content of 7.5 percent.

**Table B2. Summary of LTPP survey sheets
for ASR investigation—control section 1.**

Type	Identification code	Unit	11/29/94	11/28/95	11/21/96	12/9/97	10/22/98
Corner breaks	1L	No.	0	0	0	0	0
	1M	No.	0	0	0	0	0
	1H	No.	0	0	0	0	0
Durability cracking	2L	No.	0	0	0	0	0
	2L	M2	0	0	0	0	0
	2M	No.	0	0	0	0	0
	2M	M2	0	0	0	0	0
	2H	No.	0	0	0	0	0
	2H	M2	0	0	0	0	0
	3L	m	0	0	0	0	0
Longitudinal cracking	3L (sealed)	m	0	0	0	0	0
	3M	m	0	0	0	0	0
	3M (sealed)	m	0	0	0	0	0
	3H	m	0	0	0	0	0
	3H (sealed)	m	0	0	0	0	0
Transverse cracking	4L	No.	1	1	1	1	1
	4L	m	3.4	3.4	3.4	3.4	3.4
	4L (sealed)	m	0	0	0	0	0
	4M	No.	0	0	0	0	0
	4M	m	0	0	0	0	0
	4M (sealed)	m	0	0	0	0	0
	4H	No.	0	0	0	0	0
	4H	m	0	0	0	0	0
Transverse joint seal damage	4H (sealed)	m	0	0	0	0	0
	Sealed	Y/n	Y	Y	Y	Y	Y
	5aL	No.	1	1	1	1	1
	5aM	No.	0	0	0	0	0
Longitudinal joint seal damage	5aH	No.	0	0	0	0	0
	No. sealed	No.	2	2	2	2	0
Spalling of longitudinal joints	5b	m	12.2	12.2	12.2	12.2	12.2
	6L	m	0	0	0	0	0
	6M	m	0	0	0	0	0
Spalling of transverse joints	6H	m	0	0	0	0	0
	7L	no.	0	1	1	1	1
	7L (length)	m	0	0.2	1.8	2	2
	7M	no.	0	0	0	0	0
	7M (length)	m	0	0	0	0	0
	7H	no.	0	0	0	0	0
Map cracking	7H (length)	m	0	0	0	0	0
	8a	no.	1	7	1	1	1
Scaling	8a	m2	11.5	23.2	26.8	27.8	29.7
	8b	no.	0	0	0	0	0
Polished aggregate	8b	m2	0	0	0	0	0
Popouts	9	m2	0	0	0	0	0
Blowups	10	no./m2	0	0	0	0	0
Faulting	11	no.	0	0	0	0	0
Lane-shoulder dropoff	12	-	-	-	-	-	-
Lane-shoulder separation	13	-	-	-	-	-	-
Flexible patch deterioration	14	-	-	-	-	-	-
	15fL	no.	0	0	0	0	0
	15fL	m2	0	0	0	0	0
	15fM	no.	0	0	0	0	0
	15fM	m2	0	0	0	0	0
	15fH	no.	0	0	0	0	0
Rigid patch deterioration	15fH	m2	0	0	0	0	0
	15rL	no.	0	0	0	0	0
	15rL	m2	0	0	0	0	0
	15rM	no.	0	0	0	0	0
	15rM	m2	0	0	0	0	0
	15rH	no.	0	0	0	0	0
Bleeding and pumping	15rH	m2	0	0	0	0	0
	16	no.	0	0	0	0	0
Other	16	m	0	0	0	0	0
	17	-	-	-	-	-	-

**Table B3. Summary of LTPP survey sheets
for ASR investigation—test section 1.**

Type	Identification code	Unit	11/29/94	11/28/95	11/21/96	12/9/97	10/22/98
Corner breaks	1L	no.	0	0	0	0	0
	1M	no.	0	0	0	0	0
	1H	no.	0	0	0	0	0
Durability cracking	2L	no.	0	0	0	0	0
	2L	m2	0	0	0	0	0
	2M	no.	0	0	0	0	0
	2M	m2	0	0	0	0	0
	2H	no.	0	0	0	0	0
	2H	m2	0	0	0	0	0
	3L	m	0	0	0	0	0
Longitudinal cracking	3L (sealed)	m	0	0	0	0	0
	3M	m	0	0	0	0	0
	3M (sealed)	m	0	0	0	0	0
	3H	m	0	0	0	0	0
	3H (sealed)	m	0	0	0	0	0
Transverse cracking	4L	no.	0	0	0	0	0
	4L	m	0	0	0	0	0
	4L (sealed)	m	0	0	0	0	0
	4M	no.	0	0	0	0	0
	4M	m	0	0	0	0	0
	4M (sealed)	m	0	0	0	0	0
	4H	no.	0	0	0	0	0
	4H (sealed)	m	0	0	0	0	0
Transverse joint seal damage	Sealed	y/n	Y	Y	Y	Y	Y
	5aL	no.	1	1	1	1	1
	5aM	no.	0	0	0	0	0
	5aH	no.	0	0	0	0	0
Longitudinal joint seal damage	No. sealed	no.	2	2	2	2	2
	5b	m	12.2	12.2	12.2	12.2	12.2
Spalling of longitudinal joints	6L	m	1.5	0.5	1.8	1.8	1.8
	6M	m	0	0	0	0	0
	6H	m	0	0	0	0	0
Spalling of transverse joints	7L	no.	0	0	1	1	1
	7L (length)	m	0	0	2.1	3.4	3.4
	7M	no.	0	0	0	0	0
	7M (length)	m	0	0	0	0	0
	7H	no.	0	0	0	0	0
Map cracking	8a	no.	1	1	1	1	1
	8a	m2	11.8	21.8	28.3	29.1	31.4
Scaling	8b	no.	0	0	0	0	0
	8b	m2	0	0	0	0	0
Polished aggregate	9	m2	0	0	0	0	0
Popouts	10	no./m2	0	0	0	0	0
Blowups	11	no.	0	0	0	0	0
Faulting	12	-	-	-	-	-	-
Lane-shoulder dropoff	13	-	-	-	-	-	-
Lane-shoulder separation	14	-	-	-	-	-	-
Flexible patch deterioration	15fL	no.	0	0	0	0	0
	15fL	m2	0	0	0	0	0
	15fM	no.	0	0	0	0	0
	15fM	m2	0	0	0	0	0
	15fH	no.	0	0	0	0	0
	15fH	m2	0	0	0	0	0
Rigid patch deterioration	15rL	no.	0	0	0	0	0
	15rL	m2	0	0	0	0	0
	15rM	no.	0	0	0	0	0
	15rM	m2	0	0	0	0	0
	15rH	no.	0	0	0	0	0
Bleeding and pumping	16	no.	0	0	0	0	0
	16	m	0	0	0	0	0
Other	17	-	-	-	-	-	-

**Table B4. Summary of LTPP survey sheets
for ASR investigation—test section 2.**

Type	Identification code	Unit	11/29/94	11/28/95	12/21/96	12/9/97	10/22/98
Corner breaks	1L	no.	0	0	0	0	0
	1M	no.	0	0	0	0	0
	1H	no.	0	0	0	0	0
Durability cracking	2L	no.	0	0	0	0	0
	2L	m2	0	0	0	0	0
	2M	no.	0	0	0	0	0
	2M	m2	0	0	0	0	0
	2H	no.	0	0	0	0	0
	2H	m2	0	0	0	0	0
	3L	m	0	0	0	0	0
Longitudinal cracking	3L (sealed)	m	0	0	0	0	0
	3M	m	0	0	0	0	0
	3M (sealed)	m	0	0	0	0	0
	3H	m	0	0	0	0	0
	3H (sealed)	m	0	0	0	0	0
Transverse cracking	4L	no.	0	0	0	0	0
	4L	m	0	0	0	0	0
	4L (sealed)	m	0	0	0	0	0
	4M	no.	0	0	0	0	0
	4M	m	0	0	0	0	0
	4M (sealed)	m	0	0	0	0	0
	4H	no.	0	0	0	0	0
	4H (sealed)	m	0	0	0	0	0
Transverse joint seal damage	Sealed	y/n	Y	Y	Y	Y	Y
	5aL	no.	1	1	1	1	1
	5aM	no.	0	0	0	0	0
	5aH	no.	0	0	0	0	0
Longitudinal joint seal damage	No. sealed	no.	2	2	2	2	2
	5b	m	12.2	12.2	12.2	12.2	12.2
Spalling of longitudinal joints	6L	m	0	1.5	1.5	1.5	1.5
	6M	m	2.5	0	0	0	0
	6H	m	0	0	0	0	0
Spalling of transverse joints	7L	no.	1	1	1	1	1
	7L (length)	m	3.4	3.4	3.4	3.4	3.4
	7M	no.	0	0	0	0	0
	7M (length)	m	0	0	0	0	0
	7H	no.	0	0	0	0	0
Map cracking	8a	no.	1	1	1	1	1
	8a	m2	8	14.9	25.3	25.3	26
Scaling	8b	no.	0	0	0	0	0
	8b	m2	0	0	0	0	0
Polished aggregate	9	m2	0	0	0	0	0
Popouts	10	no./m2	0	0	0	0	0
Blowups	11	no.	0	0	0	0	0
Faulting	12	-	-	-	-	-	-
Lane-shoulder dropoff	13	-	-	-	-	-	-
Lane-shoulder separation	14	-	-	-	-	-	-
Flexible patch deterioration	15fL	no.	0	0	0	0	0
	15fL	m2	0	0	0	0	0
	15fM	no.	0	0	0	0	0
	15fM	m2	0	0	0	0	0
	15fH	no.	0	0	0	0	0
	15fH	m2	0	0	0	0	0
Rigid patch deterioration	15rL	no.	0	0	0	0	0
	15rL	m2	0	0	0	0	0
	15rM	no.	0	0	0	0	0
	15rM	m2	0	0	0	0	0
	15rH	no.	0	0	0	0	0
Bleeding and pumping	16	no.	0	0	0	0	0
	16	m	0	0	0	0	0
Other	17	-	-	-	-	-	-

**Table B5. Summary of LTPP survey sheets
for ASR investigation—control section 2.**

Type	Identification code	Unit	11/29/94	11/28/95	12/21/96	12/9/97	10/22/98
Corner breaks	1L	no.	0	0	0	0	0
	1M	no.	0	0	0	0	0
	1H	no.	0	0	0	0	0
Durability cracking	2L	no.	0	0	0	0	0
	2L	m2	0	0	0	0	0
	2M	no.	0	0	0	0	0
	2M	m2	0	0	0	0	0
	2H	no.	0	0	0	0	0
	2H	m2	0	0	0	0	0
	3L	m	0	0	0	0	0
Longitudinal cracking	3L (sealed)	m	0	0	0	0	0
	3M	m	0	0	0	0	0
	3M (sealed)	m	0	0	0	0	0
	3H	m	0	0	0	0	0
	3H (sealed)	m	0	0	0	0	0
Transverse cracking	4L	no.	0	0	0	0	0
	4L	m	0	0	0	0	0
	4L (sealed)	m	0	0	0	0	0
	4M	no.	0	0	0	0	0
	4M	m	0	0	0	0	0
	4M (sealed)	m	0	0	0	0	0
	4H	no.	0	0	0	0	0
	4H (sealed)	m	0	0	0	0	0
Transverse joint seal damage	Sealed	y/n	Y	Y	Y	Y	Y
	5aL	no.	1	1	1	1	1
	5aM	no.	0	0	0	0	0
	5aH	no.	0	0	0	0	0
Longitudinal joint seal damage	No. sealed	no.	2	2	2	2	2
	5b	m	12.2	12.2	12.2	12.2	12.2
Spalling of longitudinal joints	6L	m	0	0	0	0	0
	6M	m	0	0	0	0	0
	6H	m	0	0	0	0	0
Spalling of transverse joints	7L	no.	0	0	1	1	1
	7L (length)	m	0	0	1.2	2.1	2.1
	7M	no.	0	0	0	0	0
	7M (length)	m	0	0	0	0	0
	7H	no.	0	0	0	0	0
Map cracking	8a	no.	1	1	1	1	1
	8a	m2	6	11.1	13.9	14.9	26
Scaling	8b	no.	0	0	0	0	0
	8b	m2	0	0	0	0	0
Polished aggregate	9	m2	0	0	0	0	0
Popouts	10	no./m2	0	0	0	0	0
Blowups	11	no.	0	0	0	0	0
Faulting	12	-	-	-	-	-	-
Lane-shoulder dropoff	13	-	-	-	-	-	-
Lane-shoulder separation	14	-	-	-	-	-	-
Flexible patch deterioration	15fL	no.	0	0	0	0	0
	15fL	m2	0	0	0	0	0
	15fM	no.	0	0	0	0	0
	15fM	m2	0	0	0	0	0
	15fH	no.	0	0	0	0	0
	15fH	m2	0	0	0	0	0
Rigid patch deterioration	15rL	no.	0	0	0	0	0
	15rL	m2	0	0	0	0	0
	15rM	no.	0	0	0	0	0
	15rM	m2	0	0	0	0	0
	15rH	no.	0	0	0	0	0
Bleeding and pumping	16	no.	0	0	0	0	0
	16	m	0	0	0	0	0
Other	17	-	-	-	-	-	-

**Table B6. Summary of LTPP survey sheets
for ASR investigation—control section 3.**

Type	Identification code	Unit	11/29/94	11/28/95	12/21/96	12/9/97	10/22/98
Corner breaks	1L	no.	0	0	0	0	0
	1M	no.	0	0	0	0	0
	1H	no.	0	0	0	0	0
Durability cracking	2L	no.	0	0	0	0	0
	2L	m2	0	0	0	0	0
	2M	no.	0	0	0	0	0
	2M	m2	0	0	0	0	0
	2H	no.	0	0	0	0	0
	2H	m2	0	0	0	0	0
	3L	m	0	0	0	0	0
Longitudinal cracking	3L (sealed)	m	0	0	0	0	0
	3M	m	0	0	0	0	0
	3M (sealed)	m	0	0	0	0	0
	3H	m	0	0	0	0	0
	3H (sealed)	m	0	0	0	0	0
Transverse cracking	4L	no.	1	1	1	1	1
	4L	m	2.4	2.4	2.4	2.4	2.4
	4L (sealed)	m	0	0	0	0	0
	4M	no.	0	0	0	0	0
	4M	m	0	0	0	0	0
	4M (sealed)	m	0	0	0	0	0
	4H	no.	0	0	0	0	0
	4H (sealed)	m	0	0	0	0	0
Transverse joint seal damage	Sealed	y/n	Y	Y	Y	Y	Y
	5aL	no.	1	1	1	1	1
	5aM	no.	0	0	0	0	0
	5aH	no.	0	0	0	0	0
Longitudinal joint seal damage	No. sealed	no.	2	2	2	2	2
	5b	m	12.2	12.2	12.2	12.2	12.2
Spalling of longitudinal joints	6L	m	0	0	0	0	0
	6M	m	0	0	0	0	0
	6H	m	0	0	0	0	0
Spalling of transverse joints	7L	no.	1	0	1	1	1
	7L (length)	m	2	1	0.9	1.5	1.5
	7M	no.	0	0	0	0	0
	7M (length)	m	0	0	0	0	0
	7H	no.	0	0	0	0	0
Map cracking	8a	no.	1	1	1	1	1
	8a	m2	9.8	20.8	22	25	29.7
Scaling	8b	no.	0	0	0	0	0
	8b	m2	0	0	0	0	0
Polished aggregate	9	m2	0	0	0	0	0
Popouts	10	no./m2	0	0	0	0	0
Blowups	11	no.	0	0	0	0	0
Faulting	12	-	-	-	-	-	-
Lane-shoulder dropoff	13	-	-	-	-	-	-
Lane-shoulder separation	14	-	-	-	-	-	-
Flexible patch deterioration	15fL	no.	0	0	0	0	0
	15fL	m2	0	0	0	0	0
	15fM	no.	0	0	0	0	0
	15fM	m2	0	0	0	0	0
	15fH	no.	0	0	0	0	0
	15fH	m2	0	0	0	0	0
Rigid patch deterioration	15rL	no.	0	0	0	0	0
	15rL	m2	0	0	0	0	0
	15rM	no.	0	0	0	0	0
	15rM	m2	0	0	0	0	0
	15rH	no.	0	0	0	0	0
Bleeding and pumping	16	no.	0	0	0	0	0
	16	m	0	0	0	0	0
Other	17	-	-	-	-	-	-

**Table B7. Summary of LTPP survey sheets
for ASR investigation—control section 4.**

Type	Identification code	Unit	11/29/94	11/28/95	12/21/96	12/9/97	10/22/98
Corner breaks	1L	no.	0	0	0	0	-
	1M	no.	0	0	0	0	-
	1H	no.	0	0	0	0	-
Durability cracking	2L	no.	0	0	0	0	-
	2L	m2	0	0	0	0	-
	2M	no.	0	0	0	0	-
	2M	m2	0	0	0	0	-
	2H	no.	0	0	0	0	-
	2H	m2	0	0	0	0	-
	3L	m	0	0	0	0	-
Longitudinal cracking	3L (sealed)	m	0	0	0	0	-
	3M	m	0	0	0	0	-
	3M (sealed)	m	0	0	0	0	-
	3H	m	0	0	0	0	-
	3H (sealed)	m	0	0	0	0	-
Transverse cracking	4L	no.	1	1	1	1	1
	4L	m	3.4	3.4	3.4	3.4	3.4
	4L (sealed)	m	0	0	0	0	-
	4M	no.	0	0	0	0	-
	4M	m	0	0	0	0	-
	4M (sealed)	m	0	0	0	0	-
	4H	no.	0	0	0	0	-
	4H (sealed)	m	0	0	0	0	-
Transverse joint seal damage	Sealed	y/n	Y	Y	Y	Y	-
	5aL	no.	1	1	1	1	-
	5aM	no.	0	0	0	0	-
	5aH	no.	0	0	0	0	-
Longitudinal joint seal damage	No. sealed	no.	2	2	2	2	-
	5b	m	12.2	12.2	12.2	12.2	-
Spalling of longitudinal joints	6L	m	0	0	0	0	-
	6M	m	0	0	0	0	-
	6H	m	0	0	0	0	-
Spalling of transverse joints	7L	no.	1	0	0	0	-
	7L (length)	m	2.5	2.5	0	0	-
	7M	no.	0	0	1	1	1
	7M (length)	m	0	0	2.4	2.4	2.4
	7H	no.	0	0	0	0	-
Map cracking	7H (length)	m	0	0	0	0	-
	8a	no.	1	1	1	1	-
Scaling	8a	m2	5.3	6.3	7.5	9.5	-
	8b	no.	0	0	0	0	-
Polished aggregate	8b	m2	0	0	0	0	-
Popouts	9	m2	0	0	0	0	-
Blowups	10	no./m2	0	0	0	0	-
Faulting	11	no.	0	0	0	0	-
Lane-shoulder dropoff	12	-	-	-	-	-	-
Lane-shoulder separation	13	-	-	-	-	-	-
Flexible patch deterioration	14	-	-	-	-	-	-
	15fL	no.	0	0	0	0	-
	15fL	m2	0	0	0	0	-
	15fM	no.	0	0	0	0	-
	15fM	m2	0	0	0	0	-
	15fH	no.	0	0	0	0	-
Rigid patch deterioration	15fH	m2	0	0	0	0	-
	15rL	no.	0	0	0	0	-
	15rL	m2	0	0	0	0	-
	15rM	no.	0	0	0	0	-
	15rM	m2	0	0	0	0	-
Bleeding and pumping	15rH	no.	0	0	0	0	-
	15rH	m2	0	0	0	0	-
Other	16	no.	0	0	0	0	-
	16	m	0	0	0	0	-
Other	17	-	-	-	-	-	-

**Table B8. Summary of LTPP survey sheets
for ASR investigation—test section 3.**

Type	Identification code	Unit	11/29/94	11/28/95	12/21/96	12/9/97	10/22/98
Corner breaks	1L	no.	0	0	0	0	0
	1M	no.	0	0	0	0	0
	1H	no.	0	0	0	0	0
Durability cracking	2L	no.	0	0	0	0	0
	2L	m2	0	0	0	0	0
	2M	no.	0	0	0	0	0
	2M	m2	0	0	0	0	0
	2H	no.	0	0	0	0	0
	2H	m2	0	0	0	0	0
	3L	m	0	0	0	0	0
Longitudinal cracking	3L (sealed)	m	0	0	0	0	0
	3M	m	0	0	0	0	0
	3M (sealed)	m	0	0	0	0	0
	3H	m	0	0	0	0	0
	3H (sealed)	m	0	0	0	0	0
Transverse cracking	4L	no.	1	0	1	1	1
	4L	m	2.4	0	2.7	3.4	3.4
	4L (sealed)	m	0	0	0	0	0
	4M	no.	0	0	0	0	0
	4M	m	0	0	0	0	0
	4M (sealed)	m	0	0	0	0	0
	4H	no.	0	0	0	0	0
	4H (sealed)	m	0	0	0	0	0
Transverse joint seal damage	Sealed	y/n	Y	Y	Y	Y	Y
	5aL	no.	1	1	1	1	1
	5aM	no.	0	0	0	0	0
	5aH	no.	0	0	0	0	0
Longitudinal joint seal damage	No. sealed	no.	2	2	2	2	2
	5b	m	12.2	12.2	12.2	12.2	12.2
Spalling of longitudinal joints	6L	m	0	0	0	0	0
	6M	m	0	0	0	0	0
	6H	m	0	0	0	0	0
Spalling of transverse joints	7L	no.	0	0	1	1	1
	7L (length)	m	0	0	0.3	0.3	0.3
	7M	no.	0	0	0	0	0
	7M (length)	m	0	0	0	0	0
	7H	no.	0	0	0	0	0
Map cracking	8a	no.	1	1	1	1	1
	8a	m2	2.5	6.2	7.2	7.4	33.4
Scaling	8b	no.	0	0	0	0	0
	8b	m2	0	0	0	0	0
Polished aggregate	9	m2	0	0	0	0	0
Popouts	10	no./m2	0	0	0	0	0
Blowups	11	no.	0	0	0	0	0
Faulting	12	-	-	-	-	-	-
Lane-shoulder dropoff	13	-	-	-	-	-	-
Lane-shoulder separation	14	-	-	-	-	-	-
Flexible patch deterioration	15fL	no.	0	0	0	0	0
	15fL	m2	0	0	0	0	0
	15fM	no.	0	0	0	0	0
	15fM	m2	0	0	0	0	0
	15fH	no.	0	0	0	0	0
	15fH	m2	0	0	0	0	0
Rigid patch deterioration	15rL	no.	0	0	0	0	0
	15rL	m2	0	0	0	0	0
	15rM	no.	0	0	0	0	0
	15rM	m2	0	0	0	0	0
	15rH	no.	0	0	0	0	0
Bleeding and pumping	16	no.	0	0	0	0	0
	16	m	0	0	0	0	0
Other	17	-	-	-	-	-	-

**Table B9. Summary of LTPP survey sheets
for ASR investigation—test section 4.**

Type	Identification code	Unit	11/29/94	11/28/95	12/21/96	12/9/97	10/22/98
Corner breaks	1L	no.	0	0	0	0	0
	1M	no.	0	0	0	0	0
	1H	no.	0	0	0	0	0
Durability cracking	2L	no.	0	0	0	0	0
	2L	m2	0	0	0	0	0
	2M	no.	0	0	0	0	0
	2M	m2	0	0	0	0	0
	2H	no.	0	0	0	0	0
	2H	m2	0	0	0	0	0
	3L	m	0	0	0	0	0
Longitudinal cracking	3L (sealed)	m	0	0	0	0	0
	3M	m	0	0	0	0	0
	3M (sealed)	m	0	0	0	0	0
	3H	m	0	0	0	0	0
	3H (sealed)	m	0	0	0	0	0
Transverse cracking	4L	no.	0	0	0	0	0
	4L	m	0	0	0	0	0
	4L (sealed)	m	0	0	0	0	0
	4M	no.	0	0	0	0	0
	4M	m	0	0	0	0	0
	4M (sealed)	m	0	0	0	0	0
	4H	no.	0	0	0	0	0
	4H (sealed)	m	0	0	0	0	0
Transverse joint seal damage	Sealed	y/n	Y	Y	Y	Y	Y
	5aL	no.	1	1	2	1	1
	5aM	no.	0	0	0	0	0
	5aH	no.	0	0	0	0	0
Longitudinal joint seal damage	No. sealed	no.	2	2	2	2	2
	5b	m	12.2	12.2	12.2	12.2	12.2
Spalling of longitudinal joints	6L	m	0	0	0	0	0
	6M	m	0	0	0	0	0
	6H	m	0	0	0	0	0
Spalling of transverse joints	7L	no.	0	0	0	0	0
	7L (length)	m	0	0	0	0	0
	7M	no.	0	0	0	0	0
	7M (length)	m	0	0	0	0	0
	7H	no.	0	0	0	0	0
Map cracking	8a	no.	1	1	1	1	1
	8a	m2	6.3	8.1	13.9	13.9	33.4
Scaling	8b	no.	0	0	0	0	0
	8b	m2	0	0	0	0	0
Polished aggregate	9	m2	0	0	0	0	0
Popouts	10	no./m2	0	0	0	0	0
Blowups	11	no.	0	0	0	0	0
Faulting	12	-	-	-	-	-	-
Lane-shoulder dropoff	13	-	-	-	-	-	-
Lane-shoulder separation	14	-	-	-	-	-	-
Flexible patch deterioration	15fL	no.	0	0	0	0	0
	15fL	m2	0	0	0	0	0
	15fM	no.	0	0	0	0	0
	15fM	m2	0	0	0	0	0
	15fH	no.	0	0	0	0	0
	15fH	m2	0	0	0	0	0
Rigid patch deterioration	15rL	no.	0	0	0	0	0
	15rL	m2	0	0	0	0	0
	15rM	no.	0	0	0	0	0
	15rM	m2	0	0	0	0	0
	15rH	no.	0	0	0	0	0
Bleeding and pumping	16	no.	0	0	0	0	0
	16	m	0	0	0	0	0
Other	17	-	-	-	-	-	-

**Table B10. Summary of LTPP survey sheets
for ASR investigation—control section 5.**

Type	Identification code	Unit	11/29/94	11/28/95	12/21/96	12/9/97	10/22/98
Corner breaks	1L	no.	0	0	0	0	0
	1M	no.	0	0	0	0	0
	1H	no.	0	0	0	0	0
Durability cracking	2L	no.	0	0	0	0	0
	2L	m2	0	0	0	0	0
	2M	no.	0	0	0	0	0
	2M	m2	0	0	0	0	0
	2H	no.	0	0	0	0	0
	2H	m2	0	0	0	0	0
	3L	m	0	0	0	0	0
Longitudinal cracking	3L (sealed)	m	0	0	0	0	0
	3M	m	0	0	0	0	0
	3M (sealed)	m	0	0	0	0	0
	3H	m	0	0	0	0	0
	3H (sealed)	m	0	0	0	0	0
Transverse cracking	4L	no.	0	0	0	0	0
	4L	m	0	0	0	0	0
	4L (sealed)	m	0	0	0	0	0
	4M	no.	0	0	0	0	0
	4M	m	0	0	0	0	0
	4M (sealed)	m	0	0	0	0	0
	4H	no.	0	0	0	0	0
	4H (sealed)	m	0	0	0	0	0
Transverse joint seal damage	Sealed	y/n	Y	Y	Y	Y	Y
	5aL	no.	2	2	2	2	2
	5aM	no.	0	0	0	0	0
	5aH	no.	0	0	0	0	0
Longitudinal joint seal damage	No. sealed	no.	2	2	2	2	2
	5b	m	12.2	12.2	12.2	12.2	12.2
Spalling of longitudinal joints	6L	m	0	0	0	0	0
	6M	m	0	0	0	0	0
	6H	m	0	0	0	0	0
Spalling of transverse joints	7L	no.	2	2	2	1	1
	7L (length)	m	1	1	2.9	0.6	0.6
	7M	no.	0	0	0	1	1
	7M (length)	m	0	0	0	2.25	2.25
	7H	no.	0	0	0	0	0
Map cracking	8a	no.	1	1	1	1	1
	8a	m2	5.3	7.9	15.8	15.8	33.4
Scaling	8b	no.	0	0	0	0	0
	8b	m2	0	0	0	0	0
Polished aggregate	9	m2	0	0	0	0	0
Popouts	10	no./m2	0	0	0	0	0
Blowups	11	no.	0	0	0	0	0
Faulting	12	-	-	-	-	-	-
Lane-shoulder dropoff	13	-	-	-	-	-	-
Lane-shoulder separation	14	-	-	-	-	-	-
Flexible patch deterioration	15fL	no.	0	0	0	0	0
	15fL	m2	0	0	0	0	0
	15fM	no.	0	0	0	0	0
	15fM	m2	0	0	0	0	0
	15fH	no.	0	0	0	0	0
	15fH	m2	0	0	0	0	0
Rigid patch deterioration	15rL	no.	0	0	0	0	0
	15rL	m2	0	0	0	0	0
	15rM	no.	0	0	0	0	0
	15rM	m2	0	0	0	0	0
	15rH	no.	0	0	0	0	0
Bleeding and pumping	16	no.	0	0	0	0	0
	16	m	0	0	0	0	0
Other	17	-	-	-	-	-	-

APPENDIX C



(a) Control section 1 (C1)

Figure C1. Photographs showing typical areas of each section (Boron, CA).



(b) Methacrylate section 1 (M1)

Figure C1. Photographs showing typical areas of each section (Boron, CA). (continued)



(c) Methacrylate section 2 (M2)

Figure C1. Photographs showing typical areas of each section (Boron, CA). (continued)



(d) Control section 3 (C3)

Figure C1. Photographs showing typical areas of each section (Boron, CA). (continued)



(e) Methacrylate section 3 (M3)

Figure C1. Photographs showing typical areas of each section (Boron, CA). (continued)

Petrographic Report for Boron, CA, 1997

Two sections from each of the cores were cut and lapped. These sections were then soaked overnight, dried, and the entire lapped surface was traversed under a stereo microscope. The lapped surface was divided into five or more traverses and examined at magnifications of 10 to 30 times. All instances of cracks, alkali-silica gel, and deteriorated or reacted aggregate particles were counted.

Boron OH No. 1: The surface is worn and partially coated. This core is of smaller diameter than the other cores, and only 8 traverses were made. Twenty-two instances of cracks were counted, with no gel or distressed aggregate particles. The core is classified as slightly to moderately distressed. The core is poorly air-entrained with an estimated air content of 3 percent.

Core 97-C1-3: The surface is moderately worn with moderately frequent popouts over coarse and fine aggregate particles. One hundred ninety cracks and 67 instances of alkali-silica gel were counted. Eight coarse and 20 fine aggregate particles showed evidence of distress or reaction. The core is classified as severely distressed. The core is air-entrained with an estimated air content of 5.5 percent.

Core 97-C2-30: The surface is moderately worn with occasional popouts over aggregate particles. One hundred seventy-four cracks and 24 instances of alkali-silica gel were counted. Eleven coarse and 23 fine aggregate particles showed evidence of reaction or distress. The core is classified as severely distressed. It is air-entrained with an estimated air content of 6 percent.

Core 97-C2-32: The surface is worn and cracked with occasional popouts over aggregate particles. One hundred ninety cracks and 44 instances of alkali-silica gel were counted. Twenty-six coarse and 30 fine aggregate particles showed evidence of distress or deterioration. The core is classified as severely distressed. It is air-entrained with an estimated air content of 6 percent.

Core 97-M1-33: The surface is worn with occasional popouts over aggregate particles. One hundred ninety-one cracks and 65 instances of alkali-silica gel were counted. Twenty-three coarse and 33 fine aggregate particles showed evidence of distress or reaction. The core is classified as severely distressed. It is air-entrained with an estimated air content of 5.5 percent.

Core 97-M2-33: The surface is worn and partially coated. Popouts over aggregate particles are occasionally present. One hundred thirty-five cracks and 59 instances of alkali-silica gel were counted. Twenty-nine coarse and 24 fine aggregate particles show evidence of distress or reaction. The core is classified as moderately severely distressed. It is poorly air-entrained and with estimated air content of 3.5 percent.

Core 97-M3-32: The surface is worn and partially coated. Occasional popouts over aggregate particles are present. One hundred thirty-four cracks and 46 instances of alkali-silica gel were counted. Thirty-one coarse and 32 fine aggregate particles show evidence of reaction or distress. The core is classified as moderately severely distressed. It is air-entrained with an estimated air content of 4 percent.

Petrographic Report for Boron, CA, 1998

Sections from each of the cores were cut and lapped. These sections were then soaked overnight, dried, and the entire lapped surface was traversed under a stereo microscope. Each lapped surface was divided into five or more (except the Boron OH cores) traverse areas and examined at magnifications of 10 to 30 times. Due to their smaller diameter (95.25 mm), the Boron OH cores were divided into 4 traverses. All instances of cracks, alkali-silica gel, and deteriorated or reacted aggregate particles were counted.

Boron OH-98-1: The wearing surface is moderately worn. Two cracks intercepting each other at approximate right angles are evident on the surface, and appear to have been repaired with an elastomeric material. The core is moderately severely distressed. Two macroscopic and 29 microcracks were counted. Twenty-one instances of alkali-silica gel were counted. Seven coarse and 8 fine aggregate particles show evidence of reaction or distress. The core is non-air-entrained with an estimated air content of 3 percent.

Boron OH-98-4: The wearing surface is moderately worn. Two cracks intercepting each other at approximate right angles are evident on the surface, and appear to have been repaired with an elastomeric material. The core is moderately severely distressed. One large and 29 microcracks were counted. Thirty-six instances of alkali-silica gel were counted. Eleven coarse and 7 fine aggregate particles showed evidence of reaction or distress. The core is non-air-entrained with an estimated air content of 1.5 percent.

98-C1-40: The wearing surface is severely worn with frequently exposed fine aggregate particles. Two large cracks form a "Y" shaped intercept on the wearing surface. The core is severely distressed. Five large and 86 microcracks were counted, and 49 instances of alkali-silica gel were counted. Twenty-two coarse and 21 fine aggregate particles show evidence of distress or reaction. The core is air-entrained with an estimated air content of 5 percent.

98-C1-42: the wearing surface is moderately severely worn with frequently exposed aggregate particles. Two distinct popouts over aggregate particles are present. The core is severely distressed. Sixty microcracks and 41 instances of alkali-silica gel were counted. Twenty-three coarse and 21 fine aggregate particles show evidence of distress or reaction. The core is air-entrained with an estimated air content of 5 percent.

98-C3-41: The wearing surface is severely worn with frequently exposed aggregate particles and worn popouts. The core is severely distressed. Three large cracks, 50 microcracks, and 28 instances of alkali-silica gel were counted. Eleven coarse and 8 fine aggregate particles show evidence of reaction or distress. The core is poorly air-entrained with an estimated air content that varies locally from 2 to 5 percent.

98-C3-42: The wearing surface is severely worn with frequently exposed fine aggregate particles. The core is severely distressed. Two large and 63 microcracks were counted, as were 14 instances of alkali-silica gel. Twelve coarse and 10 fine aggregate particles showed evidence of reaction or distress. The core is air-entrained with an estimated air content of 6 percent.

98-M1-41: The wearing surface is severely worn with frequently exposed aggregate particles. The core is moderately severely distressed. One large and 51 microcracks were counted, and 20

instances of alkali-silica gel were noted. Nine coarse and nine fine aggregate particles showed evidence of distress or reaction. The core is marginally air entrained with an estimated air content of 4 percent.

98-M1-42: The wearing surface is severely worn with frequently exposed aggregate particles. The core is severely distressed. Six major and 84 microcracks were counted, and there were 32 occurrences of alkali-silica gel. Seventeen coarse and 15 fine aggregate particles showed evidence of reaction or distress. The core is poorly air-entrained with an estimated air content of 3.5 percent.

98-M2-40B: The wearing surface is severely worn. Aggregate particles are frequently exposed and polished. The core is severely distressed. Three major and 72 microcracks were counted, and there were 12 instances of alkali-silica gel. Twelve coarse and seven fine aggregate particles show evidence of distress or reaction. The core is marginally air-entrained with an estimated air content of 4 percent.

98-M2-41: The wearing surface is severely worn. Aggregate particles are frequently exposed and polished. The core is severely distressed. Three major and 89 microcracks were counted, as well as 23 occurrences of alkali-silica gel. Eighteen coarse and 16 fine aggregate particles show evidence of reaction or distress. The core is marginally air-entrained with an estimated air content of 4.5 percent.

98-M3-41: The wearing surface is severely worn, with very frequently exposed and polished aggregate particles. The core is moderately severely distressed. Sixty-six microcracks and 29 instances of alkali-silica gel were counted. Fourteen coarse and 7 fine aggregate particles show evidence of distress or reaction. The core is air-entrained and has an estimated air content of 8 percent.

98-M3-42: The wearing surface is severely worn, with very frequently exposed and polished aggregate particles. The core is moderately severely distressed. Sixty-seven microcracks and 24 instances of alkali-silica gel were counted,. Ten coarse and 13 fine aggregate particles showed evidence of reaction or distress. The core is air-entrained with an estimated air content of 6 percent.

**Table C1. Summary of LTPP survey sheets
for ASR investigation—C1-boron.**

Type	Identification code	Unit	2/28/95	11/8/95	12/9/96	10/14/97	9/29/98
Corner breaks	1L	no.	0	0	0	0	0
	1M	no.	0	0	0	0	0
	1H	no.	0	0	0	0	0
Durability cracking	2L	no.	0	0	0	0	0
	2L	m2	0	0	0	0	0
	2M	no.	0	0	0	0	0
	2M	m2	0	0	0	0	0
	2H	no.	0	0	0	0	0
	2H	m2	0	0	0	0	0
Longitudinal cracking	3L	m	0	0	0	0	0
	3L (sealed)	m	0	0	0	0	0
	3M	m	0	0	0	0	0
	3M (sealed)	m	0	0	0	0	0
	3H	m	0	0	0	0	0
	3H (sealed)	m	0	0	0	0	0
Transverse crackig	4L	no.	0	0	0	0	0
	4L	m	0	0	0	0	0
	4L (sealed)	m	0	0	0	0	0
	4M	no.	0	0	0	0	0
	4M	m	0	0	0	0	0
	4M (sealed)	m	0	0	0	0	0
	4H	no.	0	0	0	0	0
	4H	m	0	0	0	0	0
	4H (sealed)	m	0	0	0	0	0
Transverse joint seal damage	Sealed	y/n	N	N	N	N	N
	5aL	no.	0	0	0	0	0
	5aM	no.	0	0	0	0	0
	5aH	no.	0	0	0	0	0
Longitudinal jointseal damage	No. sealed	no.	0	0	0	0	0
	5b	m	0	0	0	0	0
Spalling of longitudinal joints	6L	m	1	0	0	0	0
	6M	m	0	0	0	0	0
	6H	m	0	0	0	0	0
Spalling of transverse joints	7L	no.	32	0	0	0	0
	7L (length)	m	117	0	0	0	0
	7M	no.	1	31	11	17	4
	7M (length)	m	3.7	113.3	40.2	67.2	14.6
	7H	no.	0	2	22	16	29
	7H (length)	m	0	7.4	80.2	58.5	106.1
Map cracking (for 2/28/95 survey, the 8aL and 8aM amounts were combined due to grading rule changes)	8aL	no.	remainder	remainder	remainder	remainder	remainder
	8aL	m2	524.5	499.0	496.5	449.4	387.3
	8aM	no.	32	59	47	51	39
	8aM	m2	32.9	56.3	40.5	74.8	86.3
	8aH	no.	0	2	19	15	27
	8aH	m2	0	2.1	20.4	33.2	83.8
Flexible patch deterioration	15fL	no.	4	0	7	7	7
	15fL	m2	0.5	0	0.3	0.3	0.3
	15fM	no.	1	0	0	0	0
	15fM	m2	0.1	0	0	0	0
	15fH	no.	0	3	1	1	1
	15fH	m2	0	0.4	0.1	0.1	0.1
Rigid patch deterioration	15rL	no.	1	0	1	1	1
	15rL	m2	0.1	0	0.1	0.1	0.1
	15rM	no.	0	0	1	1	1
	15rM	m2	0	0	0.1	0.1	0.1
	15rH	no.	0	0	1	1	1
	15rH	m2	0	0	0.3	0.3	0.3
Bleeding and pumping	16	no.	0	0	0	0	0
	16	m	0	0	0	0	0
Other	WP-L	no.	0	0	0	0	0
	WP-M	no.	27	0	6	10	10
	WP-H	no.	5	32	26	22	22
	CL-L	no.	26	0	3	1	0
	CL-M	no.	6	32	22	26	26
	CL-H	no.	0	0	7	5	6
Total joint length at level (from sheet 6)	L	m	117.8	62.5	33.8	30.8	0.0
	M	m	2.4	53.3	76.5	82.6	99.1
	H	m	0.5	4.9	10.4	7.6	22.2
Total joint length (from sheet 6)	Total	m	120.7	120.7	120.7008	121	121.3
	Percent L	-	98	52	28	25	0
	Percent M	-	2	44	63	68	82
	Percent H	-	0	4	9	6	18
Map cracking	Total	no.	0	0	0	0	0
	Total	m	557.4182	557.4182	557.4182	557.4182	557.4182
	Percent L	-	94	90	89	81	69
	Percent M	-	6	10	7	13	15
	Percent H	-	0	0	4	6	15
Spalling of transverse joints (using 10 rule)	Total	no.	33	33	33	33	33
	Total	m	120.7	120.7	120.4	125.7	120.7
	Percent L	-	97	0	0	0	0
	Percent M	-	3	94	33	53	12
	Percent H	-	0	6	67	47	88

**Table C2. Summary of LTPP survey sheets
for ASR investigation—C2-boron.**

Type	Identification code	Unit	2/28/95	11/8/95	12/9/96	10/14/97	9/29/98
Corner breaks	1L	no.	not tested			0	0
	1M	no.	not tested			0	0
	1H	no.	not tested			0	0
Durability cracking	2L	no.	not tested			0	0
	2L	m2	not tested			0	0
	2M	no.	not tested			0	0
	2M	m2	not tested			0	0
	2H	no.	not tested			0	0
	2H	m2	not tested			0	0
Longitudinal cracking	3L	m	not tested			0	0
	3L (sealed)	m	not tested			0	0
	3M	m	not tested			0	0
	3M (sealed)	m	not tested			0	0
	3H	m	not tested			0	0
	3H (sealed)	m	not tested			0	0
Transverse cracking	4L	no.	not tested			0	0
	4L	m	not tested			0	0
	4L (sealed)	m	not tested			0	0
	4M	no.	not tested			0	0
	4M	m	not tested			0	0
	4M (sealed)	m	not tested			0	0
	4H	no.	not tested			0	0
	4H	m	not tested			0	0
	4H (sealed)	m	not tested			0	0
	Sealed	y/n	not tested			N	N
Transverse joint seal damage	5aL	no.	not tested			0	0
	5aM	no.	not tested			0	0
	5aH	no.	not tested			0	0
	5b	m	not tested			0	0
Longitudinal joint seal damage	No. sealed	no.	not tested			0	0
	5b	m	not tested			0	0
	5b	m	not tested			0	0
Spalling of longitudinal joints	6L	m	not tested			0	0
	6M	m	not tested			0	0
	6H	m	not tested			0	0
Spalling of transverse joints	7L	no.	not tested			0	0
	7L (length)	m	not tested			0	0
	7M	no.	not tested			33	27
	7M (length)	m	not tested			120.78	98.82
	7H	no.	not tested			0	6
	7H (length)	m	not tested			0	21.96
Map cracking (for 2/28/95 survey, the 8aL and 8aM amounts were combined Due to grading rule changes)	8aL	no.	not tested			remainder	remainder
	8aL	m2	not tested			505.2982	503.9082
	8aM	no.	not tested			65	66
	8aM	m2	not tested			52.12	53.51
	8aH	no.	not tested			0	0
	8aH	m2	not tested			0	0
Flexible patch deterioration	15fL	no.	not tested			0	0
	15fL	m2	not tested			0	0
	15fM	no.	not tested			0	0
	15fM	m2	not tested			0	0
	15fH	no.	not tested			0	0
	15fH	m2	not tested			0	0
Rigid patch deterioration	15rL	no.	not tested			0	0
	15rL	m2	not tested			0	0
	15rM	no.	not tested			0	0
	15rM	m2	not tested			0	0
	15rH	no.	not tested			0	0
	15rH	m2	not tested			0	0
Bleeding and pumping	16	no.	not tested			0	0
	16	m	not tested			0	0
Other	WP-L	no.	not tested			0	0
	WP-M	no.	not tested			32	32
	WP-H	no.	not tested			0	0
	CL-L	no.	not tested			8	5
	CL-M	no.	not tested			24	27
	CL-H	no.	not tested			0	0
Total joint length at level (from sheet 6)	L	m	not tested			60.7	8.84
	M	m	not tested			60.0	109.73
	H	m	not tested			0	2.13
Total joint length (from sheet 6)	Total	m				120.7	120.7
	Percent L					50.3	7.3
	Percent M					49.7	90.9
	Percent H					0.0	1.8
Map cracking	Total	no				0	0
	Total	m				557.4182	557.4182
	Percent L					91	90
	Percent M					9	10
Spalling of transverse joints (using 10 rule)	Percent H					0	0
	Total	no.				33	33
	Total	m				120.78	120.78
	Percent L					0	0
	Percent M					100	82
Percent H					0	5	

**Table C3. Summary of LTPP survey sheets
for ASR investigation—C3-boron.**

Type	Identification code	Unit	2/28/95	11/8/95	12/9/96	10/14/97	9/29/98	
Corner breaks	1L	no.	not tested	0	0	0	0	
	1M	no.	not tested	0	0	0	0	
	1H	no.	not tested	0	0	0	0	
Durability cracking	2L	no.	not tested	0	0	0	0	
	2L	m2	not tested	0	0	0	0	
	2M	no.	not tested	0	0	0	0	
	2M	m2	not tested	0	0	0	0	
	2H	no.	not tested	0	0	0	0	
	2H	m2	not tested	0	0	0	0	
Longitudinal cracking	3L	m	not tested	0	0	0	0	
	3L (sealed)	m	not tested	0	0	0	0	
	3M	m	not tested	0	0	0	0	
	3M (sealed)	m	not tested	0	0	0	0	
	3H	m	not tested	0	0	0	0	
Transverse cracking	4L	no.	not tested	0	0	0	0	
	4L	m	not tested	0	0	0	0	
	4L (sealed)	m	not tested	0	0	0	0	
	4M	no.	not tested	0	0	0	0	
	4M	m	not tested	0	0	0	0	
	4M (sealed)	m	not tested	0	0	0	0	
	4H	no.	not tested	0	0	0	0	
	4H	m	not tested	0	0	0	0	
	4H (sealed)	m	not tested	0	0	0	0	
	Transverse joint seal damage	Sealed	y/n	not tested	N	N	N	N
		5aL	no.	not tested	0	0	0	0
5aM		no.	not tested	0	0	0	0	
5aH		no.	not tested	0	0	0	0	
Longitudinal joint seal damage	No. sealed	no.	not tested	0	0	0	0	
	5b	m	not tested	0	0	0	0	
Spalling of longitudinal joints	6L	m	not tested	6.8	12	12	12	
	6M	m	not tested	0	0	0	0	
	6H	m	not tested	0	0	0	0	
Spalling of transverse joints	7L	no.	not tested	32	19	2	0	
	7L (length)	m	not tested	117	69.5	7.32	0	
	7M	no.	not tested	0	13	30	32	
	7M (length)	m	not tested	0	47.5	109.8	117	
	7H	no.	not tested	0	0	0	0	
	7H (length)	m	not tested	0	0	0	0	
Map cracking (for 2/28/95 survey, the 8aL and 8aM amounts were combined due to grading rule changes)	8aL	no.	not tested	remainder	remainder	remainder	remainder	
	8aL	m2	not tested	557.4182	547.6182	531.4982	509.1082	
	8aM	no.	not tested	0	35	50	66	
	8aM	m2	not tested	0	9.8	25.92	48.31	
	8aH	no.	not tested	0	0	0	0	
	8aH	m2	not tested	0	0	0	0	
	Flexible patch deterioration	15fL	no.	not tested	0	0	0	0
15fL		m2	not tested	0	0	0	0	
15fM		no.	not tested	0	0	0	0	
15fM		m2	not tested	0	0	0	0	
15fH		no.	not tested	0	0	0	0	
15fH		m2	not tested	0	0	0	0	
Rigid patch deterioration	15rL	no.	not tested	0	0	0	0	
	15rL	m2	not tested	0	0	0	0	
	15rM	no.	not tested	0	0	0	0	
	15rM	m2	not tested	0	0	0	0	
	15rH	no.	not tested	0	0	0	0	
	15rH	m2	not tested	0	0	0	0	
Bleeding and pumping	16	no.	not tested	0	0	0	0	
	16	m	not tested	0	0	0	0	
Other	WP-L	no.	not tested	2	5	1	0	
	WP-M	no.	not tested	31	28	32	29	
	WP-H	no.	not tested	0	0	0	4	
	CL-L	no.	not tested	32	30	30	4	
	CL-M	no.	not tested	1	3	3	29	
	CL-H	no.	not tested	0	0	0	0	
Total joint length at level (from sheet 6)	L	m	not tested	117	100.7	80.6	2.4	
	M	m	not tested	0	16.3	36.4	114.3	
	H	m	not tested	0	0	0	0.3	
Total joint length (from sheet 6)	Total	m	0	117	117	117	117	
	Percent L	-	0	100	86.1	68.9	2.1	
	Percent M	-	0	0	13.9	31.1	97.7	
	Percent H	-	0	0	0.0	0.0	0.3	
Map cracking	Total	no.	0	0	0	0	0	
	Total	m	0	557.4182	557.4182	557.4182	557.4182	
	Percent L	-	0	100	98	95	91	
	Percent M	-	0	0	2	5	9	
	Percent H	-	0	0	0	0	0	
Spalling of transverse joints (using 10 rule)	Total	no.	0	32	32	32	32	
	Total	m	0	117	117	117.12	117	
	Percent L	-	0	100	59	6	0	
	Percent M	-	0	0	41	94	100	
	Percent H	-	0	0	0	0	0	

**Table C4. Summary of LTPP survey sheets
for ASR investigation—M1-boron.**

Type	Identification code	Unit	2/28/95	11/8/95	12/9/96	10/14/97	9/29/98
Corner breaks	1L	no.	0	0	0	0	0
	1M	no.	0	0	0	0	0
	1H	no.	0	0	0	0	0
Durability cracking	2L	no.	0	0	0	0	0
	2L	m2	0	0	0	0	0
	2M	no.	0	0	0	0	0
	2M	m2	0	0	0	0	0
	2H	no.	0	0	0	0	0
	2H	m2	0	0	0	0	0
Longitudinal cracking	3L	m	0	0	0	0	0
	3L (sealed)	m	0	0	0	0	0
	3M	m	0	0	0	0	0
	3M (sealed)	m	0	0	0	0	0
	3H	m	0	0	0	0	0
	3H (sealed)	m	0	0	0	0	0
Transverse cracking	4L	no.	0	0	0	0	0
	4L	m	0	0	0	0	0
	4L (sealed)	m	0	0	0	0	0
	4M	no.	0	0	0	0	0
	4M	m	0	0	0	0	0
	4M (sealed)	m	0	0	0	0	0
	4H	no.	0	0	0	0	0
	4H (sealed)	m	0	0	0	0	0
Transverse joint seal damage	Sealed	y/n	N	N	N	N	N
	5aL	no.	0	0	0	0	0
	5aM	no.	0	0	0	0	0
	5aH	no.	0	0	0	0	0
Longitudinal joint seal damage	No. sealed	no.	0	0	0	0	0
	5b	m	0	0	0	0	0
Spalling of longitudinal joints	6L	m	6.1	0	0	0	0
	6M	m	0	0	0	0	0
	6H	m	0	0	0	0	0
Spalling of transverse joints	7L	no.	29	0	0	0	0
	7L (length)	m	106.1	0.0	0.0	0.0	0.0
	7M	no.	2	32	32	30	24
	7M (length)	m	7.3	117.0	117.0	109.8	87.8
	7H	no.	0	0	0	2	8
	7H (length)	m	0.0	0.0	0.0	7.3	29.3
Map cracking (for 2/28/95 survey, the 8aL and 8aM amounts were combined due to grading rule changes)	8aL	no.	remainder	remainder	remainder	remainder	remainder
	8aL	m2	510.0182	511.1182	506.6182	481.1482	456.5282
	8aM	no.	26	61	60	63	64
	8aM	m2	38.5	46.3	49.1	76.27	100.89
	8aH	no.	5	0	1	0	0
	8aH	m2	8.9	0	1.7	0	0
	15fL	no.	1	0	0	0	0
Flexible patch deterioration	15fL	m2	0.2	0	0	0	0
	15fM	no.	0	0	0	0	0
	15fM	m2	0	0	0	0	0
	15fH	no.	0	0	0	0	0
	15fH	m2	0	0	0	0	0
	15rL	no.	0	0	2	2	2
Rigid patch deterioration	15rL	m2	0	0	0.3	0.3	0.3
	15rM	no.	0	0	0	0	0
	15rM	m2	0	0	0	0	0
	15rH	no.	0	0	0	0	0
	15rH	m2	0	0	0	0	0
	16	no.	0	0	0	0	0
Bleeding and pumping	16	m	0	0	0	0	0
	WP-L	no.	1	0	3	22	0
	WP-M	no.	32	33	30	11	33
	WP-H	no.	0	0	0	0	0
	CL-L	no.	31	13	33	33	8
	CL-M	no.	2	20	0	0	25
Total joint length at level (from sheet 6)	CL-H	no.	0	0	0	0	0
	L	m	119.1	39.6	64.6	52.7	28.7
	M	m	1.6	80.5	55.5	63.7	83.8
	H	m	0.0	0.0	0.6	0.6	4.6
Total joint length (from sheet 6)	Total	m	117	117	117	117	117
	Percent L	-	102	34	55	45	25
	Percent M	-	1	69	47	54	72
	Percent H	-	0	0	1	1	4
Map cracking	Total	no.	0	0	0	0	0
	Total	m	557.4182	557.4182	557.4182	557.4182	557.4182
	Percent L	-	91	92	91	86	82
	Percent M	-	7	8	9	14	18
	Percent H	-	2	0	0	0	0
Spalling of transverse joints (using 10 rule)	Total	no.	31	32	32	32	32
	Total	m	113.4	117	117	117.12	117.12
	Percent L	-	94	0	0	0	0
	Percent M	-	6	100	100	94	75
	Percent H	-	0	0	0	6	25

**Table C5. Summary of LTPP survey sheets
for ASR investigation—M2-boron.**

Type	Identification code	Unit	2/28/95	11/8/95	12/9/96	10/14/97	9/29/98
Corner breaks	1L	no.	0	0	0	0	0
	1M	no.	0	0	0	0	0
	1H	no.	0	0	0	0	0
Durability cracking	2L	no.	0	0	0	0	0
	2L	m2	0	0	0	0	0
	2M	no.	0	0	0	0	0
	2M	m2	0	0	0	0	0
	2H	no.	0	0	0	0	0
	2H	m2	0	0	0	0	0
Longitudinal cracking	3L	m	0	0	0	0	0
	3L (sealed)	m	0	0	0	0	0
	3M	m	0	0	0	0	0
	3M (sealed)	m	0	0	0	0	0
	3H	m	0	0	0	0	0
	3H (sealed)	m	0	0	0	0	0
Transverse cracking	4L	no.	0	0	0	0	0
	4L	m	0	0	0	0	0
	4L (sealed)	m	0	0	0	0	0
	4M	no.	0	0	0	0	0
	4M	m	0	0	0	0	0
	4M (sealed)	m	0	0	0	0	0
	4H	no.	0	0	0	0	0
	4H	m	0	0	0	0	0
	4H (sealed)	m	0	0	0	0	0
	Transverse joint seal damage	Sealed	y/n	N	N	N	N
5aL		no.	0	0	0	0	0
5aM		no.	0	0	0	0	0
5aH		no.	0	0	0	0	0
Longitudinal joint seal damage	No. sealed	no.	0	0	0	0	0
	5b	m	0	0	0	0	0
Spalling of longitudinal joints	6L	m	1	0	0	0	0
	6M	m	0	0	0	0	0
	6H	m	0	0	0	0	0
Spalling of transverse joints	7L	no.	32	0	3	0	0
	7L (length)	m	82.3	0	11	0	0
	7M	no.	0	32	29	32	31
	7M (length)	m	0	63.4	106.1	117.1	113.5
	7H	no.	0	0	0	0	1
	7H (length)	m	0	0	0	0	3.7
Map cracking (for 2/28/95 survey, the 8aL and 8aM amounts were combined due to grading rule changes)	8aL	no.	remainder	remainder	remainder	remainder	remainder
	8aL	m2	510.8	527.7	521.4	509.0	505.6
	8aM	no.	30	39	52	55	52
	8aM	m2	44.4	29.7	36.0	48.5	51.9
	8aH	no.	2	0	0	0	0
	8aH	m2	2.2	0.0	0.0	0.0	0.0
	Flexible patch deterioration	15fL	no.	0	0	0	0
15fL		m2	0	0	0	0	0
15fM		no.	0	0	0	0	0
15fM		m2	0	0	0	0	0
15fH		no.	0	0	0	0	0
15fH		m2	0	0	0	0	0
Rigid patch deterioration	15rL	no.	0	0	0	0	0
	15rL	m2	0	0	0	0	0
	15rM	no.	0	0	0	0	0
	15rM	m2	0	0	0	0	0
	15rH	no.	0	0	0	0	0
	15rH	m2	0	0	0	0	0
Bleeding and pumping	16	no.	0	0	0	0	0
	16	m	0	0	0	0	0
Other	WP-L	no.	0	0	17	19	0
	WP-M	no.	32	33	15	14	33
	WP-H	no.	1	0	1	0	0
	CL-L	no.	33	33	30	33	27
	CL-M	no.	0	0	3	0	6
	CL-H	no.	0	0	0	0	0
Total joint length at level (from sheet 6)	L	m	80.7	17.4	81.7	70.6	41.0
	M	m	1.6	46.0	35.4	46.2	75.7
	H	m	0.0	0.0	0.0	0.0	0.3
Total joint length (from sheet 6)	Total	m	82.3	63.4	117.0432	116.8	117
	Percent L	-	98	27	70	60	35
	Percent M	-	2	73	30	40	65
	Percent H	-	0	0	0	0	0
Map cracking	Total	no.	0	0	0	0	0
	Total	m	557.4182	557.4182	557.4182	557.4182	557.4182
	Percent L	-	91.6	94.7	93.5	91.3	90.7
	Percent M	-	8.0	5.3	6.5	8.7	9.3
	Percent H	-	0.4	0.0	0.0	0.0	0.0
Spalling of transverse joints (using 10 rule)	Total	no.	32	32	32	32	32
	Total	m	82.3	63.4	117.1	117.1	117.1
	Percent L	-	100	0	9	0	0
	Percent M	-	0	100	91	100	97
	Percent H	-	0	0	0	0	1

**Table C6. Summary of LTPP survey sheets
for ASR investigation—M3-boron.**

Type	Identification code	Unit	2/28/95	11/8/95	12/9/96	10/14/97	9/29/98
Corner breaks	1L	no.	not tested	0	0	0	0
	1M	no.	not tested	0	0	0	0
	1H	no.	not tested	0	0	0	0
Durability cracking	2L	no.	not tested	0	0	0	0
	2L	m2	not tested	0	0	0	0
	2M	no.	not tested	0	0	0	0
	2M	m2	not tested	0	0	0	0
	2H	no.	not tested	0	0	0	0
	2H	m2	not tested	0	0	0	0
Longitudinal cracking	3L	m	not tested	0	0	0	0
	3L (sealed)	m	not tested	0	0	0	0
	3M	m	not tested	0	0	0	0
	3M (sealed)	m	not tested	0	0	0	0
	3H	m	not tested	0	0	0	0
	3H (sealed)	m	not tested	0	0	0	0
Transverse cracking	4L	no.	not tested	0	0	0	0
	4L	m	not tested	0	0	0	0
	4L (sealed)	m	not tested	0	0	0	0
	4M	no.	not tested	0	0	0	0
	4M	m	not tested	0	0	0	0
	4M (sealed)	m	not tested	0	0	0	0
	4H	no.	not tested	0	0	0	0
	4H	m	not tested	0	0	0	0
	4H (sealed)	m	not tested	0	0	0	0
	Sealed	y/n	not tested	N	N	N	N
Transverse joint seal damage	5aL	no.	not tested	0	0	0	0
	5aM	no.	not tested	0	0	0	0
	5aH	no.	not tested	0	0	0	0
	No. sealed	no.	not tested	0	0	0	0
Longitudinal joint seal damage	5b	m	not tested	0	0	0	0
Spalling of longitudinal joints	6L	m	not tested	2.7	2	2	2
	6M	m	not tested	0	0	0	0
	6H	m	not tested	0	0	0	0
Spalling of transverse joints	7L	no.	not tested	8	16	14	1
	7L (length)	m	not tested	5.1	26.2	51.2	3.7
	7M	no.	not tested	12	16	19	29
	7M (length)	m	not tested	13	29.6	69.5	106.1
	7H	no.	not tested	0	0	0	3
	7H (length)	m	not tested	0	0	0	11.0
Map cracking	8aL	no.	not tested	remainder	remainder	remainder	remainder
	8aL	m2	not tested	551.7182	551.0182	551.0182	534.1982
	8aM	no.	not tested	6	17	17	43
	8aM	m2	not tested	5.7	6.4	6.4	23.22
	8aH	no.	not tested	0	0	0	0
	8aH	m2	not tested	0	0	0	0
Flexible patch deterioration	15fL	no.	not tested	0	0	0	0
	15fL	m2	not tested	0	0	0	0
	15fM	no.	not tested	0	0	0	0
	15fM	m2	not tested	0	0	0	0
	15fH	no.	not tested	0	0	0	0
	15fH	m2	not tested	0	0	0	0
Rigid patch deterioration	15rL	no.	not tested	0	0	0	0
	15rL	m2	not tested	0	0	0	0
	15rM	no.	not tested	0	0	0	0
	15rM	m2	not tested	0	0	0	0
	15rH	no.	not tested	0	0	0	0
	15rH	m2	not tested	0	0	0	0
Bleeding and pumping	16	no.	not tested	0	0	0	0
	16	m	not tested	0	0	0	0
Other	WP-L	no.	not tested		31	31	17
	WP-M	no.	not tested		2	3	17
	WP-H	no.	not tested		0	0	0
	CL-L	no.	not tested		33	33	30
	CL-M	no.	not tested		0	1	4
	CL-H	no.	not tested		0	0	0
Total joint length at level (from sheet 6)	L	m	not tested	7.9	43.2816	82.9	82.6
	M	m	not tested	14	10.0584	12.5	37.2
	H	m	not tested	0	0	0	0.9
Total joint length (from sheet 6)	Total	m	0	21.9	53.34	95.4	120.7
	Percent L	-	0	36	81	87	68
	Percent M	-	0	64	19	13	31
	Percent H	-	0	0	0	0	1
	Total	no	0	0	0	0	0
Map cracking	Total	m	0	557.4182	557.4182	557.4182	557.4182
	Percent L	-	0	99	99	99	96
	Percent M	-	0	1	1	1	4
	Percent H	-	0	0	0	0	0
	Total	no.	0	20	32	33	33
Spalling of transverse joints (using 10 rule)	Total	m	0	18.1	55.8	120.78	120.78
	Percent L	-	0	28	47	42	3
	Percent M	-	0	72	53	58	88
	Percent H	-	0	0	0	0	9

APPENDIX D

Petrographic Report for Albuquerque, NM, 1997

Sections from each of the cores were cut and lapped. These sections were then soaked overnight, dried, and the entire lapped surface was traversed under a stereo microscope. The lapped surface was divided into five traverses and examined at magnifications of 10 to 30 times. All instances of cracks, alkali-silica gel, and deteriorated or reacted aggregate particles were counted.

Core 97-1-1: The core is well air-entrained with an estimated air content of approximately 7 percent. There were numerous popouts and scales on the wearing surface. Eight microcracks were counted. No gel was detected. Three fine aggregate particles had reacted.

Core 97-2-2: The core is well air-entrained with an estimated air content of approximately 7 percent. The wearing surface appears worn but otherwise undistressed. Eight microcracks were counted. Three instances of alkali-silica gel were detected. Eleven fine aggregate particles show evidence of reaction.

Core 97-3-1: The core is marginally air-entrained with an estimated air content of approximately 4 percent. The wearing surface has occasional spalls and popouts over aggregate particles. Nine microcracks were counted. Eighteen instances of alkali-silica gel were detected. Three coarse and 15 fine aggregate particles show evidence of reaction or distress.

Core 97-4-2: The core is well to slightly over air-entrained with an estimated air content of 8 percent. There are numerous popouts and shallow spalls on the wearing surface. Five microcracks were counted. Twenty-one instances of alkali-silica gel, 5 reacted or distressed coarse aggregate particles, and 20 reacted or distressed fine aggregate particles were detected.

Core 97-5-1: The core is air-entrained with an estimated air content of 5.5 percent. There are frequent shallow spalls and popouts on the wearing surface, as well as a "Y" shaped crack. Microcracks are frequent throughout the core and distress is severe. Ninety-two of the largest cracks were counted. Thirty-six instances of alkali-silica gel, 10 reacted or distressed coarse aggregate particles, and 49 reacted or distressed fine aggregate particles were counted.

Core 97-6-1: The core is air-entrained with slightly variable air content. The air content is estimated to be approximately 4.5 percent to 6 percent. The wearing surface is slightly worn but shows no other apparent distress. Two microcracks were counted. Seven instances of alkali-silica gel were detected; two reacted or distressed coarse aggregate particles; and six reacted or distressed fine aggregate particles were counted.

Core 97-7-2: The core is air-entrained with an estimated air content of approximately 6.5 percent. Infrequent small popouts are present on the wearing surface. One microcrack was counted. Three instances of alkali-silica gel were detected. One coarse aggregate particle had reacted; 21 fine aggregate particles showed evidence of reaction or distress.

Core 97-8-2: The core is air-entrained with an estimated air content of approximately 7 percent. There are occasional popouts over fine aggregate particles on the wearing surface. Four very short microcracks were counted within approximately 13 cm of the wearing surface. Four instances of alkali-silica gel were counted. One coarse and 10 fine aggregate particles showed evidence of reaction or distress.

Core 97-9-1: The core is air-entrained with an estimated air content of approximately 6 percent. There are infrequent small popouts over fine aggregate particles on the wearing surface. Three short microcracks were counted, two near the wearing surface. Two instances of alkali-silica gel were counted. Two coarse and two fine aggregate particles showed evidence of reaction or distress.

Core 97-10-2: The core is air-entrained with an estimated air content of approximately 7 percent. There are occasional small popouts over fine aggregate particles, and two large spalls on the wearing surface. It is not clear from this core whether the spalls are due to aggregate related distress or physical damage. Two short microcracks were counted within approximately 25 cm of the wearing surface. Six instances of alkali-silica gel were counted. One coarse and 10 fine aggregate particles showed evidence of reaction or distress.

Core 97-11-1: The core is air-entrained with an estimated air content of approximately 6.5 percent. No distress, only normal wear, was evident on the wearing surface. Two microcracks extending approximately 20 cm from the wearing surface were counted. Two instances of alkali-silica gel were counted. Seven coarse aggregate and 21 fine aggregate particles showed evidence of reaction or distress.

With the exception of two cores, distress is very minor in these specimens. There is a general paucity of alkali-silica gel; cracking is usually very minor and very fine. Even where particles can be seen to have reacted, the amount of reaction or deterioration is usually minimal.

Petrographic Report for Albuquerque, NM 1998

Sections from each of the cores were cut and lapped. These sections were then soaked overnight, dried, and the entire lapped surface was traversed under a stereo microscope. Each lapped surface was divided into five or more traverse areas and examined at magnifications of 10 to 30 times. All instances of cracks, alkali-silica gel, and deteriorated or reacted aggregate particles were counted.

Core 98-1-2: The core shows scant deterioration. The wearing surface has a slightly to moderately worn coarse broomed finish with occasional popouts over aggregate particles. Three microcracks were counted, as were 24 occurrences of alkali-silica gel. Three coarse and 36 fine aggregate particles show slight evidence of reaction. The core is air-entrained with an estimated air content of 6.5 percent.

Core 98-2-2: The wearing surface has a moderately worn, coarse broomed finish on which aggregate particles are occasionally exposed. The core is minimally distressed. Seven cracks and 24 instances of alkali-silica gel were counted. Two coarse and 27 fine aggregate particles show evidence of reaction. One fine aggregate particle was severely distressed. The core is air entrained with an estimated air content of 7 percent.

Core 98-3-2: The wearing surface is moderately to severely worn with frequent exposed aggregate particles, some apparently in old, worn popouts. The core shows abundant evidence of reaction but little distress. Two microcracks and 68 occurrences of gel were detected. Two coarse and 35 fine aggregate particles show evidence of reaction or distress. The core is air-entrained with an estimated air content of 5 percent.

Core 98-4-2: The wearing surface is severely worn with frequent exposed coarse and fine aggregate particles. Surface wear is too great to determine whether any were once popouts. The core shows evidence of reaction but little distress. Five microcracks were detected, as were fifty-one instances of alkali-silica gel. Ten coarse and 51 fine aggregate particles showed evidence of distress or reaction. The core is highly air entrained with an estimated air content of 8.5 percent.

Core 98-5-2: The wearing surface is severely worn, with numerous exposed coarse and fine aggregate particles, one empty coarse aggregate particle socket, and five visible cracks, three of which intersect near the center of the core. The core is severely distressed. In addition to the features noted above, 254 microcracks and 135 instances of alkali-silica gel were counted. Fifty-two coarse and 75 fine aggregate particles show evidence of reaction or distress. The core is air-entrained with a variable entrained air content which is estimated to range from 4 to 8 percent.

Core 98-6-2: The wearing surface is moderately worn with occasional exposed coarse and fine aggregate particles. The core shows slight evidence of distress or deterioration. Twenty-six microcracks and 25 instances of alkali-silica gel were counted. Fourteen coarse and 32 fine aggregate particles show evidence of reaction or distress. The core is air-entrained with an estimated air content of 8 percent.

Core 98-7-2: The wearing surface is moderately worn with frequently exposed aggregate particles. The core shows considerable evidence of reaction but little evidence of distress. Ten microcracks and 92 occurrences of alkali-silica gel were counted. Twenty-four coarse and 54 fine aggregate particles showed evidence of distress or reaction. The core is air-entrained with an estimated air content of 7 percent.

Core 98-8-2: The wearing surface is severely worn with frequent exposed aggregate particles. There is considerable evidence of reaction but little evidence of distress. Twenty-one microcracks, chiefly contained within reacted aggregate particles, and 45 occurrences of alkali-silica gel were counted. Sixteen coarse and 36 fine aggregate particles showed evidence of reaction or distress. The core is highly air-entrained with an estimated air content of 8 percent.

Core 98-9-2: The wearing surface is moderately to severely worn with frequent exposed aggregate particles. Although the core contains substantial evidence of ASR, apparent distress is slight. Twenty-one microcracks—chiefly limited to aggregate particles—and 58 instances of alkali-silica gel were counted. Sixteen coarse and 45 fine aggregate particles show evidence of distress or reaction. The core is air-entrained with an estimated air content of 8 percent.

Core 98-10-2: The wearing surface is moderately worn with moderately frequent exposed aggregate particles. The core contains abundant evidence of reaction, but little evidence of distress. Eighteen microcracks—all contained in aggregate particles—and 77 instances of alkali-silica gel were counted. Twenty-one coarse and 51 fine aggregate particles showed evidence of reaction or distress. The core is air-entrained with an estimated air content of 6 percent.

Core 98-11-2: The wearing surface is severely worn with frequent exposed aggregate particles. The core contains frequent evidence of reaction, but little evidence of distress. Eleven microcracks and 55 instances of alkali-silica gel were counted. Sixteen coarse and 60 fine aggregate particles show evidence of distress or reaction. The core is air-entrained with an estimated air content of 6 percent.

**Table D1. Summary of LTPP survey sheets
for ASR investigation—1–1% LiOH.**

Type	Identification code	Unit	11/8/94	10/16/95	12/11/96	10/16/97	10/1/98
Corner breaks	1L	no.	0	0	0	0	0
	1M	no.	0	0	0	0	0
	1H	no.	0	0	0	0	0
Durability cracking	2L	no.	0	0	0	0	0
	2L	m2	0	0	0	0	0
	2M	no.	0	0	0	0	0
	2M	m2	0	0	0	0	0
	2H	no.	0	0	0	0	0
Longitudinal cracking	2H	m2	0	0	0	0	0
	3L	m	0	0	0	0	0
	3L (sealed)	m	0	0	0	0	0
	3M	m	0	0	0	0	0
	3M (sealed)	m	0	0	0	0	0
	3H	m	0	0	0	0	0
Transverse cracking	3H (sealed)	m	0	0	0	0	0
	4L	no.	0	0	0	0	0
	4L	m	0	0	0	0	0
	4L (sealed)	m	0	0	0	0	0
	4M	no.	0	0	0	0	0
	4M	m	0	0	0	0	0
	4M (sealed)	m	0	0	0	0	0
	4H	no.	0	0	0	0	0
Transverse joint seal damage	4H	m	0	0	0	0	0
	4H (sealed)	m	0	0	0	0	0
	Sealed	y/n	Y	Y	Y	Y	Y
	5aL	no.	2	2	2	2	2
	5aM	no.	1	1	1	1	1
Longitudinal joint seal damage	5aH	no.	0	0	0	0	0
	No. sealed	no.	2	2	2	2	2
Spalling of longitudinal joints	5b	m	0	0	0	0	0
	6L	m	0	0	0	0	0
	6M	m	0	0	0	0	0
Spalling of transverse joints	6H	m	0	0	0	0	0
	7L	no.	1	1	2	1	1
	7L (length)	m	0.8	1.1	1.2	1.3	2.7
	7M	no.	0	0	0	1	0
	7M (length)	m	0	0	0	0.4	0
	7H	no.	0	0	0	0	1
Map cracking	7H (length)	m	0	0	0	0	3
	8a	no.	0	2	4	4	1
Scaling	8a	m2	0	10	11.5	32	54
	8b	no.	0	0	0	0	0
Polished aggregate	8b	m2	0	0	0	0	0
	9	m2	0	0	0	0	0
Popouts	10	no./m2	0	0	0	0	0
Blowups	11	no.	0	0	0	0	0
Faulting	12	-	-	-	-	-	-
Lane-shoulder dropoff	13	-	-	-	-	-	-
Lane-shoulder separation	14	-	-	-	-	-	-
Flexible patch deterioration	15fL	no.	0	0	0	0	0
	15fL	m2	0	0	0	0	0
	15fM	no.	0	0	0	0	0
	15fM	m2	0	0	0	0	0
	15fH	no.	0	0	0	0	0
	15fH	m2	0	0	0	0	0
Rigid patch deterioration	15rL	no.	0	0	0	0	0
	15rL	m2	0	0	0	0	0
	15rM	no.	0	0	0	0	0
	15rM	m2	0	0	0	0	0
	15rH	no.	0	0	0	0	0
Bleeding and pumping	15rH	m2	0	0	0	0	0
	16	no.	0	0	0	0	0
Other	16	m	0	0	0	0	0
	WP-L	no.	-	-	-	-	-
	WP-M	no.	-	-	-	-	-
	WP-H	no.	-	-	-	-	-
	CL-L	no.	-	-	-	-	-
	CL-M	no.	-	-	-	-	-
Longitudinal cracking	CL-H	no.	-	-	-	-	-
	Total	m	0	0	0	0	0
	Percent L	-	0	0	0	0	0
	Percent M	-	0	0	0	0	0
	Percent H	-	0	0	0	0	0
Transverse cracking	Total	no	0	0	0	0	0
	Total	m	0	0	0	0	0
	Percent L	-	0	0	0	0	0
	Percent M	-	0	0	0	0	0
	Percent H	-	0	0	0	0	0
Spalling of transverse joints	Total	no.	1	1	2	2	2
	Total	m	0.8	1.1	1.2	1.7	5.8
	Percent L	-	100	100	100	76	47
	Percent M	-	0	0	0	24	0
	Percent H	-	0	0	0	0	52

**Table D2. Summary of LTPP survey sheets
for ASR investigation—2–0.5% LiOH.**

Type	Identification code	Unit	11/8/94	10/16/95	12/11/96	10/16/97	10/1/98
Corner breaks	1L	no.	0	0	0	0	0
	1M	no.	0	0	0	0	0
	1H	no.	0	0	0	0	0
Durability cracking	2L	no.	0	0	0	0	0
	2L	m2	0	0	0	0	0
	2M	no.	0	0	0	0	0
	2M	m2	0	0	0	0	0
	2H	no.	0	0	0	0	0
	2H	m2	0	0	0	0	0
Longitudinal cracking	3L	m	0	0	0	0	0
	3L (sealed)	m	0	0	0	0	0
	3M	m	0	0	0	0	0
	3M (sealed)	m	0	0	0	0	0
	3H	m	0	0	0	0	0
	3H (sealed)	m	0	0	0	0	0
Transverse cracking	4L	no.	0	0	0	0	0
	4L	m	0	0	0	0	0
	4L (sealed)	m	0	0	0	0	0
	4M	no.	0	0	0	0	0
	4M	m	0	0	0	0	0
	4M (sealed)	m	0	0	0	0	0
	4H	no.	0	0	0	0	0
	4H	m	0	0	0	0	0
	4H (sealed)	m	0	0	0	0	0
Transverse joint seal damage	Sealed	y/n	Y	Y	Y	Y	Y
	5aL	no.	2	2	2	2	2
	5aM	no.	0	0	0	0	0
	5aH	no.	0	0	0	0	0
Longitudinal joint seal damage	No. sealed	no.	2	2	2	2	2
	5b	m	0	0	0	0	0
Spalling of longitudinal joints	6L	m	0	0	0	0	0
	6M	m	0	0	0	0	0
	6H	m	0	0	0	0	0
Spalling of transverse joints	7L	no.	0	0	2	0	0
	7L (length)	m	0	0	0.6	0	0
	7M	no.	0	0	0	2	2
	7M (length)	m	0	0	0	1.9	5.5
	7H	no.	0	0	0	0	0
	7H (length)	m	0	0	0	0	0
Map cracking	8a	no.	0	2	5	4	1
	8a	m2	0	6	5.9	24.3	25.5
Scaling	8b	no.	0	0	0	0	0
	8b	m2	0	0	0	0	0
Polished aggregate	9	m2	0	0	0	0	0
Popouts	10	no./m2	0	0	0	0	0
Blowups	11	no.	0	0	0	0	0
Faulting	12	-	-	-	-	-	-
Lane-shoulder dropoff	13	-	-	-	-	-	-
Lane-shoulder separation	14	-	-	-	-	-	-
Flexible patch deterioration	15fL	no.	0	0	0	0	0
	15fL	m2	0	0	0	0	0
	15fM	no.	0	0	0	0	0
	15fM	m2	0	0	0	0	0
	15fH	no.	0	0	0	0	0
	15fH	m2	0	0	0	0	0
Rigid patch deterioration	15rL	no.	0	0	0	0	0
	15rL	m2	0	0	0	0	0
	15rM	no.	0	0	0	0	0
	15rM	m2	0	0	0	0	0
	15rH	no.	0	0	0	0	0
Bleeding and pumping	15rH	m2	0	0	0	0	0
	16	no.	0	0	0	0	0
	16	m	0	0	0	0	0
Other	WP-L	no.	-	-	-	-	-
	WP-M	no.	-	-	-	-	-
	WP-H	no.	-	-	-	-	-
	CL-L	no.	-	-	-	-	-
	CL-M	no.	-	-	-	-	-
	CL-H	no.	-	-	-	-	-
Longitudinal cracking	Total	m	0	0	0	0	0
	Percent L	-	0	0	0	0	0
	Percent M	-	0	0	0	0	0
	Percent H	-	0	0	0	0	0
Transverse cracking	Total	no	0	0	0	0	0
	Total	m	0	0	0	0	0
	Percent L	-	0	0	0	0	0
	Percent M	-	0	0	0	0	0
Spalling of transverse joints	Percent H	-	0	0	0	0	0
	Total	no.	0	0	2	2	2
	Total	m	0	0	0.6	1.9	5.5
	Percent L	-	0	0	100	0	0
	Percent M	-	0	0	0	100	100
Percent H	-	0	0	0	0	0	

**Table D3. Summary of LTPP survey sheets
for ASR investigation—3-Lomar.**

Type	Identification code	Unit	11/8/94	10/16/95	12/11/96	10/16/97	10/1/98
Corner breaks	1L	no.	0	0	1	0	0
	1M	no.	0	0	0	0	0
	1H	no.	0	0	0	0	0
Durability cracking	2L	no.	0	0	0	0	0
	2L	m2	0	0	0	0	0
	2M	no.	0	0	0	0	0
	2M	m2	0	0	0	0	0
	2H	no.	0	0	0	0	0
	2H	m2	0	0	0	0	0
Longitudinal cracking	3L	m	0	0	0	0	0
	3L (sealed)	m	0	0	0	0	0
	3M	m	0	0	0	0	0
	3M (sealed)	m	0	0	0	0	0
	3H	m	0	0	0	0	0
	3H (sealed)	m	0	0	0	0	0
Transverse cracking	4L	no.	0	0	0	0	0
	4L	m	0	0	0	0	0
	4L (sealed)	m	0	0	0	0	0
	4M	no.	0	0	0	0	0
	4M	m	0	0	0	0	0
	4M (sealed)	m	0	0	0	0	0
	4H	no.	0	0	0	0	0
	4H (sealed)	m	0	0	0	0	0
Transverse joint seal damage	Sealed	y/n	Y	Y	Y	Y	Y
	5aL	no.	1	2	1	1	1
	5aM	no.	1	0	1	1	1
	5aH	no.	0	0	0	0	0
Longitudinal joint seal damage	No. sealed	no.	2	2	2	2	2
	5b	m	0	0	0	0	0
Spalling of longitudinal joints	6L	m	0	0	0.5	0.5	0.5
	6M	m	0	0	0	0	0
	6H	m	0	0	0	0	0
Spalling of transverse joints	7L	no.	2	0	0	0	0
	7L (length)	m	0.2	0	0	0	0
	7M	no.	0	1	2	2	0
	7M (length)	m	0	0.5	1.2	1.6	0
	7H	no.	0	0	0	0	2
	7H (length)	m	0	0	0	0	4.3
Map cracking	8a	no.	0	0	0	1	2
	8a	m2	0	0	0	3.1	7
Sealing	8b	no.	0	0	0	0	0
	8b	m2	0	0	0	0	0
Polished aggregate	9	m2	0	0	0	0	0
Popouts	10	no./m2	0	0	0	0	0
Blowups	11	no.	0	0	0	0	0
Faulting	12	-	-	-	-	-	-
Lane-shoulder dropoff	13	-	-	-	-	-	-
Lane-shoulder separation	14	-	-	-	-	-	-
Flexible patch deterioration	15fL	no.	0	0	0	0	0
	15fL	m2	0	0	0	0	0
	15fM	no.	0	0	0	0	0
	15fM	m2	0	0	0	0	0
	15fH	no.	0	0	0	0	0
	15fH	m2	0	0	0	0	0
Rigid patch deterioration	15rL	no.	0	0	0	0	0
	15rL	m2	0	0	0	0	0
	15rM	no.	0	0	0	0	0
	15rM	m2	0	0	0	0	0
	15rH	no.	0	0	0	0	0
Bleeding and pumping	15rH	m2	0	0	0	0	0
	16	no.	0	0	0	0	0
	16	m	0	0	0	0	0
	WP-L	no.	-	-	-	-	-
Other	WP-M	no.	-	-	-	-	-
	WP-H	no.	-	-	-	-	-
	CL-L	no.	-	-	-	-	-
	CL-M	no.	-	-	-	-	-
	CL-H	no.	-	-	-	-	-
Longitudinal cracking	Total	m	0	0	0	0	0
	Percent L	-	0	0	0	0	0
	Percent M	-	0	0	0	0	0
	Percent H	-	0	0	0	0	0
Transverse cracking	Total	no.	0	0	0	0	0
	Total	m	0	0	0	0	0
	Percent L	-	0	0	0	0	0
	Percent M	-	0	0	0	0	0
Spalling of transverse joints	Percent H	-	0	0	0	0	0
	Total	no.	2	1	2	2	2
	Total	m	0.2	0.5	1.2	1.6	4.3
	Percent L	-	100	0	0	0	0
	Percent M	-	0	100	100	100	0
Percent H	-	0	0	0	0	100	

**Table D4. Summary of LTPP survey sheets
for ASR investigation—4-class F fly ash.**

Type	Identification code	Unit	11/8/94	10/16/95	12/11/96	10/16/97	10/1/98
Corner breaks	1L	no.	0	0	0	0	0
	1M	no.	0	0	0	0	0
	1H	no.	0	0	0	0	0
Durability cracking	2L	no.	0	0	0	0	0
	2L	m2	0	0	0	0	0
	2M	no.	0	0	0	0	0
	2M	m2	0	0	0	0	0
	2H	no.	0	0	0	0	0
	2H	m2	0	0	0	0	0
Longitudinal cracking	3L	m	0	0	0	0	0
	3L (sealed)	m	0	0	0	0	0
	3M	m	0	0	0	0	0
	3M (sealed)	m	0	0	0	0	0
	3H	m	0	0	0	0	0
	3H (sealed)	m	0	0	0	0	0
Transverse cracking	4L	no.	0	0	0	0	0
	4L	m	0	0	0	0	0
	4L (sealed)	m	0	0	0	0	0
	4M	no.	0	0	0	0	0
	4M	m	0	0	0	0	0
	4M (sealed)	m	0	0	0	0	0
	4H	no.	0	0	0	0	0
	4H (sealed)	m	0	0	0	0	0
Transverse joint seal damage	Sealed	y/n	Y	Y	Y	Y	Y
	5aL	no.	3	3	3	3	3
	5aM	no.	0	0	0	0	0
	5aH	no.	0	0	0	0	0
Longitudinal joint seal damage	No. sealed	no.	1	2	2	2	2
	5b	m	1.5	0	0	0	0
Spalling of longitudinal joints	6L	m	1.5	0.3	0.3	0.3	0.3
	6M	m	0	0	0	0	0
	6H	m	0	0	0	0	0
Spalling of transverse joints	7L	no.	0	0	2	3	3
	7L (length)	m	0	0	0.3	1.6	5.2
	7M	no.	0	0	0	0	0
	7M (length)	m	0	0	0	0	0
	7H	no.	0	0	0	0	0
	7H (length)	m	0	0	0	0	0
Map cracking	8a	no.	0	1	1	1	2
	8a	m2	0	1	1	1.8	1.8
Scaling	8b	no.	0	0	0	0	0
	8b	m2	0	0	0	0	0
Polished aggregate	9	m2	0	0	0	0	0
Popouts	10	no./m2	0	0	0	0	0
Blowups	11	no.	0	0	0	0	0
Faulting	12	-	-	-	-	-	-
Lane-shoulder dropoff	13	-	-	-	-	-	-
Lane-shoulder separation	14	-	-	-	-	-	-
Flexible patch deterioration	15fL	no.	0	0	0	0	0
	15fL	m2	0	0	0	0	0
	15fM	no.	0	0	0	0	0
	15fM	m2	0	0	0	0	0
	15fH	no.	0	0	0	0	0
	15fH	m2	0	0	0	0	0
Rigid patch deterioration	15rL	no.	0	0	0	0	0
	15rL	m2	0	0	0	0	0
	15rM	no.	0	0	0	0	0
	15rM	m2	0	0	0	0	0
	15rH	no.	0	0	0	0	0
Bleeding and pumping	15rH	m2	0	0	0	0	0
	16	no.	0	0	0	0	0
Other	16	m	0	0	0	0	0
	WP-L	no.	-	-	-	-	-
	WP-M	no.	-	-	-	-	-
	WP-H	no.	-	-	-	-	-
	CL-L	no.	-	-	-	-	-
	CL-M	no.	-	-	-	-	-
Longitudinal cracking	CL-H	no.	-	-	-	-	-
	Total	m	0	0	0	0	0
	Percent L	-	0	0	0	0	0
	Percent M	-	0	0	0	0	0
	Percent H	-	0	0	0	0	0
Transverse cracking	Total	no.	0	0	0	0	0
	Total	m	0	0	0	0	0
	Percent L	-	0	0	0	0	0
	Percent M	-	0	0	0	0	0
	Percent H	-	0	0	0	0	0
Spalling of transverse joints	Total	no.	0	0	2	3	3
	Total	m	0	0	0.3	1.6	5.2
	Percent L	-	0	0	100	100	100
	Percent M	-	0	0	0	0	0
	Percent H	-	0	0	0	0	0

**Table D5. Summary of LTPP survey sheets
for ASR investigation—5-class F fly ash.**

Type	Identification code	Unit	11/8/94	10/16/95	12/11/96	10/16/97	10/1/98
Corner breaks	1L	no.	0	0	0	0	0
	1M	no.	0	0	0	0	0
	1H	no.	0	0	0	0	0
Durability cracking	2L	no.	0	0	0	0	0
	2L	m2	0	0	0	0	0
	2M	no.	0	0	0	0	0
	2M	m2	0	0	0	0	0
	2H	no.	0	0	0	0	0
	2H	m2	0	0	0	0	0
Longitudinal cracking	3L	m	0	4.3	4.5	4.5	4.5
	3L (sealed)	m	0	0	0	0	0
	3M	m	0	0	0	2.1	2.1
	3M (sealed)	m	0	0	0	0	0
	3H	m	0	0	0	0	0
	3H (sealed)	m	0	0	0	0	0
Transverse cracking	4L	no.	0	1	1	1	1
	4L	m	0	0.5	0.5	1	1
	4L (sealed)	m	0	0	0	0	0
	4M	no.	1	2	2	0	0
	4M	m	3.3	6.8	7.4	0	0
	4M (sealed)	m	3.3	0	0	0	0
	4H	no.	0	0	0	2	2
	4H	m	0	0	0	6.7	7.0
	4H (sealed)	m	0	0	0	0	0
Transverse joint seal damage	Sealed	y/n	Y	Y	Y	Y	Y
	5aL	no.	2	2	2	2	2
	5aM	no.	0	0	0	0	0
	5aH	no.	0	0	0	0	0
Longitudinal joint seal damage	No. sealed	no.	2	2	2	2	2
	5b	m	0	0	0	0	0
Spalling of longitudinal joints	6L	m	0	0	0	0	0
	6M	m	0	0	0	0	0
	6H	m	0	0	0	0	0
Spalling of transverse joints	7L	no.	0	2	1	0	0
	7L (length)	m	0	7	3.7	0	0
	7M	no.	0	0	1	2	2
	7M (length)	m	0	0	3.6	7.1	7.1
	7H	no.	0	0	0	0	0
	7H (length)	m	0	0	0	0	0
Map cracking	8a	no.	0	1	1	1	1
	8a	m2	0	49	49	49	49
Scaling	8b	no.	0	0	0	0	0
	8b	m2	0	0	0	0	0
Polished aggregate	9	m2	0	0	0	0	0
Popouts	10	no./m2	0	0	0	0	0
Blowups	11	no.	0	0	0	0	0
Faulting	12	-	-	-	-	-	-
Lane-shoulder dropoff	13	-	-	-	-	-	-
Lane-shoulder separation	14	-	-	-	-	-	-
Flexible patch deterioration	15fL	no.	0	0	0	0	0
	15fL	m2	0	0	0	0	0
	15fM	no.	0	0	0	0	0
	15fM	m2	0	0	0	0	0
	15fH	no.	0	0	0	0	0
	15fH	m2	0	0	0	0	0
Rigid patch deterioration	15rL	no.	0	0	0	0	0
	15rL	m2	0	0	0	0	0
	15rM	no.	0	0	0	0	0
	15rM	m2	0	0	0	0	0
	15rH	no.	0	0	0	0	0
Bleeding and pumping	15rH	m2	0	0	0	0	0
	16	no.	0	0	0	0	0
	16	m	0	0	0	0	0
Other	WP-L	no.	-	-	-	-	-
	WP-M	no.	-	-	-	-	-
	WP-H	no.	-	-	-	-	-
	CL-L	no.	-	-	-	-	-
	CL-M	no.	-	-	-	-	-
	CL-H	no.	-	-	-	-	-
Longitudinal cracking	Total	m	0	4.3	4.5	6.6	6.6
	Percent L	-	0	100	100	68	68
	Percent M	-	0	0	0	32	32
	Percent H	-	0	0	0	0	0
	Total	no.	1	3	3	3	3
Transverse cracking	Total	m	3.3	7.3	7.9	7.7	8
	Percent L	-	0	7	6	13	12
	Percent M	-	100	93	94	0	0
	Percent H	-	0	0	0	87	88
	Total	no.	0	2	2	2	2
Spalling of transverse joints	Total	m	0	7	7.3	7.1	7.1
	Percent L	-	0	100	51	0	0
	Percent M	-	0	0	49	100	100
	Percent H	-	0	0	0	0	0

**Table D6. Summary of LTPP survey sheets
for ASR investigation—6-control.**

Type	Identification code	Unit	11/8/94	10/16/95	12/11/96	10/16/97	10/1/98
Corner breaks	1L	no.	0	0	0	0	0
	1M	no.	0	0	0	0	0
	1H	no.	0	0	0	0	0
Durability cracking	2L	no.	0	0	0	0	0
	2L	m2	0	0	0	0	0
	2M	no.	0	0	0	0	0
	2M	m2	0	0	0	0	0
	2H	no.	0	0	0	0	0
	2H	m2	0	0	0	0	0
Longitudinal cracking	3L	m	0	0	0	0	0
	3L (sealed)	m	0	0	0	0	0
	3M	m	0	0	0	0	0
	3M (sealed)	m	0	0	0	0	0
	3H	m	0	0	0	0	0
	3H (sealed)	m	0	0	0	0	0
Transverse cracking	4L	no.	0	0	0	0	0
	4L	m	0	0	0	0	0
	4L (sealed)	m	0	0	0	0	0
	4M	no.	0	0	0	0	0
	4M	m	0	0	0	0	0
	4M (sealed)	m	0	0	0	0	0
	4H	no.	0	0	0	0	0
	4H	m	0	0	0	0	0
	4H (sealed)	m	0	0	0	0	0
Transverse joint seal damage	Sealed	y/n	Y	Y	Y	Y	Y
	5aL	no.	3	3	3	3	3
	5aM	no.	0	0	0	0	0
	5aH	no.	0	0	0	0	0
Longitudinal joint seal damage	No. sealed	no.	2	2	2	2	2
	5b	m	0	0	0	0	0
Spalling of longitudinal joints	6L	m	0	0	0	0	0
	6M	m	0	0	0	0	0
	6H	m	0	0	0	0	0
Spalling of transverse joints	7L	no.	0	0	3	3	3
	7L (length)	m	0	0	0.6	2.1	7
	7M	no.	0	0	0	0	0
	7M (length)	m	0	0	0	0	0
	7H	no.	0	0	0	0	0
	7H (length)	m	0	0	0	0	0
Map cracking	8a	no.	0	0	0	2	2
	8a	m2	0	0	0	8.1	35.9
Scaling	8b	no.	0	0	0	0	0
	8b	m2	0	0	0	0	0
Polished aggregate	9	m2	0	0	0	0	0
Popouts	10	no./m2	0	0	0	0	0
Blowups	11	no.	0	0	0	0	0
Faulting	12	-	-	-	-	-	-
Lane-shoulder dropoff	13	-	-	-	-	-	-
Lane-shoulder separation	14	-	-	-	-	-	-
Flexible patch deterioration	15fL	no.	0	0	0	0	0
	15fL	m2	0	0	0	0	0
	15fM	no.	0	0	0	0	0
	15fM	m2	0	0	0	0	0
	15fH	no.	0	0	0	0	0
	15fH	m2	0	0	0	0	0
Rigid patch deterioration	15rL	no.	0	0	0	0	0
	15rL	m2	0	0	0	0	0
	15rM	no.	0	0	0	0	0
	15rM	m2	0	0	0	0	0
	15rH	no.	0	0	0	0	0
Bleeding and pumping	15rH	m2	0	0	0	0	0
	16	no.	0	0	0	0	0
	16	m	0	0	0	0	0
	WP-L	no.	-	-	-	-	-
Other	WP-M	no.	-	-	-	-	-
	WP-H	no.	-	-	-	-	-
	CL-L	no.	-	-	-	-	-
	CL-M	no.	-	-	-	-	-
	CL-H	no.	-	-	-	-	-
Longitudinal cracking	Total	m	0	0	0	0	0
	Percent L	-	0	0	0	0	0
	Percent M	-	0	0	0	0	0
	Percent H	-	0	0	0	0	0
Transverse cracking	Total	no.	0	0	0	0	0
	Total	m	0	0	0	0	0
	Percent L	-	0	0	0	0	0
	Percent M	-	0	0	0	0	0
Spalling of transverse joints	Percent H	-	0	0	0	0	0
	Total	no.	0	0	3	3	3
	Total	m	0	0	0.6	2.1	7
	Percent L	-	0	0	100	100	100
	Percent M	-	0	0	0	0	0
Percent H	-	0	0	0	0	0	

**Table D7. Summary of LTPP survey sheets
for ASR investigation—7-blended C&F.**

Type	Identification code	Unit	11/8/94	10/16/95	12/11/96	10/16/97	10/1/98
Corner breaks	1L	no.	0	0	0	0	0
	1M	no.	0	0	0	0	0
	1H	no.	0	0	0	0	0
Durability cracking	2L	no.	0	0	0	0	0
	2L	m2	0	0	0	0	0
	2M	no.	0	0	0	0	0
	2M	m2	0	0	0	0	0
	2H	no.	0	0	0	0	0
	2H	m2	0	0	0	0	0
Longitudinal cracking	3L	m	0	0.8	0.8	0.8	0.8
	3L (sealed)	m	0	0	0	0	0
	3M	m	0	0	0	0	0
	3M (sealed)	m	0	0	0	0	0
	3H	m	0	0	0	0	0
	3H (sealed)	m	0	0	0	0	0
Transverse cracking	4L	no.	1	1	2	2	1
	4L	m	3.3	3.4	4.2	4.2	1.2
	4L (sealed)	m	3.3	3.4	0	0	0
	4M	no.	1	0	0	0	0
	4M	m	3.3	0	0	0	0
	4M (sealed)	m	0	0	0	0	0
	4H	no.	0	1	1	1	2
	4H	m	0	3.4	3.7	3.7	6.7
	4H (sealed)	m	0	0	0	0	0
Transverse joint seal damage	Sealed	y/n	Y	Y	Y	Y	Y
	5aL	no.	3	3	3	3	3
	5aM	no.	0	0	0	0	0
	5aH	no.	0	0	0	0	0
Longitudinal joint seal damage	No. sealed	no.	2	2	2	2	2
	5b	m	0	0	0	0	0
Spalling of longitudinal joints	6L	m	0	0	0	0	0
	6M	m	0	0	0	0	0
	6H	m	0	0	0	0	0
Spalling of transverse joints	7L	no.	0	0	2	3	3
	7L (length)	m	0	0	0.4	4.5	7
	7M	no.	0	0	0	0	0
	7M (length)	m	0	0	0	0	0
	7H	no.	0	0	0	0	0
	7H (length)	m	0	0	0	0	0
Map cracking	8a	no.	0	0	0	3	4
	8a	m2	0	0	0	19	28.7
Scaling	8b	no.	0	0	0	0	0
	8b	m2	0	0	0	0	0
Polished aggregate	9	m2	0	0	0	0	0
Popouts	10	no./m2	0	0	0	0	0
Blowups	11	no.	0	0	0	0	0
Faulting	12	-	-	-	-	-	-
Lane-shoulder dropoff	13	-	-	-	-	-	-
Lane-shoulder separation	14	-	-	-	-	-	-
Flexible patch deterioration	15fL	no.	0	0	0	0	0
	15fL	m2	0	0	0	0	0
	15fM	no.	0	0	0	0	0
	15fM	m2	0	0	0	0	0
	15fH	no.	0	0	0	0	0
	15fH	m2	0	0	0	0	0
Rigid patch deterioration	15rL	no.	0	0	0	0	0
	15rL	m2	0	0	0	0	0
	15rM	no.	0	0	0	0	0
	15rM	m2	0	0	0	0	0
	15rH	no.	0	0	0	0	0
Bleeding and pumping	15rH	m2	0	0	0	0	0
	16	no.	0	0	0	0	0
	16	m	0	0	0	0	0
Other	WP-L	no.	-	-	-	-	-
	WP-M	no.	-	-	-	-	-
	WP-H	no.	-	-	-	-	-
	CL-L	no.	-	-	-	-	-
	CL-M	no.	-	-	-	-	-
	CL-H	no.	-	-	-	-	-
Longitudinal cracking	Total	m	0	0.8	0.8	0.8	0.8
	Percent L	-	0	100	100	100	100
	Percent M	-	0	0	0	0	0
	Percent H	-	0	0	0	0	0
	Total	no.	2	2	3	3	3
Transverse cracking	Total	m	6.6	6.8	7.9	7.9	7.9
	Percent L	-	50	50	53	53	15
	Percent M	-	50	0	0	0	0
	Percent H	-	0	50	47	47	85
	Total	no.	0	0	2	3	3
Spalling of transverse joints	Total	m	0	0	0.4	4.5	7
	Percent L	-	0	0	100	100	100
	Percent M	-	0	0	0	0	0
	Percent H	-	0	0	0	0	0
	Total	-	0	0	0	0	0

**Table D8. Summary of LTPP survey sheets
for ASR investigation—8-class F.**

Type	Identification code	Unit	11/8/94	10/16/95	12/11/96	10/16/97	10/1/98
Corner breaks	1L	no.	0	0	0	0	0
	1M	no.	0	0	0	0	0
	1H	no.	0	0	0	0	0
Durability cracking	2L	no.	0	0	0	0	0
	2L	m2	0	0	0	0	0
	2M	no.	0	0	0	0	0
	2M	m2	0	0	0	0	0
	2H	no.	0	0	0	0	0
	2H	m2	0	0	0	0	0
Longitudinal cracking	3L	m	0	0	0	0	0
	3L (sealed)	m	0	0	0	0	0
	3M	m	0	0	0	0	0
	3M (sealed)	m	0	0	0	0	0
	3H	m	0	0	0	0	0
	3H (sealed)	m	0	0	0	0	0
Transverse cracking	4L	no.	2	0	0	0	0
	4L	m	2.7	0	0	0	0
	4L (sealed)	m	0	0	0	0	0
	4M	no.	0	0	0	0	0
	4M	m	0	0	0	0	0
	4M (sealed)	m	0	0	0	0	0
	4H	no.	0	0	0	0	0
	4H	m	0	0	0	0	0
	4H (sealed)	m	0	0	0	0	0
Transverse joint seal damage	Sealed	y/n	Y	Y	Y	Y	Y
	5aL	no.	0	2	1	1	1
	5aM	no.	2	0	1	1	1
	5aH	no.	0	0	0	0	0
Longitudinal joint seal damage	No. sealed	no.	2	2	2	2	2
	5b	m	0	0	0	0	0
Spalling of longitudinal joints	6L	m	0	0	0	0	0
	6M	m	0	0	0	0	0
	6H	m	0	0	0	0	0
Spalling of transverse joints	7L	no.	0	0	0	0	0
	7L (length)	m	0	0	0	0	0
	7M	no.	2	1	1	0	0
	7M (length)	m	2.6	1.2	1.1	0	0
	7H	no.	0	1	1	2	2
	7H (length)	m	0	1.8	1.9	5.2	5.2
Map cracking	8a	no.	0	2	3	3	1
	8a	m2	0	0.7	3.9	34	45
Scaling	8b	no.	0	0	0	0	0
	8b	m2	0	0	0	0	0
Polished aggregate	9	m2	0	0	0	0	0
Popouts	10	no./m2	0	0	0	0	0
Blowups	11	no.	0	0	0	0	0
Faulting	12	-	-	-	-	-	-
Lane-shoulder dropoff	13	-	-	-	-	-	-
Lane-shoulder separation	14	-	-	-	-	-	-
Flexible patch deterioration	15fL	no.	0	0	0	0	0
	15fL	m2	0	0	0	0	0
	15fM	no.	0	0	0	0	0
	15fM	m2	0	0	0	0	0
	15fH	no.	0	0	0	0	0
	15fH	m2	0	0	0	0	0
	15rL	no.	0	0	0	0	0
Rigid patch deterioration	15rL	m2	0	0	0	0	0
	15rM	no.	0	0	0	0	0
	15rM	m2	0	0	0	0	0
	15rH	no.	0	0	0	0	0
	15rH	m2	0	0	0	0	0
Bleeding and pumping	16	no.	0	0	0	0	0
	16	m	0	0	0	0	0
Other	WP-L	no.	-	-	-	-	-
	WP-M	no.	-	-	-	-	-
	WP-H	no.	-	-	-	-	-
	CL-L	no.	-	-	-	-	-
	CL-M	no.	-	-	-	-	-
	CL-H	no.	-	-	-	-	-
Longitudinal cracking	Total	m	0	0	0	0	0
	Percent L	-	0	0	0	0	0
	Percent M	-	0	0	0	0	0
	Percent H	-	0	0	0	0	0
	Total	no.	2	0	0	0	0
Transverse cracking	Total	m	2.7	0	0	0	0
	Percent L	-	100	0	0	0	0
	Percent M	-	0	0	0	0	0
	Percent H	-	0	0	0	0	0
	Total	no.	2	2	2	2	2
Spalling of transverse joints	Total	m	2.6	3	3	5.2	5.5
	Percent L	-	0	0	0	0	0
	Percent M	-	100	40	37	0	0
	Percent H	-	0	60	63	100	95

**Table D9. Summary of LTPP survey sheets
for ASR investigation—9-control.**

Type	Identification code	Unit	11/8/94	10/16/95	12/11/96	10/16/97	10/1/98
Corner breaks	1L	no.	0	0	0	0	0
	1M	no.	0	0	0	0	0
	1H	no.	0	0	0	0	0
Durability cracking	2L	no.	0	0	0	0	0
	2L	m2	0	0	0	0	0
	2M	no.	0	0	0	0	0
	2M	m2	0	0	0	0	0
	2H	no.	0	0	0	0	0
	2H	m2	0	0	0	0	0
Longitudinal cracking	3L	m	0	0.8	0.8	0.8	0.8
	3L (sealed)	m	0	0	0	0	0
	3M	m	0	0	0	0	0
	3M (sealed)	m	0	0	0	0	0
	3H	m	0	0	0	0	0
	3H (sealed)	m	0	0	0	0	0
Transverse cracking	4L	no.	0	0	0	0	0
	4L	m	0	0	0	0	0
	4L (sealed)	m	0	0	0	0	0
	4M	no.	0	0	0	0	0
	4M	m	0	0	0	0	0
	4M (sealed)	m	0	0	0	0	0
	4H	no.	0	0	0	0	0
	4H	m	0	0	0	0	0
	4H (sealed)	m	0	0	0	0	0
Transverse joint seal damage	Sealed	y/n	Y	Y	Y	Y	Y
	5aL	no.	3	3	3	3	3
	5aM	no.	0	0	0	0	0
	5aH	no.	0	0	0	0	0
Longitudinal joint seal damage	No. sealed	no.	2	2	2	2	2
	5b	m	0	0	0	0	0
Spalling of longitudinal joints	6L	m	0	0	0.1	0.1	0.1
	6M	m	0	0	0	0	0
	6H	m	0	0	0	0	0
Spalling of transverse joints	7L	no.	0	0	2	3	3
	7L (length)	m	0	0	0.4	4.5	8.1
	7M	no.	0	0	0	0	0
	7M (length)	m	0	0	0	0	0
	7H	no.	0	0	0	0	0
	7H (length)	m	0	0	0	0	0
Map cracking	8a	no.	0	0	0	5	1
	8a	m2	0	0	0	25	47.3
Scaling	8b	no.	0	0	0	0	0
	8b	m2	0	0	0	0	0
Polished aggregate	9	m2	0	0	0	0	0
Popouts	10	no./m2	0	0	0	0	0
Blowups	11	no.	0	0	0	0	0
Faulting	12	-	-	-	-	-	-
Lane-shoulder dropoff	13	-	-	-	-	-	-
Lane-shoulder separation	14	-	-	-	-	-	-
Flexible patch deterioration	15fL	no.	0	0	0	0	0
	15fL	m2	0	0	0	0	0
	15fM	no.	0	0	0	0	0
	15fM	m2	0	0	0	0	0
	15fH	no.	0	0	0	0	0
	15fH	m2	0	0	0	0	0
	15rL	no.	0	0	0	0	0
Rigid patch deterioration	15rL	m2	0	0	0	0	0
	15rM	no.	0	0	0	0	0
	15rM	m2	0	0	0	0	0
	15rH	no.	0	0	0	0	0
	15rH	m2	0	0	0	0	0
Bleeding and pumping	16	no.	0	0	0	0	0
Other	16	m	0	0	0	0	0
	WP-L	no.	-	-	-	-	-
	WP-M	no.	-	-	-	-	-
	WP-H	no.	-	-	-	-	-
	CL-L	no.	-	-	-	-	-
	CL-M	no.	-	-	-	-	-
CL-H	no.	-	-	-	-	-	
Longitudinal cracking	Total	m	0	0.8	0.8	0.8	0.8
	Percent L	-	0	100	100	100	100
	Percent M	-	0	0	0	0	0
	Percent H	-	0	0	0	0	0
	Total	no.	0	0	0	0	0
Transverse cracking	Total	m	0	0	0	0	0
	Percent L	-	0	0	0	0	0
	Percent M	-	0	0	0	0	0
	Percent H	-	0	0	0	0	0
	Total	no.	0	0	2	3	3
Spalling of transverse joints	Total	m	0	0	0.4	4.5	8.1
	Percent L	-	0	0	100	100	100
	Percent M	-	0	0	0	0	0
	Percent H	-	0	0	0	0	0
	Total	-	0	0	0	0	0

**Table D10. Summary of LTPP survey sheets
for ASR investigation—10–1% LiOH.**

Type	Identification code	Unit	11/8/94	10/16/95	12/11/96	10/16/97	10/1/98
Corner breaks	1L	no.	0	0	0	0	0
	1M	no.	0	0	0	0	0
	1H	no.	0	0	0	0	0
Durability cracking	2L	no.	0	0	0	0	0
	2L	m2	0	0	0	0	0
	2M	no.	0	0	0	0	0
	2M	m2	0	0	0	0	0
	2H	no.	0	0	0	0	0
	2H	m2	0	0	0	0	0
Longitudinal cracking	3L	m	0	0	0	0	0
	3L (sealed)	m	0	0	0	0	0
	3M	m	0	0	0	0	0
	3M (sealed)	m	0	0	0	0	0
	3H	m	0	0	0	0	0
	3H (sealed)	m	0	0	0	0	0
Transverse cracking	4L	No.	0	0	0	0	0
	4L	m	0	0	0	0	0
	4L (sealed)	m	0	0	0	0	0
	4M	No.	0	0	0	0	0
	4M	m	0	0	0	0	0
	4M (sealed)	m	0	0	0	0	0
	4H	No.	0	0	0	0	0
	4H	m	0	0	0	0	0
	4H (sealed)	m	0	0	0	0	0
Transverse joint seal damage	Sealed	y/n	Y	Y	Y	Y	Y
	5aL	No.	2	2	2	2	2
	5aM	No.	0	0	0	0	0
	5aH	No.	0	0	0	0	0
Longitudinal joint seal damage	No. sealed	No.	2	2	2	2	2
	5b	m	0	0	0	0	0
Spalling of longitudinal joints	6L	m	0	0	0	0	0
	6M	m	0	0	0	0	0
	6H	m	0	0	0	0	0
Spalling of transverse joints	7L	No.	0	1	2	2	2
	7L (length)	M	0	0.5	0.5	2.4	5.5
	7M	No.	0	0	0	0	0
	7M (length)	M	0	0	0	0	0
	7H	No.	0	0	0	0	0
	7H (length)	M	0	0	0	0	0
Map cracking	8a	No.	0	0	1	5	1
	8a	m2	0	0	0.6	18	42.9
Scaling	8b	No.	0	0	0	0	0
	8b	m2	0	0	0	0	0
Polished aggregate	9	m2	0	0	0	0	0
Popouts	10	no./m2	0	0	0	0	0
Blowups	11	No.	0	0	0	0	0
Faulting	12	-	-	-	-	-	-
Lane-shoulder dropoff	13	-	-	-	-	-	-
Lane-shoulder separation	14	-	-	-	-	-	-
Flexible patch deterioration	15fL	No.	0	0	0	0	0
	15fL	m2	0	0	0	0	0
	15fM	No.	0	0	0	0	0
	15fM	m2	0	0	0	0	0
	15fH	No.	0	0	0	0	0
	15fH	m2	0	0	0	0	0
Rigid patch deterioration	15rL	No.	0	0	0	0	0
	15rL	m2	0	0	0	0	0
	15rM	No.	0	0	0	0	0
	15rM	m2	0	0	0	0	0
	15rH	No.	0	0	0	0	0
Bleeding and pumping	15rH	m2	0	0	0	0	0
	16	No.	0	0	0	0	0
	16	m	0	0	0	0	0
	WP-L	No.	-	-	-	-	-
Other	WP-M	No.	-	-	-	-	-
	WP-H	No.	-	-	-	-	-
	CL-L	No.	-	-	-	-	-
	CL-M	No.	-	-	-	-	-
	CL-H	No.	-	-	-	-	-
Longitudinal cracking	Total	m	0	0	0	0	0
	Percent L	-	0	0	0	0	0
	Percent M	-	0	0	0	0	0
	Percent H	-	0	0	0	0	0
Transverse cracking	Total	No.	0	0	0	0	0
	Total	m	0	0	0	0	0
	Percent L	-	0	0	0	0	0
	Percent M	-	0	0	0	0	0
Spalling of transverse joints	Percent H	-	0	0	0	0	0
	Total	No.	0	1	2	2	2
	Total	m	0	0.5	0.5	2.4	5.5
	Percent L	-	0	100	100	100	100
	Percent M	-	0	0	0	0	0
Percent H	-	0	0	0	0	0	

**Table D11. Summary of LTPP survey sheets
for ASR investigation—11-class C ash.**

Type	Identification code	Unit	11/8/94	10/16/95	12/11/96	10/16/97	10/1/98
Corner breaks	1L	no.	0	0	0	0	0
	1M	no.	0	0	0	0	0
	1H	no.	0	0	0	0	0
Durability cracking	2L	no.	0	0	0	0	0
	2L	m2	0	0	0	0	0
	2M	no.	0	0	0	0	0
	2M	m2	0	0	0	0	0
	2H	no.	0	0	0	0	0
	2H	m2	0	0	0	0	0
Longitudinal cracking	3L	m	0	0	0	0	0
	3L (sealed)	m	0	0	0	0	0
	3M	m	0	0	0	0	0
	3M (sealed)	m	0	0	0	0	0
	3H	m	0	0	0	0	0
	3H (sealed)	m	0	0	0	0	0
Transverse cracking	4L	no.	0	0	0	0	0
	4L	m	0	0	0	0	0
	4L (sealed)	m	0	0	0	0	0
	4M	no.	0	0	0	0	0
	4M	m	0	0	0	0	0
	4M (sealed)	m	0	0	0	0	0
	4H	no.	0	0	0	0	0
	4H	m	0	0	0	0	0
	4H (sealed)	m	0	0	0	0	0
Transverse joint seal damage	Sealed	y/n	Y	Y	Y	Y	Y
	5aL	no.	4	4	4	4	4
	5aM	no.	0	0	0	0	0
	5aH	no.	0	0	0	0	0
Longitudinal joint seal damage	No. sealed	no.	2	2	2	2	2
	5b	m	0	0	0	0	0
Spalling of longitudinal joints	6L	m	0	0	0	0	0
	6M	m	0	0	0	0	0
	6H	m	0	0	0	0	0
Spalling of transverse joints	7L	no.	0	2	4	4	4
	7L (length)	m	0	2.1	5	9.7	11
	7M	no.	0	0	0	0	0
	7M (length)	m	0	0	0	0	0
	7H	no.	0	0	0	0	0
	7H (length)	m	0	0	0	0	0
Map cracking	8a	no.	3	0	3	4	1
	8a	m2	0	0	5.3	48	58.5
Scaling	8b	no.	0	0	0	0	0
	8b	m2	0	0	0	0	0
Polished aggregate	9	m2	0	0	0	0	0
Popouts	10	no./m2	0	0	0	0	0
Blowups	11	no.	0	0	0	0	0
Faulting	12	-	-	-	-	-	-
Lane-shoulder dropoff	13	-	-	-	-	-	-
Lane-shoulder separation	14	-	-	-	-	-	-
Flexible patch deterioration	15fL	no.	0	0	0	0	0
	15fL	m2	0	0	0	0	0
	15fM	no.	0	0	0	0	0
	15fM	m2	0	0	0	0	0
	15fH	no.	0	0	0	0	0
	15fH	m2	0	0	0	0	0
Rigid patch deterioration	15rL	no.	0	0	0	0	0
	15rL	m2	0	0	0	0	0
	15rM	no.	0	0	0	0	0
	15rM	m2	0	0	0	0	0
	15rH	no.	0	0	0	0	0
Bleeding and pumping	15rH	m2	0	0	0	0	0
	16	no.	0	0	0	0	0
	16	m	0	0	0	0	0
Other	WP-L	no.	-	-	-	-	-
	WP-M	no.	-	-	-	-	-
	WP-H	no.	-	-	-	-	-
	CL-L	no.	-	-	-	-	-
	CL-M	no.	-	-	-	-	-
	CL-H	no.	-	-	-	-	-
Longitudinal cracking	Total	m	0	0	0	0	0
	Percent L	-	0	0	0	0	0
	Percent M	-	0	0	0	0	0
	Percent H	-	0	0	0	0	0
	Total	no.	0	0	0	0	0
Transverse cracking	Total	m	0	0	0	0	0
	Percent L	-	0	0	0	0	0
	Percent M	-	0	0	0	0	0
	Percent H	-	0	0	0	0	0
	Total	no.	0	2	4	4	4
Spalling of transverse joints	Total	m	0	2.1	5	9.7	11
	Percent L	-	0	100	100	100	100
	Percent M	-	0	0	0	0	0
	Percent H	-	0	0	0	0	0

REFERENCES

1. Hall, K. T., M. I. Darter, T. E. Hoerner, and L. Khazanovich. *LTPP Data Analysis Phase I: Validation of Guidelines for k Value Selection and Concrete Pavement Performance Prediction*, Report Number FHWA-RD-96-168. Federal Highway Administration, U.S. Department of Transportation, 1996.

